DOCTOR OF PHILOSOPHY

# Dibenzothiophene-S,S-dioxide Based Conjugated Molecular and Polymeric Materials for Organic Electronics

AL-Mashhadani, Mohammed

*Award date:*
2019

*Awarding institution:*
Bangor University

# *Dibenzothiophene-S,S-dioxide Based Conjugated Molecular and Polymeric Materials for Organic Electronics*


PRIFYSGOL
BANGOR
UNIVERSITY

**Mohammed Hussein Al-Mashhadani**

School of Natural Sciences

Bangor University

A thesis submitted to Bangor University

for the degree of Doctor of Philosophy

**Dedicated to my Parents,**

**Wife, Kids, Brothers and Sisters**

# Contents

# Declaration and Consent

---

**Details of the Work**

I hereby agree to deposit the following item in the digital repository maintained by Bangor University and/or in any other repository authorized for use by Bangor University.

**Author Name:** Mohammed Hussein Al-Mashhadani

**Title:** Dibenzothiophene-*S*,*S*-dioxide Based Conjugated Molecular and Polymeric Materials for Organic Electronics

**Supervisor/Department:** Professor Igor F. Perepichka & Dr. Juma'a R. Al-Dulayymi / Chemistry

**Funding body (if any):** The Higher Committee For Education Development in Iraq (HCED)

**Qualification/Degree obtained:** PhD in Chemistry

This item is a product of my own research endeavours and is covered by the agreement below in which the item is referred to as "the Work". It is identical in content to that deposited in the Library, subject to point 4 below.

**Non-exclusive Rights**

Rights granted to the digital repository through this agreement are entirely non-exclusive. I am free to publish the Work in its present version or future versions elsewhere.

I agree that Bangor University may electronically store, copy or translate the Work to any approved medium or format for the purpose of future preservation and accessibility. Bangor University is not under any obligation to reproduce or display the Work in the same formats or resolutions in which it was originally deposited.

**Bangor University Digital Repository**

I understand that work deposited in the digital repository will be accessible to a wide variety of people and institutions, including automated agents and search engines via the World Wide Web.

I understand that once the Work is deposited, the item and its metadata may be incorporated into public access catalogues or services, national databases of electronic theses and dissertations such as the British Library's EThOS or any service provided by the National Library of Wales.

I understand that the Work may be made available via the National Library of Wales Online Electronic Theses Service under the declared terms and conditions of use

(http://www.llgc.org.uk/index.php?id=4676). I agree that as part of this service the National Library of Wales may electronically store, copy or convert the Work to any approved medium or format for the purpose of future preservation and accessibility. The National Library of Wales is not under any obligation to reproduce or display the Work in the same formats or resolutions in which it was originally deposited.

**Statement 1:**

This work has not previously been accepted in substance for any degree and is not being concurrently submitted in candidature for any degree unless as agreed by the University for approved dual awards.

Signed …….. (candidate)

Date ……..

**Statement 2:**

This thesis is the result of my own investigations, except where otherwise stated. Where correction services have been used, the extent and nature of the correction is clearly marked in a footnote(s).Other sources are acknowledged by footnotes giving explicit references. A bibliography is appended.

Signed ……. (candidate)

Date …….

**Statement 3:**

I hereby give consent for my thesis, if accepted, to be available for photocopying, for inter-library loan and for electronic repositories, and for the title and summary to be made available to outside organisations.

Signed ……. (candidate)

Date …….

NB: Candidates on whose behalf a bar on access has been approved by the Academic Registry should use the following version of **Statement 3:**

**Statement 3 (bar):**

I hereby give consent for my thesis, if accepted, to be available for photocopying, for inter-library loans and for electronic repositories after expiry of a bar on access.

Signed …… (candidate)

Date ……

**Statement 4:**

Choose one of the following options

| | |
|---|---|
| *a) I agree to deposit an electronic copy of my thesis (the Work) in the Bangor University (BU) Institutional Digital Repository, the British Library ETHOS system, and/or in any other repository authorized for use by Bangor University and where necessary have gained the required permissions for the use of third party material.* | |
| *b) I agree to deposit an electronic copy of my thesis (the Work) in the Bangor University (BU) Institutional Digital Repository, the British Library ETHOS system, and/or in any other repository authorized for use by Bangor University when the approved bar on access has been lifted.* | |
| *c) I agree to submit my thesis (the Work) electronically via Bangor University's e-submission system, however I opt-out of the electronic deposit to the Bangor University (BU) Institutional Digital Repository, the British Library ETHOS system, and/or in any other repository authorized for use by Bangor University, due to lack of permissions for use of third party material.* | |

*Options B should only be used if a bar on access has been approved by the University.*

**In addition to the above I also agree to the following:**

1. That I am the author or have the authority of the author(s) to make this agreement and do hereby give Bangor University the right to make available the Work in the way described above.
2. That the electronic copy of the Work deposited in the digital repository and covered by this agreement, is identical in content to the paper copy of the Work deposited in the Bangor University Library, subject to point 4 below.

3. That I have exercised reasonable care to ensure that the Work is original and, to the best of my knowledge, does not breach any laws – including those relating to defamation, libel and copyright.

4. That I have, in instances where the intellectual property of other authors or copyright holders is included in the Work, and where appropriate, gained explicit permission for the inclusion of that material in the Work, and in the electronic form of the Work as accessed through the open access digital repository, or that I have identified and removed that material for which adequate and appropriate permission has not been obtained and which will be inaccessible via the digital repository.

5. That Bangor University does not hold any obligation to take legal action on behalf of the Depositor, or other rights holders, in the event of a breach of intellectual property rights, or any other right, in the material deposited.

6. That I will indemnify and keep indemnified Bangor University and the National Library of Wales from and against any loss, liability, claim or damage, including without limitation any related legal fees and court costs (on a full indemnity bases), related to any breach by myself of any term of this agreement.

Signature: ……

Date : …….

# Acknowledgements

I would like to acknowledge The Higher Committee for Education Development in Iraq (HCED) for providing me with a Scholarship to study for a PhD in Chemistry for the academic years 2015–2019, which fully covered my tuition fees and my living expenses in UK and without which this work would not have been possible. I would also like to thank the Iraqi Ministry of Higher Education and Scientific Research (MOHESR)-University of Al-Nahrain for their support.

I have been fortunate to have such well admirable supervisors, Professor Igor F. Perepichka and Dr Juma'a R. Al-Dulayymi. Their enthusiasm and advice have encouraged me enormously throughout my research work. I am always thankful to them for being a part of their research group, for their constant guidance and supervision. Big thanks to my supervisors for always finding time to discuss my research work and show a new research direction. The four years research journey with my supervisors are memorable. My further acknowledgements are to Dr Patrick Murphy and Dr Vera Fitzsimmons-Thoss for their co-supervision as Research Committee members and their encouragement towards my research work. I am also thankful to Dr Alison Jones for all her assistance throughout the project. I really appreciated her support.

I would like to acknowledge my colleagues Srikanth Kommanaboyina, Mohammed Altahan, Zahraa Al-Taie, Shayma Ahmad, Chester Blackburm, Kenny Chan and all the PhD students on the 5$^{th}$ floor for some useful discussions and exchange of ideas. I also acknowledge the contribution of Bangor undergraduate project students Thomas Davies, James Durrant, Melissa Rowlands, Rachel Tweedy, Will Fenton, Toby Carty, and Karolis Kurmis with their short projects that have made the progress of my research faster. I am thankful to visiting students in the group Lars Kornek, Sarah Mzyk, and Eloise Testu for their help with some experimental work. My thanks to PhD student James Cooper for helping me to characterise the polymers using the GPC instrument in his group. I would like to extend my acknowledgement to the Staff members of the School of Natural Sciences. I would like to thank Dr David Hughes and Nicholas Welsby for running all of the mass-spec samples in this project. I would also like to acknowledge Dr Dmitry Yufit from the Department of Chemistry Durham University, for running the X-ray crystallography of the

monomers.

Finally and most importantly, I express deep gratitude to all my family members in Iraq and Bangor. Special thanks for my wife Zainab Al-Sudani for her constant encouragement and being so patient throughout my journey towards my PhD.

# List of Abbreviations

| | |
|---|---|
| AcOH | Acetic acid |
| AN | Acetonitrile |
| Ar | Argon |
| b.p. | Boiling point |
| B3LYP | DFT calculations using Becke functional with three-parameters Li-Yang-Parr correlated functional |
| bipy | 2,2'-Bipyridyl |
| br | Broad |
| **$Br_2F$** | 2,7-Dibromo-9,9-dioctylfluorene |
| **$Br_2S$** | 3,7-Dibromodibenzothiophene-*S*,*S*-dioxide |
| **$Br_2S$-$NO_2$** | 1-Nitro-3,7-dibromodibenzothiophene-*S*,*S*-dioxide |
| **$Br_2S$-$NH_2$** | 1-Amino-3,7-dibromodibenzothiophene-*S*,*S*-dioxide |
| **$Br_2S$-OH** | 1-Hydroxy-3,7-dibromodibenzothiophene-*S*,*S*-dioxide |
| **$Br_2S$-CN** | 1-Cyano-3,7-dibromodibenzothiophene-*S*,*S*-dioxide |
| **$Br_2S$-I** | 1-Iodo-3,7-dibromodibenzothiophene-*S*,*S*-dioxide |
| **$Br_2S$-F** | 1-Fluoro-3,7-dibromodibenzothiophene-*S*,*S*-dioxide |
| **$Br_2S$-R** | 1-Functionalised-3,7-dibromodibenzothiophene-*S*,*S*-dioxide |
| **$Br_2S$-OR** | 1-Alkoxy-3,7-dibromodibenzothiophene-*S*,*S*-dioxide |
| **$Br_2S$-SR** | 1-Alkylthio-3,7-dibromodibenzothiophene-*S*,*S*-dioxide |
| **$Br_2S$-$SO_2R$** | 1-Alkylsolfonyl-3,7-dibromodibenzothiophene-*S*,*S*-dioxide |
| BT | Benzothiadiazole |
| °C | Degrees Celsius |
| $CHBr_3$ | Bromoform ($CHBr_3$) |
| $CHCl_3$ | Chloroform ($CHCl_3$) |
| CIE | Commission Internationale de L`Eclairage, chromaticity diagram according to CIE 1931 colour space |
| $cm^{-1}$ | Wavenumbers |
| COD | 1,5-Cyclooctadiene |
| COSY | Correlation spectroscopy |

| | |
|---|---|
| CV | Cyclic voltammetry |
| δ | Chemical shift |
| d | Doublet |
| dd | Double doublet |
| DCM | Dichloromethane |
| DCMP | 4-(dicyanomethylene)-2-methyl-6-(*p*-dimethylaminostyryl)-4*H*-pyran |
| DFT | Density functional theory calculations |
| DHTS | 3,7-bis(4-hexylthiophen) dibenzothiophene-*S*,*S*-dioxide |
| Diox | Dioxane |
| DMABN | *N*,*N*-Dimethylaminobenzonitrile |
| DMF | *N*,*N*-Dimethylformamide |
| DMSO | Dimethyl sulfoxide |
| EA | Ethyl acetate |
| EDG | Electron donating group |
| $E_g$ | Band gap energy (of polymer) |
| EI | Electron impact |
| EL | Electroluminescence |
| $Et_2O$ | Diethyl ether |
| EWG | Electron withdrawing group |
| **F** | 9,9-Dioctylfluorene |
| FRET | Fluorescence resonance energy transfer (Förster resonance energy transfer) |
| GC-MS | Gas chromatography – mass spectrometry |
| GPC | Gel permeating chromatography |
| h | Hours |
| HOMO | Highest occupied molecular orbital |
| Hz | Hertz |
| iAmONO | Isoamyl (isopentyl) nitrite |
| IC | Internal conversion |
| ICT | Intramolecular charge transfer |
| IR | Infra-red |
| ISC | Intersystem crossing |
| ITO | Indium-tin oxide |
| *J* | Coupling constant |
| LCD | Liquid crystal display |

| | |
|---|---|
| LE | Local excited (state) |
| LED | Light-emitting diode |
| $LiAlH_4$ | Lithum aluminium hydride |
| lit. | Literature value |
| LUMO | Lowest unoccupied molecular orbital |
| m | Multiplet |
| M | Molar (moles per liter) |
| *m*CPBA | meta-Chloroperoxybenzoic acid |
| MeCH | Methylcyclohexane |
| Me | Methyl |
| min | Minute(s) |
| mL | Milliters |
| mmol | Millimol |
| $M_n$ | Number average molecular weight |
| MS | Mass spectrometry, mass spectrum |
| $M_w$ | Weight average molecular weight |
| m.p. | Melting point |
| MS(EI+) | Mass spectra (electron impact, positive mode) |
| *m/z* | Mass to charge ratio |
| NBS | *N*-Bromosuccinimide |
| NMR | Nuclear magnetic resonance |
| OFET | Organic field-effect transistor |
| OLED | Organic light-emitting diode |
| OPV | Organic photovoltaics |
| $Pd_2(dba)_3$ | Tris(benzylideneacetone)dipalladium(0) |
| PDI | Polydispersity index |
| PE | Petroleum ether (b.p. = 40–60 °C) |
| PEDOT:PSS | Poly(3,4-ethylenedioxythiophene):poly(styrenesulfonate) |
| Ph | Phenyl |
| **PF** | Polyfluorenes |
| **PF8** | Poly(9,9-dioctylfluorene) |
| **p(S-R)** | 1-functionalised dibenzothiophene-*S*,*S*-dioxide homopolymers |
| **p(S-OR)** | 1-Alkoxydibenzothiophene-*S*,*S*-dioxide homopolymers |
| **p(S-SR)** | 1-Alkylthiodibenzothiophene-*S*,*S*-dioxide homopolymers |

| | |
|---|---|
| **p(S-$SO_2$R)** | 1-Alkylsulfonyldibenzothiophene-*S*,*S*-dioxide homopolymers |
| **p(F/S)-y** | 9,9-Dioctylfluorene/dibenzothiophene-*S*,*S*-dioxide co-polymers |
| **p(F/S-R)-y** | 9,9-Dioctylfluorene/1-functionalised dibenzothiophene-*S*,*S*-dioxide co-polymers |
| PhCl | Chlorobenzene |
| $PhCl_2$ | Dichlorobenzene |
| PhCOMe | Acetophenone |
| PhCN | Benzonitrile |
| PhOMe | Anisole |
| PL | Photoluminescence |
| PLED | Polymer light emitting diode |
| PLQY | Photoluminescence quantum yield |
| PPV | Poly-*p*-phenylenevinylene |
| $R_f$ | Retention factor (in TLC) |
| r.t | Room temperature |
| **S** | Dibenzothiophene-*S*,*S*-dioxide |
| TADF | Thermally activated delayed fluorescence |
| TCNQ | Tetracyano-*p*-quihodimethane |
| $T_d$ | Thermal decomposition |
| TGA | Thermogravimetric analysis |
| THF | Tetrahydrofuran |
| TLC | Thin layer chromatography |
| TMS | Tetramethylsilane |
| Tol | Toluene |
| TTF | Tetrathiafulvalene |
| UV | Ultraviolet |
| UV-Vis | Ultraviolet-visible electron absorption spectra (spectroscopy) |
| VR | Vibrational relaxation |
| WPLED | White-light polymer light-emitting diodes |
| $\lambda_{abs}$ | Maxima of the bands in electron absorption spectra |
| $\lambda_{PL}$ | Maxima of the bands in photoluminescence spectra |
| $\Phi_{PL}$ | Photoluminescence quantum yield |

# Abstract

Organic electronics is a rapidly developing field of both science and technology. Semiconducting conjugated polymers are performing an important role in the progression of optical electronic device applications. Photoluminescent and electroluminescent conjugated polymers have made profound scientific and technological developments in a wide range of light-emitting applications.

This thesis deals with the design, synthesis and study of a novel class of 1-functionalised dibenzothiophene-*S*,*S*-dioxide monomers and then uses them to synthesise the first novel soluble 1-functionalised dibenzothiophene-*S*,*S*-dioxide homopolymers, and co-polymers with fluorene units.

A series of novel 1-(alkoxy, alkylthio, alkylsulfonyl)-dibenzothiophene-*S*,*S*-dioxide monomers (**$Br_2$S-R**) **(I)** with various solubilising alkyl chains (linear or branched) have been synthesised and fully characterised by $^{1}H$ and $^{13}C$ NMR spectroscopy and mass spectrometry.

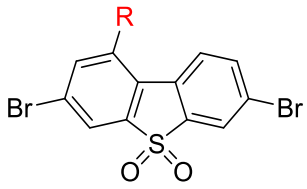


**$Br_2$S-R**

**(I)**

Polymerisation of these novel monomers *via* a Ni-mediated Yamamoto C–C homo coupling polycondensation has been employed to create the first novel soluble electron deficient homopolymers **p(S-R) (II)** based on the dibenzothiophene-*S*,*S*-dioxide moiety **p(S-R) (I)**. The photo physical studies of these polymers demonstrated an interesting phenomenon in that the polymers were blue emitting in solution and green emitting in the solid state under excitation. Thus, these studies confirm that such 1-functionalised poly(dibenzothiophene-*S*,*S*-dioxides) might be promising materials for organic electronics.

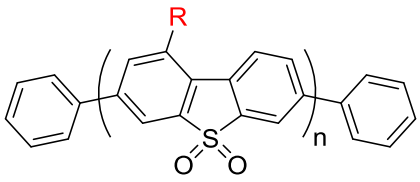


**p(S-R)**

**(II)**

Additionally a novel series of **p(F/S-R)-y (III)** co-polymers incorporating electron-withdrawing and donating groups (**R = CN, $SO_2Me$, $NO_2$, F, SMe, OMe**) onto the dibenzothiophene-*S*,*S*-dioxide moiety were prepared, to understand the structural effect of the polymer chain on the interplay between the local excited (LE) and intramolecular charge transfer (ICT) states. The pronounced donor-acceptor interaction between the **F** and **S-R** units in the excited state led to an increased contribution of ICT emission even at low concentrations of **S-R** units (~5%) in the co-polymer chain. The dual LE/ICT emission from the materials shifts their photoluminescence from deep blue to light blue, greenish-white and a purely green colour. This phenomenon could be useful in the design of highly efficient materials for white light-emitting organic light–emitting devices (WOLED) for solid state lighting applications.

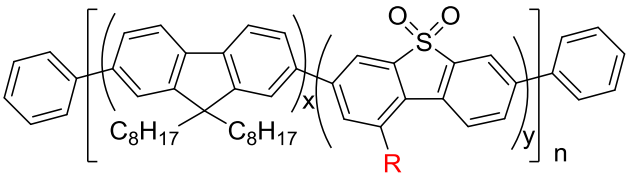


**p(F/S-R)-y**

**(III)**

# Presentations and Awards

The following presentations were based on work described in this thesis:

1. The 33rd Young Scientist Symposium hosted by The Royal Society of Chemistry, Bangor University on 22nd June 2018, presentation of a poster and talk.
2. The 32nd Annual Young Scientist Symposium hosted by The Royal Society of Chemistry, Bangor/Glyndwr at Wrexham Glyndwr University on 3rd July 2017, presentation of a poster.
3. Emerging Areas of Photochemistry: From Fundamentals to Applications hosted by Solar Fuels Network at the University of York – United Kingdom on 16-17 March 2017, and contributed to the conference by presenting a poster.
4. The Science Around Us hosted by The Royal Society of Chemistry at The University of Sheffield on 9th September 2016, and contributed to the conference by presenting a poster.
5. The 31st Annual Young Scientist Symposium hosted by The Royal Society of Chemistry, Bangor/Glyndwr at School of Chemistry, Bangor University on 19th July 2016, presentation of a poster.

The following awards were based on work described in this thesis:

1. The first poster prize for the 31st Annual Young Scientist Symposium Bangor/Glyndwr at School of Chemistry, Bangor University, on 19th July 2016.
2. The first poster prize for the 32nd Annual Young Scientist Symposium' Bangor/Glyndwr at Wrexham Glyndwr University on 3rd July 2017.
3. The first prize for the best oral presentation, the 33rd Young Scientist Symposium, Bangor University on 22nd June 2018.
4. The Andrew Johnstone Prize 2018, presented by the School of Chemistry, Bangor University. The Prize is awarded to a third-year Chemistry PhD student who presents the best lecture based on her/his work.

# CHAPTER 1

# Introduction Conjugated Molecular and Polymeric Materials

## 1.1 Organic electronics

Organic electronics is a multidisciplinary field, which includes organic chemistry, material science, physics and engineering. It deals with the synthesis of small organic molecules, oligomers and polymers with specific electrical and optical properties that make them suitable for application as active layers in electronic devices, studies of physical phenomena in such materials and the fabrication of electronic devices from them. In contrast to inorganic materials, most organic compounds are insulators. From the 1970's some new organic materials have been developed, which posses semi-conductive or even electrically conductive properties, characteristic of inorganic compounds (semiconductors based on Si and other elements, metals). This has opened a new field in material science, which is now called "organic electronics".

In 1973, Ferraris *et al.* discovered the first organic electrically conductive material with metallic type conductivity ("synthetic metal") based on a charge transfer complex between a tetrathiafulvalene (**1.1**) molecule, as an electron donor, and tetracyano-*p*-quihodimethane (**1.2**), as an electron acceptor (see **Figure 1.1**).[1]

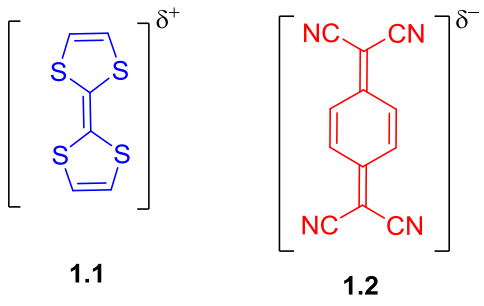


**Figure 1.1:** Structures of the compounds **1.1–1.2**.

In 1975, Shirakawa's student was preparing a polymerisation reaction and accidently added a huge amount of the catalyst (Ziegler–Natta), about a 1000 times excess. To their surprise, the product was a silvery elastic film and not a black powder as expected. Shirakawa shared the outcome with Heeger and MacDiarmid and they proved that the doping of poly acetylene with halogens increases the conductivity of polyacetylene 10 million times, to a level similar to that of silver or copper, compared to undoped polyacetylene (see **Figure 1.2 b**). This discovery, first published in 1977[2] represented a breakthrough in this field of research, which started the era of "plastic electronics", i.e. organic electronics based on organic conjugated polymers. In 2000, these three scientists were awarded the Nobel Prize for Chemistry for their discovery and development of electrically conductive and semiconductive polymers and the physical phenomena associated with their functions.[3,4,5]

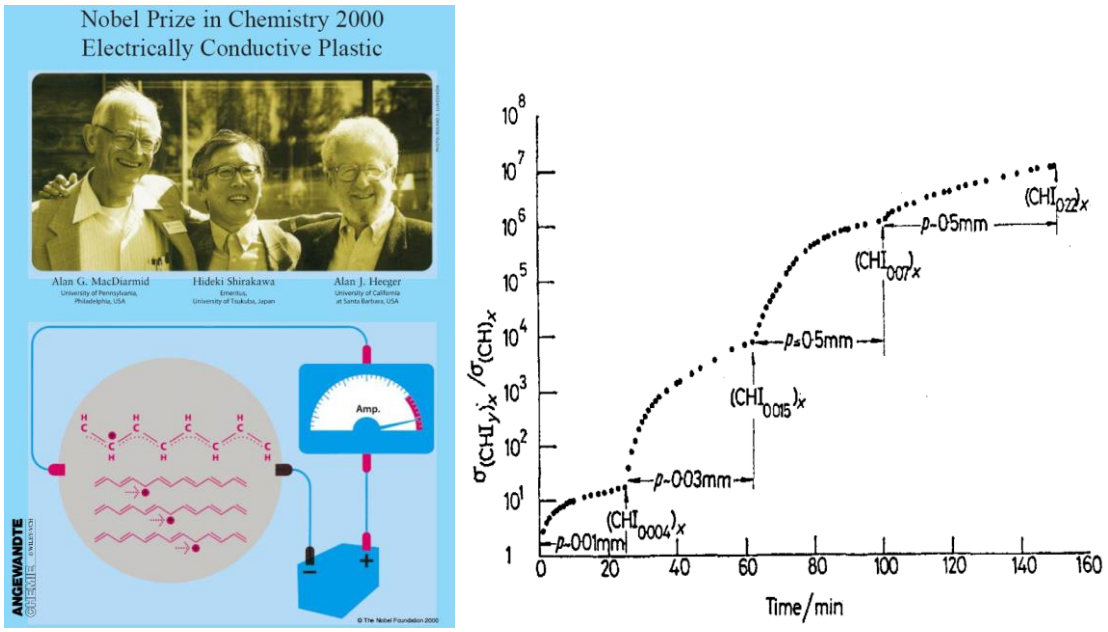


**a)** **b)**

**Figure 1.2:** a) Nobel Prize in chemistry 2000 conductive polymer (from an issue of *Angew. Chem.* with published Nobel Lectures).[3,4,5] b) An increase of the relative conductivity of *trans*-polyacetylene, $(CH)_n$, as a function of time at fixed iodine vapour pressure at room temperature (the initial room temperature conductivity was $3.2\times10^{-6}$ $\Omega^{-1}$ $cm^{-1}$).[2]

Over the last 2-3 decades, a large amount of research has been done to develop new molecular and polymeric organic materials with wonderful electronic and photo-/electro-luminescence properties.[6,7,8,9,10,11] The major advantages of organic semiconductive materials are that they are cheaper, lighter and more flexible than inorganic materials and their properties can be easily tuned by chemical functionalisations and modifications.[12] Electrical conductivity of such organic conjugated polymers can be varied over a wide range, from$10^{-6}$ to $10^{2}$ S $cm^{-1}$ approaching the conductivity of metals (**Figure 1.3**).

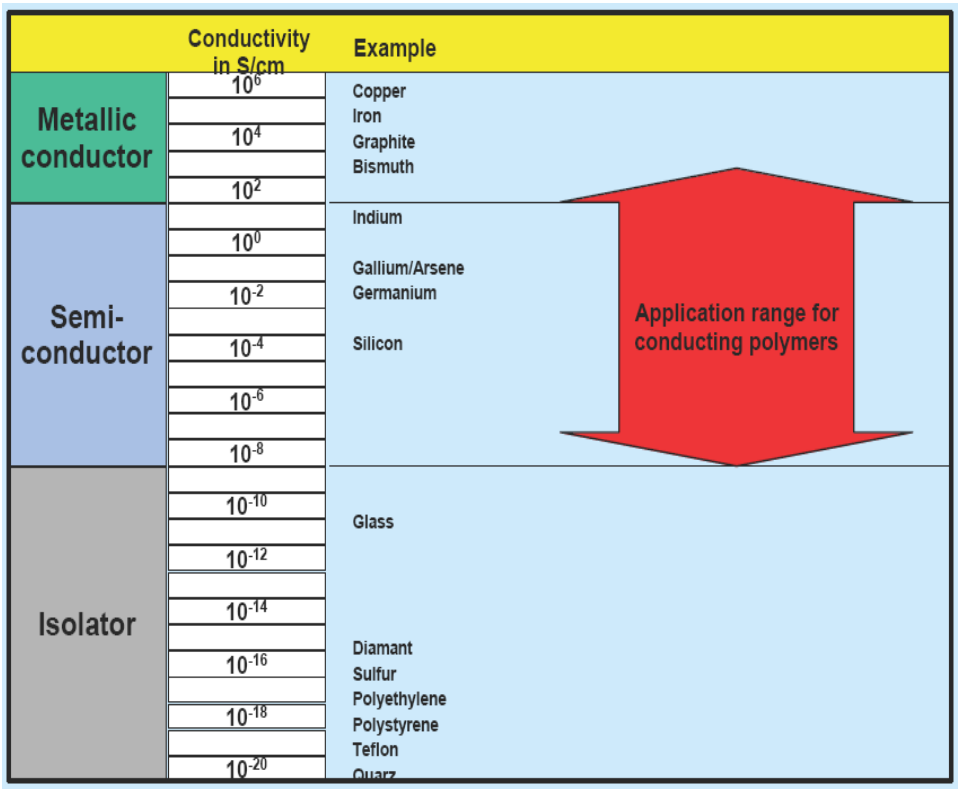


**Figure 1.3:** Organic semiconductive polymers with metallic type conductivity.[5]

## 1.2 Conjugated polymers

Conjugated polymers are a special class of polymers that can be electrically conductive or semiconductive. Their main chain consists of an alternation of double and single bonds. All carbon atoms in the backbone have $sp^2$ hybridisation, i.e. have an electron in the π orbitals allowing delocalisation of electrons along the backbone. The degree of π delocalisation depends on the structure of the monomeric building blocks, the planarity between the

monomers, and on some other factors, which all together define the effective conjugation length of the polymer chain (i.e. the degree of the excitation delocalisation in the neutral state of the polymer and the degree of polaron (radical cation/anion) delocalisation in p- and n-doped states of the polymer). The conjugation length of the polymer is the number of monomer units over which the $\pi$–$\pi^*$ molecular orbitals are delocalised along the chain. For example, the conjugation length in polyfluorene is *ca.* 11-12 fluorene units.[13] Otsubo *et al.* have published an interesting paper on specifically designed planar polythiophene which reached a conjugation length of *ca.* 96 thiophene units.[14] In their undoped (neutral) state, conjugated polymers are either insulators or semiconductors, with electrical conductivity between $10^{-10}$ and $10^{-5}$ S $cm^{-1}$. Their conductivity can be increased by several orders of magnitude by doping the polymers with electrons or holes, reaching the values of 1 to $10^4$ S $cm^{-1}$. The concept of doping distinguishes the conductive or semiconductive polymer from all other types of polymers.[5]

Conjugated polymers can be doped by redox electrochemical reactions with partial removal of electrons (oxidation, p-doping) or addition of electrons (reduction, n-doping). The doping can also be achieved by chemical methods. Chemical p-doping can be performed by reacting an oxidising agent, e.g. halogens (iodine, bromine) with the polymer to remove an electron from the $\pi$-orbitals and creating a delocalised hole (**Figure 1.4**). This leads to the charged state in which easy transfer of the delocalised electrons along the conjugated chain is observed through overlapped p orbitals with very little energy input. On the other hand, n-doping is adding an electron to the conjugated polymer chain by a reduction reaction (e.g. with an alkali metal such as sodium). This also leads to easy movement of electrons along the conjugated $\pi$ orbitals. The conjugated polymer can also be doped by the acid/base chemistry doping method and photo-doping method.[4] Some major common classes of conjugated polymers based on different aromatic / heteroaromatic and / or alkene / alkyne building blocks are shown in **Figure 1.5**.

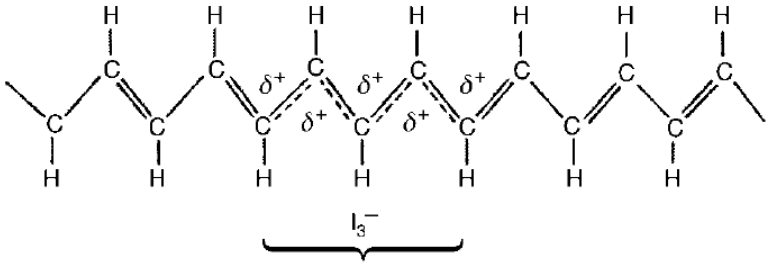

**Figure 1.4:** Chemical p-doping of polyacetylene with iodine producing positive polaron on the polymer chain.[4]

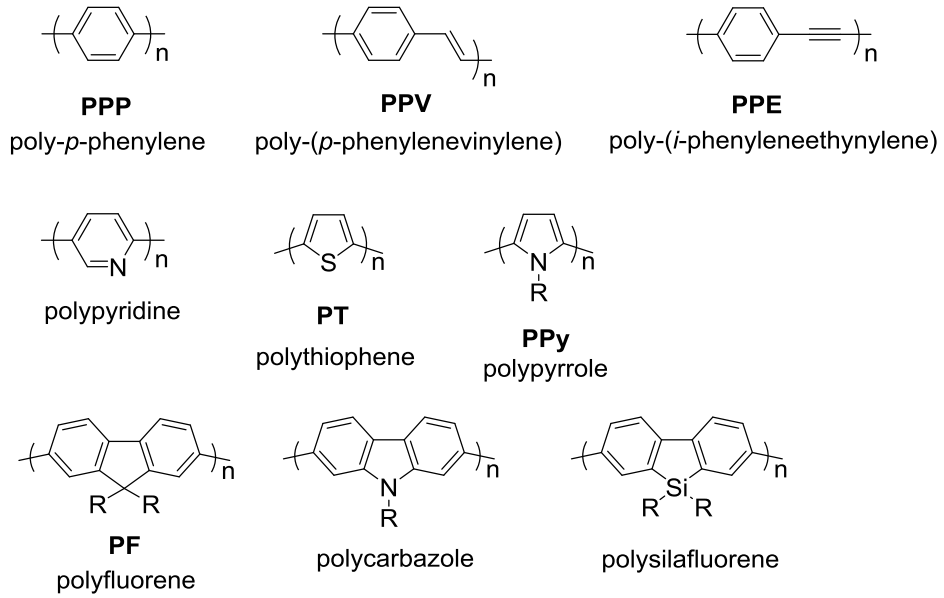


**Figure 1.5:** Examples of some well-known conjugated polymer building blocks.

## 1.3 Photophysical processes

The procedure of exciting atoms or molecules by absorption of light (photoexcitation) and release of the energy from the excited state through radiative (fluorescence or phosphorescence) or non-radiative processes without any participation of the chemical is known as photophysics. Thus, photophysics is the study of absorption and emission processes, and their investigation under different environmental conditions, all in an attempt to clarify how the materials perform. When an atom or molecule is photoexcited to higher energy states $S_1$, $S_2 \ldots S_n$ the transition happens in too short a time ($10^{-15}$ s) according to the Franck-Condon principle. Then the excited higher energy state electrons relax to the lower

excited singlet states ($S_1$) by loss of the energy through internal conversion (IC) and vibrational relaxation (VR) within the state. The photon emission happens by transition of the electron from the excited singlet state $S_1$ or triplet state $T_1$ to the ground state ($S_0$) according to Kasha's rule. [15] The deactivation paths of an excited molecule are divided into two main types of processes. The first one is a radiative process, which are fluorescence, and phosphorescence as a radiative energy transfer. Second, the non-radiative process includes the vibrational relaxation (VR), internal conversion (IC), intersystem crossing (ISC), and fluorescence resonance energy transfer (FRET) as shown in the Jablonski diagram (see **Figure 1.6**).[16]

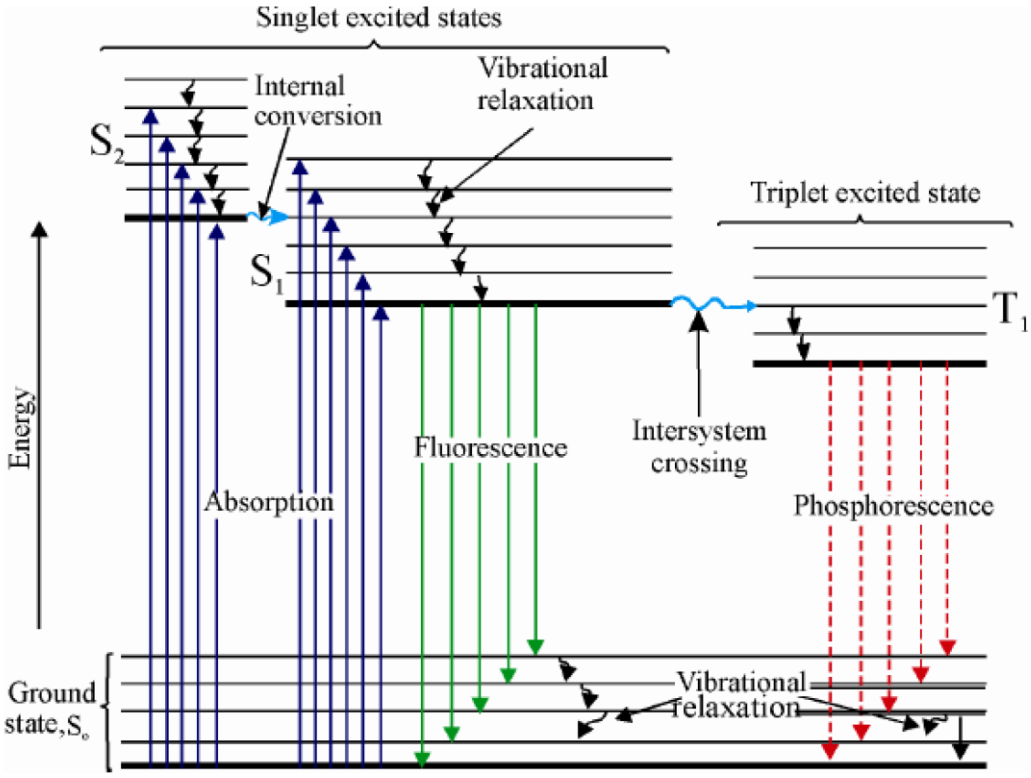


**Figure 1.6:** The Jablonski diagram showing the radiative and non-radiative processes.[16]

### 1.3.1 Singlet and triplet states

The absorption of photons leads to two types of electronic orbital configuration states, which are the singlet and triplet states. In the singlet state, the electron spins are paired anti-parallel, so the state has no spin magnetic moment, which stays as a single state in the existence of a

magnetic field. While in the triplet state, the electron spins are unpaired, *i.e.* parallel, and the state has a net spin magnetic moment and splits into the three quantised states (**Figure 1.7**). The excited triplet state has lower energy compared to the excited singlet state according to Hund's rule, owing to the repulsive spin-spin interaction between the electrons of the same spin orientation.

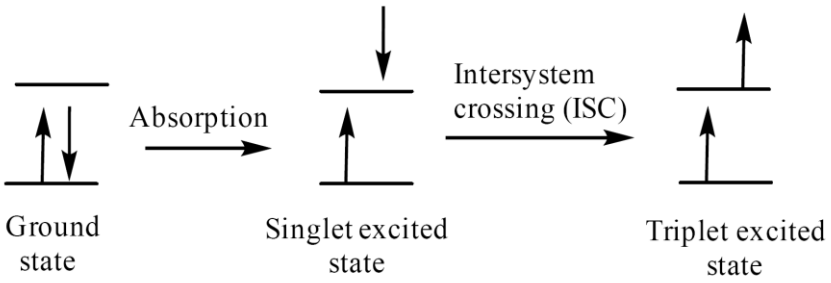


**Figure 1.7:** Singlet and triplet excited states

### 1.3.2 Non-radiative processes

After the molecule is excited from the ground state ($S_0$) to the excited stated ($S_n$), it comes back to the ground state through radiative and non-radiative processes. This section is going to focus on the non-radiative deactivation routes. The main non-radiative processes paths from the excited states of the molecule are vibrational relaxation (VR), internal conversion (IC), intersystem crossing (ISC), and fluorescence resonance energy transfer (FRET).

**1) Vibrational relaxation (VR)**: In an electronic excitation process, the electrons in a molecule are excited to a number of higher energy vibrational levels. Then, the molecule rapidly loses some energy to the surroundings through collisions with other molecules, in the form of non-radiative process. After that, it relaxes to the lowest excited singlet state $S_1$ (see **Figure 1.6**). The vibrational relaxation process is very quick, within a lifetime less than $10^{-12}$ s, which is significantly smaller than the lifetime of the lowest excited singlet state ($S_1$), which is about $10^{-8}$ s.

**2) Internal conversion (IC):** This is an intermolecular non-radiative transition process between the electronic energy states of same spin multiplicity (see **Figure 1.6**).[17] The rate constant of the IC from $S_1$ to $S_0$ is between $10^{-9}$ and $10^{-7}$ s compared to the higher energy states such as from $S_2$ to $S_1$ the rate constant is much shorter between $10^{-14}$ and

$10^{-11}$ s. Furthermore, it has been demonstrated that IC efficiency reduces with an increase of energy band gap between the $S_1$ and $S_0$ states.[18] It is also possible to see an internal conversion between the $T_2$ and $T_1$ states for some molecules.[19]

**3) Intersystem crossing (ISC):** This is a non-radiative transition process, where the transition happens between different spin multiplicity states, for example from $S_1$ to $T_1$ (**Figure 1.6**).[17] Because of the existence of a big energy gap between the excited singlet state $S_1$ and the ground state $S_0$, the straight non-radiative transition from $S_1$ to $S_0$ is difficult. Therefore, there are two ways to reach the ground state level $S_0$, either through fluorescence transition or *via* crossover to the triplet state through ISC (radiativeless process). Due to the energy of $T_1$ being lower than $S_1$ the probability of transition from $S_1$ to $T_1$ is greater than the transition from $T_1$ to $S_1$.

**4) Fluorescence resonance energy transfer (or Förster resonance energy transfer) (FRET):** This is the distance interactions between two light sensitive fluorescent molecules in the excited states. This process happens when two molecules donor and acceptor or one molecule that holds both donor and acceptor parts are excited by light. Some of the energy in the excited stated will transfer through the non-radiative process FRET from the donor to the acceptor. This is due to the donor emission overlaping with the acceptor absorption so some of the energy will be re-absorbed by the acceptor without emission of a photon. This can then relax to the ground state by radiative or non-radiative processes.

### 1.3.3 Radiative processes

Luminescence is the emission of light form the molecule when the electron relaxes from the higher energetic state to the ground state with emission of a photon. After the molecule absorbs the light the transfer from the ground state $S_0$ to the excited state $S_n$ happens followed by relaxation to the ground state through loss of energy by a radiative process with the expulsion of a photon. There are many types of luminescence depending on the type of excitation of the substance. For example, photoluminescence is the emission of light after excitation of the substance by a photon; electroluminescence is the emission of light after excitation of the molecule by applying a voltage; and chemiluminescence is the emission of light due to a chemical reaction. Other types of luminescence include bioluminescence, sonoluminescence, *etc*.

**Fluorescence**: By photoexcitation, the electrons in the ground state of a molecule are excited to one of the higher vibrational levels in the excited electronic state. This excited state is usually the first excited singlet state $S_1$. Molecules in higher vibrational levels of the excited state (such as $S_2$, $S_3$) quickly relax to the lowest level of the excited state ($S_1$) by vibrational relaxation and internal conversion. Fluorescence takes place when the electron transfers from the lowest excited singlet state $S_1$ to the ground state $S_0$ with the emission of a photon (**Figure 1.8**). This kind of transition is quantum mechanically "allowed" (spin state allowed). The fluorescence usually occurs from aromatic molecules and its lifetime is usually $10^{-8}$ s. Investigation of the Jablonski diagram (see **Figure 1.6**, **Page 6**) shows that the energy of emission is lower than the energy of absorption, therefore, fluorescence usually takes place at longer wavelengths. The difference between the maximum absorption and emission is called the Stokes shift according to the first observation of this phenomenon by G. Stokes in 1852 at the University of Cambridge.[20]

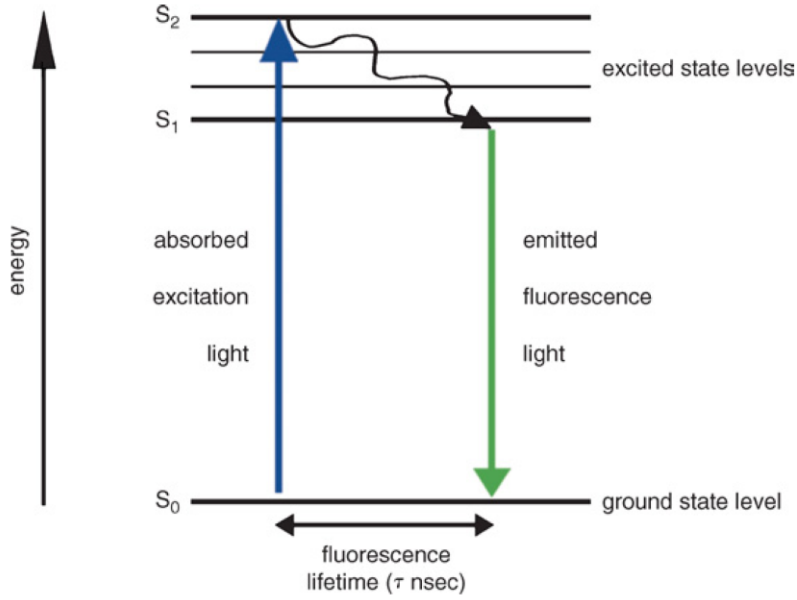


**Figure 1.8:** Jablonski diagram (fluorescence emission).[21]

**Phosphorescence:** is a slower transition process compared to the fluorescence process, its lifetime is usually from $10^{-4}$ to $10^{1}$ s. Phosphorescence takes place when the electron transfers from the excited triplet state $T_1$ (formed by ISC transition from the $S_1$ state) to the ground state $S_0$ with the emission of a photon. The straight transition from the

$S_0$ ground state to the $T_1$ excited state is impossible, due to it being a spin forbidden process. Since the lifetime of the $T_1$ state is longer than that of the $S_1$ state and the relaxation $T_1$ to $S_0$ is slower, the energy level of the $T_1$ state is lower than that of the $S_1$ state. Therefore, the phosphorescence happens at a longer wavelength compared to fluorescence. Phosphorescence displays the typical feature of slow emission where the emission carries on after the excitation source is detached (see **Figure 1.9**).

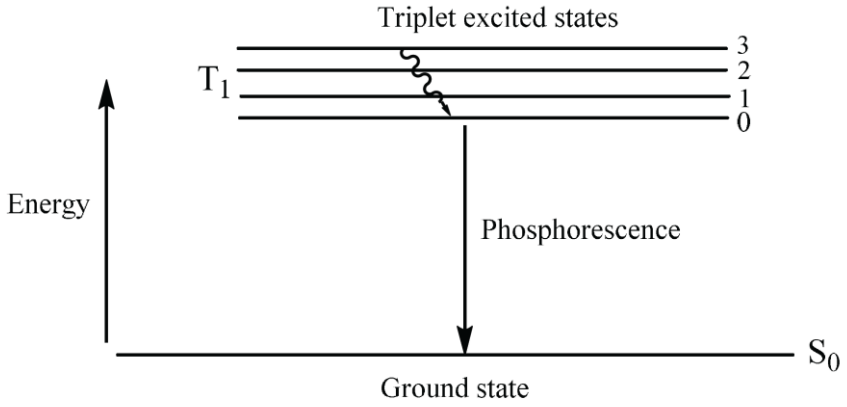


**Figure 1.9:** Jablonski diagram (phosphorescence emission).

### 1.4 Applications of conjugated polymers

In the past two decades, conjugated polymers have found a wide range of applications in the field of electronics.[22,10] In 1989 Friend *et al.*, at the Cavendish Laboratory in Cambridge, discovered that a thin film of poly(*p*-phenylenevinylene) (PPV), when sandwiched between two electrodes and a voltage applied, started to emit a green light through electroluminescence effect (conversion of the energy of electrons into the energy of photons).[23,24] This discovery opened a new era of electroluminescent organic materials for use in a new generation of displays, screens and light-emitting sources. Since then, conjugated polymers have been widely studied as a new class of promising materials in a range of electronic applications such as organic light emitting diodes (OLEDs),[30] photovoltaic devices,[25] transistors, batteries, and photo-sensors.[8]

According to development in OLED and its wide range of applications in full colour displays (**Figure 1.10**), people need to study the molecules which emit the three primary

colours (red, green, and blue) and white colour.[26,27] Materials emitting a blue colour are still a challenge because materials emitting red and green colours are more stable due to the low band gap (HOMO-LUMO) and their slower degradation during the device operation.[28,29]

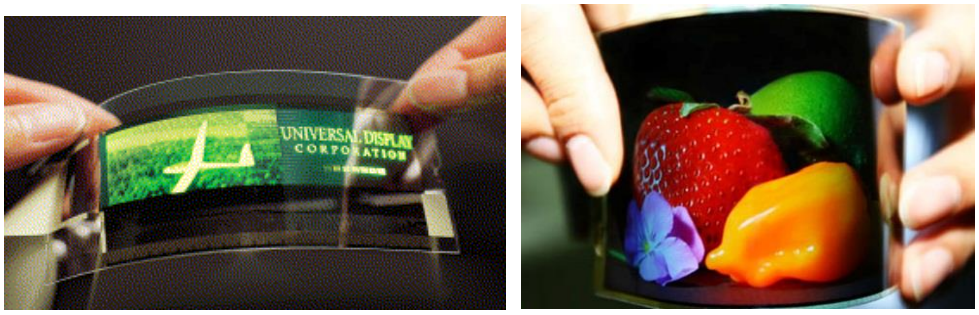


**Figure 1.10:** Flexible displays.

### 1.4.1 Organic Light Emitting Diodes (OLEDs)

OLEDs consist of a thin film of organic semiconductors sandwiched between two electrodes (e.g. indium-tin oxide as an anode and magnesium, calcium, barium or aluminium as a cathode). One of the electrodes should be transparent, and the electricity is applied to emit light as shown in **Figure 1.11**.[30] On applying the electricity, the device starts to emit the light with an energy close to the band gap of the material in the light-emitting layer. The advantages of OLED technology is that it does not require a white-light background panel as in LCD, but the material emits the light *via* the application of a small current through the material. Nowadays, people have OLEDs (2 to 5 inch) in many devices for daily use such as mobiles, smartphones, tablets, car audio and video systems, cameras *etc*. There are also many companies, which deal with the production of devices based on OLEDs, for example Sony, LG, Philips, Samsung, *etc*. Other advantages of OLEDs are their faster response times compared to LCD, lower power, higher image quality, high brightness and contrast, lower weight and lower prices *etc*. Flexibility of the devices represents the most important advantages of OLEDs.

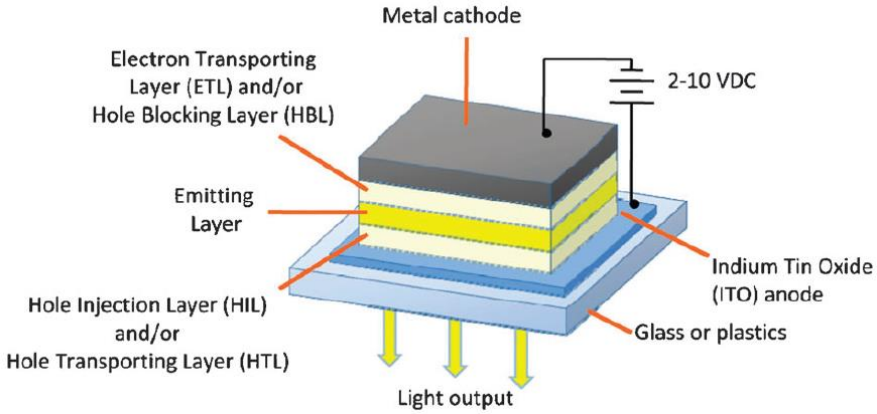


**Figure 1.11:** Schematic diagram of OLED.[30]

## 1.5 Polyfluorenes

Polyfluorenes (**1.3**) are considered as one of the most important common conjugated polymers. The possibilities of structural alterations and property relationships of homo and co-polymers of polyfluorenes made them very attractive as unique functional materials.[31,32] Fluorene is a polycyclic aromatic molecule and it is called fluorene because it has violet fluorescence. The two hydrogen atoms at position 9 are weakly acidic and can be easily substituted with e.g. alkyl groups which allows an increase in the solubility of the compound without affecting the photoluminescence properties and planarity of the polymer structure.[33,34] Fluorene undergoes electrophilic substitutions at position 2 and 7, allowing easy functionalisation through these conjugated sites to access fluorene-based conjugated polymers (**Figure 1.12**).

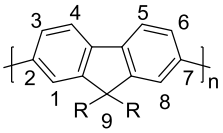


**1.3**

**Figure 1.12:** Polyfluorene showing the IUPAC enumeration of carbon atoms in the fluorene moiety.

Monomers for the synthesis of poly(9,9-dialkylfluorenes) **PF8** can be prepared either by bromination of fluorene at the 2,7-positions followed by alkylation at position 9 or by

alkylation of the 9-position first followed by bromination of the 2,7-positions, see **Scheme 1.1**.[1] Such monomers, **1.6**, can then be polymerised by different chemical methods.

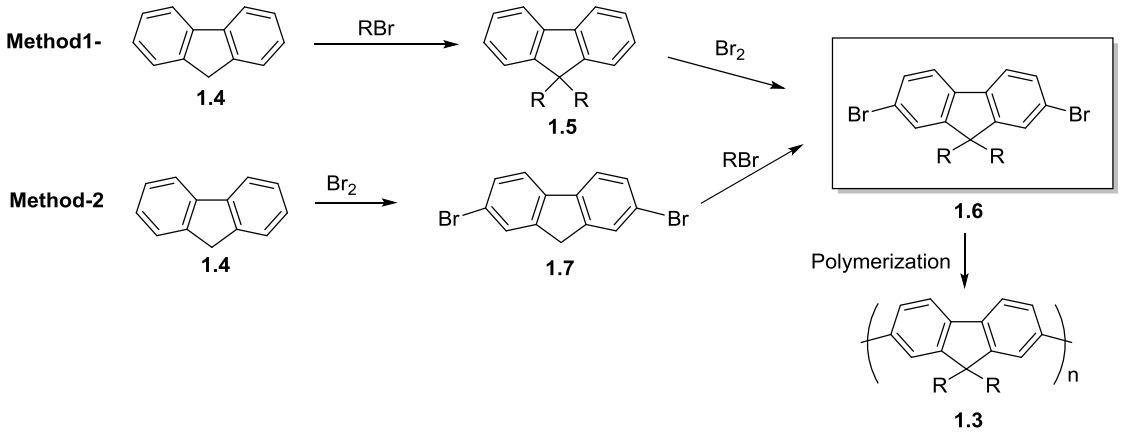


**Scheme 1.1:** Synthesis of dialkylfluorene monomer by two common methods and its polymerisation.[33]

There are many literature methods which describe the synthetic procedures to obtain poly(9,9-dialkylfluorenes).[35,36,37,38] The first one was investigated by Yoshino *et al.*[39] *via* oxidative polymerisation of 9,9-dihexylfluorene (**1.5)** by anhydrous $FeCl_3$ in chloroform, which however gave a poor quality polymer (**Scheme 1.2**).[40]

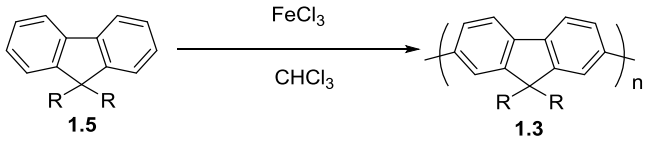


**Scheme 1.2:** Synthesis of polymer **1.3** by oxidative coupling of **1.5**.[40]

Nowadays, the two most widely used procedures for the synthesis of polyfluorenes (both under laboratory conditions and in industry) are the Yamamoto Ni(0) mediated coupling polymerisation with $Ni(COD)_2$/cyclooctadiene (COD)/bipyridyl(bipy) in DMF/toluene,[41] and the Suzuki Pd-catalysed coupling polymerisation (**Scheme 1.3**).[42] The advantages of Yamamoto's polymerisation is obtaining high molecular weight polymers using a simple and shorter process (except for the dry and oxygen free atmosphere).

However, the main disadvantage of this reaction is the use of the quite expensive $Ni(COD)_2$. On the other hand, Suzuki's coupling polymerisation requires more steps to prepare the monomers for polymerisation, but it is cheaper (**Scheme 1.3**).[43]

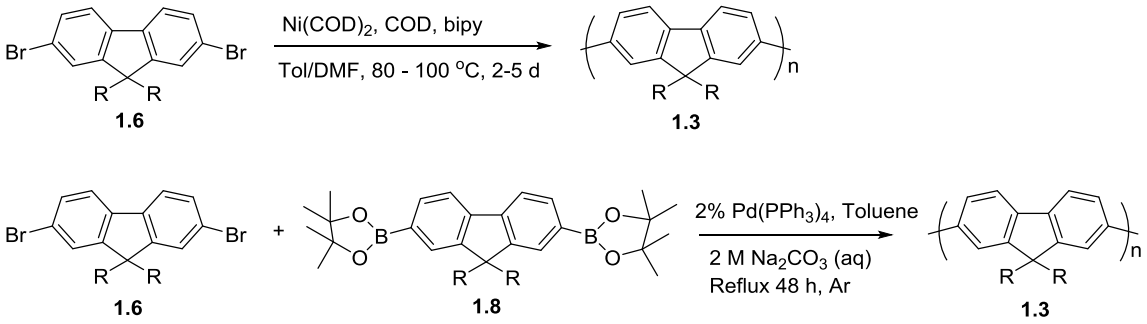


**Scheme 1.3:** Synthesis of polymers **1.3** by Yamamoto's polymerisation of monomer **1.6** and by Suzuki coupling polycondensation of **1.6** with **1.8**.[43]

Poly(9,9-dialkylfluorene) absorbs light at 385–390 nm (in solution), which refers to $\pi$–$\pi^*$ electronic transition. There is about a 5–10 nm red shift of this band in the solid state. Poly(9,9-dialkylfluorenes) emit in the blue region and show three vibrionic peaks at 418, 442, and 472 nm (**Figure 1.13**).[44,41] The photoluminescence quantum yields (PLQY) of polyfluorenes are very high, ~80% in solution and ~20–40% in the solid state.[45]

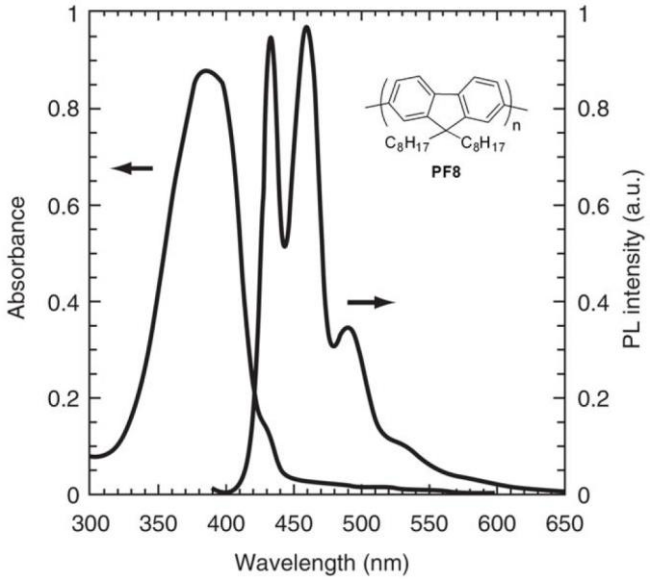


**Figure 1.13:** Absorption and emission spectra of poly(9,9-dioctylfluorene), **PF8**, in films.[50]

Janietz *et al.* determined the ionization potential (IP = –5.8 eV, related to HOMO energy level) and the electron affinity (EA = –2.12 eV, related to LUMO energy level) of poly(9,9-dioctylfluorene)[46] by cyclic voltammetry that gives the band gap for the polymer of 3.68 eV (**Figure 1.14**). The electrochemically measured band gap is somewhat higher than the optical band gap estimate from the onset of polymer absorption (~430 nm = 2.9 eV), however it is not surprising as these two methods actually measure slightly different physical parameters and such differences are often observed in conjugated polymers.

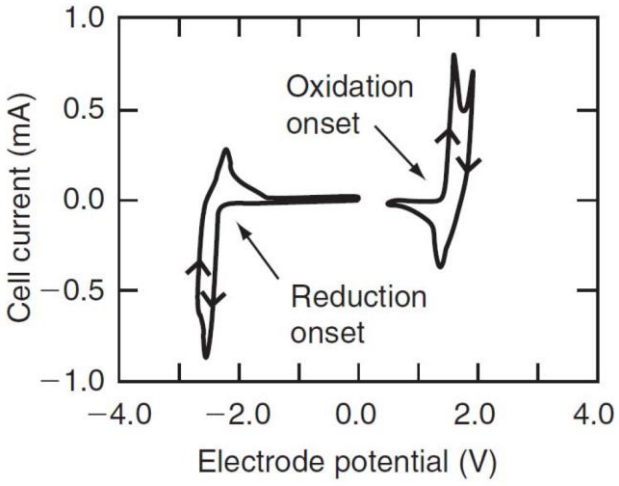


**Figure 1.14:** Cyclic voltammetry of **PF8** in thin films (potentials are vs Ag/AgCl reference electrode).[46]

However, defects in the polyfluorene structure can appear during synthesis, workup of the material or during its operation in devices. One of the main problems is that the emission of polyfluorenes is red shifted to longer wavelengths with time. The colour instability was observed in device operation with time, so the colour of emission is changed from purely blue to blue-greenish and then to green, with an increase in contribution of a new emission band at ~2.2–2.4 eV ($\lambda_{PL}$ ~535 nm). This band is called a ‘green band’ or ‘g-band’ (**Figure 1.15**).[47]

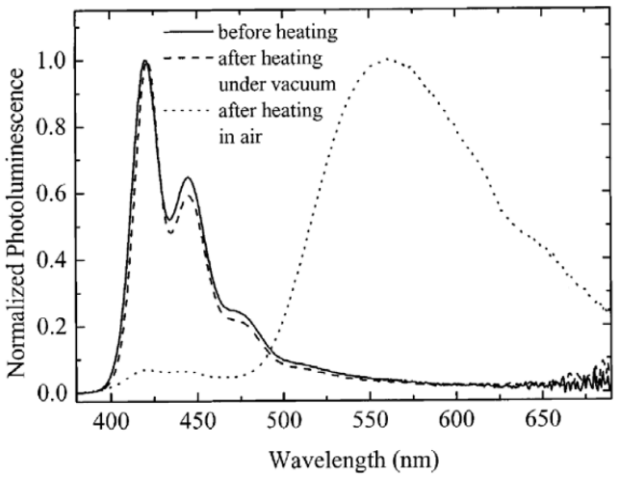


**Figure 1.15:** PL emission spectra of **PF8** before and after thermal annealing of the polymer film at 200 °C in ultra-high vacuum ($10^{-4}$ mbar) and after annealing on air (the last one quickly results in disappearance of the blue emission from **PF8** and an appearance of new green emission band).[47]

Originally, this phenomenon was attributed to the formation of the excimers (excited state dimers) in polyfluorenes and an emission from the lower energy state of the excimers.[48,49] However, later (in 2003), Moses *et al.* proved that this green emission is due to the oxidative formation of a keto group (C=O) at position 9 which leads to long wavelength emission from the fluorene-fluorenone charge transfer state (**Scheme 1.4**).[50]

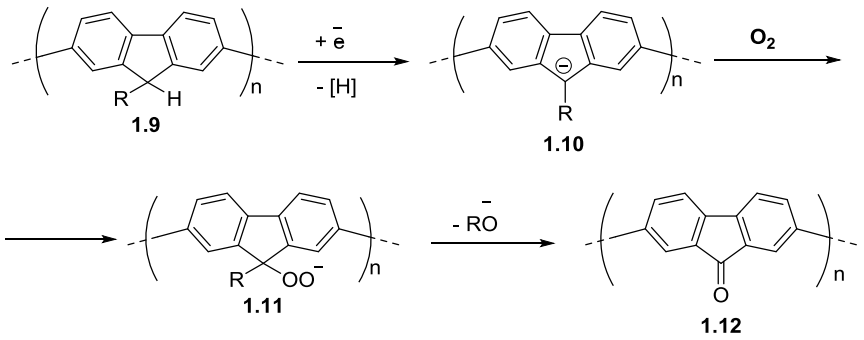


**Scheme 1.4:** Formation of keto defects on the polyfluorene chain. While it can occur on the dialkylfluorene moieties as well, the oxidation is most efficient on traces of monoalkylated fluorene sites presented in the polymer (even in amounts of <0.1%).[50]

Poly(9,9-dialkylfluorene) co-polymers prepared with other conjugated building blocks can emit at all wavelengths of the visible region. Leclerc *et al.* described the colour emitting tuning of fluorene co-polymers with thiophenes, phenylene, and phenylenevinylene segments (**Figure 1.16**).[51,52,53] They showed that changing the nature of the co-monomers leads to a change in the band gap of the polymers thus tuning the emitting colours to the entire visible spectrum. Therefore, polyfluorenes are considered as promising blue emitting polymers and many researchers have been using them to fabricate electronic devices such as polymeric light emitting diodes (PLEDs).[54,55,56]

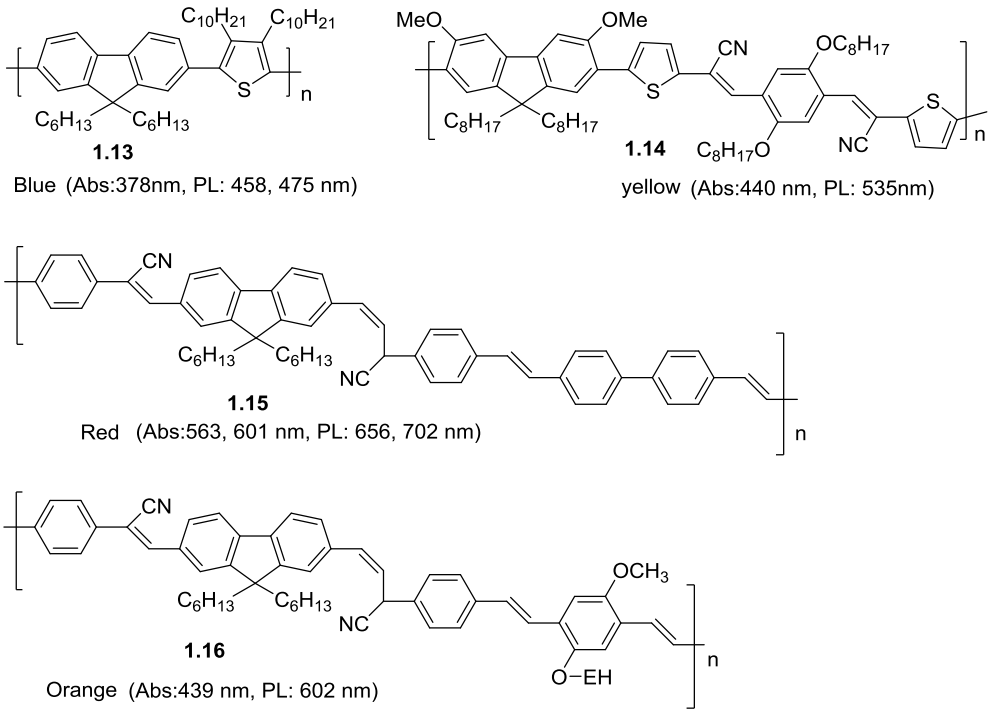


**Figure 1.16:** Various fluorene-containing co-polymers **1.13-1.16** with tuneable PL and EL colours.[51,52,53]

## 1.6 Dibenzothiophene-*S,S*-dioxide as an electron-deficient building block for organic electronics

Dibenzothiophene-*S,S*-dioxide (**1.17**) has been shown to be a strong electron-deficient building block with materials that incorporate this heterocyclic unit into the backbone having highly efficient photo- and electroluminescence. In 2005, Perepichka *et al*. published the first paper, which demonstrated the incorporation of the dibenzothiophene-*S,S*-dioxide

moiety into fluorene co-oligomers.[57] They synthesised three different co-oligomers by a Suzuki C–C cross coupling reaction and compared them with fluorene homo-oligomers (see **Figure 1.17**). Since this first seminal research, over 400 papers have been published in the literature using dibenzothiophene-*S,S*-dioxide in organic electronic materials as an electron-deficient building block, particularly for the design of new light-emitting co-polymers.[58,59,60,61,62] (*Yet, to date of writing thesis report, no dibenzothiophene-S,S-dioxide homopolymers have been reported. This is one of the aims of the present studies in our PhD program of research*).

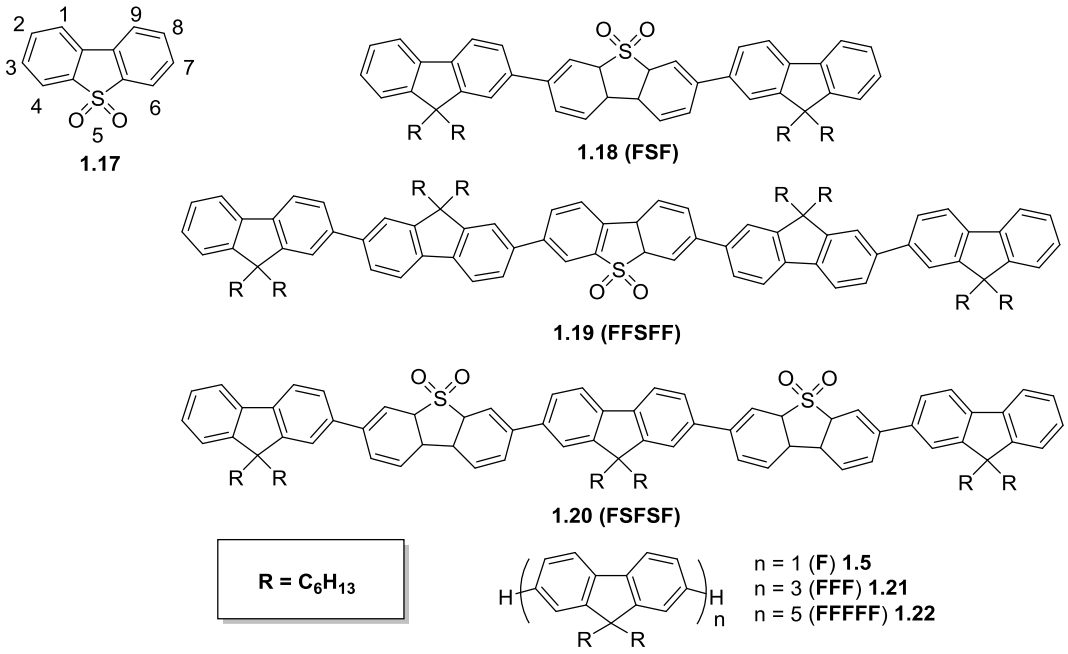


**Figure 1.17:** Dibenzothiophene-*S,S*-dioxide (**1.17**) and the IUPAC enumeration of atoms in the molecule. Fluorene–dibenzothiophene-*S,S*-dioxide co-oligomers **1.18–1.20**, and fluorene homo-oligomers **1.5, 1.21, 1.22**.[57]

In contrast to many other aromatic/heteroaromatic building blocks used for the synthesis of light-emitting conjugated polymers (see **Figure 1.5**, **Page 5**), dibenzothiophene-*S,S*-dioxide is an electron-deficient moiety due to the electron-withdrawing character of the $SO_2$ group, and its structure is topologically similar to that of fluorene. Oligomers **1.18–1.20** synthesised and studied by Perepichka *et al.* emitted blue light in solution and in the solid

state with high fluorescence efficiency ($\lambda_{PL}$ = 430–450 nm, PLQY = 65–67% in solution; $\lambda_{PL}$ = 447–462 nm, PLQY = 44–63% in the solid-state) (**Figure 1.18**).[57]

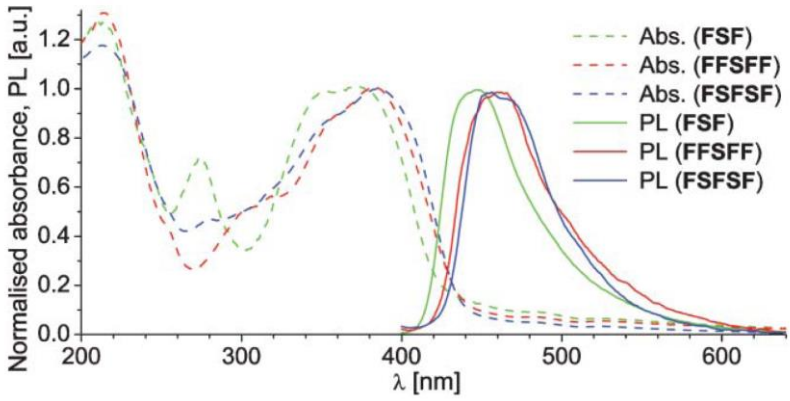


**Figure 1.18:** Normalised UV-Vis absorption and photoluminescence spectra of **1.18** (**FSF**), **1.19** (**FFSFF**) and **1.20** (**FSFSF**) co-oligomers in films ($\lambda_{exc}$ = 390 nm).[57]

The authors also showed that the incorporation of dibenzothiophene-*S*,*S*-dioxide in fluorene oligomers leads to an increase in the electron accepting properties of the oligomers due to a low-lying LUMO energy level. For example, according to DFT calculations, the LUMO energy of fluorene is –0.77 eV whereas for dibenzothiophene-*S*,*S*-dioxide it is –1.81 eV, i.e. more than 1 eV lower. For fluorene trimer **1.21** (**FFF**) LUMO = –1.40 eV whereas for its analog **FSF (1.18)** LUMO = –1.97 eV (see **Figure 1.19**). Similar differences are observed for pentamers (and polymers). This lowering of the LUMO energy levels in dibenzothiophene-*S*,*S*-dioxide based oligomers/polymers allows an increase in the electron transport properties of these materials and a decrease in the electron injection barrier in OLEDs. Dibenzothiophene-*S*,*S*-dioxide could also be a promising acceptor group for donor-acceptor (D–A) oligomers or polymers.[57]

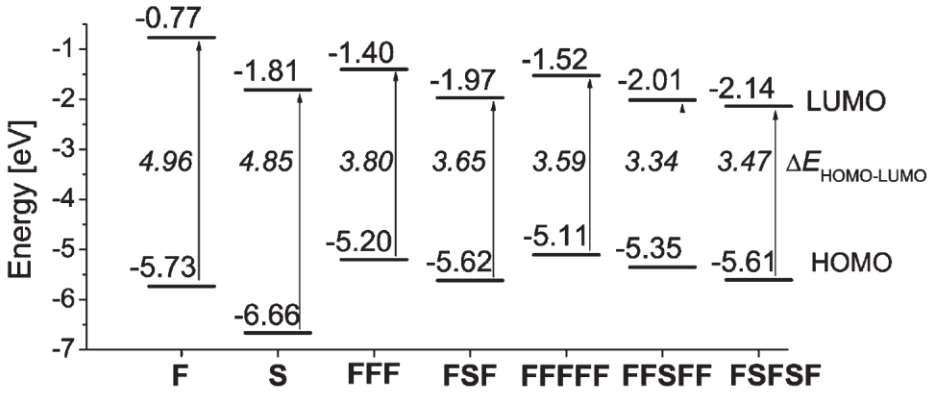


**Figure 1.19:** DFT B3LYP/6-31G(d) energy level diagram for oligofluorenes and fluorene–dibenzothiophene-*S*,*S*-dioxide co-oligomers (see **Figure 1.17** for structures).[57]

It was also observed by FTIR studies of **F-S** oligomers that the C=O group does not appear on thermal annealing of materials in the air (as commonly observed in polyfluorenes), and the undesired green emission was not observed in their PL spectra, confirming high stability of materials toward thermo/photo oxidation. Many researchers have recently used dibenzothiophene-*S*,*S*-dioxide as an electron acceptor unit in combination with various electron donor units:[63,64,65] the next sections will review some of the important research in this field.

### 1.6.1 Co-polymers containing the dibenzothiophene-*S*,*S*-dioxide moiety

Many groups investigated co-polymers containing dibenzothiophene-*S*,*S*-dioxide moieties incorporated into the backbone, of co-polymers with fluorene,[66,67,68] carbazole,[69] thiophene,[70] or other units[71,72] to obtain co-polymers with blue,[66,73] green,[74] red,[70] or white[75] colours of emission.

Perepichka *et al*. published the first paper in 2008, which described the synthesis and properties of statistic (random) 9,9-dioctylfluorene/dibenzothiophene-*S*,*S*-dioxide co-polymers **1.26**–**1.29 (PFS$_y$)** incorporating different amounts of dibenzothiophene-*S*,*S*-dioxide units into the polymer main chain (2, 5, 15, and 30%).[76] These co-polymers were synthesised by Suzuki C–C cross-coupling polymerisation by reaction of 3,7-dibromodibenzothiophene-*S*,*S*-dioxide, 9,9-dioctylfluorene-2,7-diboronic acid and 2,7-

dibromo-9,9-dioctylfluorene monomers using a different feed ratio of monomers (the polymers were end-capped with 4-*n*-BuPh-groups) (**Scheme 1.5**).[79]

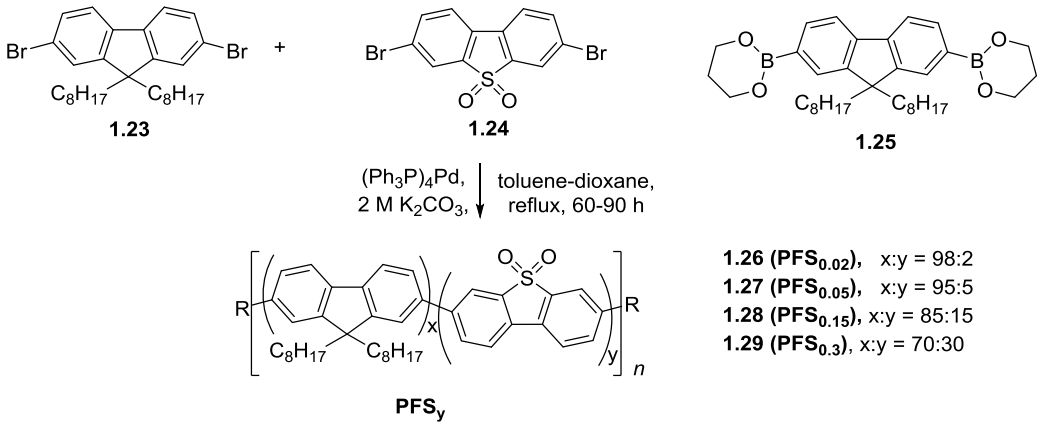


**Scheme 1.5:** Synthesis of co-polymers **1.26**–**1.29**.[79]

The photophysical properties of the co-polymers have been studied and compared with the co-oligomers **1.18**-**1.19** from previous studies (see **Figure 1.17** for chemical structures).[57] **Figure 1.20 a** shows the absorption spectra of **FSF, FFSFF, PFS0.15**, and **PFS0.3** in toluene solution. A regular red shift was demonstrated on going from the smaller oligomer **FSF** to the co-polymers **PFSy**, indicating the existence of relatively longer conjugated units in the two co-polymers. The photoluminescence spectra of the same four compounds in toluene solution are shown in **Figure 1.20 b**. Again, a bathochromic shift was demonstrated in emission with the two co-polymers emitting at longer wavelengths. Thus, there are no significant changes observed in the spectral structure between oligomers and co-polymers, and the fluorescence spectra of the pentamer, **FFSFF**, already matches well the fluorescence spectra of the co-polymers **PFS0.15,** and **PFS0.3** which have a relatively high content of S moieties, presenting a larger Stokes shift.[76]

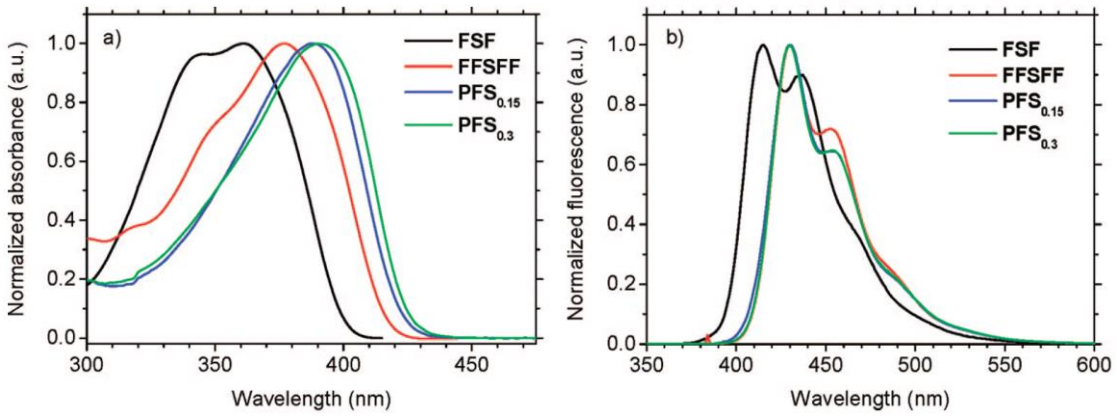


**Figure 1.20:** Normalised (a) absorption and (b) emission spectra of **1.18** (**FSF**), **1.19** (**FFSFF**), **1.28** (**PFS$_{0.15}$**), and **1.29** (**PFS$_{0.3}$**) in diluted toluene solution, $\lambda_{exc.}$ = 390 nm.[76]

As a consequence of a photo prompted charge transfer arising in the pentamer **1.19** excited states, the emission spectral structure of this oligomer shows significant alterations in polar solvents as shown in **Figure 1.21 b**.[76] The intramolecular charge transfer (ICT) excited state becomes more stable by increasing the solution polarity. Thus, the reorientation of the solvent molecules around the excited fluorophores facilitate dipole-dipole interactions.[77] In nonpolar solvents (toluene) the photoluminescence spectrum is very comparable to that of polyfluorenes, nevertheless in a moderately polar solvent (chloroform) a broad and structureless emission was demonstrated independent of the excitation wavelength.[76] **Figure 1.21 a** shows the electron absorption and photoluminescence spectra of co-polymer **1.29** in toluene and chloroform, a reasonably polar solvent. As was demonstrated, the electron absorption spectrum of **1.29** showed pretty slight alterations with solvent polarity. On the other hand, the alterations in the photoluminescence spectra for this structure are more obvious. In chloroform, only a broad featureless photoluminescence spectrum was observed, as a significance of solvent-induced stabilisation of the ICT state.[76] However, in toluene the $\lambda_{PL}$ is blue shifted and the spectra demonstrated the typical vibronic structure reported for polyfluorenes.[78]

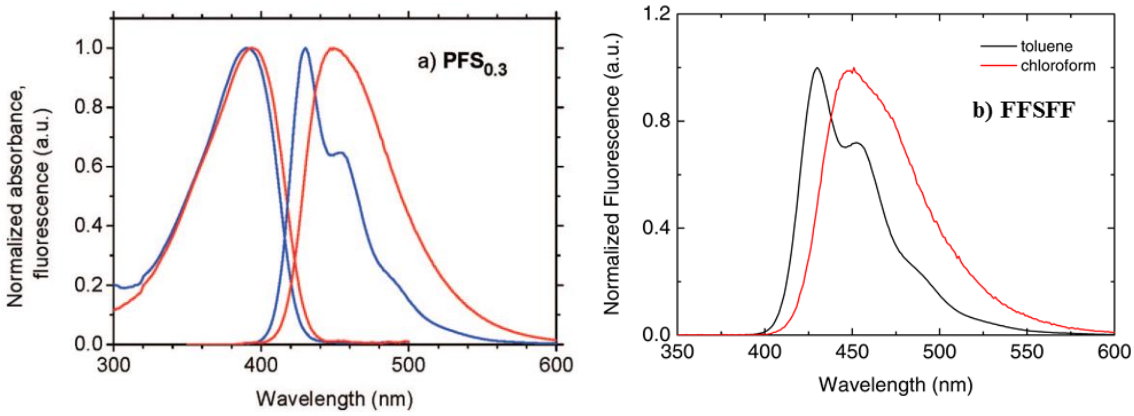


**Figure 1.21:** a) Normalised absorption and emission spectra of **1.29** (**$PFS_{0.3}$**) in toluene (blue) and chloroform (red), $\lambda_{exc}$ = 390 nm. b) Normalized emission spectra of **1.19 (FFSFF)** in toluene and chloroform dilute solution; excitation at 390 nm. Note the broad emission spectrum centered at 450 nm observed in chloroform.[76]

The photoluminescence quantum yields of co-polymers **$PFS_y$** are quite high (~56% – 69% in solution) similar to that in polyfluorenes. The solid state PLQY were also reasonably high, between 8% and 21%.[79] Studies of OLED devices fabricated with these co-polymers (single layer OLED in configuration indium tin oxide (ITO) / poly(3,4-ethylenedioxythiophene) : poly(styrenesulfonic acid) (PEDOT:PSS) / **$PFS_y$** / Ba / Al) showed that increasing the feed ratio of **S** units leads to an increase in the device performance compared to polyfluorenes under the same conditions.

The effect of introducing **S** segments into the polyfluorene backbone on the electrochemical behaviour of the co-polymers was studied. In cyclic voltammetry (CV) experiments, the co-polymer **1.29** can be reversibly p- and n-doped (see **Figure 1.22**). Comparable to the polyfluorene homopolymer **1.3**, both the oxidation and reduction potentials of **1.29** are shifted positively, with a more pronounced shift in the reduction potential compared to the oxidation potential (by onsets: 0.51 V and 0.19 V, respectively). The improved electron transport properties and easier reduction of **1.29** were presented in a positive shift in its reduction potential (by 0.51 V compared to **1.3**), so better electron injection and electron acceptor properties are expected for this polymer.[79]

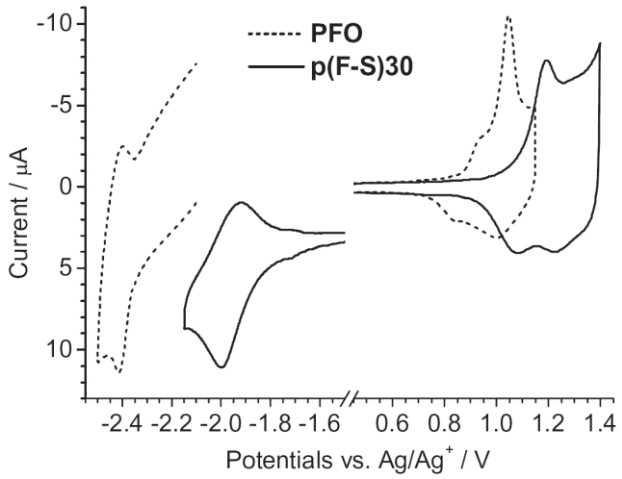


**Figure 1.22:** Cyclic voltammograms of polymers **1.29** (**P(F-S)30**) and **1.3** (**PFO** = **PF8**) in films on a glassy carbon electrode, 0.1 M $Bu_4NPF_6$ in acetonitrile, scan rate 40 mV $s^{-1}$, Estimated by onsets electrochemical bandgaps: $E_g^{CV}$ = 2.91 eV, **1.29 (p(F-S)30)**, 3.23 eV, **1.3 (PFO)**.[79]

In addition to the improved device performance, it was also demonstrated that **PFS$_y$** co-polymers show broadened photo- and electroluminescence spectra (due to dual LE/ICT emission) throughout the visible spectrum from the blue to green region and emit greenish-white light (see **Figure 1.23**), and as such can be used as materials for white-light emission OLEDs (WPLEDs).[79]

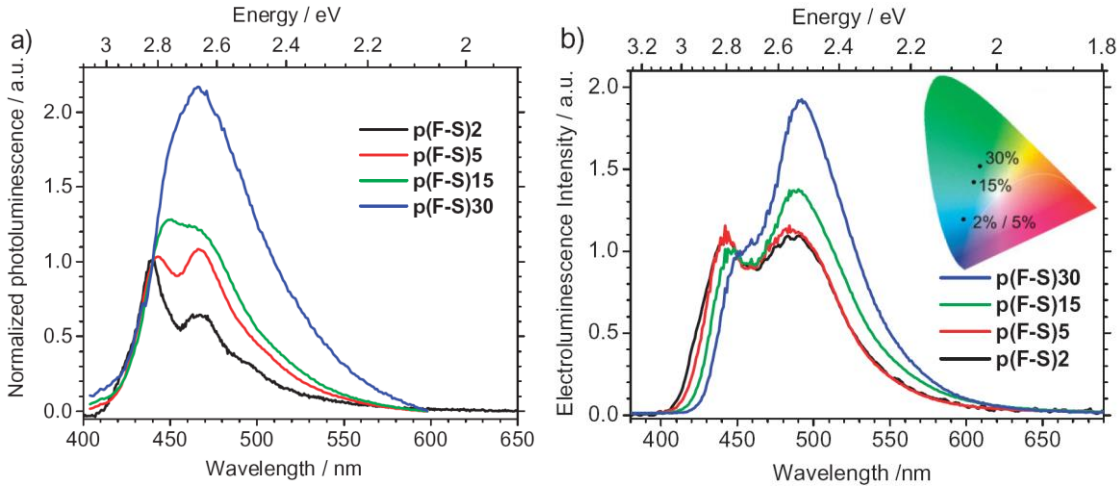


**Figure 1.23:** a) PL spectra of **1.26**–**1.29** co-polymers in films normalised to λ = 440nm, and b) electroluminescence spectra of **1.26**–**1.29** co-polymers for device structures ITO/PEDOT:PSS/**p(F-S)**$_y$/Ba/Al measured at 5 V.[79]

In 2008, a paper was published by Liu *et al.* that described the synthesis and characterisation (photoluminescence and electroluminescence) of co-polymers with the incorporation of dibenzothiophene-*S*,*S*-dioxide into poly[9,9-bis(4-(2-ethylhexyloxy)phenyl)fluorene-2,7-diyl] (**Figure 1.24**).[80]

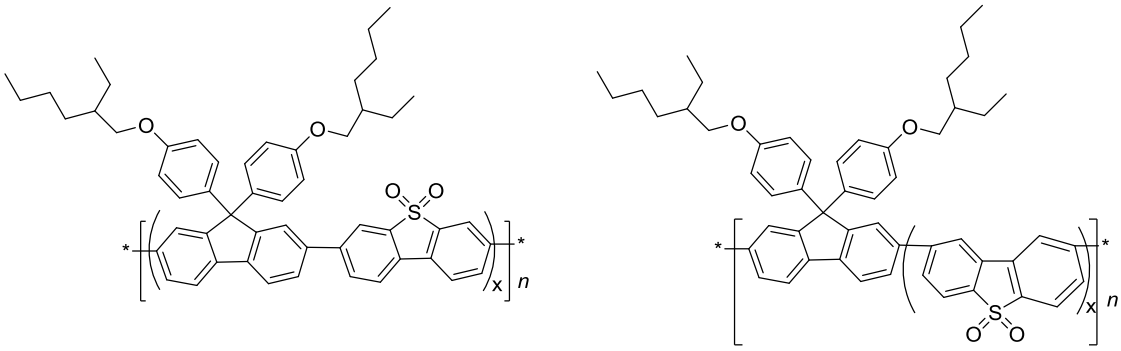

**x=0, 1.30 (PPF)**
**x=0.05, 1.31 (PPF-3,7SO5)**
**x=0.10, 1.32 (PPF-3,7SO10)**
**x=0.20, 1.33 (PPF-3,7SO20)**

**x=0.01, 1.34 (PPF-2,8SO1)**
**x=0.03, 1.35 (PPF-2,8SO3)**
**x=0.05, 1.36 (PPF-2,8SO5)**
**x=0.07, 1.37 (PPF-2,8SO7)**
**x=0.10, 1.38 (PPF-2,8SO10)**

**Figure 1.24:** Structures of co-polymers **1.30**–**1.38**.[80]

Blue-light emission was observed for these polymers, (see **Figure 1.25**), with high PLQY (~55–59%) comparable to that for the polyfluorene analogue **1.30** (PLQY = 49%).

The co-polymers showed high colour stability of their emission in devices, even at a high current flow (>360 mA/cm$^2$) through the devices, and the co-polymers annealed at high temperatures of ~200 °C, without showing undesired green emission (polyfluorenes normally show the appearance of a green band when annealed at temperatures of > 120–140 °C).[80]

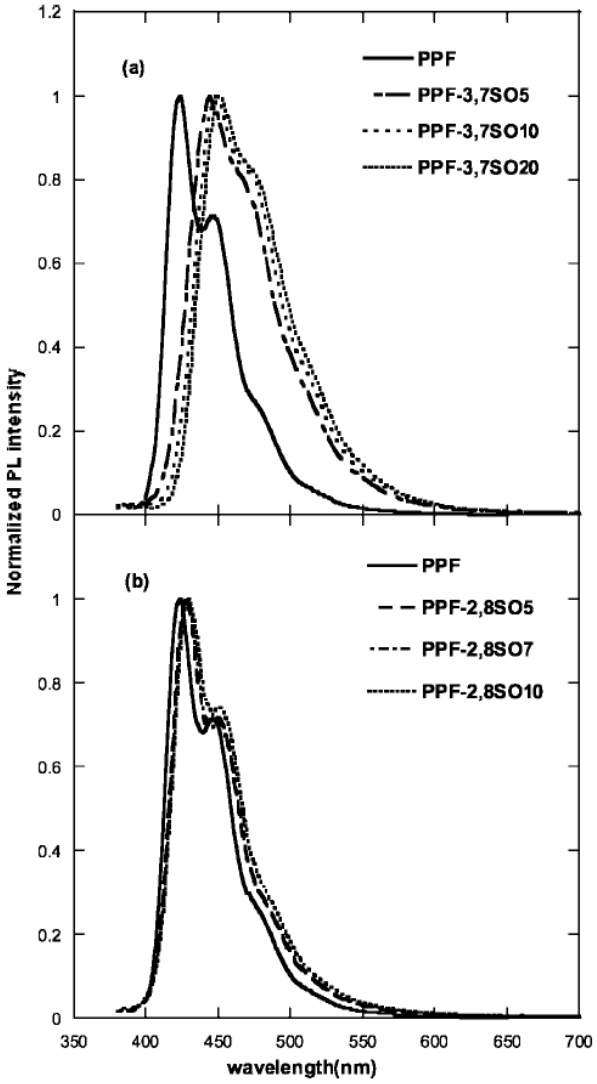


**Figure 1.25:** PL spectra of polymers (a) **1.30**–**1.33** (**PPF, PPF-3,7SO5, PPF-3,7SO10, PPF-3,7SO20)** and (b) **1.30 (PPF), 1.36**–**1.38** (**PPF-2,8SO5, PPF-2,8SO7, PPF-2,8SO10)**.[80]

In 2003, Nemoto *et al.* published a paper that studied the synthesis of three co-polymers containing dibenzothiophene (**Scheme 1.6**).[81] It was demonstrated that these

polymers emit blue light $\lambda_{PL}$ = 381–406 nm in chloroform (see **Figure 1.26**). However, they did not study the PLQY efficiency, PL properties in the solid state or electroluminescence properties of these co-polymers.

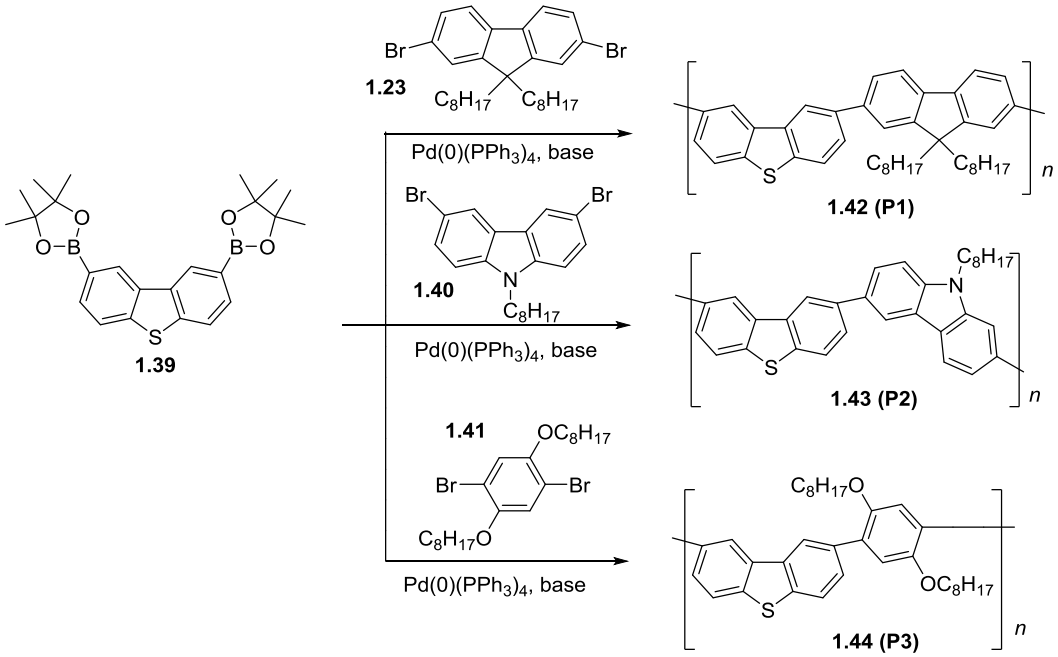


**Scheme 1.6:** Synthesis **1.42**–**1.44** (**P1**–**P3**).[81]

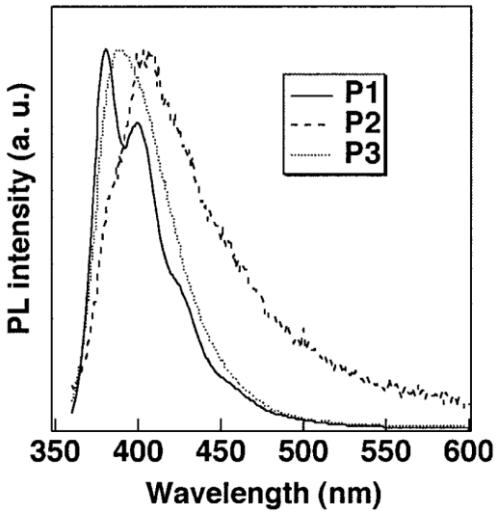


**Figure 1.26:** Photoluminescence spectra of **1.42**–**1.44** (**P1**–**P3**) in chloroform.[81]

In 2013, Liu *et al.* described complex random co-polymers based on dibenzothiophene-*S*,*S*-dioxide (SO), fluorene (F), benzothiadiazole (BT) or 4,7-di(4-hexylthien-2-yl)benzothiadiazole (DHTBT) units, prepared by Suzuki C–C cross-coupling polymerisation (**Figure 1.27**).[82]

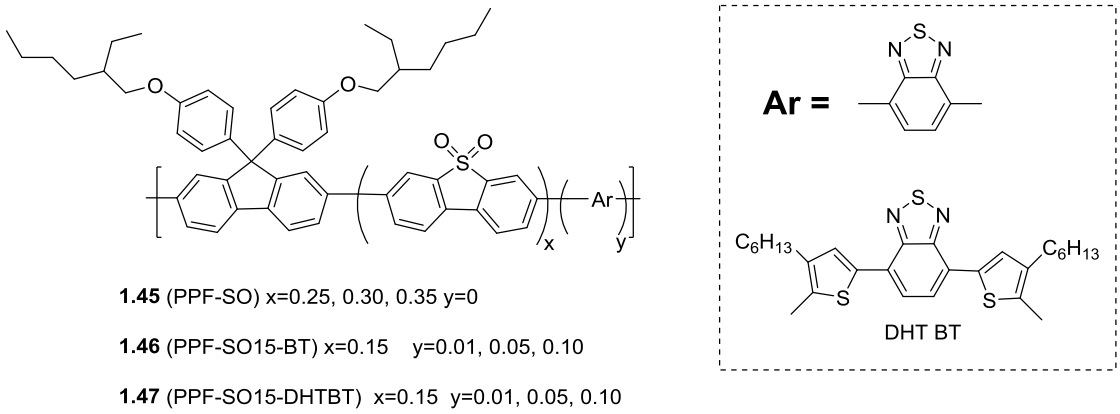


**1.45** (PPF-SO) x=0.25, 0.30, 0.35 y=0

**1.46** (PPF-SO15-BT) x=0.15 y=0.01, 0.05, 0.10

**1.47** (PPF-SO15-DHTBT) x=0.15 y=0.01, 0.05, 0.10

**Figure 1.27:** Structures of the co-polymers **1.45–1.47** (PFSO, PSSOBT, and PFSOTHDBT).[82]

The PL spectra of these co-polymers showed blue, green or red emission depending on the feed ratio of monomer units. Thus, co-polymer **1.45** emitted blue light ($\lambda_{PL}$ = 430 nm), PL emission of **1.46** is shifted to a longer wavelength ($\lambda_{PL}$ = 520 nm, green colour) and polymer **1.47** emits red light ($\lambda_{PL}$ = 605 nm) (**Figure 1.28**).

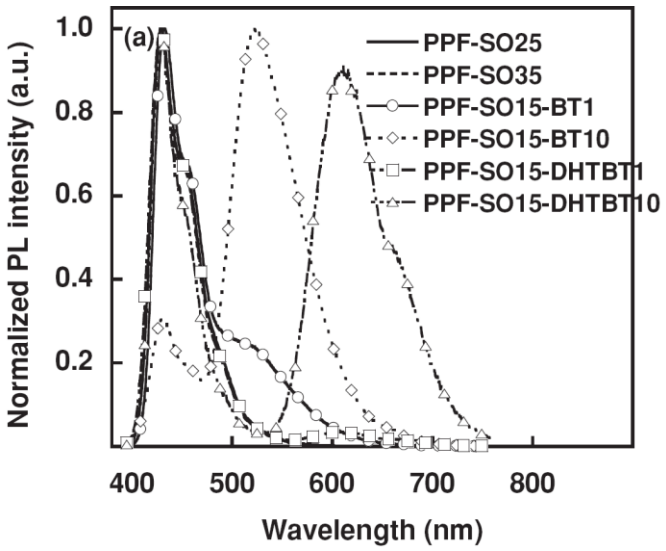


**Figure 1.28:** PL spectra of co-polymers **1.45-1.47 (**PFSO, PSSOBT, and PFSOTHDBT) in toluene.[82]

The PLQY values of solid films of these co-polymers have been found to be quite high: PLQY = 53% (for the blue light emitting polymer), 67% (for the green light emitting polymer), 56% (for the red emitting polymer). So, it was suggested that they might be suitable materials for the fabrication of white-light emitting devices by blending them in WPLEDs.[82]

Recently (in 2018), Yong *et al.* have synthesized bipolar blue light-emitting polyfluorenes **1.48** containing electron-deficient dibenzothiophene-*S*,*S*-dioxide and an electron-rich carbazole moiety (see **Figure 1.29**).[83] All the co-polymers presented a great thermal stability with decomposition temperatures above 400 °C and higher photoluminescence quantum yields. The highest occupied molecular orbital HOMO energy levels somewhat improve and the lowest unoccupied molecular orbital LUMO energy levels moderately reduce with the increase of carbazole ratio in the co-polymers. PL spectra of the polymers display a significant bathochromic shift and broadening with an increase in solvent polarity, indicating a substantial intramolecular charge transfer (ICT) effect in the polymers. Electroluminescence (EL) spectra of the co-polymers showed a broadening tendency with increasing carbazole moiety content in the co-polymers.

Green light-emitting polyfluorenes (**1.49**) having a 3,7-bis(4-hexylthiophene) dibenzothiophene-*S*,*S*-dioxide (**DHTS**) moiety were designed and synthesised (see **Figure 1.29**).[84] The polymers showed improved highest occupied molecular orbital energy

levels ($E_{HOMO's}$) and depressed lowest unoccupied molecular orbital energy levels ($E_{LUMO's}$) with the increase of the **DHTS** unit in polymers. The photoluminescence (PL) spectra of the polymers showed a significant bathochromic shift with the increase of solvent polarities, indicating a significant intramolecular charge transfer (ICT) effect in the polymers containing the **DHTS** moiety. The photoluminescence quantum yields (PLQY) are in the range of 34−67% for polymers **1.49** in film. The device made of the polymer containing 15% of the **DHTS** unit demonstrated green emission with the CIE coordinates of (0.26, 0.59).

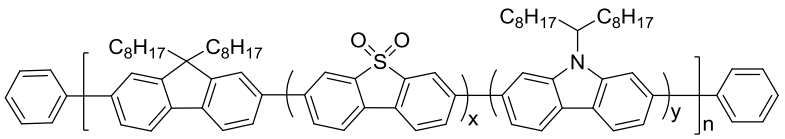


**1.48**

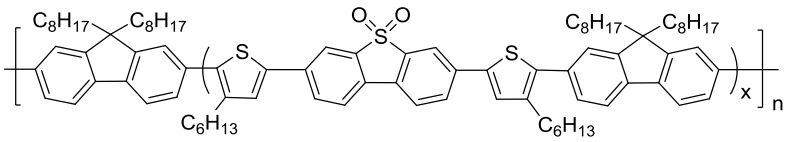


**1.49**

**Figure 1.29:** Structures of the co-polymers **1.48–1.49**.

In 2016, Cao's group synthesised and designed a polyfluorene-based blue-light emitting co-polymer **1.50** containing an aromatic dibenzothiophene-*S*,*S*-dioxide unit in the alkane side chain (see **Figure 1.30**).[85] The UV\Vis, PL spectra and wide-angle X-ray diffraction measurements of the resulting polymer showed that the introduction of such an aromatic moiety could induce the formation of the β-phase. The resulting polymer **1.50** containing the dibenzothiophene-*S*,*S*-dioxide moiety demonstrated enhanced electroluminescence properties relative to the original polyfluorene film. A maximum luminous efficiency of 2.25 cd $A^{-1}$ with CIE coordinates of (0.17, 0.09) was achieved from the light-emitting device based on the polymer containing the dibenzothiophene-*S*,*S*-dioxide unit, it also demonstrated stable electroluminescent spectra. In 2017, the same group published another blue light-emitting polyfluorene **1.51** containing a dibenzothiophene-*S*,*S*-dioxide unit in the alkyl side chain of the carbazole (see **Figure 1.30**).[86] They demonstrated that the HOMO and LUMO energy levels of the co-polymers slightly reduced with an

increase of dibenzothiophene-*S*,*S*-dioxide content in side chain. PL spectra of the polymers show a somewhat bathochromic shift and broadening with an increase in solvent polarity, indicating a typical intramolecular charge transfer (ICT) effect in the co-polymers holding dibenzothiophene-*S*,*S*-dioxide unit in the alkyl side chain. These clarifications indicate that the introduction of the aromatic unit in the side chain is a promising strategy to obtain stable blue-light emitting polyfluorenes with improved efficiency.

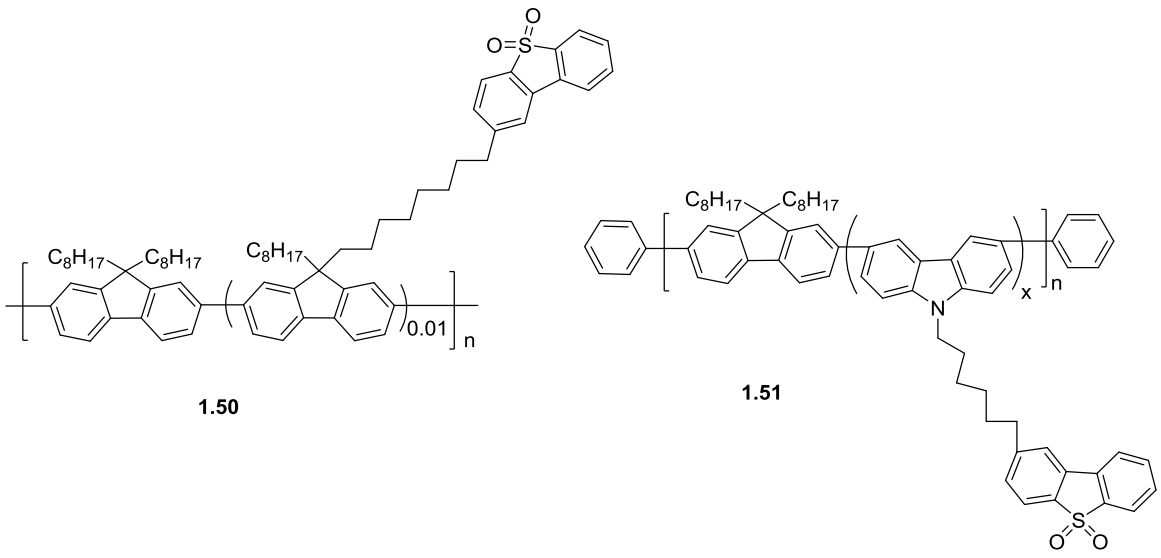


**Figure 1.30:** Structures of the co-polymers **1.50–1.51**.

Peng *et al.* presented an effective strategy to enhance the electroluminescent performance of poly[(fluorene)-co-dibenzothiophene-*S*,*S*-dioxide] derivatives by end-capping, which was carried out by presenting the *N*-([1,1'-biphenyl]-4-yl)-*N*-(4-phenyl)-9,9-dimethyl-9*H*-fluoren-2-amine unit (TF) at the end of the polymerisation (see **Figure 1.31**).[87] In comparison with the original co-polymers, **PFS**$_y$, that were end capped by a phenyl moiety, the TF-end-capped co-polymers **1.52** showed enhanced HOMO levels, which can assist hole injection and hence lead to more balanced charge carrier transport in the emissive layer. Thus, the resulting co-polymers **1.52** could be used to fabricate single-layer devices without a hole transport layer, which decreased driving voltage and clearly improved luminous efficiency relative to the device fabricated from the co-polymer **PFS**$_y$ that was end capped by a phenyl moiety.

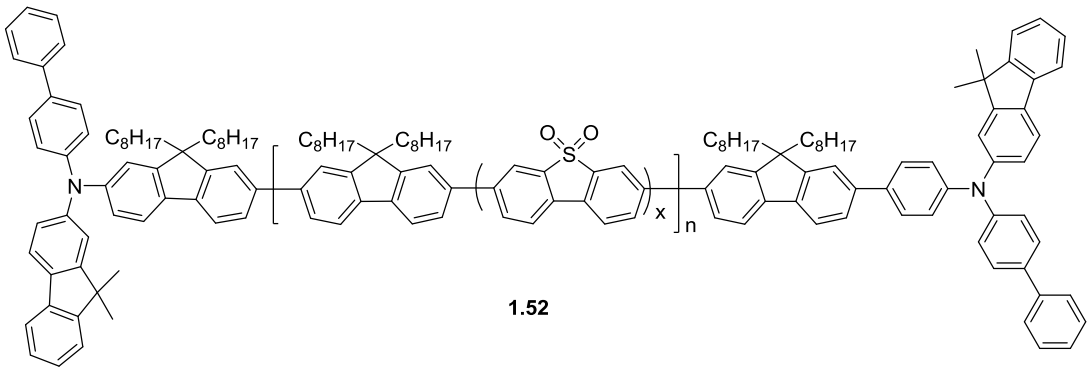


**Figure 1.31:** Structure of the co-polymer **1.52**.

### 1.6.2 Co-polymers with 2,8-disubstituted dibenzothiophene-*S*,*S*-dioxide

It should be mentioned that in 2002 Ancora *et. al.* reported the co-polymer **1.53** of 2,8-dimethyldibenzothiophene-*S*,*S*-dioxide and phenylenevinylene (**Figure 1.32**).[88] However, they did not study the photo and electro properties of this polymer and other results showed weak interest in this material.

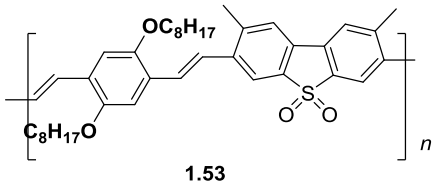


**Figure 1.32:** Structure of co-polymer **1.53** 2,8-dimethyl dibenzothiophene-*S*,*S*-dioxide and phenylenevinylene.[88]

Dibenzothiophene-*S*,*S*-dioxide as a blue light-emitting unit has been used in many research papers to prepare co-oligomers or co-polymers[89,90,91] as described above. However, there are only a few research papers that describe substituted dibenzothiophene-*S*,*S*-dioxide co-polymers. In 2010, Bryce's group reported the synthesis of a series of co-polymers **1.57-1.59** by reacting monomers **1.25** and **1.23** with different percentages (15, 30, or 50%) of **1.56** *via* a Suzuki polycondensation reaction (see **Scheme 1.7**).[92] It was noticed that the hexyl groups linked to dibenzothiophene-*S*,*S*-dioxide participate to increase the solubility of the co-polymers compared to the analogous unsubstituted co-polymers.[76,79] The presence of a hexyl group also affected the emission of the co-polymers. Thus, polymer **1.58** (70:30)

with hexyl groups showed $\lambda_{PL}$ = 412 nm (toluene), 412 nm ($CHCl_3$), and 426 nm (film), whereas polymer **1.29** (**$PFS_{0.3}$**) with the same ratio (70:30) but without hexyl groups substituted at the dibenzothiophene-*S*,*S*-dioxide moiety showed red-shifted emission, $\lambda_{PL}$ = 427 nm (toluene), 443 nm ($CHCl_3$), and 469 nm (film) (**Figure 1.33**).[79] This is proof that the hexyl groups at the sterically hindered 2,8-positions reduce the conjugation in the polymer due to increasing the dihedral angles between the building blocks in the polymers backbone and leads to an increase in the band gap of the polymer.[92]

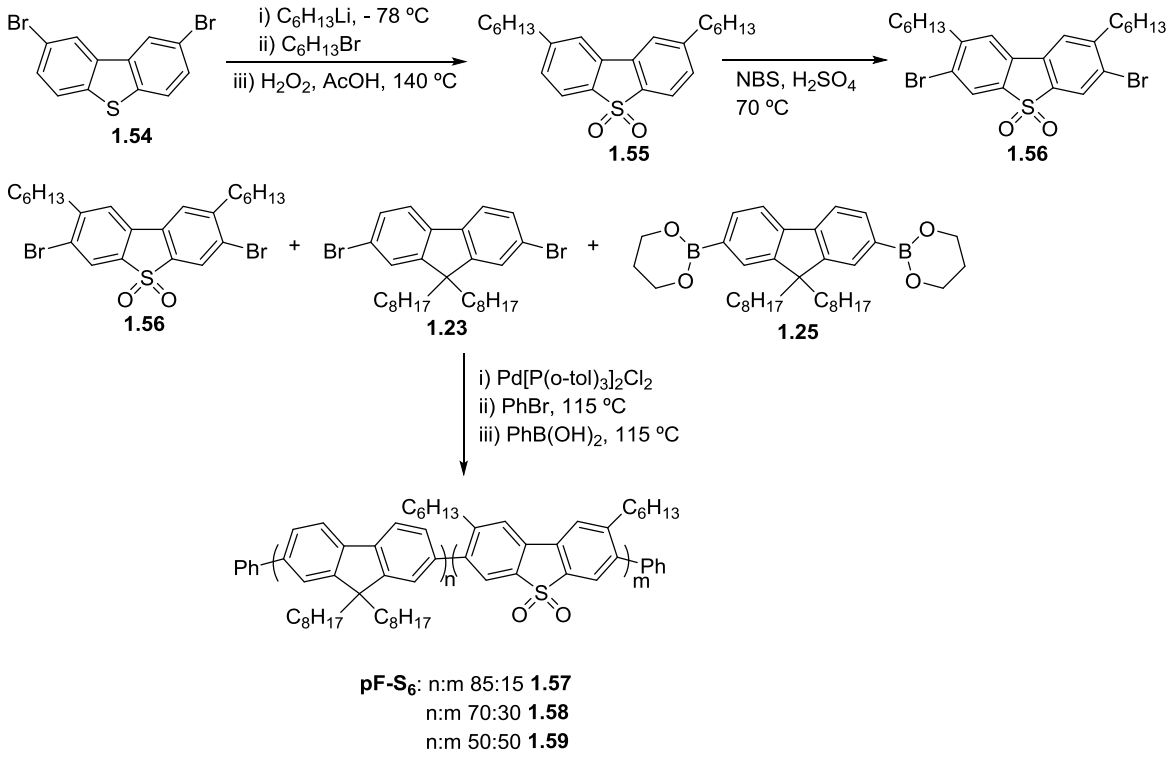


**Scheme 1.7:** Synthetic route to polymers **1.57-1.59**.[92]

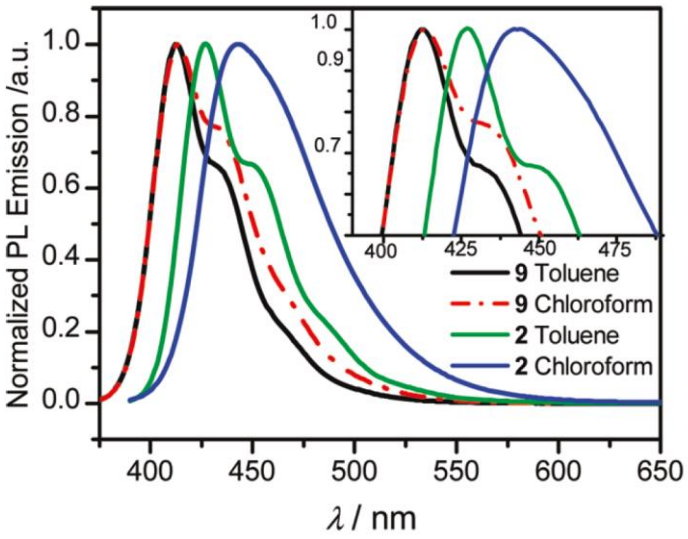


**Figure 1.33:** Photoluminescence spectra of **1.58 (9)** black line in toluene, red line in chloroform and **1.29 (2)** green line in toluene, blue line in chloroform. Inset shows a magnification of the $\lambda_{max}$ region.[92]

More recently (in 2014), Bryce's group reported two series of seven fluorene/dibenzothiophene-*S*,*S*-dioxide co-polymers **1.60–1.66** (**P1**-**P7**) with 2,8-dialkoxy groups on the dibenzothiophene-*S*,*S*-dioxide units.[93] They synthesised polymers **1.60–1.62** with different ratios of dibenzothiophene-*S*,*S*-dioxide, and with *meta*-linkage at the fluorene moiety, as well as co-polymers **1.63–1.66** with *para*-linkage at the fluorene moiety (**Figure1.34**). All these co-polymers were synthesised by a Suzuki C–C coupling reaction with an end-capping phenyl group.

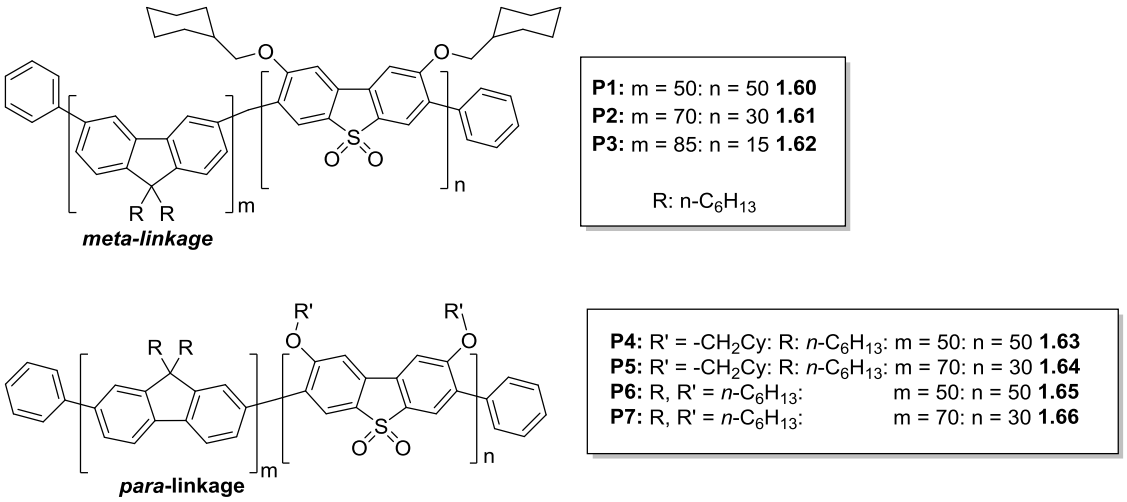


**Figure 1.34:** Synthesis and structures of co-polymers **1.60–1.66** (**P1**–**P7**).[93]

The polymers showed negligibly small solvatochromism (or no solvatochromism): for example polymer **1.61,** $\lambda_{PL}$ = 412 nm (ethyl acetate), 413 nm (cyclohexane). They also showed an observable blue shift of ~ 30 nm for the polymers with a *meta*-linkage compared to those with a *para*-linkage (in films, $\lambda_{PL}$ = 420 nm for **1.61,** 450 nm for **1.64**) (**Figure 1.35**). This difference was attributed to a broken conjugation in polymers **1.60–1.62 (P1**–**P3)**. It was shown that the percentage of dibenzothiophene-*S*,*S*-dioxide segments in the polymers does not affect the absorption and emission of the polymers. For example, absorption of all three polymers **1.60–1.62** in the solid state is observed at $\lambda_{max}$ = 350 nm. The same is observed for the photoluminescence: $\lambda_{PL}$ = 424 nm (**1.60**), 420 nm (**1.61, 1.62**).

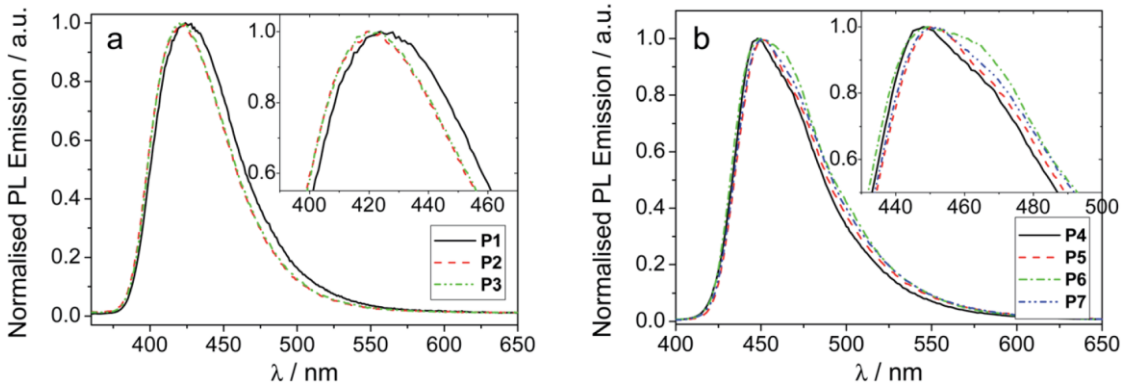


**Figure 1.35:** Normalised PL emission spectra for (a) polymers **1.60-1.62 (P1**–**P3)** and (b) polymers **1.63-1.66 (P4**–**P7)** in thin film. Insets show an expansion of the $\lambda_{max}$ regions.[93]

In 2014, Xiao *et al.* described a series of co-polymers containing substituted dibenzothiophene-*S*,S-dioxide at positions 2, and 8 (R = H, $C_8H_{17}$, or $OC_8H_{17}$) with di(aminoalkyl)fluorene (see **Figure 1.36**).[94] The co-polymers **1.67–1.69** were synthesised by a Suzuki C-C cross coupling polymerisation reaction. All synthesised co-polymers were slightly soluble in common organic solvents such as THF, chloroform or toluene and they were soluble in polar solvents *N*,*N*-dimethylformamide (DMF) and dimethyl sulfoxide (DMSO). Some other co-polymers of this series (structures are not shown) are readily soluble in methanol and in water containing trace amounts of acetic acid.

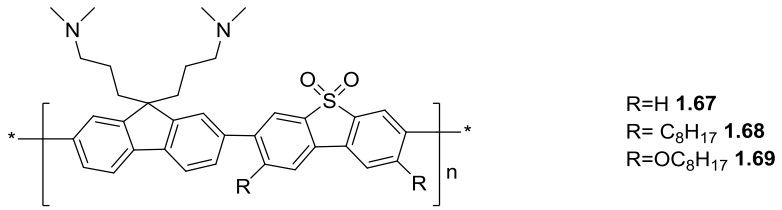


**Figure 1.36:** Structures of polymers **1.67–1.69**.[94]

### 1.6.3 Co-oligomers and small molecules containing dibenzothiophene-*S*,*S*-dioxide unit

In 2010, Bryce's group reported several ambipolar oligomeric compounds (donor–acceptor–donor) with fluorene, carbazole and arylamine as electron donor segments and dibenzothiophene-*S*,*S*-dioxide as the electron acceptor segment (see **Figure 1.37**).[95] These trimers **1.18, 1.70–1.75** were prepared by a Suzuki C–C coupling reaction.

Investigations of their photophysical properties showed a regular red-shift in both absorption and emission spectra, in accordance with an increase in the strength of the donor units: fluorene < carbazole < arylamine. For example, the emission in toluene: $\lambda_{PL}$ = 433 nm (**1.18**),[3] 450 nm (**1.70**), 471 nm (**1.75**), and in chloroform: $\lambda_{PL}$ = 427 nm (**1.18**, deep blue), 458 nm (**1.70**, sky blue ), 520 nm (**1.75**, green) (see **Figure 1.38**). The authors also observed the positive solvachromatism for all the trimers due to the intramolecular charge transfer. For instance, for the trimer **1.74** in toluene $\lambda_{PL}$ = 482 nm but in chloroform $\lambda_{PL}$ = 520 nm.[95]

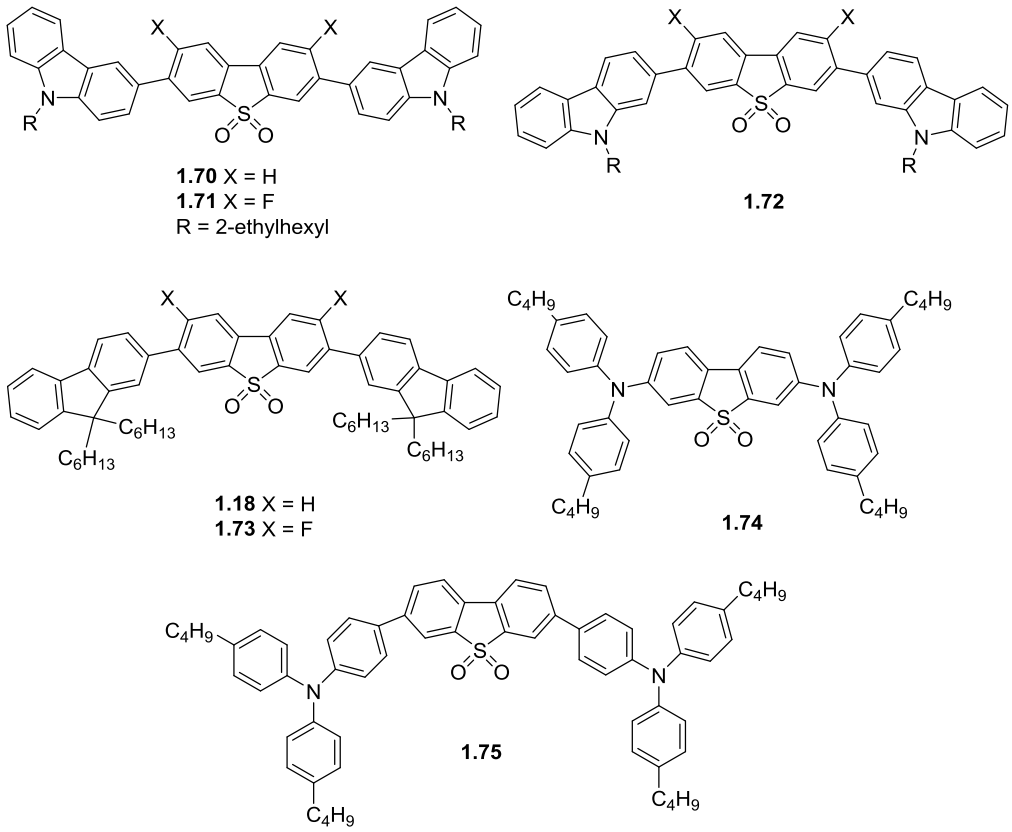


**Figure 1.37:** Structures of trimers **1.18, 1.70–1.75** containing dibenzothiophene-*S*,*S*-dioxide moieties.[95]

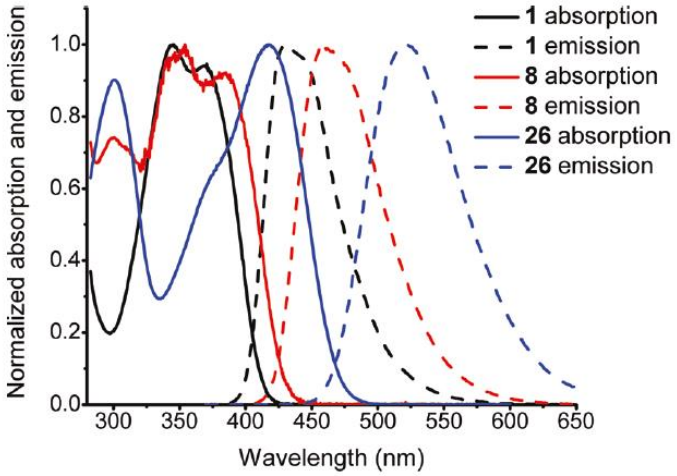


**Figure 1.38:** Influence of the donor substituents on the absorption and emission spectra of oligomers **1.18 (1)**, **1.70 (8)**, and **1.75 (26)** in chloroform.[95]

Huang *et al.* have prepared dipolar compounds by linking two arylamine fragments to dibenzothiophene-*S*,*S*-dioxide (compounds **1.76–1.79, Figure 1.39**).[96] The compounds

**1.76** and **1.79** were synthesised by using Hartwig's method (C-N coupling reaction), and compounds **1.77** and **1.78** were prepared by a Stille C–C coupling reaction. The photophysical properties of these compounds were studied and it was shown that the charge transfer from the donor (arylamine) to acceptor (dibenzothiophene-*S*,*S*-dioxide) is observed for all materials. They showed absorption in the region from 250 to 300 nm (π-π* and n-π*) with large solvatochromism due to the strong intramolecular charge transfer between the donor and the acceptor moieties. It was demonstrated that the emission could be tuneable over a wide range, from blue to orange depending on solvent polarity. For example, compound **1.77**: $\lambda_{PL}$ = 444 nm (toluene), 524 nm (DCM), 572 nm (acetonitrile). Compound **1.79** emits at the highest wavelength among these four compounds. It was also found that compounds **1.77** and **1.78** have high PLQY in toluene (98% and 48%, respectively), much higher than compounds **1.76** and **1.79** (7%) in the same solvent. However, all of these four compounds showed low PLQY in acetonitrile (between 4% to 14%). These compounds were also used to fabricate single layer electroluminescent devices with high performance.[96]

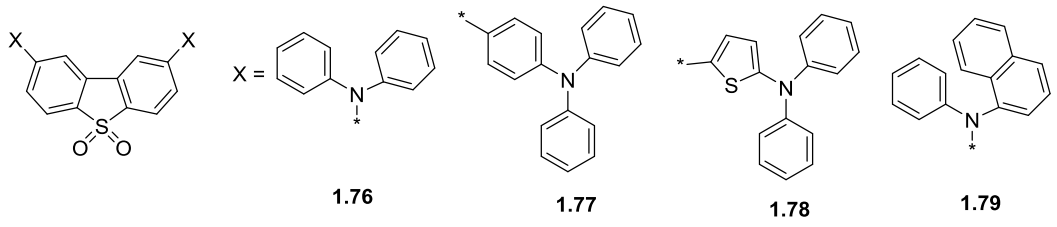


**Figure 1.39:** Bipolar dibenzothiophene-*S*,*S*-dioxide compounds **1.76–1.79**.[96]

The same group (in 2006) reported another series of small conjugated molecules with dibenzothiophene or dibenzothiophene-*S*,*S*-dioxide central moieties. Compounds **1.88–1.91** have been synthesised in three steps: i) a Sonogashira coupling reaction with phenyl acetylene; ii) oxidation of the alkyne groups; and iii) a condensation reaction of the carbonyl groups with a diamine in quinoxaline or pyrazine (see **Scheme 1.8**).[97] All molecules showed two absorption peaks, with $\lambda_{abs}$ ~ 257–281 nm for the first peak and 335–373 nm for the second peak. The emission peaks of these compounds are in the range of 419–475 nm in DCM or in the solid state (**Figure 1.40**). These molecules showed quite high electron mobility, and OLEDs with good performances could be fabricated by utilizing **1.88–1.91** as electron-transporting materials.

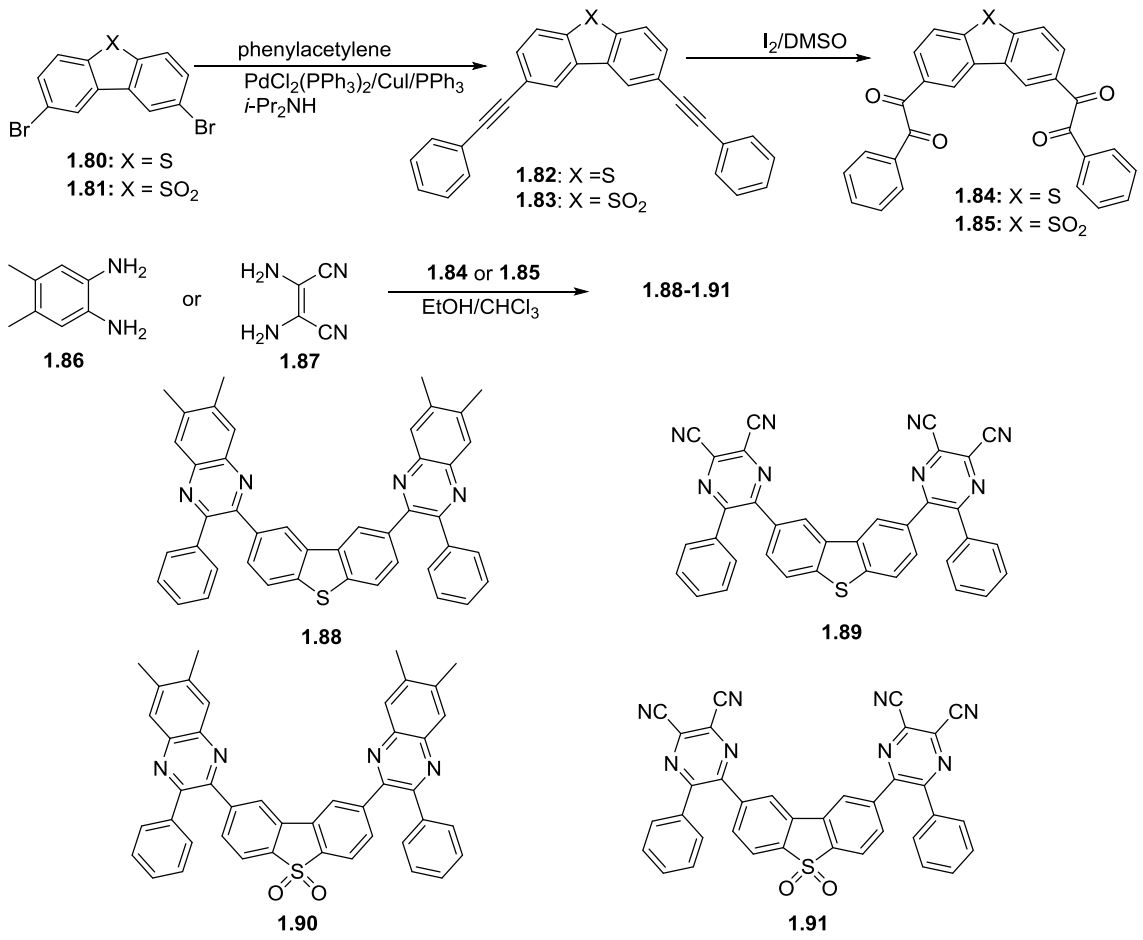


**Scheme 1.8:** Synthetic route to compounds **1.88–1.91**.[97]

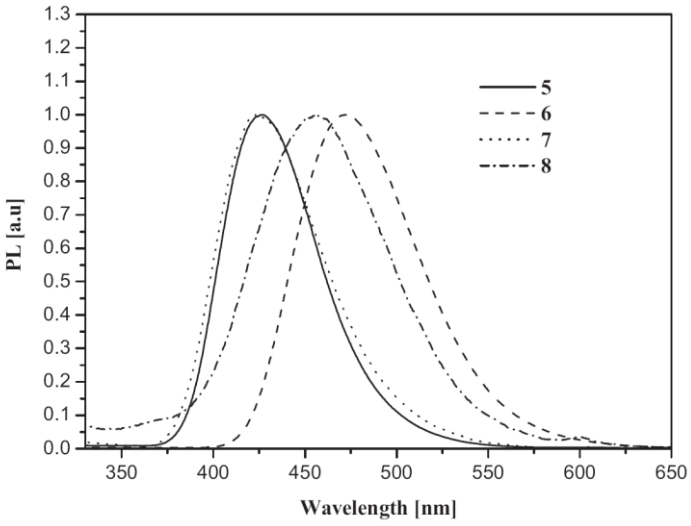


**Figure 1.40:** The emission spectra of **1.88–1.91(5 – 8)**, in dichloromethane, $\lambda_{exc.}$ = 350 nm.[97]

## 1.7 Aims of the project

Since the first significant paper introducing dibenzothiophene-*S*,*S*-dioxide as a versatile building block for conjugated organic molecules and polymers for organic electronics,[57] more than 400 papers have been published reporting different variations in structures, studies of their optoelectronic properties and testing of the materials in various devices (mainly in OLEDs, but applications in other devices have also been studied). The dibenzothiophene-*S*,*S*-dioxide moiety is topologically similar to fluorene, however, fluorene can be easily functionalised at position 9 to improve the solubility to the materials. Dibenzothiophene-*S*,*S*-dioxide itself shows lower solubility than fluorene and even in the case of its co-polymers with dialkylfluorenes, the amount of incorporated dibenzothiophene-*S*,*S*-dioxide units can not normally exceed 25–30% (for 2,8-dialky- or 2,8-dialkoxydibenzothiophene-*S*,*S*-dioxide moieties it can be higher, but such substitution decreases the effective conjugation length of the co-polymers due to steric interactions in the main chain).

In recent research, Perepichka's group have developed a series of novel light-emitting 4-functionalised polyfluorenes.[98] Such substitution at position 4 of the fluorene moiety does not sterically disturb the main chain of the polymers, but allows efficient tuning of the electronic properties of the polymers. As a logical expansion of this research programme, this work is focussed on 1-substituted dibenzothiophene-*S*,*S*-dioxide conjugated polymers and co-polymers (position 1 here is an equivalent of position 4 in fluorene, due to different IUPAC enumeration of these molecules).

The first aim of this project is an elaboration of synthetic methods to synthesise the first (yet unknown as a class) soluble conjugated dibenzothiophene-*S*,*S*-dioxide **p(S-R)** homopolymers as n-type electron deficient polymers. To achieve this goal, synthetic methods for the introduction of solubilising groups (alkoxy, alkylthio and alkylsulfonyl) at position 1 of the dibenzothiophene-*S*,*S*-dioxide moiety will be elaborated, to make and to study conjugated polymers based on this structural moiety (see **Scheme 1.9**). This will be described in detail in Chapter 3.

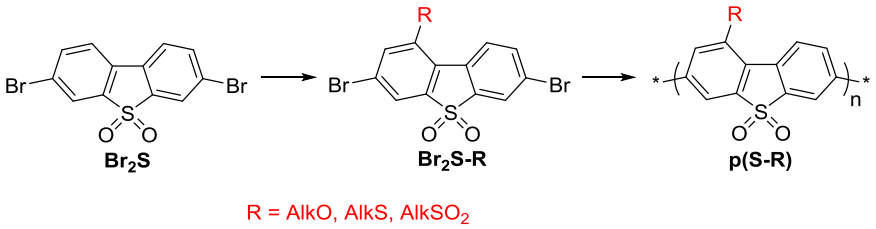


**Scheme 1.9:** General scheme showing synthetic route to soluble 1-substituted dibenzothiophene-*S*,*S*-dioxide **p(S-R)** homopolymers.

The second aim of the project is the development of novel light-emitting co-polymers incorporating 1-substituted dibenzothiophene-*S*,*S*-dioxide **Br2S-R** moieties (see **Scheme 1.10**). The goal of this task is to the achieve efficient tuning of electronic and optical properties of co-polymers by electronic effects from electron donating (EDG) or electron withdrawing groups (EWG) at the 1-position. After elaboration of synthetic methods to monomers **Br2S-R**, they can also be used for developing other classes of co-polymers with other (not only fluorene) conjugated building blocks. This work will be described in detail in Chapter 4.

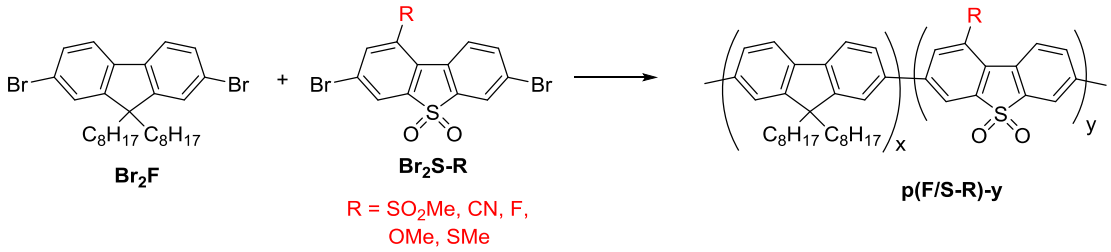


**Scheme 1.10:** General scheme describe synthesis of co-polymers **p(F/S-R)-y**.

To achieve these goals, it was necessary to elaborate synthetic methods for the introduction of different groups at position 1 of the dibenzothiophene-*S*,*S*-dioxide moiety. It was considered that a convenient synthetic pathway would be electrophilic substitution of 3,7-dibromodibenzothiophene-*S*,*S*-dioxide **Br2S**, which should proceed at position 1. A nitration reaction seems a good choice as it allows further transformation of the $NO_2$ group to $NH_2$ to give access to a wide range of other functionalities *via* diazonium chemistry (see **Scheme 1.11**). The synthesis of these monomers will be discussed in Chapter 2.

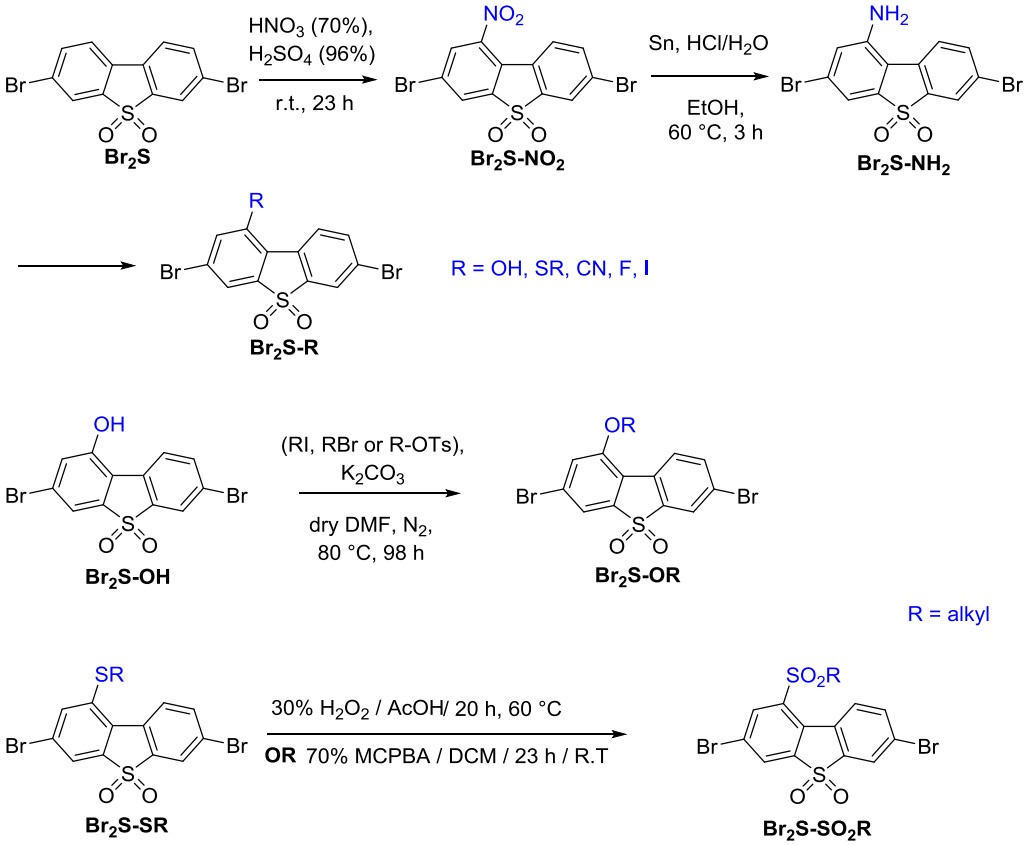


**Scheme 1.11:** General scheme for the substitution of **Br2S** at position 1.

## References


1 J. Ferraris, D. O. Cowan, V. Walatka, and J. H. Perlstein, Electron transfer in a new highly conducting donor-acceptor complex, *J. Am. Chem. Soc.*, **1973**, *2*, 948–949.

2 H. Shirakawa, E. J. Louis, A. G. MacDiarmid, C. K. Chiang, and A. J. Heeger, Synthesis of electrically conducting organic polymers : halogen derivatives of polyacetylene, (CH)x, *Chem. Commun.*, **1977**, *16*, 578–580.

3 H. Shirakawa, The discovery of polyacetylene film: the dawning of an era of conducting polymers (Nobel Lecture), *Angew. Chem. Int. Ed.*, **2001**, *40*, 2574–2580. DOI: 10.1002/1521-3773(20010716)40:14<2574

4 A. G. MacDiarmid, Synthetic metals a novel role for organic polymers (Nobel Lecture), *Angew. Chem. Int. Ed*. **2001**, *40*, 2581–2590. DOI: 10.1002/1521-3773(20010716)40:14<2581

5 A. J. Heeger, Semiconducting and metallic polymers: the fourth generation of polymeric materials (Nobel Lecture), *Angew. Chem. Int. Ed.*, **2001**, *40*, 2591–2611. DOI: 10.1002/1521-3773(20010716)40:14<2591

6 D. F. Perepichka, I. F. Perepichka, H. Meng, and F. Wudl, Light-emitting polymers. In Book: *Organic Light-Emitting Materials and Devices*, Z. R. Li, and H. Meng (Eds.), CRC Press, Boca Raton, FL, **2006**, Chapter 2, pp. 45–293.

7 T. A. Skotheim, and J. R. Reynolds (Eds.), Handbook of Conducting Polymers (3rd Edition). *Conjugated Polymers. Vol.1: Theory, Synthesis, Properties and Characterization; Vol. 2: Processing and Applications*, CRC Press, Boca Raton, FL, **2007**.

8 Y. Chujo (Ed.), *Conjugated Polymer Synthesis*, Wiley–VCH, **2010**.

9 M. Leclerc and J.-F. Morin (Eds.), *Design and Synthesis of Conjugated Polymers*, Wiley–VCH, **2010**.

10 A. C. Grimsdale, K. L. Chan, R. E. Martin, P. G. Jokisz, and A. B. Holmes, Synthesis of Light-Emitting Conjugated Polymers for Applications in Electroluminescent Devices, *Chem. Rev.*, **2009**, *109*, 897–1091. DOI: 10.1021/cr000013v

11 X. Zhaoab, and X. Zhan, Electron transporting semiconducting polymers in organic electronics, *Chem. Soc. Rev*., **2011**, *40*, 3728–3743. DOI: 10.1039/c0cs00194e

12 S. Forrest, and N. C. Moore, Energy efficiency with organic electronics, *MRS Bulletin*, **2012**, *37.06*, 552–553. DOI: 10.1557/mrs.2012.125

13 K. Asada, T. Kobayashi, and H. Naito, Control of Effective Conjugation Length in Polyfluorene Thin Films, *Jpn. J. Appl. Phys.*, **2006**, *45*, L247–L249. DOI: 10.1143/JJAP.45.L247

14 T. Izumi, S. Kobashi, K. Takimiya, Y. Aso, and T. Otsubo, Synthesis and spectroscopic properties of a series of β-blocked long oligothiophenes up to the 96-mer: revaluation of effective conjugation length, *J. Am. Chem. Soc.*, **2003**, *125*, 5286–5287. DOI: 10.1021/ja034333i

15 M. Kasha, Characterization of electronic transitions in complex molecules, *Discuss. Faraday Soc.*, **1950**, *9*, 14–19. DOI: 10.1039/DF9500900014

16 A. Jablonski, Efficiency of Anti-Stokes Fluorescence in Dyes, *Nature*, **1933**, *131*, 839–840. DOI:10.1038/131839b0

17 K. L. Litvinenko, N. M. Webber, and S. R. Meech, Internal Conversion in the Chromophore of the Green Fluorescent Protein: Temperature Dependence and Isoviscosity Analysis, *J. Phys. Chem. A*, **2003**, *107*, 2616–2623. DOI: 10.1021/jp027376e

18 L. S. Föster and Dadby, The luminescence of fluorescein dyes, *J. Phys. Chem.*, **1962**, *66*, 838–840. DOI: 10.1021/j100811a017

19 K. Hamanoue, T. Nakayama, and M. Ito, Existence of the Second Excited Triplet State of 1,8-Dibromoanthraquinone observed by Picosecond Laser Photolysis in Solutions at Room Temperature, *Chem. Soc. Faraday Trans.*, **1991**, *87*, 3487–3493. DOI: 10.1039/FT9918703487

20 G. G. Stokes, On the change of refrangibility of light, *Phil Trans R Soc Lond.*, **1852**, *142*, 463–562.

21 D. Llères, S. Swift, and A. I. Lamond, Detecting Protein-Protein Interactions In Vivo with FRET using Multiphoton Fluorescence Lifetime Imaging Microscopy (FLIM), *Current Protocols in Cytometry*, **2007**, *42*, 12.10.1–12.10.19. DOI: 10.1002/0471142956.cy1210s42

22 M. T. Bernius, M. Inbasekaran, J. O'Brien, and W. Wu, Progress with light-emitting polymers, *Adv. Mater.*, **2000**, *12*, 1737–1750. DOI: 10.1002/1521-4095(200012)12:23<1737

23 J. H. Burroughes, D. D. C. Bradley, A. R. Brown, R. N. Marks, K. Makcay, R. H. Friend, P. L. Burn, and A. B. Holmes, Light-emitting-diodes based on conjugated polymers, *Nature*, **1990**, *347*, 539–541. DOI: 10.1038/347539a0

24 R. H. Friend, G. J. Denton, J. J. M. Halls, N. T. Harrison, A. B. Holmes, A. Köhler, A. Luxb, S. C. Moratti, K. Pichler, N. Tessler, and K. Towns, Electronic processes of conjugated polymers in semiconductor device structures, *Synth. Metals*, **1997**, *84*, 463–470. DOI:10.1016/S0379-6779(97)80830-2

25 K. Zhao, L. Ye, W. Zhao, S. Zhang, H. Yao, B. Xu, M. Sun, and J. Hou, Enhanced efficiency of polymer photovoltaic cells via the incorporation of a water-soluble naphthalene diimide derivative as a cathode interlayer, *J. Mater. Chem. C*, **2015**, *3*, 9565–9571. DOI: 10.1039/c5tc02172c

26 S. Liu, C. Zhong, S. Dong, J. Zhang, X. Huang, C. Zhou, J. Lu, L. Ying, L. Wang, F. Huang, and Y. Cao, Novel aminoalkyl-functionalized blue-, green- and red-emitting polyfluorenes, *Org. Electronics*, **2014**, *15*, 850–857. DOI: 10.1016/j.orgel.2014.01.016

27 R. He, J. Xu, Y. Xue, D. Chen, L. Ying, W. Yang, and Y. Cao, Improving the efficiency and spectral stability of white-emitting polycarbazoles by introducing a dibenzothiophene-*S*,*S*-dioxide unit into the backbone, *J. Mater. Chem. C*, **2014**, *2*, 7881–7890. DOI: 10.1039/c4tc01089b

28 Y. Li, H. Wu, J. Zou, L. Ying, W. Yang, and Y. Cao, Enhancement of spectral stability and efficiency on blue light-emitters via introducing dibenzothiophene-*S*,*S*-dioxide isomers into polyfluorene backbone, *Org. Electronics*, **2009**, *10*, 901–909. DOI: 10.1016/j.orgel.2009.04.021

29 L. Hu, Y. Yang, J. Xu, J. Liang, T. Guo, B. Zhang, W. Yang, and Y. Cao, Blue light-emitting polymers containing fluorenebased benzothiophene-*S*,*S*-dioxide derivatives, *J. Mater. Chem. C*, **2016**, *4*, 1305–1312. DOI: 10.1039/c5tc03197d

30 G. M. Farinola, and R. Ragni, Electroluminescent materials for white organic light emitting diodes, *Chem. Soc. Rev.*, **2011**, *40*, 3467–3482. DOI: 10.1039/c0cs00204f

31 H. Cheun, X. Liu, F. J. Himpsel, M. Knaapila, U. Scherf, M. Torkkeli, and M. J. Winokur, Polarized optical absorption spectroscopy, NEXAFS, and GIXRD measurements of chain alignment in polyfluorene thin films, *Macromolecules*, **2008**, *41*, 6463–6472. DOI: 10.1021/ma702579r

32 R. C. Evans, A. G. Macedo, S. Pradhan, U. Scherf, L. D. Carlos, and H. D. Burrows, Fluorene based conjugated polyelectrolyte/silica nanocomposites: charge-mediated phase aggregation at the organic–inorganic interface, *Adv. Mater.*, **2010**, *22*, 3032–3037. DOI: 10.1002/adma.200904377

33 U. Scherf, and E. J. W. List, semiconducting polyfluorenes-towards relibale structure-poperty relationships, *Adv. Mater.*, **2002**, *14*, 477–487. DOI: 10.1002/1521-4095(20020404)14:7<477

34 A. J. Cadby, P. A. Lane, M. Wohlgenannt, C. An, Z. V. Vardeny, and D. D. C. Bradley, Optical studies of photoexcitations of poly(9,9-dioctylfluorene), *Synth. Metals*, **2000**, *111*, 515–518. DOI: 10.1016/S0379-6779(99)00409-9

35 Q. Pei, and Y. Yang, Efficient photoluminescence and electroluminescence from a soluble polyfluorene, *J. Am. Chem. Soc.*, **1996**, *118*, 7416–7417. DOI: 10.1021/ja9615233

36 M. Ranger, D. Rondeau, and M. Leclerc, New well-defined poly(2,7-fluorene) derivatives: photoluminescence and base doping, *Macromolecules*, **1997**, *30*, 7686–7691. DOI: 10.1021/ma970920a

37 S. B. Jhaveri, J. J. Peterson, and K. R. Carter, Organolithium-activated nickel (OLAN) catalysis: a new synthetic route for polyarylates, *Macromolecules*, **2008**, *41*, 8977–8979. DOI: 10.1021/ma801243x

38 R. M. Walczak, R. N. Brookins, A. M. Savage, E. M. van der Aa, and J. R. Reynolds, Convenient synthesis of functional polyfluorenes via a modified one-pot Suzuki-Miyaura condensation reaction, *Macromolecules*, **2009**, *42*, 1445–1447. DOI: 10.1021/ma802462v

39 M. Fukuda, K. Sawada, S. Morita, and K. Yoshino, Novel characteristics of conducting poly(9-alkylfluorene), poly(9,9-dialkylfluorene) and poly(1,10-bis(9′-alkylfluorenyl) alkane), *Synth. Metals*, **1991**, *41*, 855–858. DOI: 10.1016/0379-6779(91)91510-H)

40 M. Fukuda, K. Sawada, and K. Yoshino, Fusible conducting poly(9-alkylfluorene) and poly(9,9-dialkylfluorene) and their characteristics, *Jpn. J. Appl. Phys. Pt. 2 Letters*, **1989**, *28*, L 1433–L 1435.

41 T. Yamamoto, Electrically conducting and thermally stable pi-conjugated poly(arylene)s prepared by organometallic processes, *Prog. Polym. Sci.*, **1992**, *17*, 1153–1205. DOI: 10.1016/0079-6700(92)90009-N

42 M. Ranger, and M. Leclerc, Novel base-dopable poly(2,7-fluorenylene) derivatives, *Chem. Commun.*, **1997**, 1597–1598. DOI: 10.1039/A703076B

43 G. Klaerner, and R. D. Miller, polyfluorene derivatives: effective conjugation lengths from well-defined oligomers, *Macromolecules*, **1998**, *31*, 2007–2009. DOI: 10.1021/ma971073e

44 M. Fukuda, K. Sawada, and K. Yoshino, Synthesis of fusible and soluble conducting polyfluorene derivatives and their characteristics, *J. Polym. Sci., Part A: Polym. Chem.*, **1993**, *31*, 2465–2471. DOI: 10.1002/pola.1993.080311006

45 M. Kreyenschmidt, G. Klaerner, T. Fuhrer, J. Ashenhurst, S. Karg, W. D. Chen, V. Y. Lee, J. C. Scott, and R. D. Miller, Thermally stable blue-light-emitting copolymers of poly(alkylfluorene), *Macromolecules*, **1998**, *31*, 1099–1103. DOI: 10.1021/ma970914e

46 S. Janietz, D. D. C. Bradley, M. Grell, C. Giebeler, M. Inbasekaran, and E. P. Woo, Electrochemical determination of the ionization potential and electron affinity of poly(9,9-dioctylfluorene), *Appl. Phys. Lett.*, **1998**, *73*, 2453–2455. DOI: 10.1063/1.122479

47 M. Gaal, E. J. W. List, and U. Scherf, Excimers or emissive on-chain defects?, *Macromolecules*, **2003**, *36*, 4236–4237. DOI: 10.1021/ma021614m

48 Bliznyuk, V. N. Carter, S. Scott, J. C. Klärner, G. Miller, R. D. Miller, and D. C. Miller, Electrical and photoinduced degradation of polyfluorene based films and light-emitting devices, *Macromolecules*, **1999**, *32*, 361–369. DOI: 10.1021/ma9808979

49 G. Zeng, W.-L. Yu, S.-J. Chua, and W. Huang, Spectral and thermal spectral stability study for fluorene-based conjugated polymers, *Macromolecules*, **2002**, *35*, 6907–6914. DOI: 10.1021/ma020241m

50 X. Gong, P. K. Iyer, D. Moses, G. C. Bazan, A. J. Heeger, and S. S. Xiao, Stabilized blue emission from polyfluorene-based light-emitting diodes: elimination of flourenone defects, *Adv. Funct. Mater.*, **2003**, *13*, 325–330. DOI: 10.1002/adfm.200304279

51 A. Donat-Bouillud, I. Levesque, Y. Tao, M. D'Iorio, S. Beaupré, P. Blondin, M. Ranger, J. Bouchard, and M. Leclerc, light-emitting diodes from fluorene-based π-conjugated polymers, *Chem. Mater.*, **2000**, *12*, 1931–1936. DOI: 10.1021/cm0001298

52 I. Lévesque, A. Donat-Bouillud, Y. Tao, M. D'Iorio, S. Beaupré, P. Blondin, M. Ranger, J. Bouchard, and M. Leclerc, Organic tunable electroluminescent diodes from polyfluorene derivatives, *Synth. Metals*, **2001**, *122*, 79–81. DOI: 10.1016/S0379-6779(00)01368-0

53 S. Beaupré, and M. Leclerc, Optical and electrical properties of π-conjugated polymers based on electron-rich 3,6-dimethoxy-9,9-dihexylfluorene unit, *Macromolecules*, **2003**, *36*, 8986–8991. DOI: 10.1021/ma035064j

54 J. Zhang, S. Dong, K. Zhang, A. Liang, X. Yang, F. Huang, and Y. Cao, A series of blue supramolecular polymers with different counter ions for polymer light-emitting diodes, *Chem. Commun.*, **2014**, *50*, 8227–8230. DOI: 10.1039/c4cc03080j

55 C. D. Muller, A. Falcou, N. Reckefuss, M. Rojahn, V. Wiederhirn, P. Rudati, H. Frohne, O. Nuyen, H. Becker, and K. Meerholz, Multi-colour organic light-emitting displays by solution processing, *Nature*, **2003**, *421*, 829–833. DOI: 10.1038/nature01390

56 Y. Li, J. Ding, M. Day, Y. Tao, J. Lu, and M. Diorio, Synthesis and properties of random and alternating fluorene/carbazole copolymers for use in blue light-emitting devices, *Chem. Mater.*, **2004**, *16*, 2165–2173. DOI: 10.1021/cm030069g

57 I. I. Perepichka, I. F. Perepichka, M. R. Bryce, and L.-O. Pälsson, Dibenzothiophene-*S*,*S*-dioxide–fluorene co-oligomers. Stable, highly-efficient blue emitters with improved electron affinity, *Chem. Commun.*, **2005**, *1*, 3397–3399. DOI: 10.1039/b417717g

58 F. Yang, K. Sun, Z. J. Cao, Z. H. Li, and M. S. Wong, Synthesis and functional properties of oligofluorenyl-dibenzothiophene-*S*,*S*-dioxides end-capped by diphenylamine moieties, *Synth. Metals*, **2008**, *158*, 391–395. DOI: 10.1016/j.synthmet.2008.02.012

59 S. Fujii, Z. Duan, T. Okukawa, Y. Yanagi, A. Yoshida, T. Tanaka, G. Zhao, Y. Nishioka, and H. Kataura, Synthesis of novel thiophenephenylene oligomer derivatives with a dibenzothiophene-5,5-dioxide core for use in organic solar cells, *Phys. Status Solidi*, **2012**, *B249*, 2648–2651. DOI: 10.1002/pssb.201200439

60 F. B. Dias, K. N. Bourdakos, V. Jankus, K. C. Moss, K. T. Kamtekar, V. Bhalla, J. Santos, M. R. Bryce, and A. P. Monkman, triplet harvesting with 100% efficiency by way of thermally activated delayed fluorescence in charge transfer OLED emitters, *Adv. Mater.*, **2013**, *25*, 3707–3714. DOI: 10.1002/adma.201300753

61 X. Zhan, Z. Wu, Y. Lin, S. Tang, J. Yang, J. Hu, Q. Peng, D. Ma, Q. Lia, and Z. Li, New AIEgens containing dibenzothiophene-*S*,*S*-dioxide and tetraphenylethene moieties: similar structures but very different hole/electron transport properties, *J. Mater. Chem. C*, **2015**, *3*, 5903–5909. DOI: 10.1039/c5tc01028d

62 C. Fan, C. Duan, Y. Wei, D. Ding, H. Xu, and W. Huang, dibenzothiophene-based phosphine oxide host and electron-transporting materials for efficient blue thermally activated delayed fluorescence diodes through compatibility optimization, *Chem. Mater.*, **2015**, *27*, 5131−5140. DOI: 10.1021/acs.chemmater.5b02012

63 R. Grisorio, C. Piliego, P. Cosma, P. Fini, P. Mastrorilli, G. Gigli, G. P. Suranna, and C. F. Nobile, Random poly(fluorenylene-vinylene)s containing 3,7-dibenzothiophene-5,5-dioxide units: synthesis, photophysical, and electroluminescence properties, *J. Polym. Sci., Part A: Polym. Chem.*, **2009**, *47*, 2093–2104. DOI: 10.1002/pola.23291

64 R. He, J. Xu, Y. Yang, P. Cai, D. Chen, L. Ying, W. Yang, and Y. Cao, Dibenzothiophene-*S*,*S*-dioxide based medium-band-gap polymers for efficient bulk heterojunction solar cells, *Org. Electronics*, **2014**, *15*, 2950–2958. DOI: 10.1016/j.orgel.2014.08.026

65 Y. Wang, Y. Gao, L. Chen, Y. Fu, D. Zhu, Q. He, H. Cao, J. Cheng, R. Zhang, S. Zheng, and S. Yan, Fluorescent diphenylfluorene-pyrenyl copolymer with dibenzothiophene-*S*,*S*-dioxide and adamantane units for explosive vapor detection, *RSC Adv.*, **2015**, *5*, 4853–4860. DOI: 10.1039/c4ra12966k

66 S. M. King, I. I. Perepichka, I. F. Perepichka, F. B. Dias, M. R. Bryce, and A. P. Monkman, Exploiting a dual-fluorescence process in fluorene–dibenzothiophene-*S*,*S*-dioxide co-polymers to give efficient single polymer LEDs with broadened emission, *Adv. Funct. Mater.*, **2009**, *19*, 586–591. DOI: 10.1002/adfm.200801237

67 D. W. Bright, K. C. Moss, K. T. Kamtekar, M. R. Bryce, and A. P. Monkman, The β phase formation limit in two poly(9,9-di-n-octylfluorene) based copolymers, *Macromol. Rapid Commun.*, **2011**, *32*, 983–987. DOI: 10.1002/marc.201100221

68 Y. Yang, L. Yu, Y. Xue, Q. Zou, B. Zhang, L. Ying, W. Yang, J. Peng, and Y. Cao, Improved electroluminescence efficiency of polyfluorenes by simultaneously incorporating dibenzothiophene-*S*,*S*-dioxide unit in main chain and oxadiazole moiety in side chain, *Polymer*, **2014**, *55*, 1698–1706. DOI: 10.1016/j.polymer.2014.02.032

69 R. He, S. Hu, J. Liu, L. Yu, B. Zhang, N. Li, W. Yang, H. Wu, and J. Peng, Bipolar blue-emitting poly(N-9-heptadecanyl-carbazole-2,7-diyl-codibenzothiophene-*S*,*S*-dioxide-3,7-diyl)s, *J. Mater. Chem.*, **2012**, *22*, 3440–3446. DOI: 10.1039/c2jm14926e

70 P. Camurlu, T. Durak, and L. Toppare, Solution processable donor acceptor type dibenzothiophen-*S*,*S*-dioxide derivatives for electrochromic applications, *J. Electroanal. Chem.*, **2011**, *661*, 359–366. DOI: 10.1016/j.jelechem.2011.08.018

71 C.-L. Ho, S.-Y. Poon, P.-K. Lo, M.-S. Wong, and W.-Y. Wong, Synthesis, characterization and photophysical properties of metallopolyynes and metallodiynes of platinum(II) with dibenzothiophene derivatives, *J. Inorg. Organomet. Polym.*, **2013**, *23*, 206–215. DOI 10.1007/s10904-012-9761-1

72 C. Li, Y. Wang, D. Sun, H. Li, X. Sun, D. Ma, Z. Ren, and S. Yan, Thermally Activated Delayed Fluorescence Pendant Copolymers with Electron- and Hole-Transporting Spacers, *ACS Appl. Mater. Interfaces*, **2018**, *10*, 5731–5739. DOI: 10.1021/acsami.8b00136

73 X. Wang, L. Zhao, S. Shao, J. Ding, L. Wang, X. Jing, and F. Wang, Poly(spirobifluorene)s containing nonconjugated diphenylsulfone moiety: toward blue emission through a weak charge transfer effect, *Macromolecules*, **2014**, *47*, 2907−2914. DOI: 10.1021/ma500407m

74 H. Xiao, L. Yu, Y. Li, W. Yang, B. Zhang, W. Yang, H. Wu, and Y. Cao, Novel green light-emitting polyfluorenes containing dibenzothiophene-*S*,*S*-dioxide-arylamine derivatives, *Polymer*, **2012**, *53*, 2873–2883. DOI: 10.1016/j.polymer.2012.05.011

75 A. Li, Y. Li, W. Cai, G. Zhou, Z. Chen, H. Wua, W.-Y. Wong, W. Yang, J. Peng, and Y. Cao, Realization of highly efficient white polymer light-emitting devices via interfacial energy transfer from poly(N-vinylcarbazole), *Org. Electronics*, **2010**, *11*, 529–534. DOI: 10.1016/j.orgel.2009.12.008

76 F. B. Dias, S. King, A. P. Monkman, I. I. Perepichka, M. A. Kryuchkov, I. F. Perepichka, and M. R. Bryce, Dipolar stabilization of emissive singlet charge transfer excited states in polyfluorene copolymers, *J. Phys. Chem. B*, **2008**, *112*, 6557–6566. DOI: 10.1021/jp800068d

77 F. Terenziani, A. Painelli, C. Katan, M. Charlot, and M. Blanchard-Desce, Charge Instability in Quadrupolar Chromophores: Symmetry Breaking and Solvatochromism, *J. Am. Chem. Soc.*, **2006**, *128*, 15742–15755. DOI: 10.1021/ja064521j

78 D. F. Perepichka, I. F. Perepichka, H. Meng, and F. Wudl, Light- Emitting Polymers. In Organic Light-Emitting Materials and Devices, Z. Li, and H. Meng, Eds., *CRC Press: Boca Raton, FL*, **2007**, *Chapter 2*, 45–293.

79 S. M. King, I. I. Perepichka, I. F. Perepichka, F. B. Dias, M. R. Bryce, and A. P. Monkman, Exploiting a dual-fluorescence process in fluorene dibenzothiophene-*S*,*S*-dioxide co-polymers to give efficient single polymer LEDs with broadened emission, *Adv. Funct. Mater.*, **2009**, *19*, 586–591. DOI: 10.1002/adfm.200801237

80 J. Liu, J. Zou, W. Yang, H. Wu, C. Li, B. Zhang, J. Peng, and Y. Cao, Highly efficient and spectrally stable blue-light-emitting polyfluorenes containing a dibenzothiophene-*S*,*S*-dioxide unit, *Chem. Mater.*, **2008**, *20*, 4499–4506. DOI: 10.1021/cm800129h

81 N. Nemoto, H. Kameshima, Y. Okano, and T. Endo, Synthesis of novel π-conjugating polymers based on dibenzothiophene, *J. Polym. Sci., Part A: Polym. Chem.*, **2003**, *41*, 1521–1526. DOI: 10.1002/pola.10693

82 L. Yu, J. Liu, S. Hu, R. He, W. Yang, H. Wu, J. Peng, R. Xia, and D. D. C. Bradley, Red, green, and blue light-emitting polyfluorenes containing a dibenzothiophene-*S*,*S*-dioxide unit and efficient high-color-rendering-index white-light-emitting diodes made therefrom, *Adv. Funct. Mater.*, **2013**, *23*, 4366–4376. DOI: 10.1002/adfm.201203675

83 L. Li, L. Jie, Z. Yuhao, H. Liwen, G. Ting, Y. Wei and C. Yong, Bipolar Blue Light-emitting Polyfluorenes Containing Dibenzothiophene-*S*,*S*-dioxide/Carbazole Units, *Chem. Res. Chin. Univ.*, **2018**, *34(3)*, 506–512. DOI: 10.1007/s40242-018-7311-2

84 L. Hu, L. Liang, Y. Yang, T. Guo, Y. Zhang, W. Yang, and Y. Cao, Green-emitting Polyfluorenes Containing Hexylthiophen-dibenzothiophene-*S*,*S*-dioxide Unit with Large Two-photon Absorption Cross Section, *Chinese J. Polym. Sci.*, **2018**, *36*, 546–554. DOI: 10.1007/s10118-018-2017-y

85 S. Zhao, J. Liang, T. Guo, Y. Wang, X. Chen, D. Fu, J. Xiong, L. Ying, W. Yang, J. Peng, and Y. Cao, Formation of poly(9,9-dioctylfluorene) β-phase by incorporating aromatic moiety in side chain, *Organic Electronics*, **2016**, *38*, 130–138. DOI: 10.1016/j.orgel.2016.08.007

86 Y. Fang, J. Liu, Y. Zhang, T. Guo, F. Huang, W. Yang, and Y. Cao, Blue light-emitting polyfluorenes containing dibenzothiophene-*S*,*S*-dioxide unit in alkyl side chain, *Sci China Chem*, **2017**, *60*, 1356–1366. DOI: 10.1007/s11426-017-9100-0

87 F. Peng, T. Guo, L. Ying, W. Yang, J. Peng, and Y. Cao, Improving electroluminescent performance of blue light-emitting poly(fluorene-co-dibenzothiophene-*S*,*S*-dioxide) by end-capping, *Organic Electronics*, **2017**, *48*, 118–126. DOI: 10.1016/j.orgel.2017.05.037

88 R. Ancora, F. Babudri, G. M. Farinola, F. Naso, and R. Ragni, Synthesis of conjugated polymers by coupling between arenediazonium tetrafluoroborates and vinyl silanes, *Eur. J. Org. Chem.*, **2002**, 4127–4130. DOI: 10.1002/1099-0690(200212)2002:24<4127

89 J. Yang, L. Zhao, X. Wang, S. Wang, J. Ding, L. Wang, X. Jing, and F. Wang, Green-light-emitting poly(spirobifluorene)s with an electron-rich unit in the side chain and an electron-defi cient unit in the main chain, *Macromol. Chem. Phys.*, **2014**, *215*, 1107−1115. DOI: 10.1002/macp.201400046

90 T. Guo, L. Yu, B. Zhao, L. Ying, H. Wu, W. Yang, and Y. Cao, Blue light-emitting hyperbranched polymers using fluorene-co-dibenzothiophene-*S*,*S*-dioxide as branches, *J. Polym. Sci., Pt A: Polym. Chem.*, **2015**, *53*, 1043–1051. DOI: 10.1002/pola.27532

91 H. Ye, B. Zhao, D. Li, D. Chen, G. Xie, S.-J. Su, W. Yang, and Y. Cao, Highly efficient non-doped single-layer blue organic light-emitting diodes based on light-emitting conjugated polymers containing trifluoren-2-ylamine and dibenzothiophene-*S*,*S*-dioxide, *Synth. Metals*, **2015**, *205*, 228–235. DOI: 10.1016/j.synthmet.2015.04.008

92 K. T. Kamtekar, H. L. Vaughan, B. P. Lyons, A. P. Monkman, S. U. Pandya, and M. R. Bryce, Synthesis and spectroscopy of poly(9,9-dioctylfluorene-2,7-diyl-co-2,8-dihexyldibenzothiophene-*S*,*S*-dioxide-3,7-diyl)s: solution-processable, deep-blue emitters with a high triplet energy, *Macromolecules*, **2010**, *43*, 4481–4488. DOI: 10.1021/ma100566p

93 J. H. Cook, J. Santos, H. Li, H. A. Al-Attar, M. R. Bryce, and A. P. Monkman, Efficient deep blue fluorescent polymer light emitting diodes (PLEDs), *J. Mater. Chem. C*, **2014**, *2*, 5587–5592. DOI: 10.1039/c4tc00896k

94 H. Xiao, J. Miao, J. Cao, W. Yang, H. Wu, and Y. Cao, Alcohol-soluble polyfluorenes containing dibenzothiophene-*S*,*S*-dioxide segments for cathode interfacial layer in PLEDs and PSCs, *Org. Electronics*, **2014**, *15*, 758–774. DOI: 10.1016/j.orgel.2014.01.006

95 K. C. Moss, K. N. Bourdakos, V. Bhalla, K. T. Kamtekar, M. R. Bryce, M. A. Fox, H. L. Vaughan, F. B. Dias, and A. P. Monkman, Tuning the intramolecular charge transfer emission from deep blue to green in ambipolar systems based on dibenzothiophene-*S*,*S*-dioxide by manipulation of conjugation and strength of the electron donor units, *J. Org. Chem.*, **2010**, *75*, 6771–6781. DOI: 10.1021/jo100898a

96 T.-H. Huang, J. T. Lin, L.-Y. Chen, Y.-T. Lin, and C.-C. Wu, Dipolar dibenzothiophene-*S*,*S*-dioxide derivatives containing diarylamine: materials for single-layer organic light-emitting devices, *Adv. Mater.*, **2006**, *18*, 602–606. DOI: 10.1002/adma.200502078

97 T.-H. Huang, W.-T. Whang, J. Y. Shen, Y.-S. Wen, J. T. Lin, T.-H. Ke, L.-Y. Chen, and C.-C. Wu, Dibenzothiophene/oxide and quinoxaline/pyrazine derivatives serving as electron-transport materials, *Adv. Funct. Mater.*, **2006**, *16*, 1449–1456. DOI: 10.1002/adfm.200500823

98 S. Kommanaboyina, Conjuated Polymers Based on 4-Substituted Fluorenes and Fluorenones, PhD Thesis, Bangor University, **2016**.

# CHAPTER 2

# Synthesis of 1-Substituted-3,7-Dibromodibenzothiophene-*S,S*-dioxide as Monomers for 1-Functionalised Dibenzothiophene-*S,S*-dioxide Homo and Co-polymers

## 2.1 Introduction

Since the first important paper introducing dibenzothiophene-*S,S*-dioxide as a versatile building block for conjugated organic molecules and polymers for organic electronics,[1] more than 400 papers have been published reporting different variations in structures, studies on their optoelectronic properties and testing the materials in various devices (mainly in OLEDs, but applications in other devices have also been studied).

In 2010, Bryce's group reported the synthesis of a series of co-polymers by incorporating 3,7-dibromo-2,8-dihexyldibenzothiophene-*S,S*-dioxide **1.56** with a fluorene unit *via* a Suzuki polycondensation reaction.[2] The synthetic route to monomer moiety **1.56** is described in **Scheme 2.1**. 2,8-Dibromodibenzothiophene **1.54** underwent halogen-lithium exchange with *n*-hexyllithium and subsequent quenching with *n*-bromohexane to yield the dihexylated product which was oxidized in *situ* with refluxing hydrogen peroxide in acetic acid to give sulfone derivative **1.55**. Compound **1.55** was then brominated with *N*-bromosuccinimide (NBS) in sulfuric acid to yield monomer **1.56**.[2]

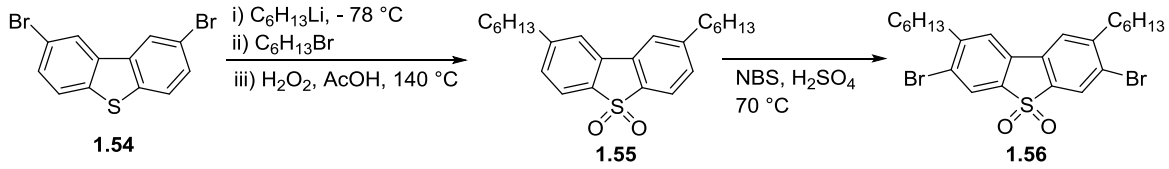


**1.54** **1.55** **1.56**

**Scheme 2.1:** Synthetic route to monomer **1.56**.[2]

The dibenzothiophene-*S*,*S*-dioxide moiety is topologically similar to fluorene. However, fluorene can be easily functionalised at the 9- position, which brings solubility to the materials. Dibenzothiophene-*S*,*S*-dioxide itself shows lower solubility than fluorene and even in the case of its co-polymers with dialkylfluorenes, the amount of incorporated dibenzothiophene-*S*,*S*-dioxide units cannot normally exceed 25–30% (for 2,8-dialky- or 2,8-dialkoxydibenzothiophene-*S*,*S*-dioxide moieties it can be higher, but such substitution decreases the effective conjugation length of the copolymers due to steric interactions in the main chain).[3,4]

### 2.1.1 Aims of the Chapter

The main objective of the research described in this chapter was elaboration of convenient synthetic methods for the synthesis of monomers **Br$_2$S-R** which will be used for the synthesis of homopolymers (Chapter 3) and co-polymers (Chapter 4) respectively. The route used for the synthesis of these monomers proceeded *via* the key intermediate 1-$NH_2$-3,7-dibromodibenzothiophene-*S*,*S*-dioxide (**Br$_2$S-NH$_2$**). This intermediate was prepared from **Br$_2$S** by a nitration reaction to give **Br$_2$S-NO$_2$**, which could then be converted to the required compound by reduction with tin powder. Having this intermediate in hand access to a wide range of monomers was possible *via* diazonium chemistry (**Scheme 2.2**).

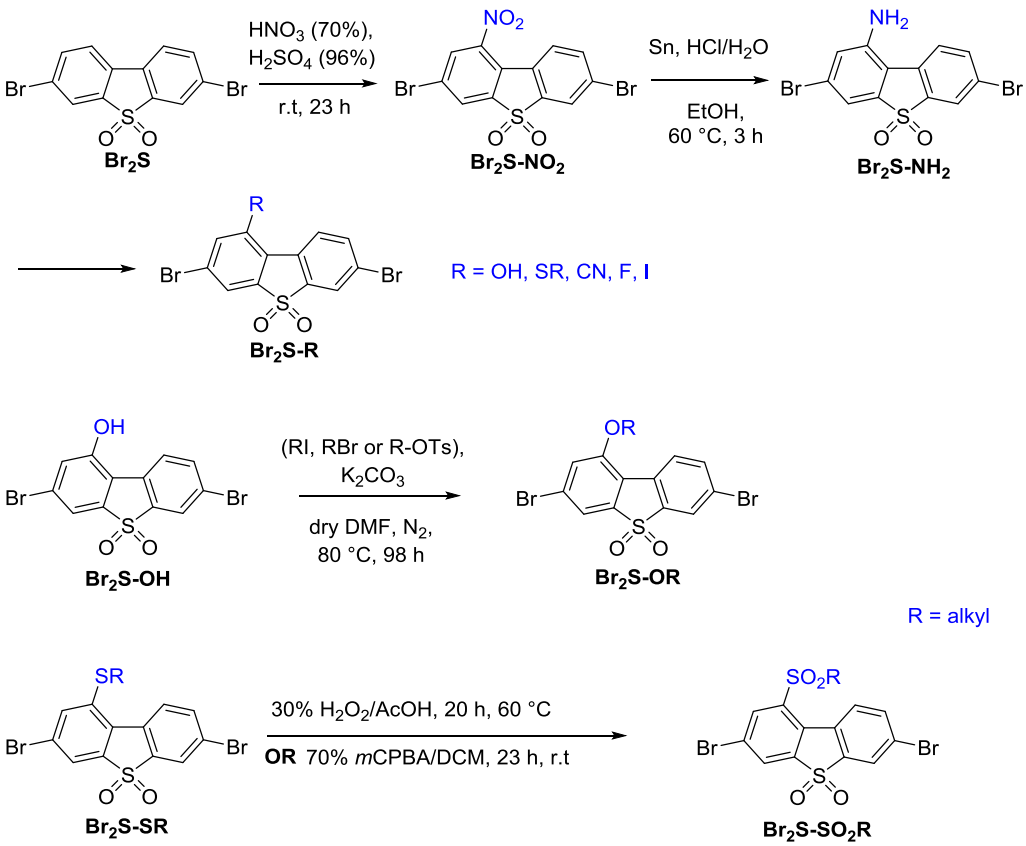


**Scheme 2.2:** Describing the substitution at position 1.

Having prepared **Br2S-OH**, and **Br2S-SR** these monomers can then be converted into the alkoxy and alkylsulfonyl analogues, **Br2S-OR** and **Br2S-SO2R**. All the monomers can then be used for the synthesis of homopolymers and co-polymers as will be discussed in later chapters.

## 2.2 Results and Discussion

### 2.2.1 Synthesis of key intermediate 1-amino-3,7-dibromodibenzothiophene-*S*,*S*-dioxide (**Br$_2$S-NH$_2$**)

For the synthesis of 1-substituted dibenzothiophene-*S*,*S*-dioxide based polymers and copolymers the corresponding 1-R-3,7-dibromodibenzothiophene-*S*,*S*-dioxide monomers needed to be prepared, which can be then polymerized by Ni-mediated or Pd-catalyzed C-C coupling methods. To access such monomers, appropriate methods of functionalisation of 3,7-dibromodibenzothiophene-*S*,*S*-dioxide (**Br$_2$S**) at position 1 were utilised. Considering 1-amino-3,7-dibromodibenzothiophene-*S*,*S*-dioxide (**Br$_2$S-NH$_2$**) as a useful synthon, it can then be converted into a wide range of 1-substituted dibenzothiophene-*S*,*S*-dioxide monomers *via* diazonium chemistry.[5] The multistep reaction route to the key intermediate, **Br$_2$S-NH$_2$**, from commercially available dibenzothiophene **2.1** is shown in **Scheme 2.3**. Attention was also paid to scaling up the reactions and optimisation of the conditions, to elaborate convenient and efficient methods of their synthesis and purification.

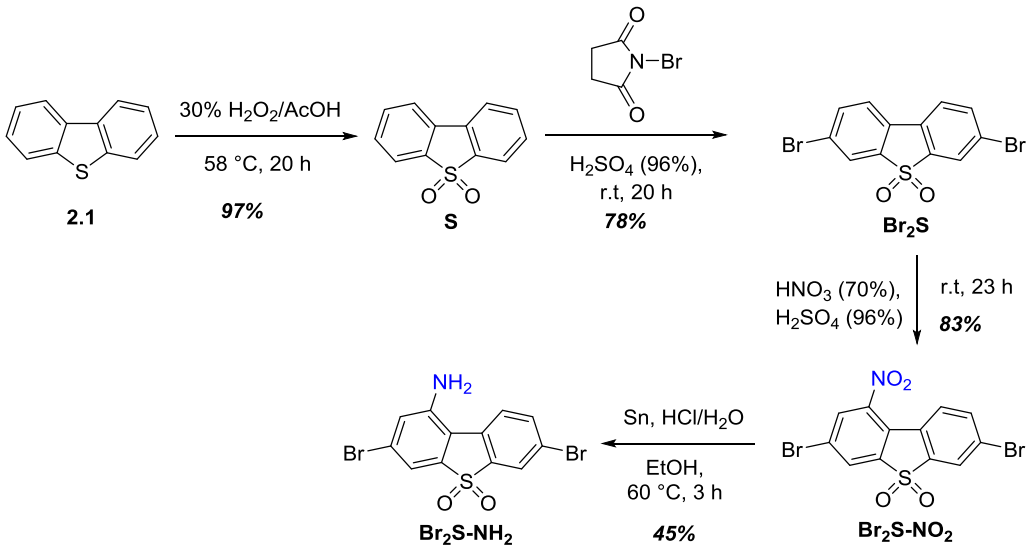


**Scheme 2.3:** Synthetic route to 1-amino-3,7-dibromodibenzothiophene-*S*,*S*-dioxide **(Br$_2$S-NH$_2$)**.

Dibenzothiophene-*S*,*S*-dioxide (**S**) was synthesised according to the literature[6] by oxidation of dibenzothiophene **2.1** with $H_2O_2$ in acetic acid on a large scale (200 g) and gave almost pure product (according to $^1$H NMR spectroscopy) in 97% yield. Bromination of **S**

with *N*-bromosuccinimide (NBS) in concentrated sulfuric acid at room temperature, according to a previously described method,[1] gave 3,7-dibromodibenzothiophene-*S*,*S*-dioxide (**Br$_2$S**) as the major product (see **Scheme 2.3**), which could be easily separated (due to its low solubility) from other isomers (mono-, tri- and tetra-brominated products) by direct filtration from the reaction mixture. This reaction was performed on a scale of up to 120 g of **S**, to give **Br$_2$S** in yields of *ca.* 78% after two recrystallisations (from acetic acid and then from chlorobenzene). This reaction was repeated four times, on a large scale, to obtain sufficient amounts of **Br$_2$S** for further studies.

The nitration of **Br$_2$S** was studied in a mixture of concentrated (70%) or fuming (90 %) $HNO_3$ with concentrated (96%) $H_2SO_4$ at ambient or elevated temperatures (see **Scheme 2.3**), varying the ratio of reagents and the reaction time. Initial experiments on a gram scale (or below) showed that nitration occurs at the desired 1- position of the dibenzothiophene-*S*,*S*-dioxide moiety, but the product was contaminated by the starting material **Br$_2$S** and by some by-products (presumably dinitro-compounds) and possibly other mono-nitrated isomers, according to $^1$H NMR analysis of the crude material. While by-products can be relatively easily removed by recrystallisation from appropriate solvents (toluene, AcOH, $CHCl_3$ and dioxane were tested, among which dioxane showed the best results), removal of the starting **Br$_2$S** was more difficult due to its low solubility and co-crystallisation with the product. Column purification was also problematic due to the close $R_f$ of **Br$_2$S-NO$_2$** and **Br$_2$S**. In addition, flash chromatography was an unsuitable method for a large scale (>10 g) purification.

Therefore, an optimisation of this reaction was performed varying the amounts of $HNO_3$/$H_2SO_4$, concentrations and the reaction time, and analysing the yields and the purities of the crude products. From these studies reasonably good conditions for the selective mono-nitration were found, with high yields of ~95% for the crude product, which had a purity of 85–90% (according to $^1$H NMR and GC-MS data). To optimise the reaction time further, the reaction was monitored by taking samples of the reaction mixture and analysing them by GC-MS (both the disappearance of **Br$_2$S** and the appearance of **Br$_2$S-NO$_2$** were monitored). These kinetic studies showed that the reaction is nearly finished after 24 h at ambient temperature (reaction half-time, $t_{1/2}$ is ~2–2.5 h). However, because the reaction is heterogeneous, the concentration of the starting **Br$_2$S** did not go to zero at $10t_{1/2}$ and *ca.* 5% of the starting **Br$_2$S** was still present in the mixture. An increase in reaction time led to

substantial formation of by-products (dinitration), but did not lead to the complete disappearance of the starting **$Br_2S$**.

The results were somewhat improved by using finely powdered **$Br_2S$** and vigorously stirring the reaction mixture. Eventually, the reaction was scaled up to ~160 g of starting material, **$Br_2S$**, and the desired **$Br_2S$-$NO_2$** was obtained in high yields (~97–98%) and reasonably high purity (~96% as shown by $^1$H NMR spectroscopy) after recrystallisation in dioxane **$Br_2S$-$NO_2$** was obtained in 83% yield and high purity 99% as shown by $^1$H NMR spectroscopy (see **Figure 2.1**, and Appendix 6.1 for more information). **Figure 2.1** shows the $^1$H NMR spectrum of the aromatic region for both the starting compound **$Br_2S$** and the target product **$Br_2S$-$NO_2$** which demonstrated three environments for the starting compound and five environments for the product. It also shows that the protons at positions 2 and 4 (*ortho* and *para* position relative to the **$NO_2$** group) are highly shifted downfield due to the **$NO_2$** group, which is a strong electron withdrawing group and therefore causes deshielding around the protons and hence shifting the signal downfield.

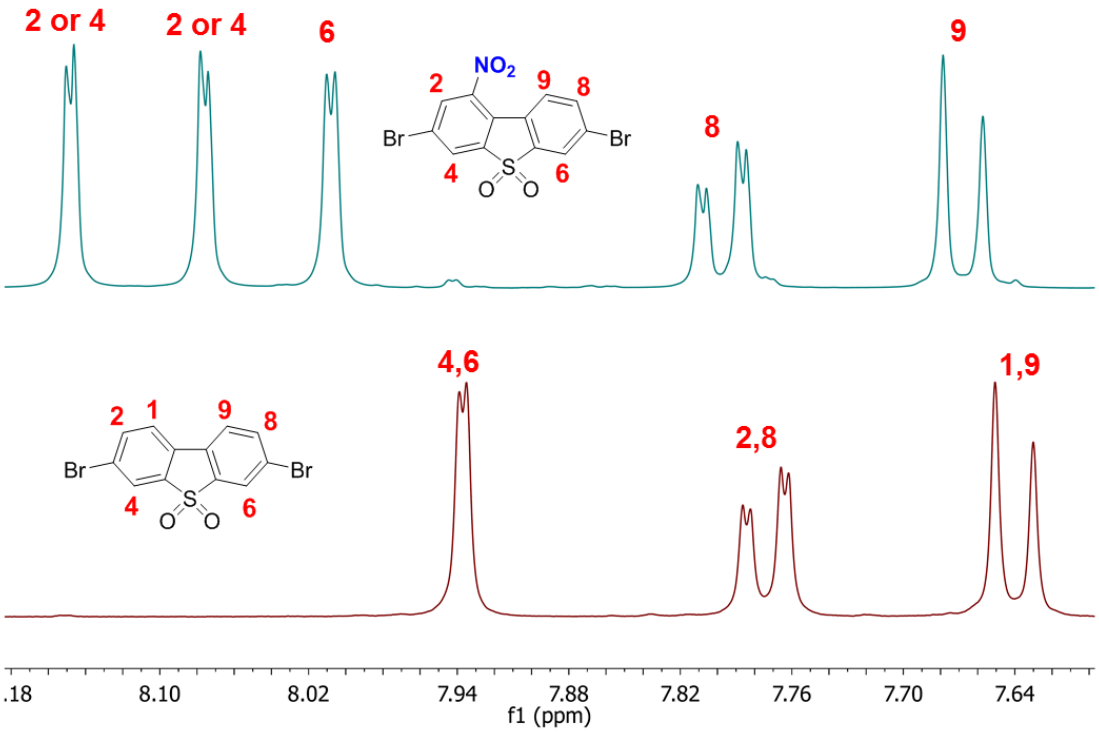


**Figure 2.1:** $^{1}$H NMR spectrum of 3,7-dibromo dibenzothiophene-*S*,*S*-dioxide (**Br$_2$S**) (bottom), and 1-nitro-3,7-dibromo dibenzothiophene-*S*,*S*-dioxide (**Br$_2$S-NO$_2$**) (top), with signal assignments.

Nitro groups in nitro aromatic compounds can be reduced to an amino group by using hydrogen in the presence of palladium on carbon (Pd/C) as a catalyst and generally the reaction proceeds efficiently giving arylamines with high yields (up to 100%).[7] Before carrying out the reduction of the **Br$_2$S-NO$_2$** compound the reduction of **Br$_2$S** was carried out in order to determine the stability of the Br and sulfonyl groups under the reaction conditions. Due to the low solubility of **Br$_2$S** in common solvents used for Pd/C–$H_2$ reduction (very low solubility in ethylacetate, insoluble in alcohols), the reaction was performed in dioxane at 40 °C where it is partly soluble. The **Br$_2$S** suspension (partly soluble) in dioxane was stable when stirred with Pd/C under a hydrogen atmosphere during the first day, however prolonged stirring at 40 °C indicated the formation of a product (second spot on TLC, - perhaps, reduction of the $SO_2$ group or debromination; $^{1}$H NMR spectroscopy also showed signals from an unidentified product apart from the starting **Br$_2$S**). Reduction of **Br$_2$S-NO$_2$** with 10% Pd/C under a hydrogen atmosphere gave a brown powder,

which represented a complex mixture (TLC, $^1$H NMR), from which the isolation of the target **Br$_2$S-NH$_2$** was problematic (see **Scheme 2.4** below).

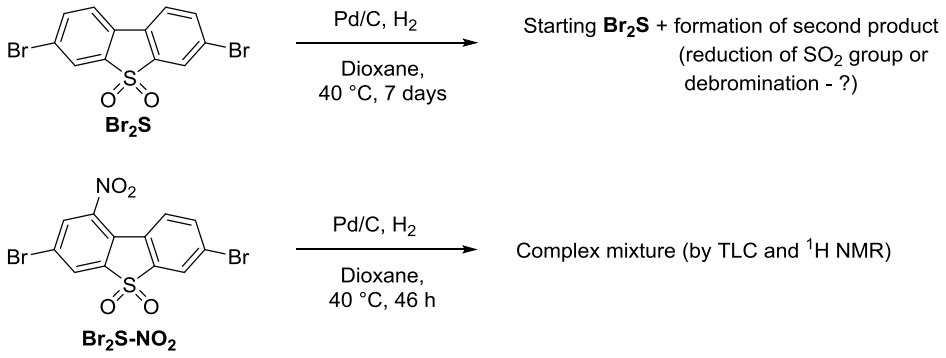


**Scheme 2.4:** Testing the stability of **Br$_2$S** in $H_2$–Pd/C system and an attempt to reduce the nitro group in **Br$_2$S-NO$_2$** using palladium on carbon and hydrogen.

Thus, it was decided not to continue an optimisation of this reaction but instead turn to using a reduction by another common method, namely by using tin powder–hydrochloric acid in an ethanol-water system. This reaction works well in many cases and it has been used for the reduction of nitrofluorenes to aminofluorenes.[8,9] Reduction of nitrofluorenes by Sn/HCl in ethanol was completed in 2–4 hours and the stability of **Br$_2$S** was tested under these conditions. Even with a high excess of tin and prolonged stirring under reflux no transformation of **Br$_2$S** was observed (monitoring by TLC) and the starting material was recovered (confirmed by $^1$H NMR spectroscopy; **Scheme 2.5**).

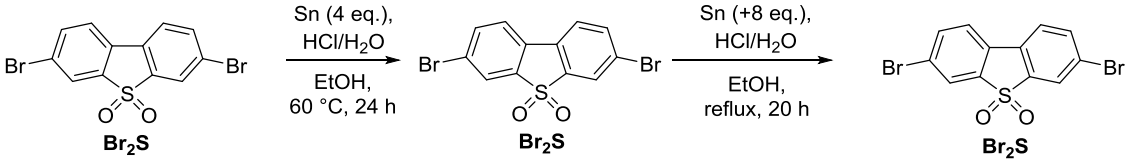


**Scheme 2.5:** Testing the stability of **Br$_2$S** in Sn/HCl/EtOH-$H_2O$ system.

Having established the stability of the **Br$_2$S** compound under the above reaction conditions the reduction of **Br$_2$S-NO$_2$** using tin powder (4–5 eq.)/concentrated HCl in an EtOH–$H_2O$ mixture at 60 °C was carried out and the reaction proceeded smoothly and was

completed in 3–4 hours to give 1-amino-3,7-dibromodibenzothiophene-*S*,*S*-dioxide (**Br$_2$S-NH$_2$**) (**Scheme 2.3, Page 55**). In small scale reactions, after basification and extraction of the product with ethyl acetate, it was purified by column chromatography to give analytically pure samples. However, this workup and purification method were found to be unsuitable for scaling up. Therefore, finding a different procedure for isolation and purification of **Br$_2$S-NH$_2$** was important. After completion of the reduction, the mixture was basified with sodium carbonate to adjust the pH to 9 and the solution was evaporated to dryness. The residue was transferred into a soxhlet apparatus with a ~6 – 7 cm silica gel layer on the bottom and **Br$_2$S-NH$_2$** was extracted with tetrahydrofuran (thus passing the extract through the silica gel layer) for ~20–30 h. The extracted crude product was then recrystallised twice from dioxane to afford **Br$_2$S-NH$_2$** in ~45% yield and ~96% purity according to $^1$H NMR spectroscopy. This method for the synthesis and purification showed reproducible results on a ~100 g scale synthesis (in smaller scale syntheses (~10 g) the yields were somewhat higher, ~70%).

Thus, efficient synthetic methods to afford the **Br$_2$S-NH$_2$** intermediate have been developed and scaled up to hundred(s) gram syntheses under laboratory conditions.

### 2.2.2 Transformation of 1-amino-3,7-dibromodibenzothiophene-*S*,*S*-dioxide using diazonium chemistry

This section describes the transformation of **Br$_2$S-NH$_2$** into 4 other 1-substituted dibenzothiophene-*S*,*S*-dioxides, replacing the amino group (*via* diazonium salts) by an **OH**, **CN**, **I** and **F** group (**Scheme 2.6**). 1-Hydroxy-3,7-dibenzothiophene-*S*,*S*-dioxide (**Br$_2$S-OH**) was synthesised with the aim of preparing the first series of soluble dibenzothiophene-*S*,*S*-dioxide homopolymers, named poly(1-alkoxydibenzothiophene-*S*,*S*-dioxides) (see Section 2.2.3 and Chapter 3). Two other compounds, **Br$_2$S-CN** and **Br$_2$S-F** have been prepared for the synthesis of novel fluorene–dibenzothiophene-*S*,*S*-dioxide copolymers, structurally similar to the previously reported copolymers **1.26–1.29** described in Chapter 1, which showed broadened simultaneous emission from both local excited (LE) and intramolecular charge transfer (ICT) states and have been shown to be promising materials for the development of white light-emitting polymers for WPLEDs.[10,11] The introduction of electron withdrawing groups (EWG) into the **S** moiety in such types of copolymers should

increase the contribution from ICT emission leading to polymers with emissions shifted from greenish-white (**Figure 1.19**, Chapter 1) to CIE coordinates closer to the white point. In addition, **Br$_2$S-OMe**, **Br$_2$S-SMe**, and **Br$_2$S-SO$_2$Me** were synthesised for the same reason as will be described in the next sections. On the other hand, **Br$_2$S-I** and all other monomers **Br$_2$S-R** were prepared to use in the synthesis of new thermal activated delayed fluorescence (TADF) molecules.

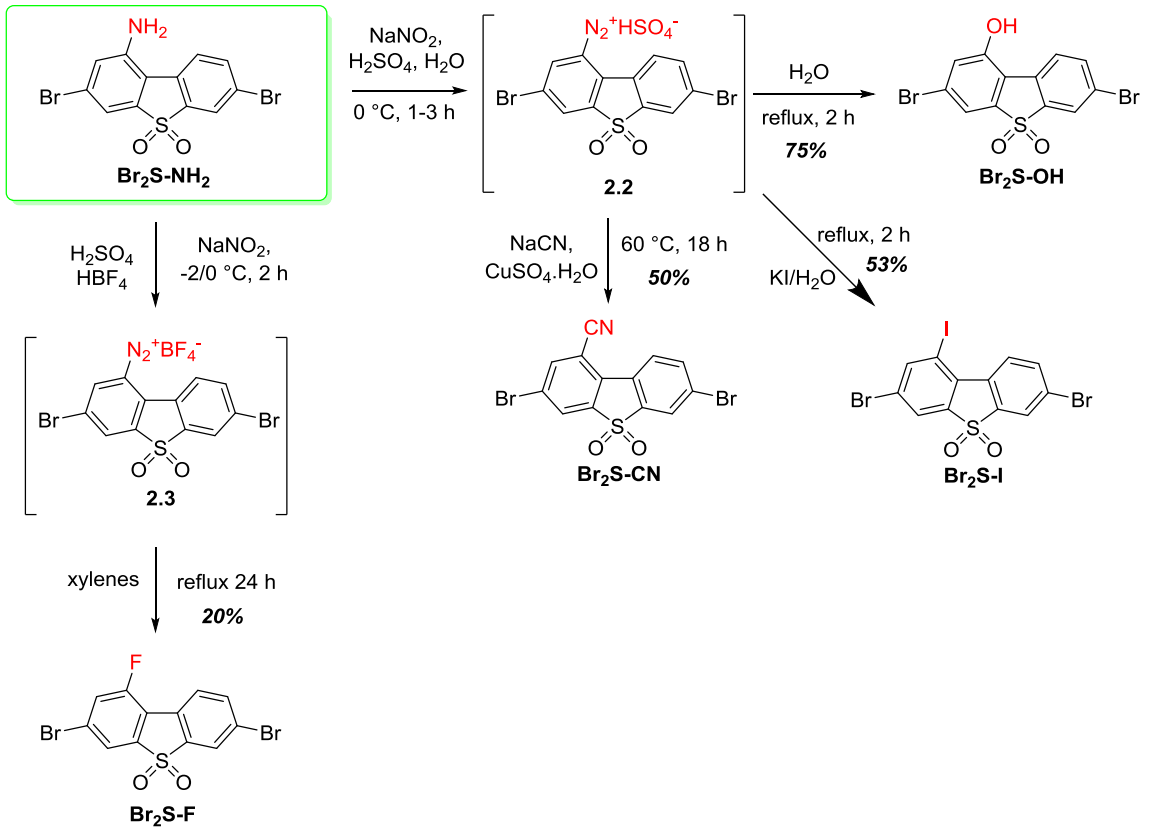


**Scheme 2.6:** Synthetic routes to 1-substituted 3,7-dibromodibenzothiophene-*S*,*S*-dioxides **Br$_2$S-OH**, **Br$_2$S-CN**, **Br$_2$S-I** and **Br$_2$S-F**.

1-Hydroxy-3,7-dibenzothiophene-*S*,*S*-dioxide (**Br$_2$S-OH**) was obtained by diazotization of **Br$_2$S-NH$_2$** with $NaNO_2$ in sulfuric acid and reaction of the formed diazonium salt **2.2** with water under reflux (**Scheme 2.6**). Diazotization of **Br$_2$S-NH$_2$** in concentrated $H_2SO_4$ at 0 °C, followed by dilution of the formed diazonium salt with water and heating the mixture gave very low yields (10–13%) of the target **Br$_2$S-OH**. Diazotization in 50% aqueous $H_2SO_4$ proceeded under heterogeneous conditions due to the

low solubility of **$Br_2S$-$NH_2$** and again gave quite low yields of ~14%. In both cases, a substantial amount of the deamination product **$Br_2S$** was formed, which was difficult to separate from the required **$Br_2S$-OH**. Attempts to perform the reaction in the presence of $Cu_2O$ and $Cu(NO_3)_2$ as catalysts in a Sandmeyer reaction[12] were also unsuccessful. Better results were obtained when the procedure of the reaction of diazonium salt **2.2** with water was changed slightly to involve the dropwise addition of a suspension of **2.2** in 50% aqueous $H_2SO_4$ into stirring boiling water[13] and heating the mixture under reflux for 2 hours. This resulted in higher yields of **$Br_2S$-OH**, however it was still substantially contaminated with **$Br_2S$**. The latter was difficult to separate by either flash chromatography or recrystallisation from different solvents. Their separation was done through the phenolate (**$Br_2S$-ONa**) by dissolution of the crude product in an aqueous solution of NaOH with heating, hot filtration to remove the insoluble **$Br_2S$** and precipitation of **$Br_2S$-OH** after acidification of the filtrate. This procedure removed **$Br_2S$** from the crude product almost completely and, on a gram scale reaction, the **$Br_2S$-OH** obtained was sufficiently pure.[a] To obtain analytically pure samples, it was further purified by flash chromatography with a gradient eluent from toluene to Tol : $Et_2O$, 1:1 (or to 100% $Et_2O$). The latter flash chromatography procedure was essential when crude **$Br_2S$-$NH_2$** was used in the synthesis of **$Br_2S$-OH** in large scale reactions.

1-Cyano-3,7-dibromodibenzothiophene-*S*,*S*-dioxide **($Br_2S$-CN)** was synthesised by a Sandmeyer reaction[14,15,] of diazonium salt **2.2** (prepared from **$Br_2S$-$NH_2$** as described above) with CuCN obtained *in situ* from NaCN and $CuSO_4 \cdot 5H_2O$ with heating (see **Scheme 2.6**). Normally, this reaction works better under neutral conditions[16] to avoid formation of highly toxic and volatile HCN from cyanide salts. However, it was difficult to isolate diazonium salt **2.2** (very fine suspension was formed resulting in large losses on filtration) and the reaction did not work well. Therefore, the reaction was performed by direct addition of NaCN and $CuSO_4 \cdot 5H_2O$ into an acidic suspension of diazonium salt **2.2** followed by heating of the reaction mixture (**Table 2.1**).

Apart from the target **$Br_2S$-CN**, other by-products were formed in the reaction, as shown by $^1$H NMR analysis of the crude products and comparison with NMR spectra for

[a] ***NB:*** *it is important to ensure complete removal of* ***$Br_2S$*** *from* ***$Br_2S$-OH*** *as the presence of even small amounts of* ***$Br_2S$*** *in the monomers might affect the properties of the synthesised polymers.*

authentic samples (**Table 2.1**). Optimisation of the reaction by using a large excess of $NaCN/CuSO_4 \cdot 5H_2O$ and prolonged stirring of the diazonium salt at room temperature before heating allowed the content of **Br$_2$S-CN** to reach 69% of the crude product, as determined by $^1$H NMR spectroscopy. Separation of **Br$_2$S-CN** from **Br$_2$S-OH** was easily achieved by flash chromatography with a non-polar eluent (toluene), in which the hydroxyl by-product remains on the silica, followed by recrystallisation from dichloromethane to yield pure **Br$_2$S-CN** (50% yield, 98% purity by $^1$H NMR spectroscopy).

**Figure 2.2** shows the $^1$H NMR spectrum of the aromatic region for compounds **Br$_2$S-OH** and **Br$_2$S-CN**, which shows a clear assignment of all the protons for both compounds. Protons 2 and 4 had shifted greatly from 7.36 and 7.71 ppm to 8.60 and 8.79 ppm respectively, which were shifts of ~1.24 and 1.08 ppm. This result concurs with our predictions as protons 2/4 are the closest to the new groups (**OH** or **CN**) that were added to the compound. The **CN** is a strong electron withdrawing group and therefore causes deshielding around the protons and hence shifting the signal downfield. Whereas, the **OH** group is electron donating and hence the protons were shielded and shifted greatly upfield.

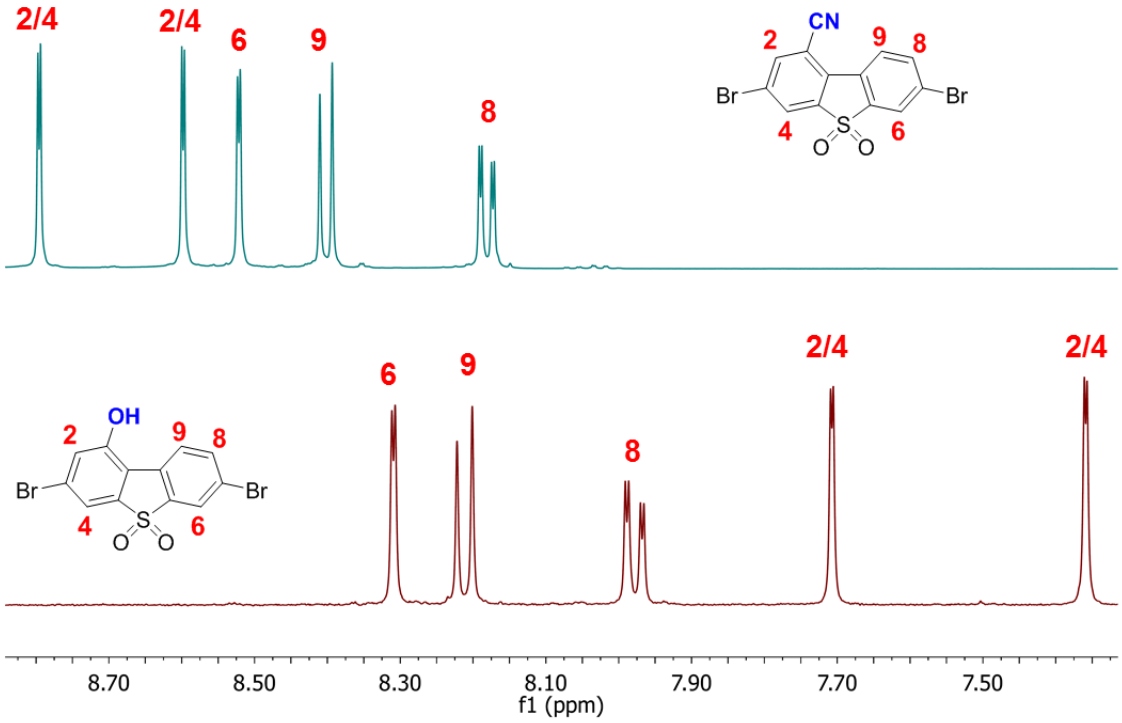


**Figure 2.2:** $^{1}$H NMR spectrum of 1-hyroxy-3,7-dibromo dibenzothiophene-*S*,*S*-dioxide (**Br$_2$S-OH**) (bottom), and 1-cyano-3,7-dibromo dibenzothiophene-*S*,*S*-dioxide (**Br$_2$S-CN**) (top), with signal assignments.

**Table 2.1:** Synthesis of 1-cyano-3,7-dibromodibenzothiophene-*S*,*S*-dioxide (**Br2S-CN**) from amine **Br2S-NH2** through diazonium salt **2.2**, and identified by-products in the reaction (by $^{1}$H NMR analysis of crude product).

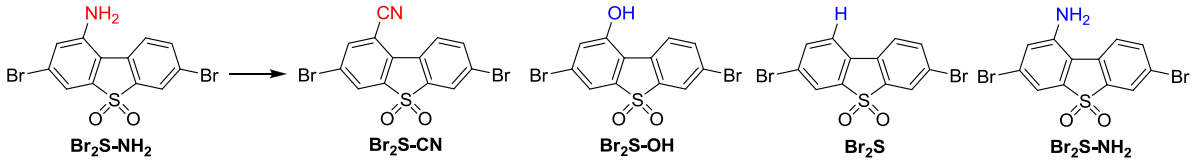


| **Br2S-NH2** (g) | $CuSO_4 \cdot 5H_2O$ (g) / [eq.] | NaCN (g) / [eq] | Reaction conditions | Crude yield (%) | **Br2S-CN** (%) | **Br2S-OH** (%) | **Br2S** (%) | **Br2S-NH2** (%) |
|---|---|---|---|---|---|---|---|---|
| 1.00 | 1.85 [2.9 eq.] | 2.08 [17 eq.] | 0 °C, 18 h reflux, 3 h | 30 | – | – | 30 | – |
| 1.00 | 1.85 [2.9 eq.] | 2.08 [2.9 eq.] | r.t, 2.25 h 50 °C, 21 h 90 °C, 1 h | 95 | 52 | 18 | 30 | – |
| 0.70 | 0 | 1.62 [12 eq.] | r.t, 67 h 50 °C, 1 h 80 °C, 4.5 h | ND | – | 53 | 32 | 15 |
| 0.70 | 2.70 [5.6 eq.] | 3.17 [33 eq.] | 60 °C, 22 h r.t, 37 h | 96 | 50 | 8 | 25 | 17 |
| 0.70 | 2.70 [5.6 eq.] | 3.17 [33 eq.] | r.t, 67 h 50 °C, 1 h 80 °C, 4.5 h | 81 | **68** | 24 | 8 | – |
| 4.00 | 55.2 [11 eq] | 32.5 [69] | r.t, 16 h 80 °C, 3 h | 103 | **69** | 12 | 12 | 7 |

ND = Not Determined

1-amino-3,7-dibromodibenzothiophene-*S*,*S*-dioxide **(Br2S-NH2)** was used as the key starting compound to access a series of 1-R-3,7-dibromodibenzothiophene-*S*,*S*-dioxide (**Br2S-R**) derivatives through diazonium chemistry. In the synthesis of **(Br2S-I)**,[9] diazotization with $NaNO_2$ was performed in sulfuric acid at 0 °C and the formed diazonium salt was involved *in situ* in a nucleophilic substitution reaction with KI under heating. The

crude product was purified by column chromatography on silica gel using PE : Tol 1:1 as eluent, resulting in the desired product **($Br_2$S-I)**.

To introduce the fluorine group, a two-step process was applied. 1-amino-3,7-dibromodibenzothiophene-*S,S*-dioxide **($Br_2$S-$NH_2$)** was firstly diazotized using $NaNO_2$ in concentrated $H_2SO_4$ / 48% tetrafluoroboric acid to give the yellow coloured diazonium salt **2.3**, which was precipitated from the reaction mixture and isolated by filtration. In the second step, following a Balz-Schiemann reaction,[17] the diazonium salt was heated to reflux in a high boiling solvent (xylene). Thermal decomposition of the tetrafluoroborate compound **2.3** afforded the corresponding 1-fluoro-3,7-dibromodibenzothiophene-*S,S*-dioxide **($Br_2$S-F)** in a 20% yield (**Scheme 2.6**). Its structure was confirmed by $^1$H NMR and $^{19}$F NMR spectroscopy (the $^1$H NMR shows appropriate F-1 coupling with adjacent H-2).

When only (48%) tetrafluoroboric acid was used in the first step the diazonium salt was not formed. This could be due to the very poor solubility of the starting compound. The same observation was noted when using acetic acid/$HBF_4$, HCl/$HBF_4$, and THF/$HBF_4$ instead of $H_2SO_4$/$HBF_4$.[18,19,20]

### 2.2.3 Synthesis of 1-alkoxy-3,7-dibromodibenzothiophene-*S,S*-dioxide monomers ($Br_2$S-OR) for use in the synthesis of homopolymers and co-polymers

Before preparing the alkoxy monomers (**$Br_2$S-OR**), from **$Br_2$S-OH**, that were needed for polymerisation, alkyl bromide **2.5** and alkyl tosylates **2.7**, and **2.9** needed to be prepared, so that they could be reacted with compound **$Br_2$S-OH**. These were prepared in good yields from the corresponding commercially available alcohols (see **Scheme 2.7**) following common procedures for the conversion of a hydroxyl group into a bromide (by using concentrated HBr)[21] or a tosylate (by using TsCl/$Et_3$N).[22,23] The products were purified by distillation or flash chromatography.

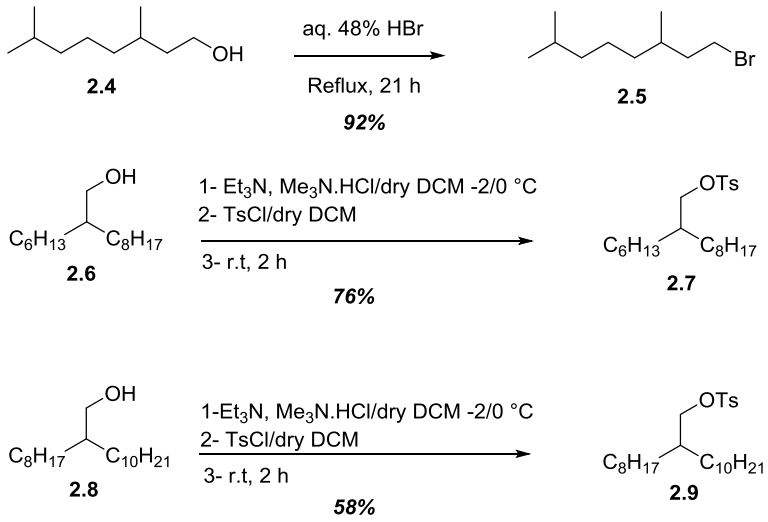


**Scheme 2.7:** Synthesis of alkyl bromide **2.5** and alkyl tosylates **2.7**, **2.9**.

In addition, alkyl tosylate **2.13** was also prepared from the alcohol **2.12** in a similar manner, however as the starting alcohol was not commercially available it was synthesised *via* a Grignard reaction from alkyl bromide **2.10**. Heptadecan-9-ol (**2.12**) was prepared by reaction of Grignard reagent **2.11** (obtained from 1-bromooctane (**2.10**)) with ethylformate according to a previously described method (see **Scheme 2.8**).[22] It was found that the product was contaminated with an unidentified impurity, which was difficult to remove even after 3 vacuum distillations. GC-MS, $^{1}H$ and $^{13}C$ NMR analyses verified that this by-product was heptadecan-9-one (which was presumably formed due to accidental oxidation of the intermediate magnesium alcoholate). Therefore, the crude product was successfully reduced with $NaBH_4$ to convert heptadecan-9-one into heptadecan-9-ol. The obtained heptadecan-9-ol (**2.12**) was then converted into tosylate **2.13** as described in **Scheme 2.8**.[22]

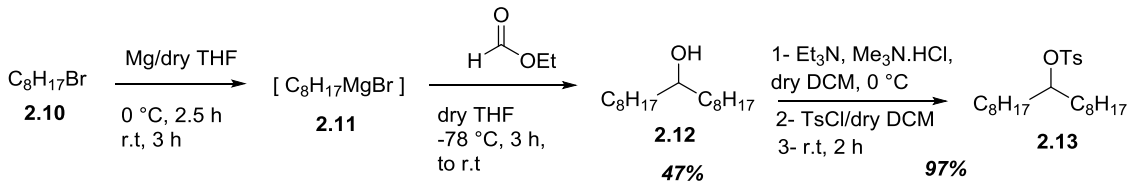


**Scheme 2.8:** Synthesis of alkyl alcohol **2.12** and alkyl tosylate **2.13**.

The monomers **Br$_2$S-OR** with different linear or branched alkyl groups could then be prepared by alkylation of **Br$_2$S-OH** with the alkyl halides or alkyl tosylates **2.5**, **2.7**, **2.9**,

**2.13** in DMF in the presence of $K_2CO_3$ (**Scheme 2.9**), by analogy with common procedures for the alkylation of phenols.[24]

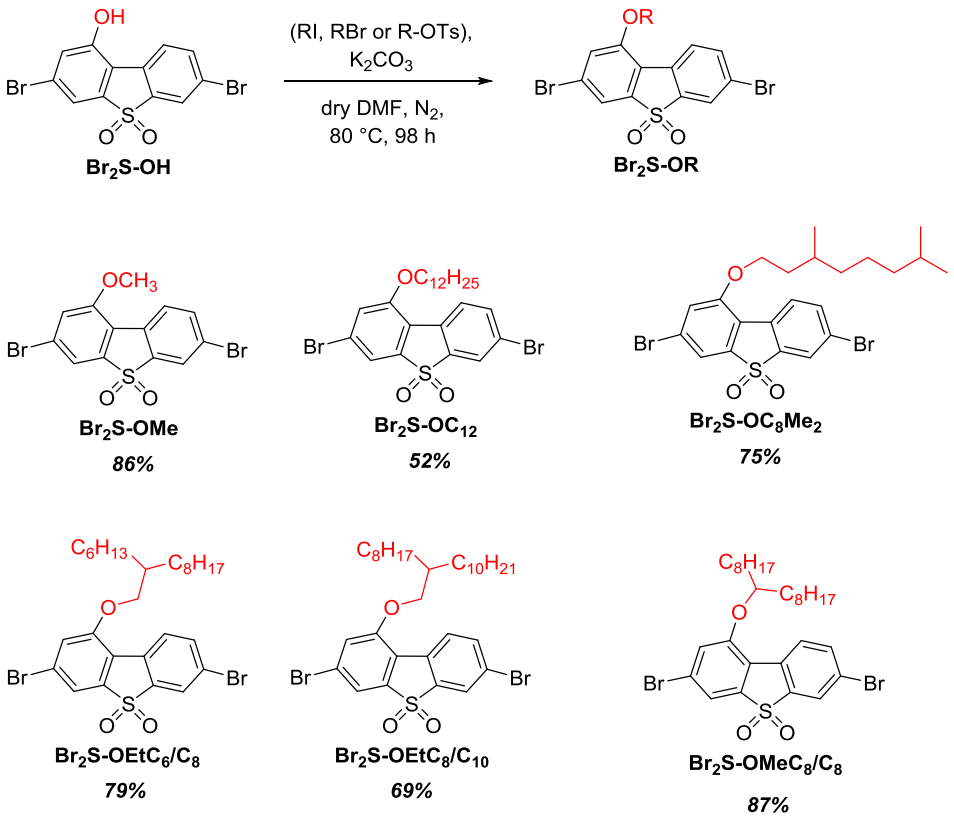


**Scheme 2.9:** Synthesis of monomers (**Br2S-OMe, Br2S-OC12**, **Br2S-OC8Me2**, **Br2S-OEtC6/C8**, **Br2S-OEtC8/C10** and **Br2S-OMeC8/C8**) by alkylation of phenol **Br2S-OH**.

In the case of monomers **Br2S-OMe, Br2S-OC12** and **Br2S-OC8Me2**, they were first dried under high vacuum (20 – 40 μbar) for 2–3 days to remove an excess of the alkyl halide and then purified twice by flash chromatography. In the case of reaction with tosylates **2.7**, **2.9**, and **2.13**, the crude products showed ≥80% purity with some amount of the unreacted tosylates (according to $^1$H NMR data). As the tosylates showed very close $R_f$ values by TLC to the corresponding alkoxydibenzothiophene-*S*,*S*-dioxides **Br2S-OEtC6/C8, Br2S-OEtC8/C10**, and **Br2S-OMeC8/C8**, the crude products were treated with ammonia in DMF to decompose the tosylates (saturating the DMF solutions of the products with gaseous $NH_3$ and heating the solutions for 17 hours at 80 °C) followed by purification of the products by column chromatography. The monomers obtained **Br2S-OR** were characterised by $^1$H and

$^{13}$C NMR spectroscopy and GC-MS and showed a high degree of purity (>98–99%), suitable for the preparation of polymers.

### 2.2.4 Synthesis of 1-(alkylthio and alkyl sulfonyl)-3,7-dibromodibenzothiophene-*S*,*S*-dioxide monomers for homopolymers and co-polymers

For the synthesis of 1-substituted dibenzothiophene-*S*,*S*-dioxide based polymers and co-polymers the corresponding 1-alkylthio or alkyl sulfonyl-3,7-dibromodibenzothiophene-*S*,*S*-dioxide monomers were required, which could then be polymerised by Ni-mediated or Pd-catalyzed C-C coupling methods.

#### 2.2.4.1 Attempted syntheses of 1-alkylthio-3,7-dibromodibenzothiophene-*S*,*S*-dioxides using $Na_2S_2O_3$ as sulfureting reagent

In recent years, Jiang and co-workers have developed convenient methods for C-S bond construction using $Na_2S_2O_3$ as the sulfureting reagent.[25,26] An interesting reaction they found during these studies was the Cu-catalysed transformation of arylamines into arylalkylsulfides or arylbenzylsulfides by reaction with $Na_2S_2O_3$ and alkyl (or benzyl) halides in an alcohol/water mixture (**Scheme 2.10**).[27] The described procedure[27] included a two-step one-pot reaction. First, the sulfureting reagent was prepared by reaction of an alkyl halide with $Na_2S_2O_3{\cdot}5H_2O$ and the Cu catalyst was prepared from $CuSO_4{\cdot}5H_2O$ and 2,2'-bipyridine in MeOH/$H_2O$ for 2 h at 80 °C. Then, after cooling the mixture to 0 °C, arylamine and *tert*-butylnitrite were added for diazotization and reaction with the *S*-nucleophile spontaneously occurred (**Scheme 2.10**).

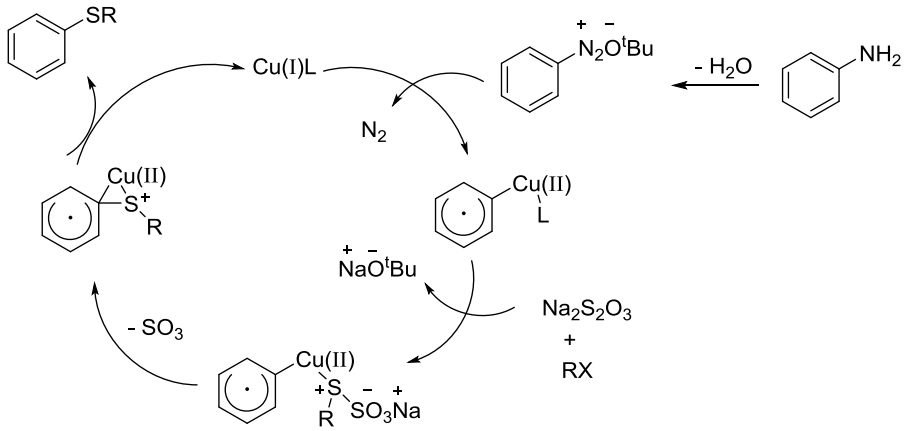


**Scheme 2.10:** Proposed mechanism for Cu-catalysed transformation of arylamines into aryl-alkylsulfides using $Na_2S_2O_3$/alkylhalide as sulfureting reagent with diazotisation by alkylnitrites.[27]

This seemed a very attractive and convenient way to access a range of alkylthio- (and then alkylsulfonyl-) 3,7-dibromodibenzothiophene-*S,S*-dioxides with wide variations of alkyl solubilising groups (**Scheme 2.11**), which could be used for the synthesis of a new series of dibromodibenzothiophene-*S,S*-dioxide homopolymers. Several attempts of this methodology were carried out, from direct reproduction of the reaction conditions described[27] to different variations of reagents, solvents and reaction conditions, but all attempts to obtain 1-alkylthio-3,7-dibromodibenzothiophene-*S,S*-dioxides from **Br$_2$S-NH$_2$** by this reaction (**Scheme 2.11**) were unsuccessful (see Appendices 6.7 for the details of the experiments). Only in some trials were crude materials isolated in very low yields of 2–3%, which presumably were impure 1-alkylthio-substituted products. One possible reason for the negative results in these trials could be the extremely low solubility of **Br$_2$S-NH$_2$** in the MeOH/$H_2O$ mixture preventing its diazotisation and trapping the intermediate by the sulfureting reagent. Attempts to use other organic solvents were also unsuccessful, possibly due to inefficient formation of the sulfureting reagent from $Na_2S_2O_3$ and alkylhalides in these cases.

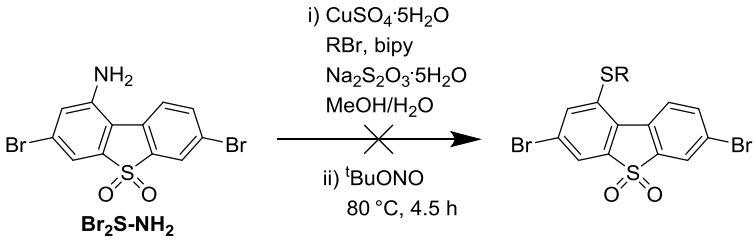


**Scheme 2.11:** General reaction scheme for the attempted synthesis of **Br$_2$S-SR** analogues

### 2.2.4.2 Syntheses of 1-alkylthio and alkyl sulfonyl -3,7-dibromodibenzothiophene-S,S-dioxides

As the route described in Section 2.2.4.1 was found to be unsuitable for the formation of the required alky-thio and alkyl-sulfonyl monomers an alternative route needed to be used. This involved the reaction of **Br$_2$S-NH$_2$** *via* diazonium chemistry with a dialkyl disulfide to obtain the **Br$_2$S-SR** monomers,[28] which can be oxidised to access the **Br$_2$S-SO$_2$R** monomers (**Scheme 2.12**). As some of the disulfides needed to prepare the target monomers were not commercially available they needed to be synthesised from the corresponding alkyl halides, which could themselves be prepared from the corresponding alcohols.

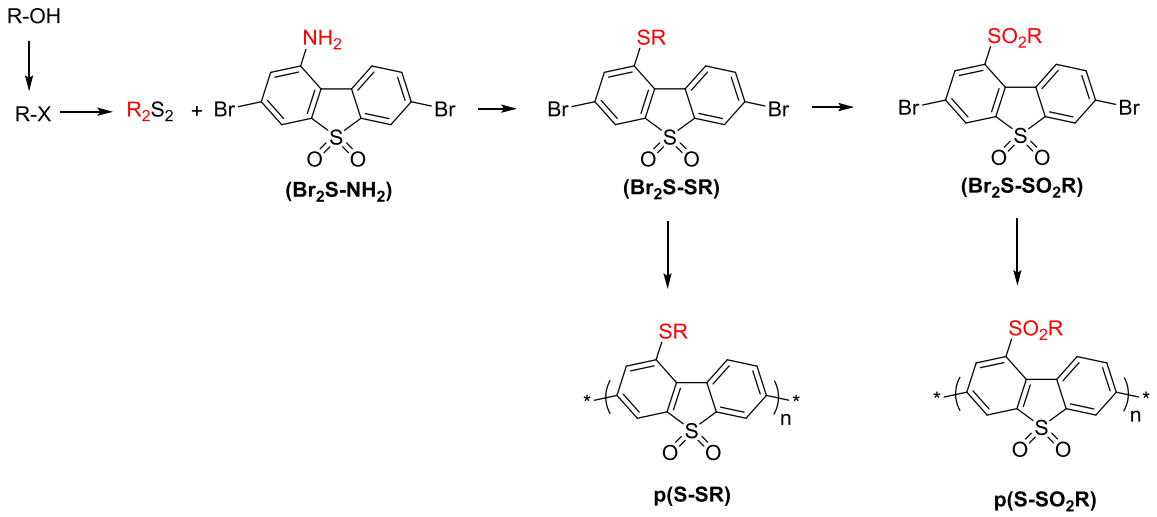


**Scheme 2.12:** General scheme showing synthetic route to soluble **p(S-SR)** and **p(S-SO$_2$R)** homopolymers.

Alkyl bromides **2.14** and **2.15** were prepared in yields of 81% and 76% respectively from the corresponding commercially available alcohols by common procedures[29] of reflux with concentrated HBr and purification by distillation and/or column chromatography (**Scheme 2.13**).

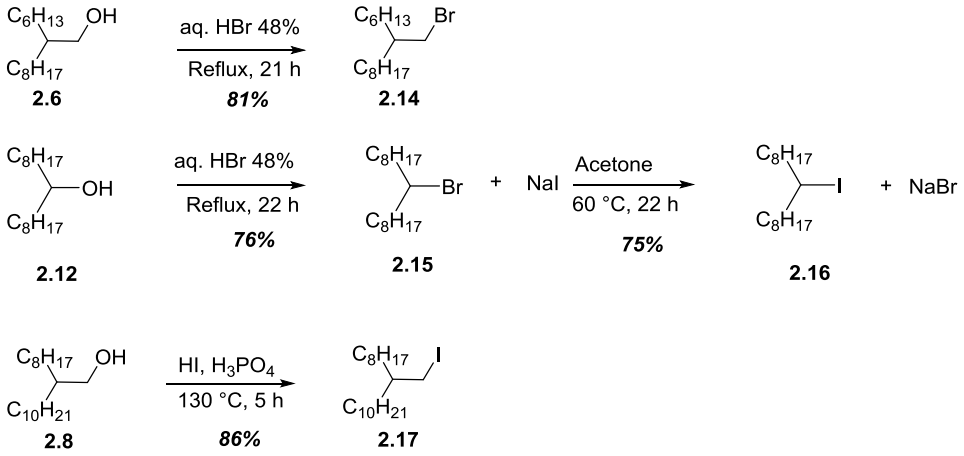


**Scheme: 2.13** Synthesis of alkyl halides **2.14–2.17**.

It was noticed that alkyl bromides are not efficient enough to prepare the dialkyl disulfide ($R_2S_2$) (see attempted reaction with **2.14**, **Scheme 2.15**, below) so it was decided to convert them to the corresponding alkyl iodides as bromine was not as susceptible to substitution as iodine; iodine is bigger in size and is therefore a better leaving group, thus giving a better yield and was more suitable for further substitution reactions. Compound **2.16** was therefore synthesised according to previous literature methods.[30] The main issue encountered with this reaction was formation of an alkene by-product (heptadec-8-ene, during each reaction step, as identified by the peak in the $^1$H NMR spectra at 5.41–5.32 (m, 2H, CH=CH). This issue was not encountered with other compounds such as **2.14**. This was a consequence of compound **2.16**, which forms a secondary carbocation intermediate *via* the $S_N1$ mechanism. It was impossible to remove this alkene by recrystallization or column chromatography. However, the alkene was removed by vacuum distillation of the first fraction which was collected at (101 °C, 46 µB) then the remaining material from the distillation was collected to obtain the target product **2.16** in 75% yield, and 96% purity as determined by $^1$HNMR spectroscopy. The synthesis of 9-(iodomethyl)nonadecane **2.17** was initiated using 2-octyldodecan-1-ol which was commercially available as described in the

literature[31] (**Scheme 2.13**). The simple substitution reaction was successful and the product was easily purified by being passed through a short silica column using PE as eluent to remove colour impurities, which were not visible by NMR spectroscopy. The target product **2.17** was obtained in 86% yield and >99% purity as determined by $^1$HNMR spectroscopy.

Having successfully prepared the alkyl halides **2.14**, **2.16**, and **2.17** they, along with commercially available 1-iododododecane (**2.18**), could be converted to the corresponding dialkyl disulfides. Recently, M. Abbasi *et al.* have developed convenient methods for the conversion of alkyl halides to symmetrical dialkyl disulfides by reacting alkyl halides with $Na_2S_2O_3$ in wet DMSO. An interesting reaction they found during these studies involved three-steps in a one-pot reaction. First, *S*-alkylthiosulfate was prepared by a nucleophilic substitution reaction of an alkyl halide with $Na_2S_2O_3 \cdot 5H_2O$. Next, the thiol was formed by hydrolysis of the salts. Finally, the generated mercaptan (*in situ*) underwent oxidative coupling by DMSO to produce the dialkyl disulfide (**Scheme 2.14**).[32]

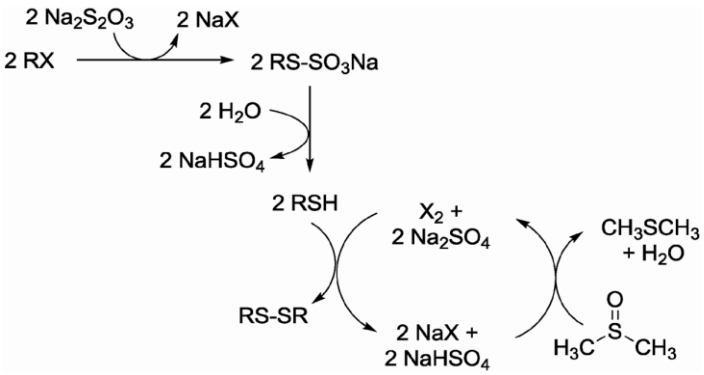


**Scheme 2.14:** Proposed reaction mechanism for the preparation of symmetrical dialkyl disulfides from alkyl halides and $Na_2S_2O_3$ in wet DMSO.[32]

Using this protocol, **2.19** and **2.21** were synthesised by heating the corresponding alkyl halides with $Na_2S_2O_3.5H_2O$, and wet DMSO at 60 °C for 23 hours to 2 days (**Scheme 2.15**). The crude products, obtained as a light orange solid or dark orange oil for **2.19** and **2.21** respectively, which were purified by flash chromatography using PE as eluent to give compound **2.19** in 92% yield (99% purity by $^1$HNMR) and compound **2.21** in 97% yield (93% purity with 7% thiol by $^1$H NMR). The trial reactions were monitored by litmus paper and $^1$H NMR spectroscopy to check the acidity of the reaction mixture and to determine the best conditions for the reaction and then the reactions were scaled up.

In the case of the branched alkyl bromide **2.14**, compound **2.20** was synthesised in the same fashion. However, after 21 h the reaction mixture was still neutral and after 30 h the reaction mixture still contained 41% of the starting material, with the target product accounting for 46%, and the thiol 13%, as determined by $^{1}$HNMR spectroscopy. Therefore, the time and temperature of the reaction was increased and after 50 h of stirring at 75 °C the purity of the target product **2.20** was only 74% with 26% of the thiol by $^{1}$HNMR spectroscopy. Also purification by column chromatography, recrystallisation, or vacuum distillation was not feasible. Therefore, the reaction was done with alkyl iodides rather than alkyl bromides due to the larger size of the iodide which makes it a better leaving group and speeds up the first step of the reaction.[b]

Compound **2.22** was difficult to synthesise because the starting alkyl halide **2.16** is secondary and has the ability to undergo an elimination reaction at high temperature. Therefore, many trial reactions were conducted on a 1 g or 0.5 g scale to optimize the conditions of the reaction. Ultimately, it was found that the optimum temperature was 60 °C for 21 days. Apart from the target product **2.22**, other by-products were formed in the reaction (30% alkene, and 21% thiol as shown by $^{1}$H NMR spectroscopy). The alkene was removed by vacuum distillation (101 °C, 46 μB) to afford the target product **2.22** in a yield of 42% and a purity of 70% with 30% thiol by $^{1}$H NMR spectroscopy.

*b Compound **2.14** was not converted to the corresponding alkyl iodide due to all of it being consumed in this trial. It was decided not to prepare more material as the solubility of the polymer in this branch (**$C_6$/$C_8$**) was expected to be similar to (**$C_8$/$C_{10}$**) branched polymer formed from **2.21**.*

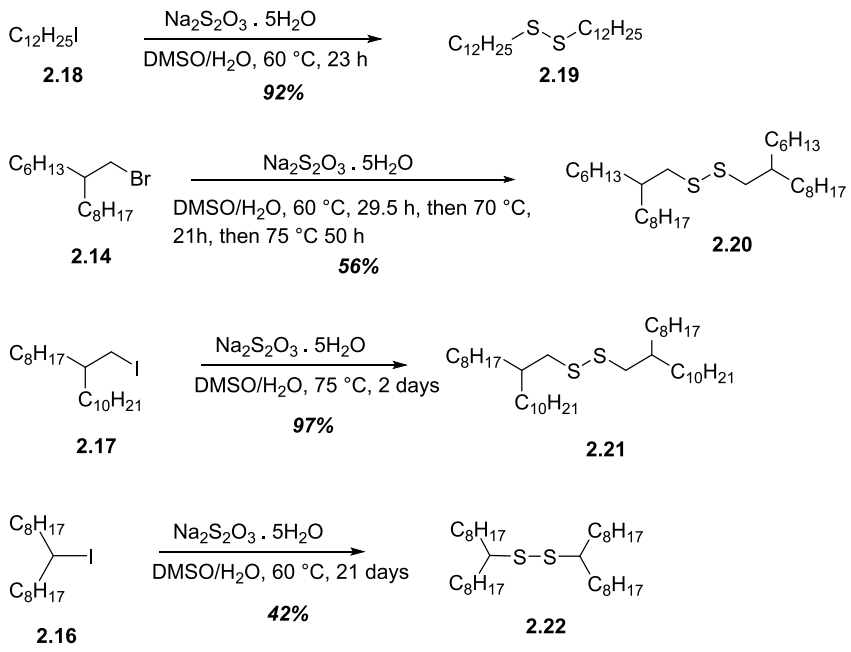


**Scheme 2.15:** Synthesis of symmetrical dialkyl disulfides **2.19–2.22** from alkyl halides and $Na_2S_2O_3$ in wet DMSO.

With the commercially available dimethyl disulfide and dialkyl disulfides **2.19** and **2.21–2.22** in hand they could be reacted with **Br$_2$S-NH$_2$** to give the target monomers **Br$_2$S-SR** (**Scheme 2.16**).

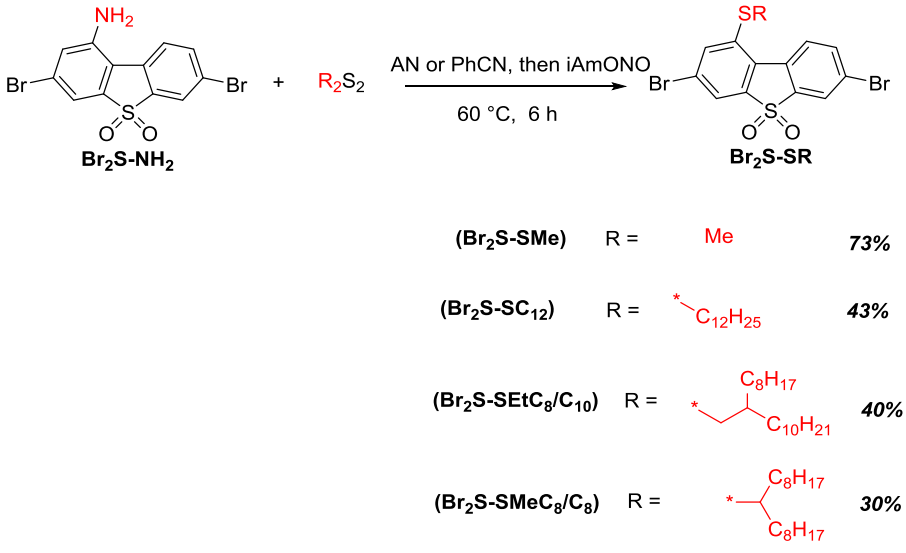


**Scheme 2.16:** Synthesis of monomers (**Br$_2$S-SMe, Br$_2$S-SC$_{12}$, Br$_2$S-SEtC$_6$/C$_8$, Br$_2$S-SEtC$_8$/C$_{10}$** and **Br$_2$S-SMeC$_8$/C$_8$**) by transformation of **Br$_2$S-NH$_2$** into **Br$_2$S-SR**

Replacement of the $NH_2$ group in **$Br_2S$-$NH_2$** by an SR group using the classical reaction *via* a diazonium salt ($-N_2^+$) was not possible as the diazonium salt oxidises thiols or disulfides instead of a nucleophilic substitution reaction occurring. This transformation can be performed by other methods in milder conditions using non-metallic thio-group sources.[33,34] Among them, the versatile method for conversion of an amino group into an alkylthio group is based on the reaction with alkylnitrites (iso-amyl nitrite, *tert*-butylnitrite) as nitration reagents in organic solvents.[35,36,37,38,39]

Using these protocols, **$Br_2S$-SMe** was synthesised by heating **$Br_2S$-$NH_2$** with iso-amyl nitrite and dimethyl disulfide in acetonitrile at 60 °C for 3 h (**Scheme 2.18**), affording the crude product in 83% yield. Further purification by flash chromatography using DCM as eluent and recrystallisation from dioxane gave pure **$Br_2S$-SMe** (>98% purity by $^1$H NMR spectroscopy). The first trial reaction was done using 750 mg of **$Br_2S$-$NH_2$** and then the reaction was scaled up to a 5 g batch giving **$Br_2S$-SMe** in 53% yield (>99% purity by $^1$H NMR spectroscopy).

In the case of compound **$Br_2S$-$SC_{12}$** acetonitrile was not an ideal solvent due to the poor solubility of the compound. In order to identify the best solvent for the reaction of the disulfide compounds with **$Br_2S$-$NH_2$** trials were conducted using the commercially available dimethyl disulfide. A range of different solvents were used, and it was found that THF did not work as the purity of the products was lower than 5% (by $^1$H NMR spectroscopy). Ethylacetate was also used as a solvent and afforded the crude product in 109% yield and ~88% purity (by $^1$H NMR spectroscopy), however, it didn't work with the preparation of **$Br_2S$-$SC_{12}$** (crude product with 13% yield and ~64% purity (by $^1$H NMR spectroscopy). Benzonitrile was also investigated and gave a good yield and purity when using dimethyl disulfide and it was found that this solvent was also suitable for the other disulfides. Eventually, in benzonitrile the pure target product **$Br_2S$-$SC_{12}$** was obtained in a 43% yield (>99% purity by $^1$H NMR).

In addition, the ratios between the chemicals was investigated and in the preparation of **$Br_2S$-$SC_{12}$**, for one equivalent of **$Br_2S$-$NH_2$**, 6 equivalents of **2.19** ($(C_{12}H_{25})S_2$) and 5 equivalents of iso-amyl nitrite were used. Finally, the reaction was repeated 7 times, the first reaction was started with 14 g of disulfide **2.19** then after each reaction the disulfide was recovered by column chromatography using PE to get the starting disulfide then DCM to get the crude product. The recovered starting disulfide was used in the next reaction. Lastly,

all crude products from these seven reactions were combined and the main byproduct was where the the amino group had been replaced with hydrogen. The crude product was purified by column chromatography using PE : Tol (1:1) as eluent, followed by recrystallization from heptane to afford more than 5 g of pure product **$Br_2S$-$SC_{12}$** in 43% yield (>99% purity by $^1$H NMR spectroscopy).

Compound **$Br_2S$-$SEtC_8/C_{10}$** was synthesised in the same fashion as compound **$Br_2S$-$SC_{12}$**. Also the ratio of the compound **$Br_2S$-$SEtC_8/C_{10}$** was changed from what was used previously. In the previous experiment **$Br_2S$-$SC_{12}$**, the ratio was 1:6 (**$Br_2S$-$NH_2$ : 2.19**) however, changing the ratio to 1:8 gave better yields. Other issues regarding this reaction were that, apart from the target product **$Br_2S$-$SEtC_8/C_{10}$** and dibenzothiophene-*S*,*S*-dioxide (**$Br_2S$**) there were other by-products in the aromatic region. Therefore, the crude products were combined and purified by column chromatography twice using PE : Tol (1:1) as eluent to give the target product **$Br_2S$-$SEtC_8/C_{10}$** in 40% yield (>99% purity by $^1$HNMR spectroscopy).

In the synthesis of **$Br_2S$-$SMeC_8/C_8$** shown in **Scheme 2.17**, the ratio used was 6 equivalents dialkyl disulfide **2.22** to 1 equivalent **$Br_2S$-$NH_2$** to 5 equivalents iso-amyl nitrite. A mixture of dibenzothiophene-*S*,*S*-dioxide **$Br_2S$-$SMeC_8/C_8$** and dibenzothiophene-S-oxide **2.23** is synthesised during this reaction due to the reducing nature of the disulfide and was separated using flash chromatography into three fractions with two fractions containing either **$Br_2S$-$SMeC_8/C_8$** or **2.23** and a mixed fraction. The pure **$Br_2S$-$SMeC_8/C_8$** fraction was used for polymerisation and the other two fractions were oxidised in the next step as separation of the mixed fraction would be technically difficult and result in the loss of product. Dibenzothiophene-*S*-oxide **2.23** would be oxidised back to the dioxide during the oxidation without the loss of product.

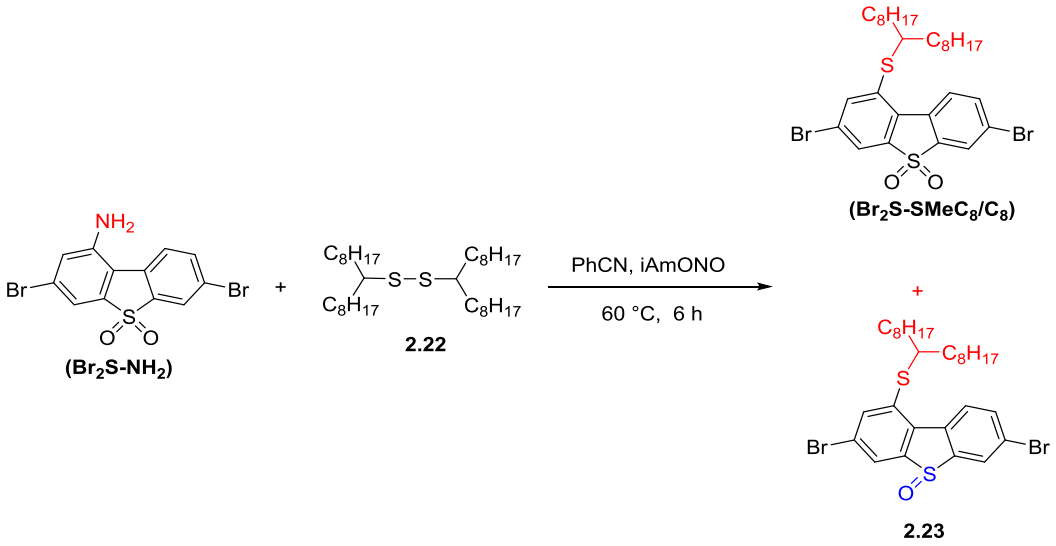


**Scheme 2.17:** Synthesis of monomer (**$Br_2S$-$SMeC_8/C_8$**) by transformation of **$Br_2S$-$NH_2$** into **$Br_2S$-SR** along with by-product dibenzothiophene-*S*-oxide **2.23**.

Having successfully prepared the alkylthio monomers (**$Br_2S$-SR**) they could then be used to obtain the corresponding alkylsulfonyl monomers (**$Br_2S$-$SO_2R$**). The **S-Me** group in **$Br_2S$-SMe** was converted to the **$SO_2Me$** group by oxidation with hydrogen peroxide in glacial acetic acid at 60 °C for 20 hours (**Scheme 2.18**). The solid was filtered off and washed with water to afford the crude product with a lot of **($Br_2S$-SOMe)** (10% or more). This was oxidized with hydrogen peroxide in glacial acetic acid at 65 °C for 50 hours again to afford the product **$Br_2S$-$SO_2Me$** in 97 % yield and a purity of ~ 96% (by $^1$H NMR spectroscopy). It was then purified by recrystallization in acetic acid to afford the product **$Br_2S$-$SO_2Me$** in 86 % yield as an off white solid in a purity of 100% according to $^1$H NMR spectroscopy.

For the oxidation of **$Br_2S$-$SC_{12}$**, **$Br_2S$-$SEtC_8/C_{10}$** and **$Br_2S$-$SMeC_8/C_8$** *m*-chloroperbenzoic acid **(***m*CPBA) was used as the oxidizing agent instead of $H_2O_2$ as hydrogen peroxide easily decomposes to give water which would make the reaction mixture heterogeneous (**Scheme 2.18**). The reaction was left for 23 h although after the reaction was repeated on a similar scale and after being monitored by probes ($^1$H NMR spectroscopy) it was found that four hours would be sufficient for the reaction to be completed and to get the target product **$Br_2S$-$SO_2C_{12}$** in 94% yield (>99% purity by $^1$HNMR), and **$Br_2S$-$SO_2EtC_8/C_{10}$** in 97% yield (>99% purity by $^1$H NMR spectroscopy). However, compound **$Br_2S$-$SMeC_8/C_8$** needed more time (5 days) to oxidize the S to $SO_2$ group which could be

due to steric hindrance of the sulfur atom due to the secondary alkyl group rather than a primary group.

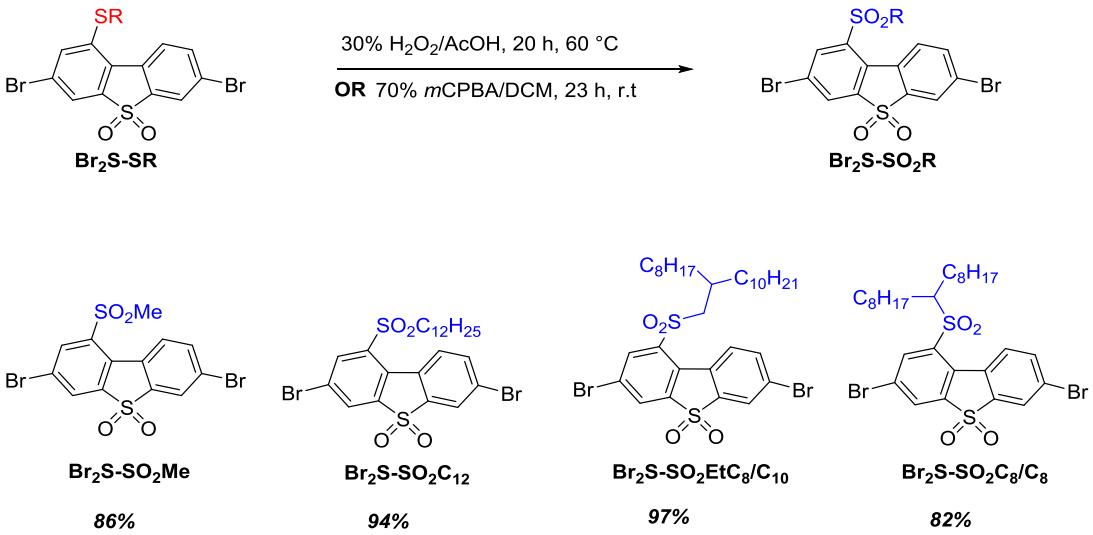


**Scheme 2.18:** Synthesis of monomers (**$Br_2S$-$SO_2Me$, $Br_2S$-$SO_2C_{12}$, $Br_2S$-$SO_2EtC_8/C_{10}$** and **$Br_2S$-$SO_2MeC_8/C_8$**) by transformation of **$Br_2S$-SR** into **$Br_2S$-$SO_2R$**.

$^1$H-$^1$H COSY NMR was performed for compounds **$Br_2S$-$SEtC_8/C_{10}$** and **$Br_2S$-$SO_2EtC_8/C_{10}$** to determine the position of the protons on the benzene rings (see **Figure 2.3**). The $^1$H-$^1$H COSY NMR gave a clear assignment of all protons for compounds **$Br_2S$-$SEtC_8/C_{10}$** and **$Br_2S$-$SO_2EtC_8/C_{10}$**. Proton 2 had shifted greatly from ~7.63 ppm to ~8.55 ppm which was a shift of ~0.92 ppm. This result concurs with our predictions as proton 2 is the closest to the new group that was added to the compound. The $SO_2$ group is a strong electron withdrawing group and therefore causes deshielding around the proton and hence shifting the signal downfield. Whereas before oxidation, the SR group was electron donating and hence the proton was shielded and hence shifted slightly upfield.

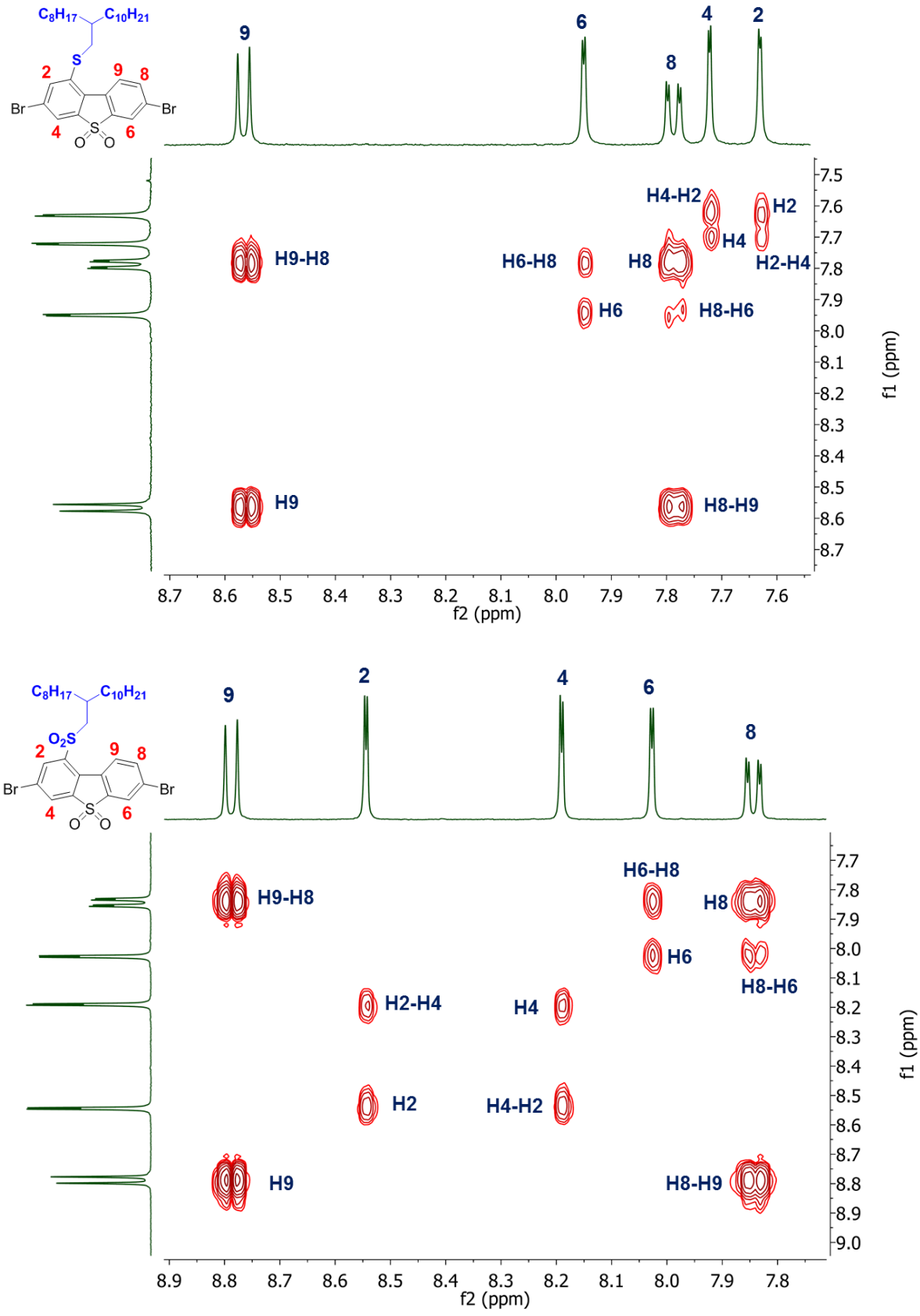


**Figure 2.3:** $^{1}$H-$^{1}$H COSY NMR structure top **$Br_2$S-SEt$C_8$/$C_{10}$** and bottom **$Br_2$S-$SO_2$Et$C_8$/$C_{10}$.**

### 2.2.5 Conversion of the -$SO_2$- group in $Br_2S$-$SEtC_8/C_{10}$ into an –S- group by reduction with lithium aluminium hydride ($LiAlH_4$)

The conversion of the **-$SO_2$-** group in **$Br_2S$-$SEtC_8/C_{10}$** into an **-S-** group was achieved by reduction with $LiAlH_4$ in dry diethyl ether at –10 °C for 20 min (**Scheme 2.19**). The crude product was purified by flash column chromatography on silica gel eluting with PE to afford the desired product **2.24** as a colourless highly viscous liquid in 59 % yield and a purity of ~ 100% according to $^1$H NMR.

Three significant points were considered in this reaction: the solvent, the temperature, and the reaction time. When using dry THF as solvent three or more spots were observed by TLC, which could be because the reactivity of $LiAlH_4$ is better in THF compared to diethyl ether, which led to substitution of the Br group with a hydrogen atom. The same thing was observed when increasing the temperature or time, four or more spots were observed by TLC, which indicates a mixture of by-products. Hence, it is important to keep the temperature below –10 °C and the time of the reaction to only 20 minutes.

The reason of synthesising the **2.24** monomer was to convert it into a homopolymer, so that it's optical and electronic properties could be compared with those of the corresponding homopolymers prepared from monomers **$Br_2S$-$SEtC_8/C_{10}$** and **$Br_2S$-$SO_2EtC_8/C_{10}$**. Unfortunately, the polymerisation of this monomer was not successful, and in three trials all the starting materials was lost (more details in Chapter 3, Section 3.2.1).

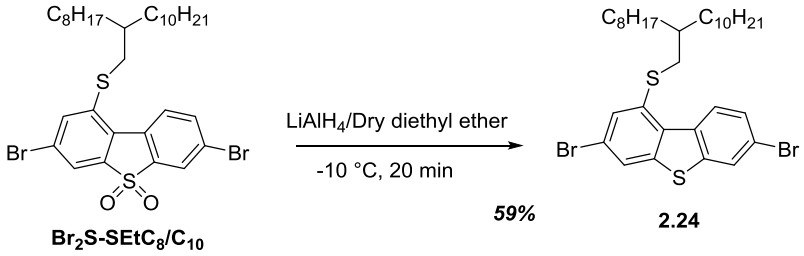


**Scheme 2.19:** Synthesis of monomer **(2.24)**.

### 2.2.6 X-ray single crystal structure of some of the monomers

The structures of five of the monomers **Br$_2$S-R** (**R** = **OMe**, **OC$_{12}$H$_{25}$**, **NO$_2$**, **SMe** and **CN**; IPER9-13 Durham codes)[c] discussed above were further confirmed by single crystal X-ray crystallography studies (see **Figures 2.4–2.8**). Crystals of all monomers were obtained by slow evaporation from a mixture of toluene : DCM (1 : 2–5). The molecules of 1-substituted 3,7-dibromodibenzothiophene-*S*,*S*-dioxides **Br$_2$S-R** are essentially planar excluding oxygen atoms of $SO_2$-groups and hydrogen atoms of substituents. Even the extended hydrocarbon chain in **Br$_2$S-OC$_{12}$** is coplanar with the aromatic ring (see **Figure 2.7**). The only other exception is molecule **Br$_2$S-NO$_2$** (see **Figure 2.4**), where the mean plane of the nitro group makes dihedral angle of 42.4(1)° with the plane of corresponding phenyl ring. Not surprisingly, the planar molecules in crystal show π...π stacking arrangements. Even lengthy side chains in structure **Br$_2$S-OC$_{12}$** cannot prevent formation of anti-parallel aromatic dimers. Of course, it is impossible to rank intermolecular interactions without proper calculations of pair-wise energies for the close molecular environment. Nevertheless, on the basis of presence of direction-specific intermolecular contacts, the Br...Br, H...Br halogen bonds and weak hydrogen bonds of C-H...O/S/π type may be detected in structures **Br$_2$S-R**. All crystal data and structure refinement for **Br$_2$S-R** monomers are collated in **Table 2.2**.

*c These measurements were done by Dr Dmitry Yufit from the Department of Chemistry Durham University.*

**Table 2.2:** Crystal data and structure refinement for 1-substituted 3,7-dibromodibenzothiophene-*S*,*S*-dioxides **$Br_2S$-R**.

| Identification code | IPER9 **$Br_2S$-OMe** | IPER10 **$Br_2S$ -$OC_{12}$** | IPER11 **$Br_2S$ -$NO_2$** | IPER12 **$Br_2S$ -SMe** | IPER13 **$Br_2S$ -CN** |
|---|---|---|---|---|---|
| Empirical formula | $C_{13}H_8Br_2O_3S$ | $C_{24}H_{30}Br_2O_3S$ | $C_{12}H_5Br_2NO_4S$ | $C_{13}H_8Br_2O_2S_2$ | $C_{13}H_5Br_2NO_2S$ |
| Formula weight | 404.07 | 558.36 | 419.05 | 420.13 | 399.06 |
| Temperature/K | 200.0 | 120.0 | 120.0 | 120.0 | 120.0 |
| Crystal system | monoclinic | monoclinic | monoclinic | triclinic | monoclinic |
| Space group | C2/m | $P2_1/c$ | $P2_1/n$ | P-1 | $P2_1/c$ |
| a/Å | 18.4915(8) | 11.9942(18) | 12.2059(7) | 7.7992(5) | 9.6638(6) |
| b/Å | 6.8608(3) | 18.330(3) | 8.0463(5) | 8.3305(5) | 9.2977(6) |
| c/Å | 11.0101(4) | 12.837(2) | 13.4744(8) | 10.7359(6) | 14.7640(10) |
| α/° | 90 | 90 | 90 | 76.808(2) | 90 |
| β/° | 103.1887(16) | 107.230(6) | 106.245(2) | 85.628(2) | 103.933(3) |
| γ/° | 90 | 90 | 90 | 78.464(2) | 90 |
| Volume/$Å^3$ | 1359.97(10) | 2695.6(7) | 1270.52(13) | 665.06(7) | 1287.53(15) |
| Z | 4 | 4 | 4 | 2 | 4 |
| $\rho_{calc}g/cm^3$ | 1.974 | 1.376 | 2.191 | 2.098 | 2.059 |
| $\mu/mm^{-1}$ | 6.113 | 3.105 | 6.556 | 6.401 | 6.452 |
| F(000) | 784.0 | 1136.0 | 808.0 | 408.0 | 768.0 |
| Reflections collected | 15075 | 58525 | 27163 | 14549 | 25604 |
| Independent refl., $R_{int}$ | 2140, 0.0390 | 7847, 0.0567 | 3702, 0.0386 | 3866, 0.0293 | 3423, 0.0491 |
| Data/ parameters | 2140/115 | 7847/272 | 3702/181 | 3866/173 | 3423/188 |
| GOOF on $F^2$ | 1.036 | 1.081 | 1.054 | 1.063 | 1.099 |
| $R_1$ [I≥2σ (I)] | 0.0342 | 0.0297 | 0.0211 | 0.0200 | 0.0547 |
| $wR_2$ [all data] | 0.0895 | 0.0723 | 0.0500 | 0.0505 | 0.1892 |
| Largest diff. peak/hole / e $Å^{-3}$ | 0.64/-0.69 | 0.44/-0.38 | 0.46/-0.40 | 0.66/-0.45 | 0.74/-1.39 |

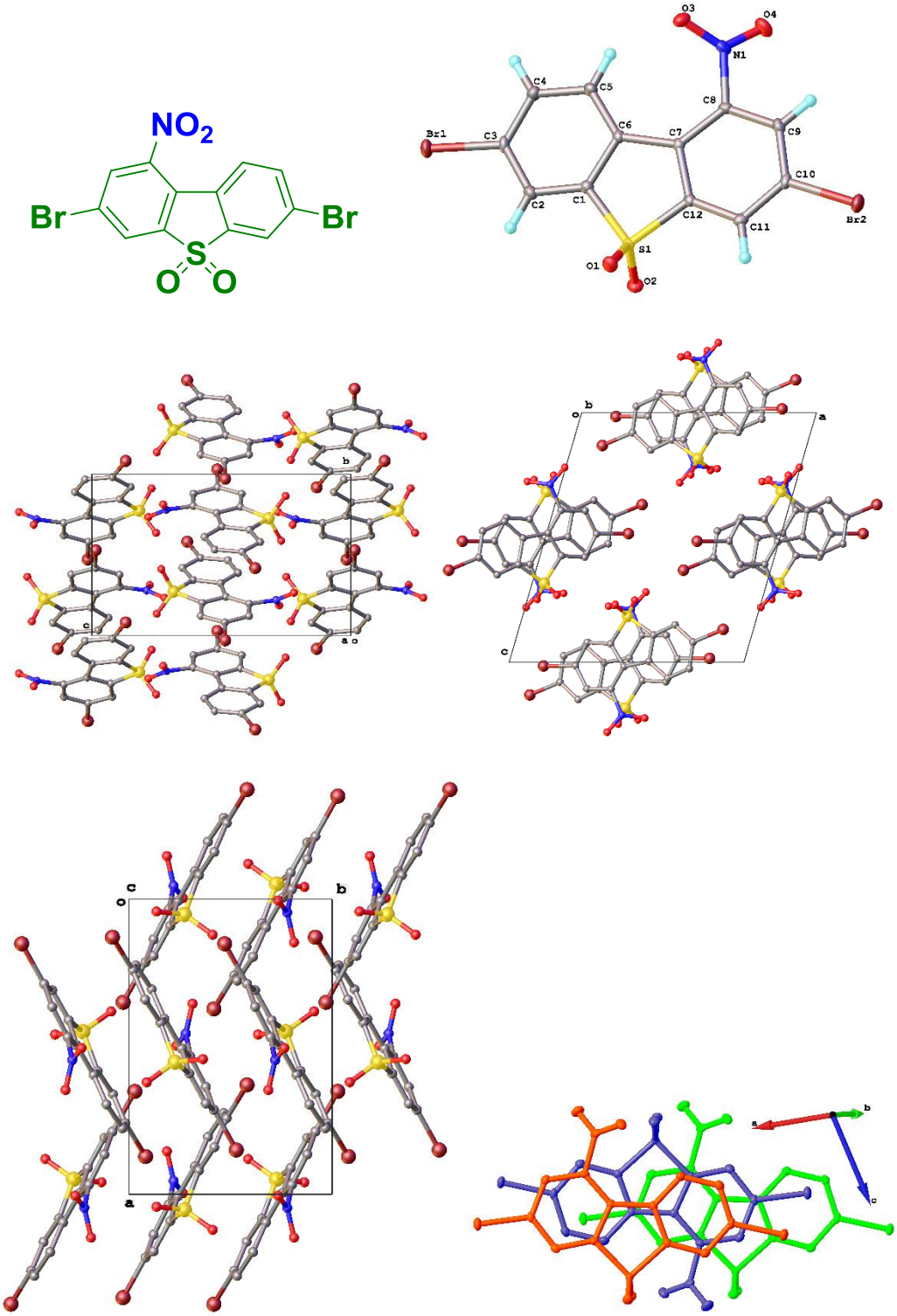


**Figure 2.4:** Single crystal x-ray molecular and crystal structure of compound **$Br_2S$-$NO_2$**.

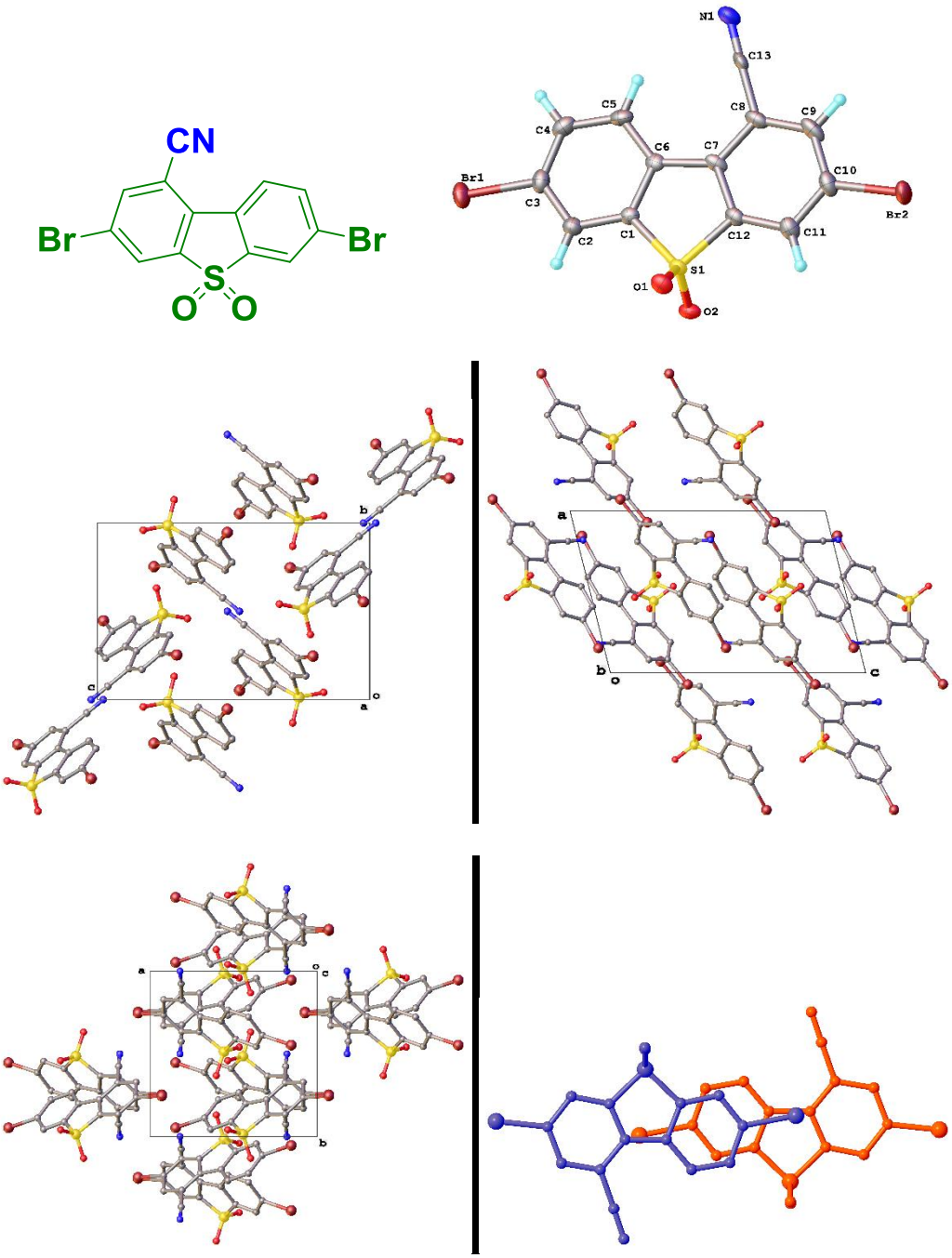


**Figure 2.5:** Single crystal x-ray molecular and crystal structure of compound **$Br_2$S-CN**.

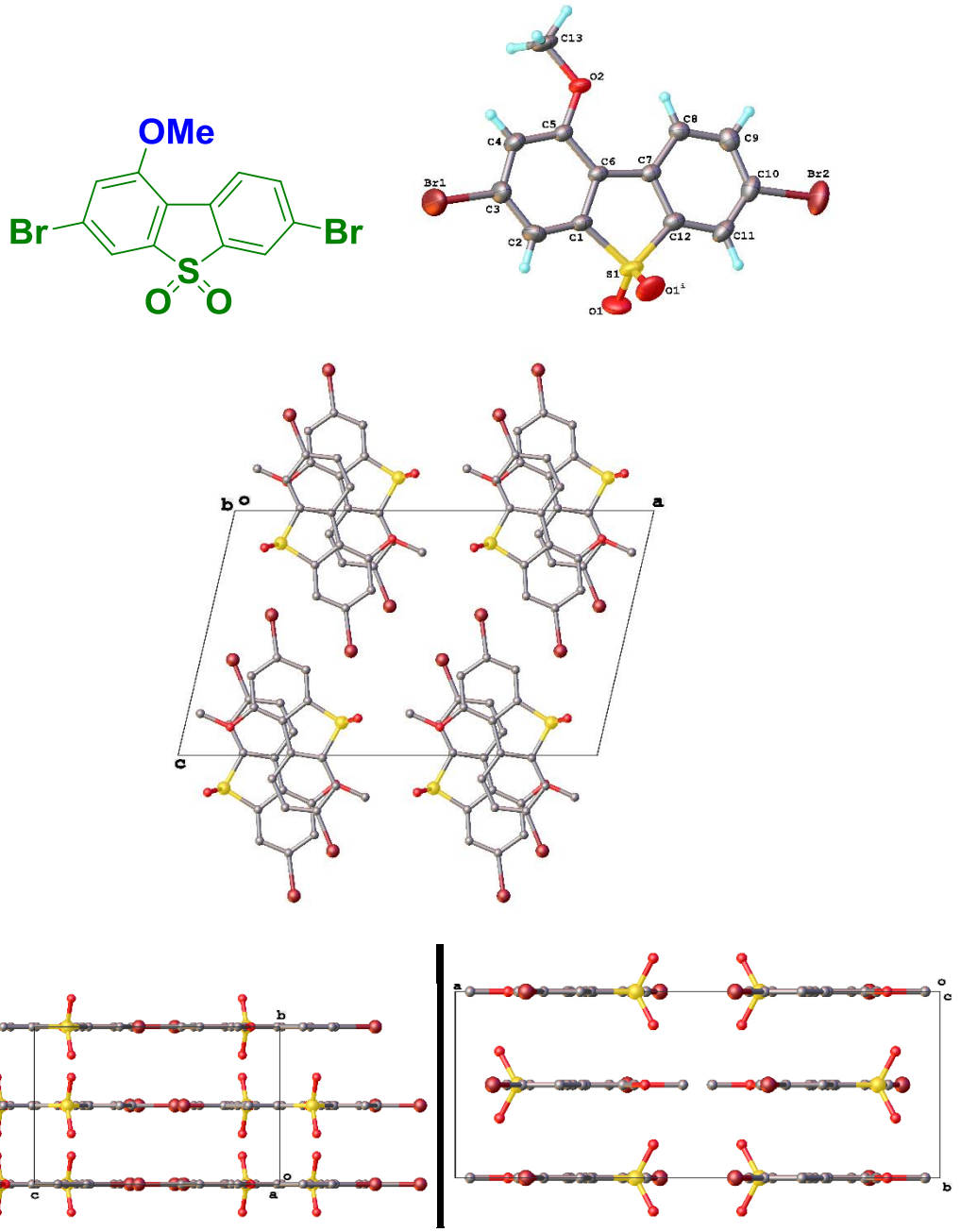


**Figure 2.6:** Single crystal x-ray molecular and crystal structure of compound **$Br_2$S-OMe**.

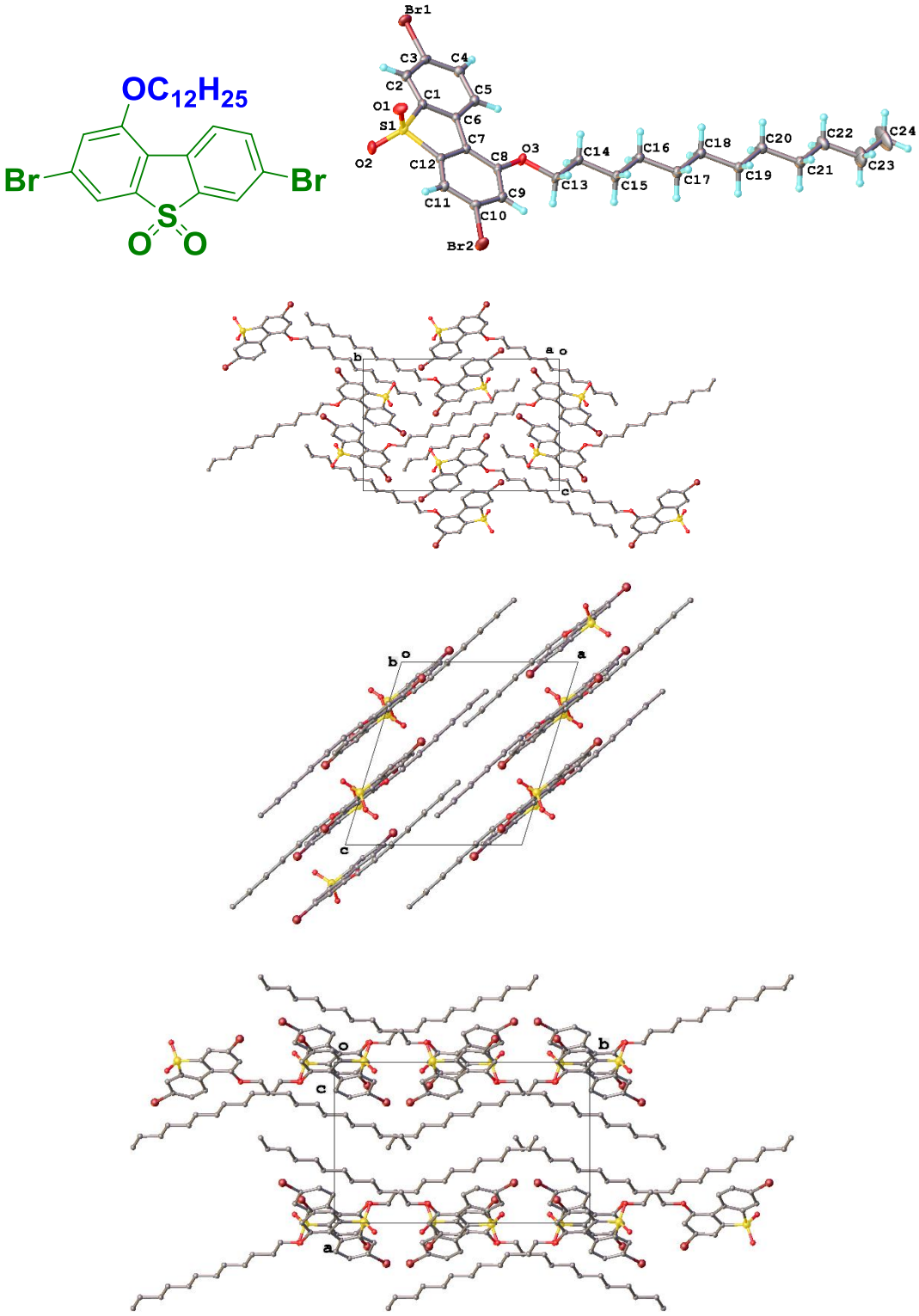


**Figure 2.7:** Single crystal x-ray molecular and crystal structure of compound **$Br_2$S-$OC_{12}$**.

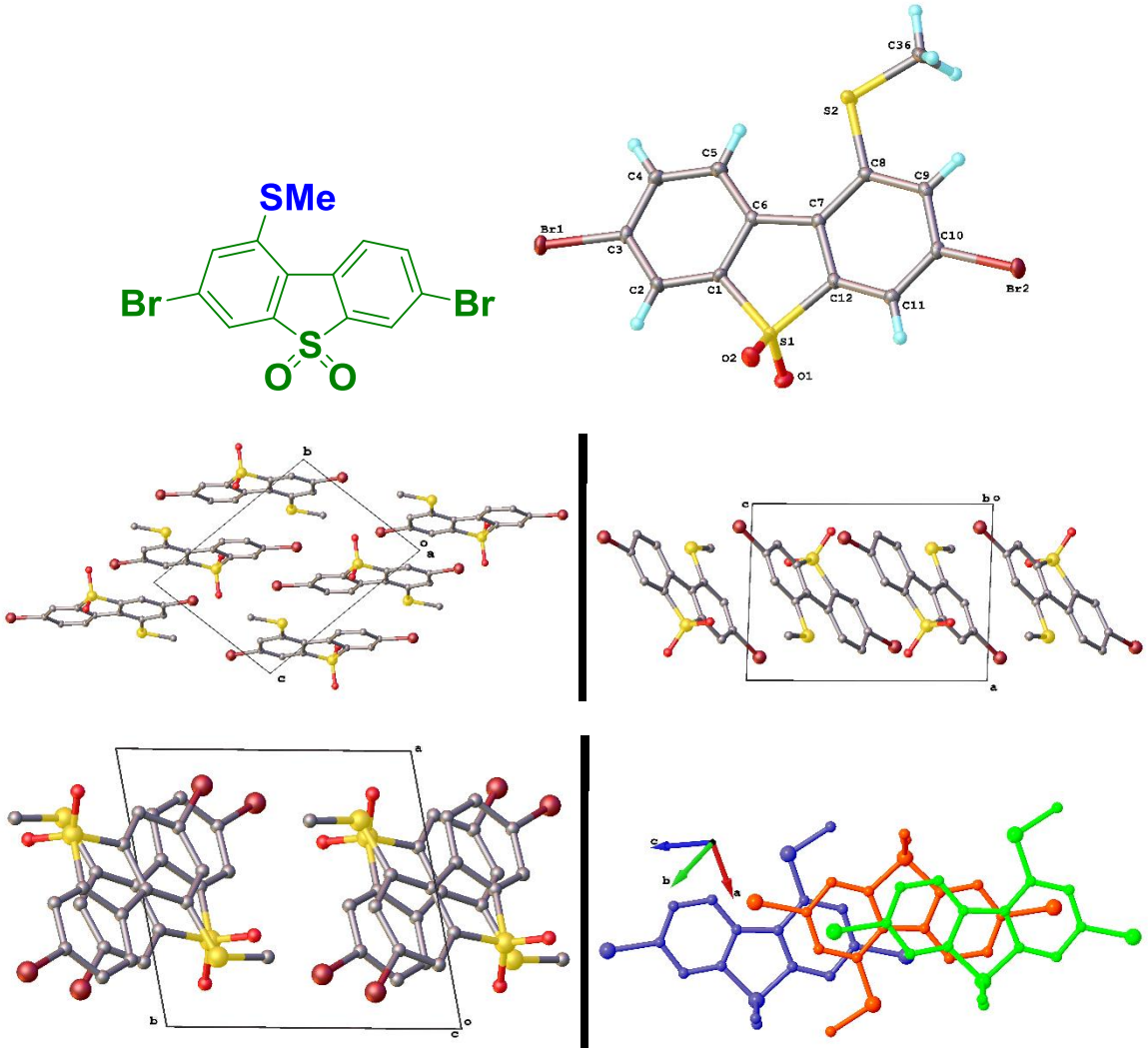


**Figure 2.8:** Single crystal x-ray molecular and crystal structure of compound **$Br_2$S-SMe**.

## 2.3 Conclusion

Synthetic methodologies to introduce a wide range of both electron-donating and electron-withdrawing substituents onto position 1 of the 3,7-dibromodibenzothiophene-*S*,*S*-dioxide **Br$_2$S-R** monomers have been elaborated. 1-Amino-3,7-dibromodibenzothiophene-*S*,*S*-dioxide (**Br$_2$S-NH$_2$**) was considered as a useful synthon for this work, which was then converted into a wide range of 1-substituted dibenzothiophene-*S*,*S*-dioxide monomers *via* diazonium chemistry. The multistep reaction route to the key intermediate, **Br$_2$S-NH$_2$**, started from commercially available dibenzothiophene, followed by oxidation, bromination, nitration, and reduction. Attention was also paid to scaling up the reactions and optimisation of the conditions, to elaborate convenient and efficient methods for their synthesis and purification. Having the **Br$_2$S-NH$_2$** monomer in hand, the amino group was converted (*via* diazonium salts) into four different groups (OH, CN, I and F). A series of 1-alkoxy-3,7-dibromodibenzothiophene-*S*,*S*-dioxide **Br$_2$S-OR** monomers were then synthesised by alkylation of **Br$_2$S-OH** with alkyl halides and alkyl tosylates. Replacement of the $NH_2$ group in **Br$_2$S-NH$_2$** by an SR group by classical reaction *via* a diazonium salt ($-N_2^+$) was not possible as diazonium salts oxidise thiols or disulfides instead of a nucleophilic substitution reaction occuring. This transformation was, therefore performed by other methods under milder conditions using iso-amyl nitrite as nitrosation reagents in organic solvents. After obtaining the **Br$_2$S-SR** monomers, they were then successfully oxidised to obtain **Br$_2$S-SO$_2$R** monomers.

## 2.4 Experimental Section

### 2.4.1 Chemicals and instruments

All the solvents and commercial chemicals, which were used without further purification, were supplied from Aldrich, Fisher, Acros, AlfaAesar, and Apollo Scientific chemical companies. Thin layer chromatography (TLC) was performed on alumina silica gel plates 20 × 20 cm (Merck) with visualisation by UV lamp 254/360 nm. For alcohols, TLC plates were developed with iodine vapour. Flash chromatography purification was performed on silica gel (40–60 μm) on Teledyne Isco Combiflash chromatograph, model Rf 200. Shimadzu UV-Vis 3600 spectrophotometer was used for recording the absorption spectra of the crude products for proper selection of the wavelengths for monitoring the separation process. VirTis BenchTop Pro 8L freeze dryer connected to a high-vacuum pump was used for vacuum drying of the samples at ambient temperature (<30–50 μbar). Microwave-assisted reactions were carried out using a CEM Discovery SP microwave reactor (300 W). NMR spectra were recorded on a Bruker Avance 400+ NMR spectrometer operating at 400 MHz (for $^{1}$H NMR) and 100 MHz (for $^{13}$C NMR) in $CDCl_3$ or DMSO-$d_6$ solutions relative to tetramethylsilane (TMS) as an internal standard (δ = 0.00 ppm). Gas chromatography – mass spectrometry measurements (GC-MS) were performed with electron impact (EI) ionisation in a positive mode (EI+) on a Thermo Scientific ITQ 900 GC/MS Ion Trap mass spectrometer, and the samples were prepared in chloroform or methanol. Melting points were measured on a Büchi M-565 automatic melting point apparatus. Infrared spectra were recorded on a Bruker Alpha ATR-FTIR as either a solid or as a neat liquid.

The single crystal X-ray crystallography data have been collected using λMoKα radiation (λ =0.71073Å) on a Bruker D8Venture (Photon100 CMOS detector, IμS-microsource, focusing mirrors) and Agilent XCalibur (Sapphire-3 CCD detector, fine-focus sealed tube, graphite monochromator) diffractometers equipped with a Cryostream (Oxford Cryosystems) open-flow nitrogen cryostats at the temperature 120.0(2)K. Crystals **Br$_2$S-OMe** shattered on attempts of flash freezing, so data for this compound were collecting at 200 K after slow (2°C/min) cooling the crystal from room temperature. All structures were solved by direct method and refined by full-matrix least squares on $F^2$ for all data using OLEX2[40] and SHELXTL[41] software. All non-disordered non-hydrogen atoms were refined

anisotropically, hydrogen atoms were placed in the calculated positions and refined in riding mode. Disordered atoms in structure **10b'** were refined isotropically with fixed SOF = 0.8 and 0.2. Structure **Br$_2$S-OC$_{12}$** also contained severely disordered toluene molecule (semi-solvate) which could not be modelled and refined satisfactorily. Their contribution was taken into account using MASK procedure of the OLEX2 program package. Crystal data and parameters of refinement are listed in **Table 2.2**.

### 2.4.2 Kinetics of nitration of 3,7-dibromodibenzothiophene-*S*,*S*-dioxide by GC-MS

The nitration of **Br$_2$S** compound was monitored by GC-MS. A sample was taken from the reaction mixture each hour for 23 hours, which was filtered, washed with water and dried under high vacuum followed by GC-MS analysis to check the progress of the reaction.

### 2.4.3 Electron absorption spectra measurements

UV-Vis electron absorption spectra were recorded on a Shimadzu UV-3600 spectrophotometer in 10 mm quartz cells in DCM, chloroform, toluene or chlorobenzene at ambient temperature (for measurements UV-Vis spectra for flash chromatography purification different solvents were used depending on the mobile phase used for chromatography). For measurements of UV-Vis spectra the concentrations were prepared to give an absorbance in the range of ~0.6–1.0 a.u.

### 2.4.4 Synthesis

**Dibenzothiophene-*S*,*S*-dioxide (S).**[6]

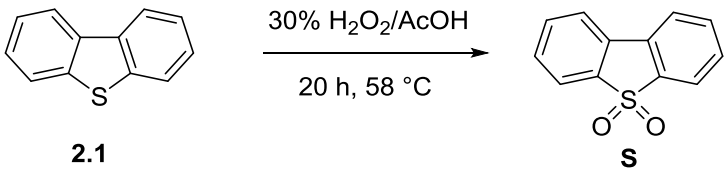


**2.1** **S**

Dibenzothiophene **2.1** (200.1 g, 1.09 mol) and acetic acid (2.0 L) were placed into a 3 L three-neck round bottom flask equipped with a stirring bar, thermometer and reflux condenser. The mixture was heated with stirring at ~58 °C until full dissolution of dibenzothiophene occurred and then 30% hydrogen peroxide (490 mL, 16.0 mol) was added

dropwise over ~1 hour. The mixture was stirred at 58 °C for 20 h, during which time the product was precipitated as a white solid. After cooling the mixture to room temperature, the solid was filtered off, washed with 70% aqueous acetic acid (150 mL) and dried *in vacuo* to afford dibenzothiophene-*S*,*S*-dioxide (**S**) (228 g, 97%) as a colourless crystalline product. $^1$H NMR spectroscopy showed that the material was sufficiently pure and it was therefore used in the next synthesis without further purification, mp. 232 – 233 °C. Lit.[42] mp. 233 – 235 °C, which showed $\delta_H$ (400 MHz, $CDCl_3$): 7.84 (d, *J* = 7.6 Hz, 2H, H-4,6), 7.81 (d, *J* = 7.7 Hz, 2H, H-1,9), 7.67 (td, *J* = 7.6, 0.92 Hz, 2H, H-3,7), 7.56 (td, *J* = 7.6, 0.7 Hz, 2H, H-2,8)

**3,7-Dibromodibenzothiophene-*S*,*S*-dioxide ($Br_2S$).**[1]

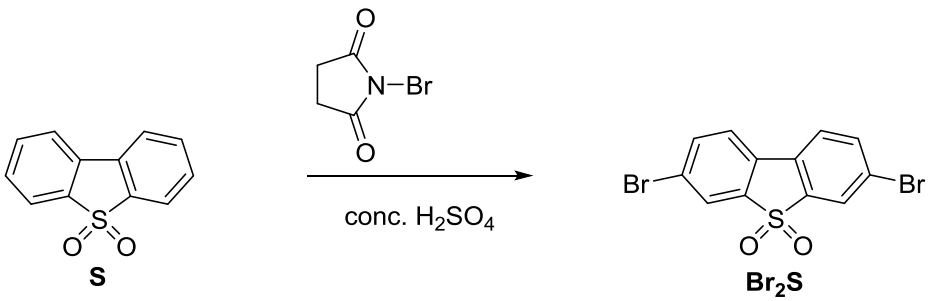


**S** **$Br_2S$**

Dibenzothiophene-*S*,*S*-dioxide (**S**) (120.0 g, 555 mmol) and conc. $H_2SO_4$ (3.6 L) were charged into a 5 L conical flask with a large magnetic stirring bar (12 × 3 cm) and stirred at room temperature until full dissolution. To this, NBS (206 g, 1107 mmol) was added slowly in portions over a period of 2 h and the reaction was stirred for 20 h. The precipitate was filtered off and washed with 90–92% conc. $H_2SO_4$. (400 mL). The reaction was carried out twice and the products (acidic!) were combined for purification. The combined products were carefully washed with water (warm/hot water in the end) and dried *in vacuo* to afford the crude product as a white powder (389 g, 94%). The crude product was added to a 4 L round bottom flask with 3 L of acetic acid. The mixture was stirred under reflux for 2 h (not full dissolution) and left to crystallise. On cooling to room temperature, the solid was filtered, washed with acetic acid (400 mL) and dried *in vacuo* in a freeze dryer to yield a white powder of partly purified product (371 g, 89%). This product was then recrystallized in two separate batches from chlorobenzene. Batch 1 (163 g) was recrystallised from 1.6 L of chlorobenzene and batch two (208 g) was recrystallised from 2.2 L of chlorobenzene. The products that crystallised on cooling were combined and collected by filtration, washed with

chlorobenzene (125 mL), and dried *in vacuo* to afford pure 3,7-dibromodibenzothiophene-*S*,*S*-dioxide (**$Br_2S$**) (322 g, 78%) as a shiny white crystalline material, mp. 299 – 300 °C. Lit.[43] mp. 288 – 290 °C, which showed $\delta_H$ (400 MHz, $CDCl_3$): 7.94 (d, *J* = 1.6 Hz, 2H), 7.78 (dd, *J* = 8.2, 1.8 Hz, 2H), 7.64 (d, *J* = 7.6, 2H); $\delta_C$ (100 MHz, $CDCl_3$): 139.9, 137.1, 129.6, 125.6, 124.6, 122.9; MS (EI+): *m/z* 371.83 ($M^+$, $^{79}Br/^{79}Br$, 54%), 373.76 ($M^+$, $^{79}Br/^{81}Br$, 100%), 375.81 ($M^+$, $^{81}Br/^{81}Br$, 53%). Calculated for $C_{12}H_6Br_2O_2S$: 373.84 (100%), 371.85 (51.4%), 375.84 (48.6%); $\nu_{max}$: 3079, 1298, 1158, 1142, 1131, 825, 652, 429 $cm^{-1}$.

**1-Nitro-3,7-dibromodibenzothiophene-*S*,*S*-dioxide (Br2S-NO2)**.

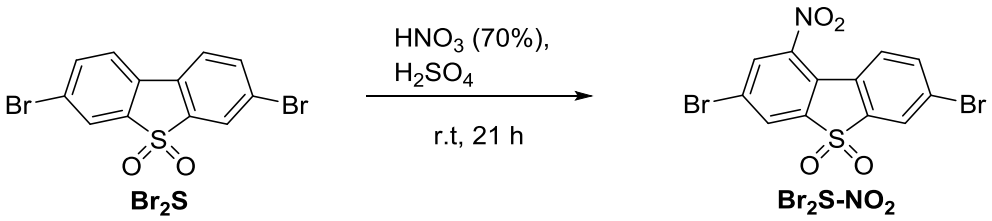


A 5 L conical flask with a large stirring bar was charged with 3,7-dibromodibenzothiophene-*S*,*S*-dioxide (**$Br_2S$**) (159 g, 423 mmol) and conc. $H_2SO_4$ (1.6 L) and stirred vigorously for 30 minutes at 0 °C. The mixture appears as a white cloudy solution/suspension. To this, concentrated $HNO_3$ (70%) (800 mL, 12.6 mol) was added dropwise over 45 minutes. The reaction mixture was stirred at room temperature for 21 h. The reaction mixture represented a heterogeneous suspension, with a pale pink suspension. After this time the reaction mixture was poured onto crushed ice (2.4 kg) and a creamy white precipitate was filtered off, washed with water until the filtrate was neutral (pH 7) and dried in an oven at 110 °C and then *in vacuo* to afford the product **$Br_2S$-$NO_2$** (175 g, 98%), purity ~ 94% by $^1H$ NMR. The crude product was recrystallized from dioxane (2 L) to afford the pure target product **$Br_2S$-$NO_2$** as a white powder (149 g, 83%), mp. 264 – 265 °C, which showed $\delta_H$ (400 MHz, $CDCl_3$): 8.15 (d, *J* = 1.7 Hz, 1H), 8.08 (d, *J* = 1.7 Hz, 1H), 8.01 (d, *J* = 1.8 Hz, 1H), 7.80 (dd, *J* = 8.5, 1.9 Hz, 1H), 7.67 (d, *J* = 8.5 Hz, 1H); $\delta_C$ (100 MHz, $CDCl_3$): 145.9, 141.1, 139.0, 137.7, 131.7, 129.1, 126.8, 126.7, 125.9, 125.2, 124.7, 122.4; MS (EI+): *m/z* 416.73 ($M^+$, $^{79}Br/^{79}Br$, 46%), 418.79 ($M^+$, $^{79}Br/^{81}Br$, 100%), 420.71 ($M^+$, $^{81}Br/^{81}Br$, 51%). Calculated for $C_{12}H_5Br_2NO_4S$: 416.83 (51.4%), 418.83 (100%), 420.83 (48.6%)%); $\nu_{max}$: 3080, 1582, 1555, 1536, 1427, 1316, 1155, 1137, 1087, 830, 576, 526,423 $cm^{-1}$.

**1-Amino-3,7-dibromo dibenzothiophene-*S*,*S*-dioxide ($Br_2S$-$NH_2$).**

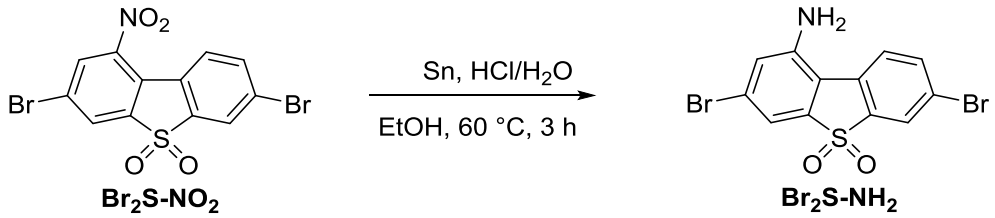


Compound **$Br_2S$-$NO_2$** (104 g, 250 mmol), ethanol (800 mL), 37% concentrated HCl (320 mL, 3.97 mol) and water (220 mL) were charged into a 3 L round bottom flask. The mixture was stirred for 1 h, producing a white suspension. Tin powder (118 g, 991 mmol) was slowly added over 1 h. The mixture was heated to 60 °C and stirred for 3 h, producing a greenish-yellow suspension. The mixture was cooled down to room temperature, diluted with water (1 L) and basified with solid $Na_2CO_3$ until pH~9 was achieved. After stirring for 1 h, it was evaporated under reduced pressure to dryness. The solid was extracted on a Soxhlet apparatus (with ~6 – 7 cm silica gel layer on the bottom to pass the solution through the silica gel layer for removal of inorganic and some by-products) with THF for 21 h. The THF was evaporated and the residue was dried *in vacuo* to afford the crude product as a yellow powder. The crude product was recrystallized from dioxane (1.9 L) to afford a yellow powder (67.2 g, 70%). A second recrystallization from dioxane (1.3 L) gave pure **$Br_2S$-$NH_2$** (43.6 g, 45%) as a light yellow powder, mp. 322 – 323 °C, which showed $\delta_H$ (400 MHz, $CDCl_3$): 7.96 (d, *J* = 1.7 Hz, 1H), 7.76 (dd, *J* = 8.3, 1.8 Hz, 1H), 7.66 (d, *J* = 8.2 Hz, 1H), 7.40 (d, *J* = 1.5, 1H), 7.12 (d, *J* = 1.5, 1H), 4.28 (s, 2H, $NH_2$); $\delta_C$ (100 MHz, DMSO-$d_6$): 146.7, 139.2, 136.9, 136.5, 129.1, 125.7, 124.4, 123.6, 123.3, 120.8, 111.6, 110.9; MS (EI+): *m/z* 386.87 ($M^+$, $^{79}Br/^{79}Br$, 46%), 388.81 ($M^+$, $^{79}Br/^{81}Br$, 100%), 390.77 ($M^+$, $^{81}Br/^{81}Br$, 52%). Calculated $C_{12}H_7Br_2NO_2S$: 386.86 (51.4%), 388.85 (100%), 390.85 (48.6%); $\nu_{max}$: 3445, 3365, 3253, 3069, 1639, 1584, 1274, 1165, 1135, 1083, 869, 618, 576, 532 $cm^{-1}$.

(The mother liquor from the first recrystallisation was evaporated to yield a dark yellow powder (29.2 g, 30%), which was used in the synthesis of additional amounts of **$Br_2S$-OH**. The mother liquor from the second recrystallization was combined with the product from the next synthesis for purification).

**1-Hydroxy-3,7-dibromo dibenzothiophene-*S*,*S*-dioxide ($Br_2S$-OH)**.

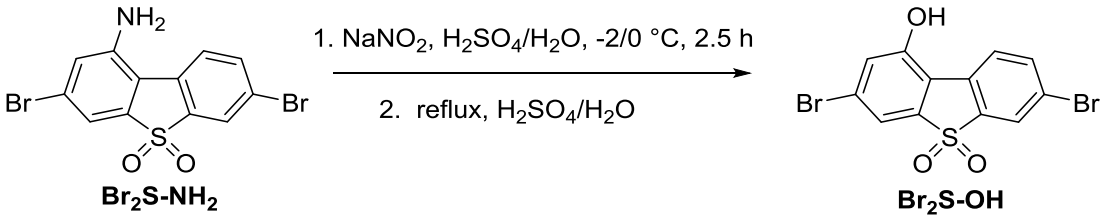


1-Amino-3,7-dibromodibenzothiophene-*S*,*S*-dioxide **($Br_2S$-$NH_2$)** (2.85 g, 7.3 mmol) in concentrated (95%) $H_2SO_4$ (75 mL) was stirred to give a dark green solution, to which water (75 mL) was added dropwise to form a yellowish suspension and the mixture was cooled down to –2/0 °C. With stirring, a solution of $NaNO_2$ (0.630 g, 9.1 mmol) in water (5 mL) was added dropwise to this mixture over 45 min and the mixture was stirred at –2/0 °C for 2 h. Urea (~600 mg) was added to this mixture to destroy any excess nitrite ion (KI-starch paper still showed a purple colour). The mixture was then slowly added dropwise over 30 min to stirred boiling water (400 mL) with concentrated (95%) $H_2SO_4$ (50 mL) and the resulting mixture was stirred under reflux for 20 min. After cooling down to room temperature, the precipitate that had formed was filtered off, washed with water until the filtrate was neutral (pH 7) and dried *in vacuo* to yield the crude product as a light brown powder. The crude product was added to 5% NaOH solution (280 mL) and heated to reflux to form a dark green solution with some precipitate, which was removed by hot filtration. After cooling down to room temperature, the solution was acidified with HCl to form a cream coloured precipitate, which was filtered off, washed with water until the filtrate was neutral (pH~7) and dried *in vacuo* to afford the target product **$Br_2S$-OH** (2.15 g, 75%) as a pale cream powder, mp. 311 – 312 °C, which showed $\delta_H$ (400 MHz, $CDCl_3$): 8.11 (d, $J$ = 8.4 Hz, 1H), 7.92 (d, $J$ = 1.8, Hz, 1H), 7.76 (dd, $J$ = 8.4, 1.8 Hz, 1H), 7.54 (d, $J$ = 1.4 Hz, 1H), 7.20 (d, $J$ = 1.4 Hz, 1H), 6.22 (s, 1H, OH); $\delta_H$ (400 MHz, DMSO-$d_6$): 8.31 (d, $J$ = 1.8 Hz, 1H), 8.21 (d, $J$ = 8.4, Hz, 1H), 7.98 (dd, $J$ = 8.4, 1.9, Hz, 1H), 7.71 (d, $J$ = 1.5 Hz, 1H), 7.36 (d, $J$ = 1.5 Hz, 1H); $\delta_C$ (100 MHz, DMSO-$d_6$): 156.3, 140.1, 138.2, 138.0, 129.3, 127.8, 125.4, 124.7, 124.6, 122.9, 115.8, 115.79; MS (EI+): *m/z* 388.04 ($M^+$, $^{79}Br/^{79}Br$, 49%), 389.98 ($M^+$, $^{79}Br/^{81}Br$, 100%), 391.96 ($M^+$, $^{81}Br/^{81}Br$, 53%). Calculated $C_{12}H_7Br_2NO_2S$: 387.84 (51.4%), 389.84 (100%), 391.84 (48.6%); $\nu_{max}$: 3318 br, 3073, 1587, 1457, 1447, 1417, 1288, 1277, 1266, 1075, 936, 838, 623, 540 $cm^{-1}$.

**1-Cyano 3,7-dibromodibenzothiophene-*S*,*S*-dioxide ($Br_2S$-CN).**

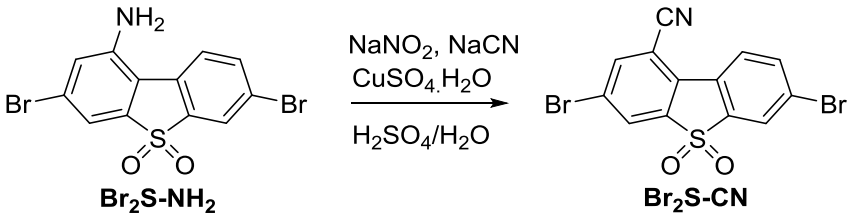


1-Amino-3,7-dibromodibenzothiophene-*S*,*S*-dioxide (**$Br_2S$-$NH_2$**) (4.00 g, 10 mmol) and $H_2SO_4$ (150 mL) were charged into a 2-neck round bottom flask. To this, water (140 mL) was added slowly with stirring maintaining the temperature below 30 °C. The mixture was then cooled to 0/-2 °C, and a solution of $NaNO_2$ (0.862 g, 12.5 mmol) in water (20 mL) was added dropwise over 30 min at 0 °C to the mixture which was then stirred at 0 °C for 2 h. To this mixture, a solution of $CuSO_4 \cdot 5H_2O$ (55.2 g, 112 mmol) in water (110 mL) was added dropwise over 30 min. Then, a solution of NaCN (32.5 g, 664 mmol) in water (70 mL) was added dropwise over the next 30 min. The mixture was allowed to warm to room temperature and left to stir for 16 h. The temperature was raised to 80 °C and the mixture was stirred for a further 3 h. The mixture was then cooled to room temperature and the solid was filtered off, washed with water and dried to afford the crude product, which indicated a mixture of **$Br_2S$-CN** (69%), **$Br_2S$-OH** (12%), **$Br_2S$** (12%) and starting **$Br_2NH_2$** (7%) (according to $^1$H NMR spectroscopy). The crude product was purified by flash chromatography on silica gel eluting with toluene (this was carried out 2 times), followed by recrystallisation from dichloromethane to yield the target product **$Br_2S$-CN** (1.99 g, 50%) as a light yellow powder, mp. 288 – 289 °C, which showed $\delta_H$ (400 MHz, $CDCl_3$): 8.49 (d, *J* = 8.5 Hz, 1H), 8.15 (d, *J* = 1.7 Hz, 1H), 8.03 (d, *J* = 1.7 Hz, 1H), 8.01 (d, *J* = 1.8 Hz, 1H), 7.89 (dd, *J* = 8.5, 1.8 Hz, 1H); $\delta_C$ (100 MHz, $CDCl_3$): 140.6, 140.2, 138.9, 138.86, 137.1, 131.3, 129.6, 127.0, 126.8, 124.6, 124.3, 115.5, 108.3; MS (EI+): *m/z* 397.07 ($M^+$, $^{79}Br/^{79}Br$, 53%), 398.95 ($M^+$, $^{79}Br/^{81}Br$, 100%), 400.97 ($M^+$, $^{81}Br/^{81}Br$, 53%). Calculated for $C_{13}H_5Br_2NO_2S$: 396.84 (51.4%) 398.84 (100%), 400.84 (48.6%); $\nu_{max}$: 3085, 3065, 2238, 1584, 1427, 1308, 1161, 1140, 1099, 1056, 803, 692, 573, 416 $cm^{-1}$.

**1-Iodo-3,7-dibromodibenzothiophene-*S*,*S*-dioxide ($Br_2S$-I).**

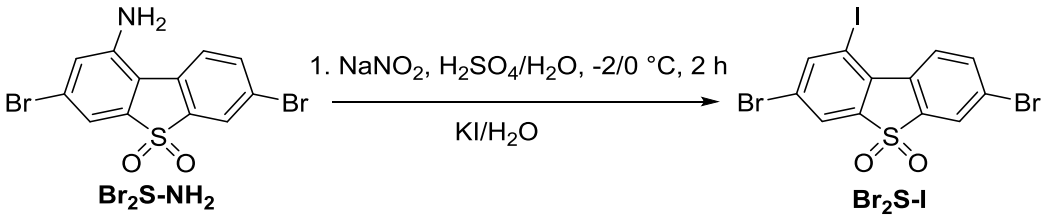


**$Br_2S$-$NH_2$** **$Br_2S$-I**

A 3 L round bottom flask was charged with 1-amino-3,7-dibromodibenzothiophene-*S*,*S*-dioxide **($Br_2S$-$NH_2$)** (20.0 g, 51.4 mmol), 95% concentrated $H_2SO_4$ (600 mL) and $H_2O$ (600 mL). The mixture was cooled to 0 °C, and a solution of $NaNO_2$ (4.79 g, 69.4 mmol) in $H_2O$ (40 mL) was slowly added with stirring over a period of 30 minutes and the reaction mixture was stirred for 2 h maintaining the temperature at –2/0 °C (internal temperature). A solution of potassium iodide (140 g, 843 mmol) in $H_2O$ (200 mL) was added and the mixture was stirred at room temperature for 30 minutes and then heated under reflux for 2 h. The mixture was cooled down to room temperature, the brown precipitate was filtered off, washed with 2 M aqueous NaOH (4 × 100 mL), then with water until the filtrate was neutral (pH ~ 7) and dried to give the crude product. Which was purified by column chromatography on silica gel eluting with (PE : Tol 1:1) to afford the pure target product **($Br_2S$-I)** as an off-white solid (13.7 g, 53%), mp. 250 – 251 °C, which showed $\delta_H$ (400 MHz, $CDCl_3$): 9.02 (d, *J* = 8.6 Hz, 1H), 8.30 (d, *J* = 1.6 Hz, 1H), 7.97 (d, *J* = 1.8, Hz, 1H), 7.94 (d, *J* = 1.7 Hz, 1H), 7.85 (dd, *J* = 8.5, 1.7 Hz 1H); $\delta_C$ (100 MHz, $CDCl_3$): 148.6, 140.5, 138.8, 136.4, 130.6, 129.7, 125.6, 125.3, 125.26, 124.3, 124.25, 89.6; MS (EI+): *m/z* 497.97 ($M^+$, $^{79}Br/^{79}Br$, 50%), 499.95 ($M^+$, $^{79}Br/^{81}Br$, 100%), 501.86 ($M^+$, $^{81}Br/^{81}Br$, 54%). Calculated for $C_{12}H_5Br_2IO_2S$: 497.74 (51.4%) 499.74 (100%), 501.74 (48.6%); $\nu_{max}$: 3057, 1560, 1429, 1300, 1166, 1137, 1087, 827, 699, 593, 577, 514, 446 $cm^{-1}$.

**1-Fluoro-3,7-dibromodibenzothiophene-*S*,*S*-dioxide ($Br_2$S-F).**

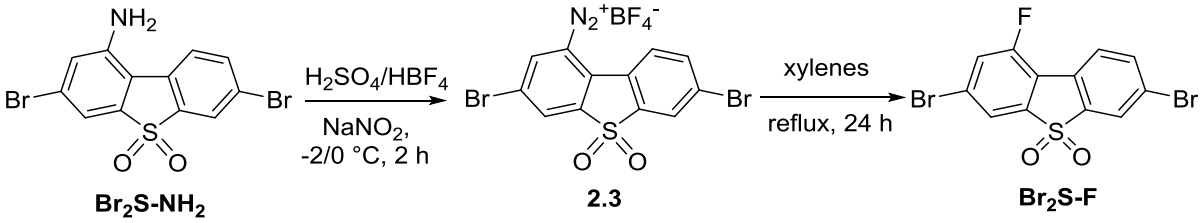


**$Br_2$S-$NH_2$** **2.3** **$Br_2$S-F**

1-Amino-3,7-dibromodibenzothiophene-*S*,*S*-dioxide **($Br_2$S-$NH_2$)** (7.00 g, 18.0 mmol), 95% concentrated $H_2SO_4$ (350 mL) and $HBF_4$ (350 mL) were charged in a 2 L round bottom flask. The mixture was cooled to 0 °C and a solution of $NaNO_2$ (3.72 g, 54.0 mmol) in $H_2O$ (20 mL) was slowly added with stirring over a period of 30 minutes and the reaction mixture was stirred for 2 h maintaining the temperature at –2/0 °C (internal temperature). The mixture was filtered, and the solid washed with cooled $HBF_4$, water and diethyl ether then dried under high vacuum overnight to obtain the diazonium salt as a yellow powder (9.84 g, 112% by mass). The solid compound was dissolved in xylene (o-/m-/p-mixture, 120 mL) and stirred at reflux for 3 h. The mixture was cooled to room temperature, passed through a short column using DCM as eluent. The solvent was evaporated under reduced pressure and the residue was dried in vacuo to give the crude product as a dark brown powder. The crude product was purified by flash chromatography on silica gel using PE : Tol 1:1 as eluent then purified further by recrystallization in toluene to afford the pure target product **($Br_2$S-F)** as off-white crystals (1.43 g, 20%), mp. 255 – 256 °C, which showed $\delta_H$ (400 MHz, $CDCl_3$): 7.96 (d, *J* = 1.3 Hz, 1H), 7.87 (d, *J* = 8.3 Hz, 1H), 7.81 (dd, *J* = 8.3, 1.2 Hz, 1H), 7.77 (br. d, 1H), 7.55 (dd, *J* = 9.4, 1.2 Hz 1H); $\delta_F$ (400 MHz, $CDCl_3$): –113.27 (d, *J* = 10.0 Hz, 1F); $\delta_C$ (100 MHz, $CDCl_3$): 159.4, 156.8, 140.6, 140.5, 138.7, 137.5, 126.9, 126.8, 126.53, 126.5, 125.6, 125.1, 124.9, 124.86, 121.8, 121.7, 117.9, 117.7; MS (EI+): *m/z* 390.02 ($M^+$, $^{79}Br/^{79}Br$, 52%), 391.98 ($M^+$, $^{79}Br/^{81}Br$, 100%), 393.97 ($M^+$, $^{81}Br/^{81}Br$, 51%). Calculated for $C_{12}H_5Br_2FO_2S$: 389.84 (51.4%) 391.83 (100%), 393.83 (48.6%); $\nu_{max}$: 3086, 1583, 1424, 1412, 1385, 1311, 1237, 1138, 831, 796, 688, 574, 538, 447 $cm^{-1}$.

Impure fraction (~ 60% purity, 1.12 g, 16%).

**1-Bromo-3,7-dimethyloctane (2.5).**[44]

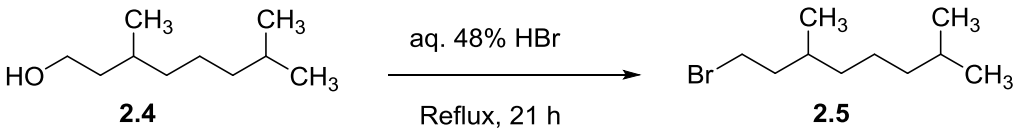


**2.4** **2.5**

3,7-Dimethyloctan-1-ol (50.0 g, 316 mmol) was added to concentrated 48% HBr (750 mL) and the solution was stirred and heated under reflux at 125 °C for 21 h. After cooling, it was extracted with PE (4 × 75 mL), and the combined organic layers were washed with a saturated solution of $NaHCO_3$ (75 mL) and evaporated. Distillation of the crude product via a fractional column afforded the pure target compound **2.5** as a colourless liquid (64.5 g, 92%, b.p. 91–93 °C / 8.9 mbar), which showed $\delta_H$ (400 MHz, $CDCl_3$): 3.50 – 3.37 (m, 2H), 1.92 – 1.83 (m, 1H), 1.71 – 1.58 (m, 2H), 1.56 – 1.48 (m, 1H), 1.33 – 1.21 (m, 3H), 1.19 – 1.09 (m, 3H), 0.89 (d, $J$ = 7.2, 3H), 0.87 (d, $J$ = 6.9, 6H); $\delta_C$ (100 MHz, $CDCl_3$): 40.1, 39.2, 36.7, 32.2, 31.7, 28.0, 24.6, 22.7, 22.6, 19.0; $\nu_{max}$: 2954, 2925, 2869, 1459, 1380, 1365, 1260, 1065, 1055, 648, 568 $cm^{-1}$.

**2-Hexyldecyl-4-methylbenzenesulfonate (2.7).**[45]

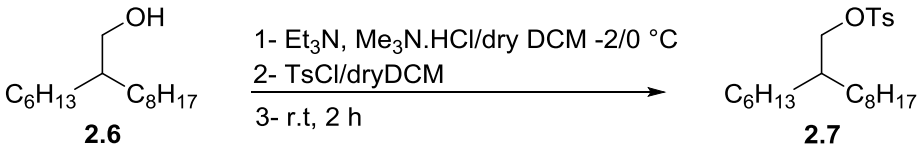


**2.6** **2.7**

Under a nitrogen atmosphere, 2-hexyldecan-1-ol (10.0 g, 41.3 mmol), $Me_3N{\cdot}HCl$ (4.57 g, 47.8 mmol) and dry $Et_3N$ (12.2 g, 120 mmol) were added to dry DCM (40 mL) and the solution was cooled to –2 °C. A solution of *p*-toluenesulfonyl chloride (11.5 g, 60.2 mmol) in dry DCM (39 mL) was added dropwise to this solution for 1.5 h. ***NB:*** *it was observed that the p-toluenesulfonyl chloride was not fully dissolved in the DCM (suspected partly hydrolysed reagent*). Therefore, a new portion of $Et_3N$ (6.00 g, 59.3 mmol) and *p*-toluenesulfonyl chloride (fresh sample: 6.00 g, 31.5 mmol) in dry DCM (20 mL) were added dropwise to the reaction mixture over 45 mins. The reaction mixture was stirred at room temperature for 2 h, quenched with water (40 mL) and the DCM layer was separated and the aqueous layer was extracted with DCM (7 × 20 mL). The combined DCM layers were washed with brine (3 × 50 mL), dried over $MgSO_4$, filtered, evaporated and dried *in vacuo* to afford the crude product as a viscous orange liquid. The crude product was purified by

flash chromatography on silica gel (PE : iPrOH, 10:1) to afford the pure target compound **2.7** as a viscous colourless liquid (12.5 g, 76%), which showed $\delta_H$ (400 MHz, $CDCl_3$): δ (ppm) = 7.79 (d, *J* = 8.2 Hz, 2H), 7.34 (d, *J* = 8.2 Hz, 2H), 3.91 (d, *J* = 5.3 Hz, 2H), 2.45 (s, 3H), 1.61 – 1.55 (m, 1H), 1.3 – 1.1 (m, 24H), 0.88 (t, *J* = 6.9 Hz, 6H); $\delta_C$ (100 MHz, $CDCl_3$): 144.6, 133.2, 129.8 (2C), 127.9 (2C), 72.9, 37.6, 31.9, 31.7, 30.6 (2C), 29.8, 29.5, 29.4, 29.3, 26.5, 26.4, 22.7, 22.6, 21.6, 14.1, 14.07; MS (ESI+) *m/z*: 419.46 $[M+Na]^+$ (14.8 %), 815.96 $[M_2+Na]^+$ (100 %). Calculated for $C_{23}H_{40}O_3S$: 396.61; calculated for $C_{23}H_{40}O_3SNa$: 419.26; $\nu_{max}$: 2955, 2924, 2855, 1598, 1458, 1362, 1306, 1187, 1175, 1097, 951, 812, 687, 554 $cm^{-1}$.

**2-Octyldodecyl tosylate (2.9)**.[46]

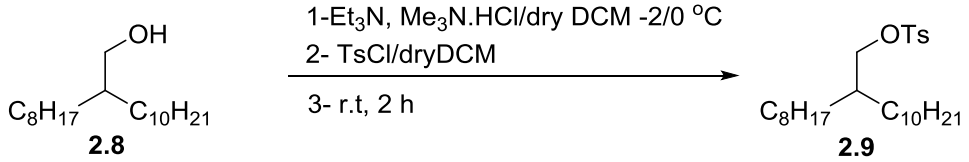


Under a nitrogen atmosphere, 2-octyldodecan-1-ol (10.0 g, 33.5 mmol), $Me_3N{\cdot}HCl$ (3.74 g, 39.1 mmol) and dry $Et_3N$ (9.91 g, 97.9 mmol) were added to dry DCM (40 mL) and cooled to –2 °C. A solution of *p*-toluenesulfonyl chloride (9.40 g, 49.3 mmol) in dry DCM (39 mL) was added dropwise to this solution over 1.5 h and the mixture was allowed to warm to room temperature and stirred for 2 h. The reaction was quenched with water (40 mL), the DCM layer was separated and the aqueous layer was extracted with DCM (7 × 20 mL). The combined DCM layers were washed with brine (3 × 50 mL), dried over $MgSO_4$ and filtered off, evaporated and dried *in vacuo* to afford the crude product as a viscous colourless liquid. The crude product was purified by flash chromatography on silica gel (PE : iPrOH, 20:1) to afford the pure compound **2.9** as a viscous colourless liquid (8.82 g, 58%), which showed $\delta_H$ (400 MHz, $CDCl_3$): 7.78 (d, *J* = 8.2 Hz, 2H), 7.33 (d, *J* = 8.2, Hz, 2H), 3.91 (d, *J* = 5.3 Hz, 2H) 2.45 (s, 3H), 1.62 – 1.54 (m, 1H), 1.34 – 1.07(m, 32H), 0.88 (t, *J* = 6.8, Hz, 6H); $\delta_C$ (100 MHz, $CDCl_3$): 144.6, 133.2, 129.8 (2C), 127.9 (2C), 72.9, 37.6, 31.9, 31.88, 30.6 (2C), 29.8 (2C), 29.6 (2C), 29.55, 29.5, 29.3, 29.28, 26.5 (2C), 22.7, 22.68, 21.6, 14.1 (2C); $\nu_{max}$: 2954, 2922, 2853, 1598, 1457, 1363, 1187, 1176, 1097, 954, 812, 665, 554 $cm^{-1}$.

**9-Heptadecyl tosylate (2.13).**[47]

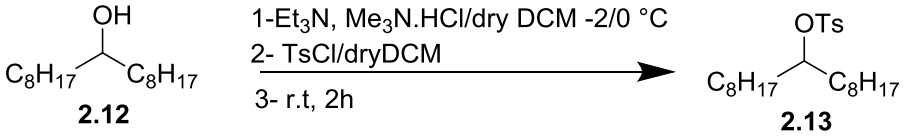


Under a nitrogen atmosphere, 9-heptadecanol (5.00 g, 16.8 mmol), $Me_3N{\cdot}HCl$ (3.20 g, 33.5 mmol) and dry $Et_3N$ (6.93 g, 58.6 mmol) were added to dry DCM (20 mL) and the solution was cooled down to –2 °C. A solution of p-toluenesulfonyl chloride (7.18 g, 37.7 mmol) in dry DCM (20 mL) was added dropwise to this solution over 1.5 h, the mixture allowed to warm to room temperature and stirred for 2 h. The reaction was quenched with water (20 mL), DCM layer was separated and the aqueous layer was extracted with DCM (7 × 10 mL). The combined DCM layers were washed with brine (3 × 25 mL), dried over $MgSO_4$, filtered off, evaporated and dried *in vacuo* to afford crude product as a viscous colourless liquid. The crude product was purified by flash chromatography on silica gel (PE : iPrOH, 20:1) to afford pure compound **2.13** as a viscous colourless liquid (6.64 g, 97%), which showed $\delta_H$ (400 MHz, $CDCl_3$): 7.78 (d, *J* = 8.2 Hz, 2H), 7.32 (d, *J* = 8.2, Hz, 2H), 4.57 – 4.50 (m, 1H), 2.44 (s, 3H), 1.62 – 1.54 (m, 1H), 1.55 – 1.50 (m, 4H), 1.25 – 1.10 (m, 24H), 0.88 (t, *J* = 6.9, Hz, 6H); $\delta_C$ (100 MHz, $CDCl_3$): 144.3, 134.8, 129.6 (2C), 127.7 (2C), 84.7, 34.1 (2C), 31.9 (2C), 29.4 (2C), 29.3 (2C), 29.2 (2C), 24.7 (2C), 22.7 (2C), 21.6, 14.1 (2C); $\nu_{max}$: 2924, 2854, 1598, 1507, 1395, 1187, 1174, 865, 813, 737, 664, 553 $cm^{-1}$.

**9-Heptadecanolol (2.12)**.[22]

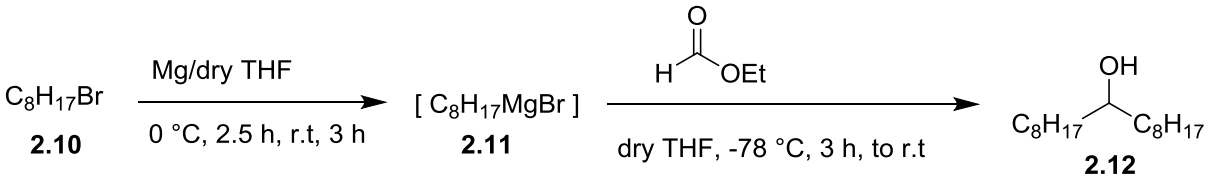


Under a nitrogen atmosphere, dried magnesium turnings (26.0 g, 1.07 mol) were suspended in dry THF (375 mL) in a 1 L oven dried (120 °C) two-neck round bottom flask. The mixture was cooled down to 0/2 °C and 1-bromooctane (123 mL, 703 mmol) was added dropwise *via* syringe over 2.5 hours to form a grey suspension and the mixture was stirred at room temperature for 3 h to complete the formation of octylmagnesium bromide **2.11**. In a separate 1 L three-neck round bottom flask, a solution of ethyl formate (25 mL, 310 mmol) in dry

THF (250 mL) under nitrogen was prepared and cooled to –78 °C. To this solution, the suspension of octylmagnesium bromide **2.11** from the first flask was transferred through a cannula over a period of 3.5 hours at -70 – -80 °C (***NB:*** *(1) during this step, the cannula was blocked four times and the temperature increased at times to –50 °C; (2) a lot of Mg turnings and another white solid (MgO, $Mg(OH)_2$ - ?) was left in the first flask*).

The reaction mixture was stirred at room temperature overnight (15 hours), then methanol 100 mL) and saturated aqueous $NH_4Cl$ (100 mL) were added. The product was extracted with DCM (7 × 50 mL), and the combined extracts were evaporated and the residue was dried *in vacuo* to give the crude product (61.8 g, 77.9%) as a yellowish liquid which was slowly crystallised at room temperature ($^1$H NMR analysis of this crude sample showed ~21% impurities, GC-MS showed ~83% contents of the main product, with an extra three peaks). The crude product was partly purified by vacuum distillation, removing the first fraction (b.p. ~80 – 120 °C, 150 μbar), then collecting the main broad fraction (b.p. 120 – 140 °C, 150 μbar). The vacuum distillation was repeated twice collecting the middle narrow b.p. fractions, but the GC-MS and $^1$H NMR still showed one impurity which was difficult to remove. A combination of $^1$H, $^{13}$C NMR and GC–MS analysis allowed this by-product to be identified as 9-heptadecanone. Therefore, this crude product of heptadecan-9-ol containing ~15% of heptadecan-9-one (38.3 g, 37.3 mmol) was dissolved in propan-2-ol (100 mL) under $N_2$ and added dropwise to a stirred mixture of $NaBH_4$ (1.03 g, 27.2 mmol) in propan-2-ol (400 mL). The mixture was stirred at room temperature for 22 h, diluted with water and extracted with diethyl ether. The combined extracts were flushed through a short silica gel column and the column was further washed with diethyl ether. The diethyl ether was then evaporated and the residue was dried *in vacuo* to afford the pure compound **2.12** as a white solid (37.5 g, 47%), which showed $\delta_H$ (400 MHz, $CDCl_3$): 3.62 – 3.55 (m, 1H), 1.43 – 1.25 (m, 28H), 0.88 (t, $J$ = 6.6 Hz, 6H); $\delta_C$ (100 MHz, $CDCl_3$): 72.1, 37.5 (2C), 31.9 (2C), 29.7 (2C), 29.6 (2C), 29.3 (2C), 25.7 (2C), 22.7 (2C), 14.1 (2C); MS (EI+) *m/z*: 239.04 (100 %), 255.28 (20.0 %), 256.31 (8.0 %). Calculated for $C_{17}H_{36}O$: 256.28; $\nu_{max}$: 3312 br, 2956, 2916, 2873, 2848, 1541, 1507, 1375, 1088, 1066, 1054, 894, 846, 721 $cm^{-1}$.

**1-Methyloxy-3,7-dibromodibenzothiophene-*S,S*-dioxide ($Br_2S$-OMe)**.

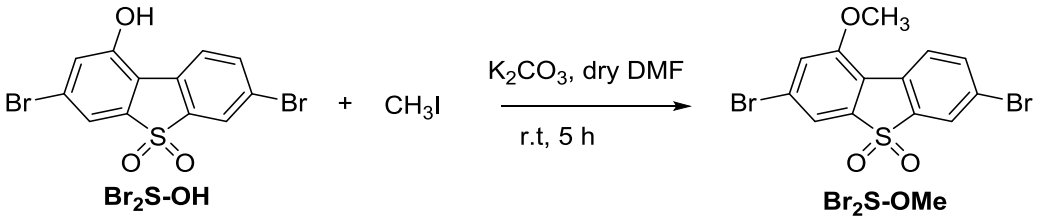


Under a nitrogen atmosphere, 1-hydroxy-3,7-dibromodibenzothiophene-*S,S*-dioxide (**$Br_2S$-OH**) (2.00 g, 5.13 mmol), iodomethane (7.28 g, 51.3 mmol) and potassium carbonate ($K_2CO_3$) (2.13 g, 15.4 mmol) were added to dry DMF (15 mL), and the reaction mixture was stirred at r.t for 5 h. The DMF was evaporated and the excess iodomethane was also evaporated under vacuum then the mixture was passed through a short column using DCM as eluent. The organic solvent was evaporated and the residue was dried *in vacuo* to afford the crude product as a brown solid. The crude product was purified by flash chromatography on silica gel using toluene as eluent to afford the pure compound **$Br_2S$-OMe** as a white solid (1.78 g, 86%), mp. 309 – 310 °C, which showed $\delta_H$ (400 MHz, $CDCl_3$): 8.09 (d, *J* = 8.3 Hz, 1H), 7.91 (d, *J* = 1.6 Hz, 1H), 7.72 (dd, *J* = 8.3, 1.5 Hz, 1H), 7.55 (d, *J* = 1.0 Hz, 1H), 7.29 (d, *J* = 1.0 Hz, 1H), 4.05 (s, 3H); $\delta_C$ (100 MHz, $CDCl_3$): 156.9, 139.9, 138.3, 137.0, 128.9, 127.5, 125.2, 125.0, 123.4, 119.7, 117.9, 117.2, 56.5; MS (EI+) *m/z*: 402.02 ($M^+$, $^{79}Br/^{79}Br$, 54%), 404.01 ($M^+$, $^{79}Br/^{81}Br$, 100%) 406.08 ($M^+$, $^{81}Br/^{81}Br$, 48%). Calculated for $C_{13}H_8Br_2O_3S$: 401.86 (51.4 %), 403.85 (100.0%), 405.85 (48.6%); $\nu_{max}$: 3094, 3066, 2985, 2901, 1585, 1559, 1433, 1404, 1306, 1137, 1093, 1032, 836, 628, 572, 537, 451 $cm^{-1}$.

**1-Dodecyloxy-3,7-dibromodibenzothiophene-*S,S*-dioxide ($Br_2S$-$OC_{12}$)**.

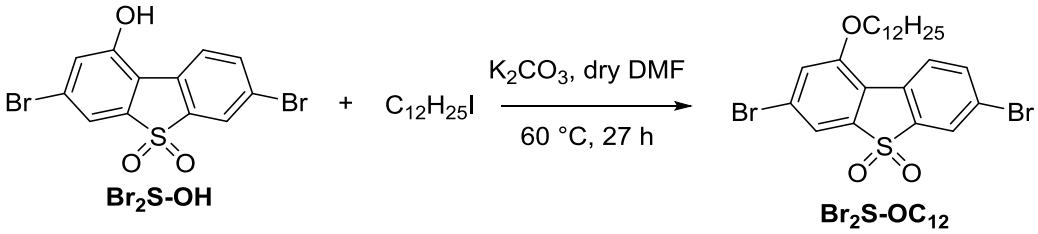


Under a nitrogen atmosphere, 1-hydroxy-3,7-dibromodibenzothiophene-*S,S*-dioxide **($Br_2S$-OH)** (1.49 g, 3.81 mmol), 1-iododododecane (1.24 g, 4.19 mmol) and potassium carbonate (1.58 g, 11.4 mmol) were added to dry DMF (10.5 mL). The reaction mixture was heated to 60 °C and stirred for 6 h. The reaction was quenched with diluted 5% aqueous $NH_4OH$ (35

mL) and extracted with diethyl ether (7 × 15 mL). The combined organic extracts were evaporated and the residue was dried *in vacuo* to afford the crude product as a brown solid. The crude product was twice purified by flash chromatography on silica gel (PE : EA, 5:1, followed by toluene) to afford the pure compound **$Br_2S$-$OC_{12}$** as a white solid (1.11 g, 52%), mp. 115 – 116 °C, which showed $\delta_H$ (400 MHz, $CDCl_3$): 8.35 (d, *J* = 1.7 Hz, 1H), 8.14 (d, *J* = 8.4 Hz, 1H), 8.00 (dd, *J* = 8.4, 1.8, Hz, 1H), 7.87 (d, *J* = 1.2 Hz, 1H), 7.70 (d, *J* = 1.1 Hz, 1H), 4.30 (t, *J* = 6.4 Hz, 2H), 1.86 (quintet, *J* = 7.0 Hz, 2H), 1.50 – 1.43 (m, 2H), 1.39 – 1.17 (m, 16H), 0.84 (t, *J* = 6.5 Hz, 3H); $\delta_C$ (100 MHz, $CDCl_3$): 156.5, 139.9, 138.4, 137.0, 129.1, 127.3, 125.2, 125.0, 123.3, 120.3, 117.8, 116.9, 69.7, 31.9, 29.7 (2C), 29.6, 29.5, 29.4, 29.2, 28.9, 26.0, 22.7, 14.1; MS (EI+) *m/z*: 556.01 ($M^+$, $^{79}Br/^{79}Br$, 49.3%), 557.98 ($M^+$, $^{79}Br/^{81}Br$, 100%) 560.07 ($M^+$, $^{81}Br/^{81}Br$, 33.0%). Calculated for $C_{24}H_{30}Br_2O_3S$: 556.03 (51.4 %), 558.03 (100.0%), 560.02 (48.6%); $\nu_{max}$: 3081, 2951, 2921, 2848, 1580, 1557, 1468, 1444, 1386, 1282, 1138, 1043, 903, 859, 705, 619, 574, 448 $cm^{-1}$.

**1-(3,7-Dimethyloctyloxy)-3,7-dibromodibenzothiophene-*S*,*S*-dioxide (Br$_2$S-OC$_8$Me$_2$).**

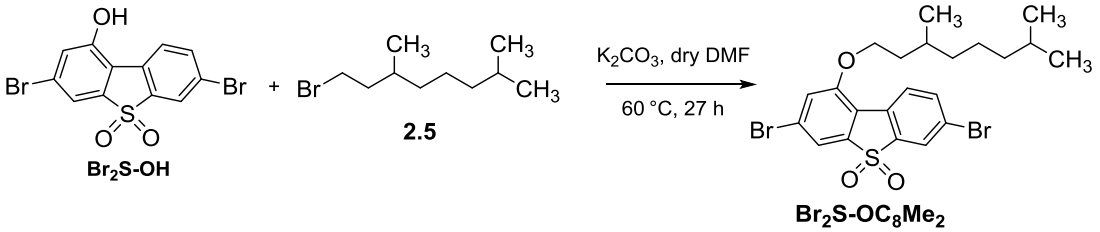


Under a nitrogen atmosphere, 1-hydroxy-3,7-dibromodibenzothiophene-*S*,*S*-dioxide (1.20 g, 3.08 mmol) and 1-bromo-3,7-dimethyloctane (0.816 g, 3.69 mmol) were added to dry DMF (8.5 mL), followed by the addition of potassium carbonate (1.28 g, 9.23 mmol). The reaction mixture was heated to 60 °C and stirred for 24 h. The reaction was quenched with diluted 5% aqueous $NH_4OH$ (24 mL) and extracted with diethyl ether (7 × 15 mL). The combined organic extracts were evaporated and the residue was dried *in vacuo* to afford the crude product as a brown solid. The crude product was twice purified by flash chromatography (toluene, followed by PE : Tol, 1:1) to afford the pure target compound **Br$_2$S-OC$_8$Me$_2$** as a white solid (1.22 g, 75%), mp. 136 – 137 °C, which showed $\delta_H$ (400 MHz, $CDCl_3$): 8.09 (d, *J* = 8.4 Hz, 1H), 7.90 (d, *J* = 1.8 Hz, 1H), 7.72 (dd, *J* = 8.4, 1.8 Hz, Hz, 1H), 7.53 (d, *J* = 1.3 Hz, 1H), 7.28 (d, *J* = 1.2 Hz, 1H), 4.25 – 4.16 (m, 2H), 2.03 – 1.95 (m, 1H), 1.79 – 1.72 (m, 2H), 1.60 – 1.52 (m, 1H), 1.39 – 1.12 (m, 6H), 1.00 (d, *J* = 6.2 Hz,

3H), 0.88 (d, $J$ = 6.6 Hz, 6H); $\delta_C$ (100 MHz, $CDCl_3$): 156.4, 139.9, 138.3, 137.0, 129.1, 127.3, 125.2, 125.0, 123.3, 120.3, 117.8, 116.9, 68.2, 39.2, 37.2, 36.0, 30.0, 28.0, 24.7, 22.7, 22.6, 19.7; MS (EI+): *m/z*: 528.00 ($M^+$, $^{79}Br/^{79}Br$, 38.0%), 529.99 ($M^+$, $^{79}Br/^{81}Br$, 78.5%), 532.00 ($M^+$, $^{81}Br/^{81}Br$, 45.5%). Calculated for $C_{22}H_{26}Br_2O_3S$: 528.00 (51.4%), 529.99 (100.0%), 531.99 (48.6%); $\nu_{max}$: 3095, 2951, 2922, 2866, 1584, 1467, 1385, 1307, 1290, 1161, 1039, 925, 834, 705, 616, 595, 539, 449 $cm^{-1}$.

**1-(2-Hexyldecyloxy)-3,7-dibromodibenzothiophene-*S*,*S*-dioxide ($Br_2$S-OEt$C_6/C_8$)**.

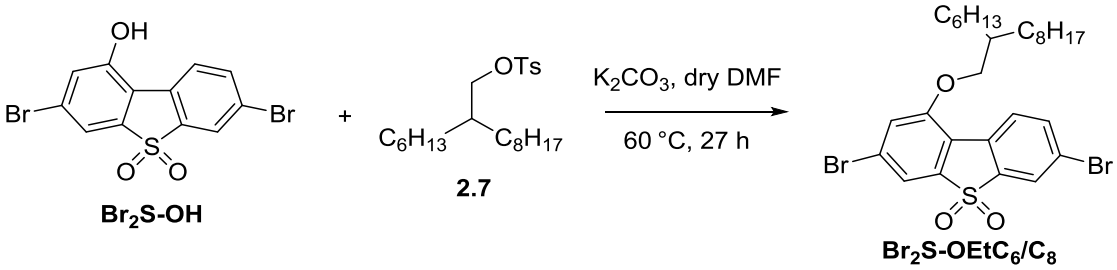


Under a nitrogen atmosphere, 1-hydroxy-3,7-dibromodibenzothiophene-*S*,*S*-dioxide **($Br_2$S-OH)** (1.00 g, 2.56 mmol) and 2-hexyldecyl tosylate (1.02 g, 2.56 mmol) were added to dry DMF (7 mL), followed by the addition of potassium carbonate (1.06 g, 7.69 mmol). The reaction mixture was heated to 60 °C and stirred for 26 h. The reaction was quenched with diluted 5% $NH_4OH$ (24 mL), and then extracted with diethyl ether (7 × 15 mL). The combined organic extracts were evaporated and the residue was dried *in vacuo* to afford the crude product as a brown solid. The crude product was twice purified by dissolving in dry DMF (4 mL), bubbling ammonia gas into the solution for 30 mins, sealing the reaction tube and stirring the solution at 60 °C for 18 h. The reaction was quenched with 5% $NH_4OH$ (24 mL), and extracted with diethyl ether (10 × 20 mL). The combined organic extracts were evaporated and the residue was dried *in vacuo* to afford the target compound as a dark brown viscous semi-solid (1.50 g, 95%) with ~96% purity (by $^1H$ NMR). The product was then purified by flash chromatography on silica gel using toluene as eluent to afford the pure compound **$Br_2$S-OEt$C_6/C_8$** as an off-white solid (1.25 g, 79%), mp. 77 – 78 °C, which showed $\delta_H$ (400 MHz, $CDCl_3$): 8.10 (d, $J$ = 8.4 Hz, 1H), 7.91 (d, $J$ = 1.8 Hz, 1H), 7.73 (dd, $J$ = 8.4, 1.8 Hz, 1H), 7.53 (d, $J$ = 1.4 Hz, 1H), 7.28 (d, $J$ = 1.2 Hz, 1H), 4.06 (d, $J$ = 5.4 Hz, 2H), 1.97 – 1.88 (m, 1H), 1.53 – 1.44 (m, 4H), 1.41 – 1.23 (m, 20H), 0.88 (t, $J$ = 7.0, 6H); $\delta_C$ (100 MHz, $CDCl_3$): 156.7, 139.9, 138.4, 137.0, 129.2, 127.3, 125.2, 125.1, 123.3, 120.3,

117.9, 116.9, 72.4, 37.9, 31.9, 31.8, 31.5 (2C), 29.9, 29.6, 29.5, 29.3, 26.82, 26.8, 22.7, 22.65, 14.1, 14.08; MS (EI+) *m/z*: 612.19 ($M^+$, $^{79}Br/^{79}Br$, 45.5%), 614.15 ($M^+$, $^{79}Br/^{81}Br$, 100%) 616.09 ($M^+$, $^{81}Br/^{81}Br$, 39.2%). Calculated for $C_{28}H_{38}Br_2O_3S$: 612.09 (51.4%), 614.09 (100.0%), 616.09 (48.6%); $\nu_{max}$: 3095, 2952, 2920, 2852, 1581, 1464, 1304, 1260, 1160, 1137, 1076, 1019, 910, 825, 794, 622, 594, 449 $cm^{-1}$.

**1-(2-Octyldodecyloxy)-3,7-dibromodibenzothiophene-*S*,*S*-dioxide ($Br_2$S-OEt$C_8/C_{10}$)**.

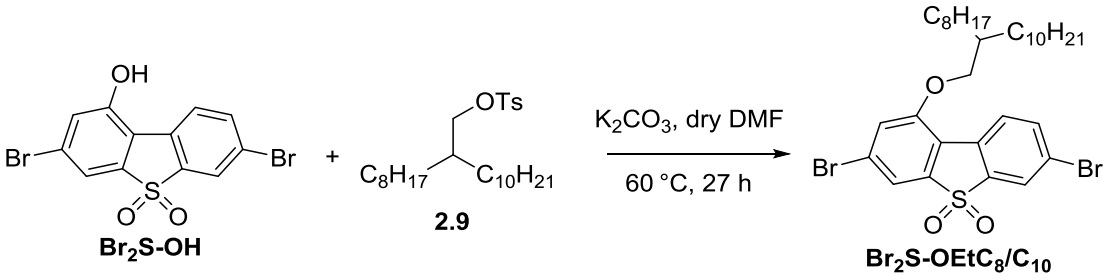


Under a nitrogen atmosphere, 1-hydroxy-3,7-dibromodibenzothiophene-*S*,*S*-dioxide (0.669 g, 1.72 mmol) and 2-octyldodecyl tosylate (0.854 g, 1.89 mmol) were added to dry DMF (3 mL), followed by the addition of potassium carbonate (0.782 g, 5.66 mmol). The reaction mixture was heated to 60 °C and stirred for 27 h. The reaction was quenched with diluted 5% $NH_4OH$ (30 mL), and the aqueous layer was extracted with diethyl ether (7 × 15 mL). The combined organic extracts were washed with water (30 mL), concentrated and dried *in vacuo* to afford the crude product as a dark brown solid. The crude product was purified by flash chromatography (PE : EA, 10:1) to afford the crude compound **$Br_2$S-OEt$C_8/C_{10}$** as a light orange viscous semi-solid (1.09 g, 95%, ~71% purity by $^1H$ NMR, contains starting tosylate). This product was further purified twice by dissolving in dry DMF (4 mL), bubbling ammonia gas into the solution for 30 mins, sealing the reaction tube and stirring the solution at 60 °C for 18 h. The reaction was quenched with a diluted 5% $NH_4OH$ (24 mL), and the aqueous layer was extracted with diethyl ether (10 × 20 mL). The combined organic extracts were evaporated and the residue was dried *in vacuo* to afford the target compound as a light orange viscous semi-solid (0.90 g, 78%; ~96% purity by $^1H$ NMR). The product was further purified by flash chromatography on silica gel using toluene as eluent to afford the pure compound **$Br_2$S-OEt$C_8/C_{10}$** as a clear viscous semi-solid (0.796 g, 69%; ~99% purity by $^1H$ NMR), mp. 71 – 72 °C, which showed $\delta_H$ (400 MHz, $CDCl_3$): 8.10 (d, *J* = 8.4 Hz, 1H), 7.91 (d, *J* = 1.8 Hz, 1H), 7.73 (dd, *J* = 8.4, 1.8 Hz, 1H), 7.53 (d, *J* = 1.3 Hz, 1H), 7.28 (d, *J* = 1.2

Hz, 1H), 4.06 (d, *J* = 5.3 Hz, 2H), 1.95 – 1.89 (m, 1H), 1.52 – 1.44 (m, 4H), 1.43 – 1.21 (m, 28H), 0.88 (t, *J* = 7.0, 6H); $\delta_C$ (100 MHz, $CDCl_3$): 156.7, 139.9, 138.4, 137.0, 129.2, 127.3, 125.2, 125.1, 123.3, 120.3, 117.9, 116.9, 72.4, 37.9, 31.9, 31.89, 31.5 (2C), 29.9 (2C), 29.7, 29.64, 29.6, 29.5, 29.34, 29.3, 26.8 (2C), 22.7, 22.67, 14.1 (2 C); MS (EI+): *m/z:* 668.15 ($M^+$, $^{79}Br/^{79}Br$, 52.0%), 670.13 ($M^+$, $^{79}Br/^{81}Br$, 100%), 672.15 ($M^+$, $^{81}Br/^{81}Br$, 62.0%). Calculated for $C_{32}H_{46}Br_2O_3S$: 668.15 (51.4%), 670.15 (100.0%), 672.15 (48.6%); $\nu_{max}$: 3090, 2955, 2921, 2852, 1582, 1507, 1464, 1442, 1415, 1304, 1263, 1195, 1075, 1000, 826, 796, 623, 593, 576, 448 $cm^{-1}$.

**1-(1-Octylnonyloxy)-3,7-dibromodibenzothiophene-*S*,*S*-dioxide ($Br_2$S-OMe$C_8/C_8$)**.

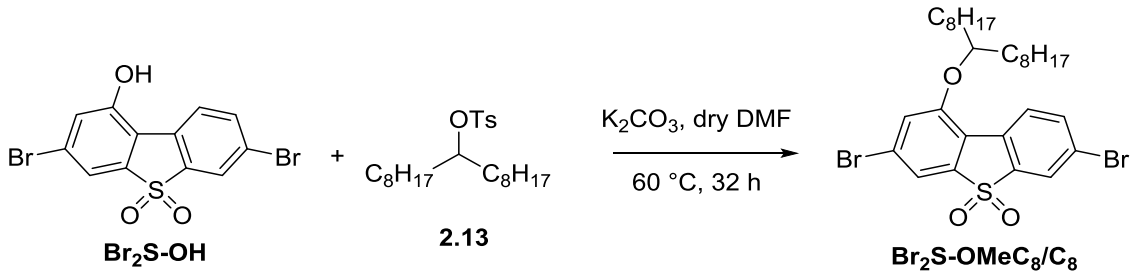


Under a nitrogen atmosphere, 1-hydroxy-3,7-dibromodibenzothiophene-*S*,*S*-dioxide (**$Br_2$S-OH**) (0.984 g, 2.52 mmol) and compound **2.13** (1.04 g, 2.52 mmol) were added to dry DMF (9 mL), followed by the addition of potassium carbonate (1.05 g, 7.56 mmol). The reaction mixture was heated to 60 °C and stirred for 32 h. The reaction was quenched with diluted 5% $NH_4OH$ (25 mL), and then extracted with DCM (7 × 15 mL). The combined organic extracts were evaporated and the residue was dried *in vacuo* to afford the crude product as a light brown solid. The product was purified by flash chromatography on silica gel using (PE : Tol 1:1) as eluent to afford **$Br_2$S-OMe$C_8/C_8$** in 99% purity (by $^1$H NMR) as an off-white solid (1.37 g, 87%), mp. 97 – 98 °C, which showed $\delta_H$ (400 MHz, $CDCl_3$): 8.10 (d, *J* = 8.4 Hz, 1H), 7.90 (d, *J* = 1.8 Hz, 1H), 7.73 (dd, *J* = 8.4, 1.8 Hz, 1H), 7.49 (d, *J* = 1.1 Hz, 1H), 7.22 (d, *J* = 0.6 Hz, 1H), 4.53 – 4.41 (m, 1H), 1.85 – 1.70 (m, 4H), 1.53 – 1.19 (m, 24H), 0.88 (t, *J* = 6.6, 6H); $\delta_C$ (100 MHz, $CDCl_3$): δ (ppm) = 156.1, 140.1, 138.3, 137.1, 129.3, 127.2, 125.1, 125.0, 123.2, 121.1, 118.2, 116.6, 80.3, 33.6, 31.8, 29.5, 29.4, 29.2, 25.2, 22.6, 14.1; MS (EI+) *m/z*: 625.83 ($M^+$, $^{79}Br/^{79}Br$, 49%), 627.85 ($M^+$, $^{79}Br/^{81}Br$, 100%) 629.83 ($M^+$, $^{81}Br/^{81}Br$, 51%). Calculated for $C_{29}H_{40}Br_2O_3S$: 626.11 (51.4%), 628.10 (100.0%), 630.10

(48.6%); $\nu_{max}$: 3095, 2949, 2920, 2853, 1581, 1468, 1429, 1386, 1308, 1254, 1161, 1101, 1021, 990, 890, 828, 704, 618, 576, 550, 448 $cm^{-1}$.

**2-Hexyl-1-bromodecane (2.14)**.[48]

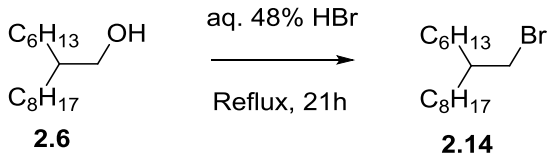

**2.6** **2.14**

To a one neck 250 mL round bottom flask 2-hexyl-1-decanol (**2.6**) (10.8 g, 44.6 mmol) and aqueous 48% HBr (110 mL, 2.03 mol) were added. The yellow solution was stirred and heated under reflux at 125 °C for 21 h. After cooling, it was extracted with PE (4 × 25 mL), and the combined organic extracts were washed with a saturated solution of $NaHCO_3$ (25 mL) and evaporated under reduced pressure. The crude product was purified by column chromatography on silica gel using PE as eluent to afford the pure target product **2.14** as a colourless, viscous liquid (11.1 g, 81%), which showed $\delta_H$ (400 MHz, $CDCl_3$): 3.45 (d, *J* = 4.8 Hz, 2H), 1.59 – 1.54 (m, 1H), 1.18 – 1.42 (m, 24H), 0.88 (t, *J* = 6.6 Hz, 6H, 2 × $CH_3$); $\delta_C$ (100 MHz, $CDCl_3$): 39.7, 39.5, 32.6, 32.59, 31.9, 31.8, 29.8, 29.6, 29.5, 29.3, 26.6, 26.56, 22.7, 22.67, 14.12, 14.1; $\nu_{max}$: 2956, 2922, 2853, 1457, 1394, 1340, 1231, 1066, 1056, 722, 651, 621 $cm^{-1}$.

**9-Bromoheptadecane (2.15).**[49]

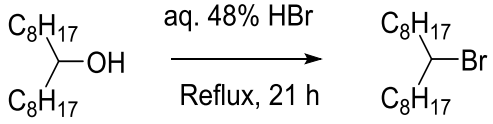

**2.12** **2.15**

To a one neck 500 mL round bottom flask 9-heptadecanol (**2.12**) (20.9 g, 81.4 mmol) and aqueous 48% HBr (195 mL, 1.75 mol) were added. The colourless suspension was stirred and heated under reflux at 120 °C for 21 h. After cooling, it was extracted with PE (10 × 25 mL) and the combined organic extracts were washed with a saturated solution of $NaHCO_3$ (25 mL) and evaporated under reduced pressure. The crude product was purified by column chromatography on silica gel using PE as eluent then by vacuum distillation with a vigreux

column (1.5 cm × 11 cm) to remove the alkene. The first phase was taken between 75 °C and 82 °C at 34 µbar to afford a colourless liquid (1.74g, 6.6%) which contained 79% of alkene by-product by $^1$H NMR. The remaining materials in the flask and in the column were collected with PE. The PE was evaporated to afford the target product **2.15** as a light yellow, viscous liquid. (19.7 g, 76%) with 97% purity (by $^1$H NMR), which showed $\delta_H$ (400 MHz, $CDCl_3$): 4.06 – 4.00 (m, 1H, CH-Br), 1.89 – 1.74 (m, 4H), 1.55 – 1.19 (m, 24H), 0.88 (t, *J* = 6.7 Hz, 6H, 2 × $CH_3$); $\delta_C$ (100 MHz, $CDCl_3$): 59.1, 39.2, 31.9, 29.5, 29.3, 29.1, 27.6, 22.7, 14.1; $\nu_{max}$: 2955, 2922, 2854, 1457, 1377, 1056, 722, 616 cm$^{-1}$.

**9-Iodoheptadecane (2.16).**[50]

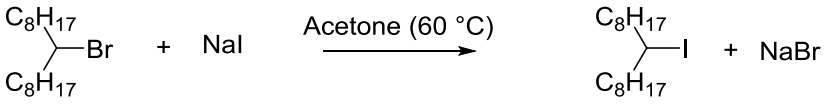


**2.15** **2.16**

Compound **2.15** (31.5 g, 98.6 mmol), NaI (29.6 g, 197 mmol) and acetone (350 mL) were combined and left to stir at 60 °C for 22 h. After cooling, the solvent was evaporated under reduced pressure and DCM (100 mL) was added. The mixture was then washed with water (10 × 25 mL) and the organic layer was evaporated on the rotary evaporator. The product was then purified by dissolving in PE, and passing it through a short column, followed by further purification by vacuum distillation. The first fraction containing the alkene was distilled off at 46 µB pressure and 101 °C. The remaining orange liquid was the pure target compound **2.16** (27.0 g, 75%), which showed $\delta_H$ (400 MHz, $CDCl_3$): 4.15 – 4.09 (m, 1H, CH-I), 1.90 – 1.78 (m, 2H,), 1.72 – 1.61 (m, 2H,), 1.56 – 1.42 (m, 2H), 1.41 – 1.17 (m, 22H), 0.88 (t, *J* = 6.6 Hz, 6H, 2 × $CH_3$); $\delta_H$ (100 MHz, $CDCl_3$): 40.7, 31.9, 29.5, 29.46, 29.3, 29.1, 28.9, 22.7, 14.1; MS (EI+) *m/z:* 364.94 (100.0%), 365.93 (21.5%). Calculated for $C_{17}H_{35}I$: 366.18; $\nu_{max}$: 2955, 2922, 2853, 1457, 1377, 1149, 1129, 1056, 721, 588 cm$^{-1}$.

For alkene (8-Heptadecene)[51]

$\delta_H$ (400 MHz, $CDCl_3$): 5.41–5.32 (m, 2H, CH=CH), 2.05 – 1.91 (m, 4H,), 1.40 – 1.17 (m, 22H,), 0.88 (t, *J* = 6.6 Hz, 6H, 2 × $CH_3$); $\nu_{max}$: 2956, 2921, 2852, 1558, 1520, 1488, 1457, 1066, 1056, 891, 721 cm$^{-1}$.

**9-(Iodomethyl)nonadecane (2.17).**[31]

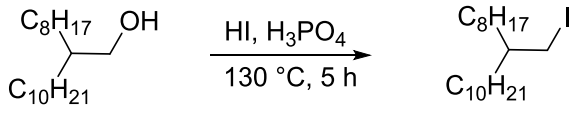


**2.8** **2.17**

2-Octyldodecan-1-ol (**2.8**) (60 mL 0.17 mol), HI (60 mL 0.79 mol) and $H_3PO_4$ (60 mL 1.03 mol) were added to a round bottom flask and the reaction mixture was heated to 130 °C and stirred for 5 h. The reaction mixture was then cooled to room temperature and water (60 mL) and PE (60 mL) were added, however no separation occurred. Sodium sulphite solution (20 mL) was therefore added and the layers became clear. The product was then extracted with PE (10 × 60 mL) and the combined organic layers were washed with water (4 × 240 mL). The crude product was then passed through a silica column using PE as eluent and the solvent was evaporated to give the target product **2.17** as a pale red oil (59.4 g, 86% yield), which showed $\delta_H$ (400 MHz, $CDCl_3$): 3.27 (d, $J$ = 4.6 Hz, 2H, I-$CH_2$), 1.56 – 1.52 (m, 1H) 1.35 – 1.05 (m, 32H), 0.88 (t, $J$ = 6.7 Hz, 6H, 2 × $CH_3$); $\delta_C$ (100 MHz $CDCl_3$): 38.7, 34.4 (2C), 31.92, 31.9, 29.7(2C), 29.6 (2C), 29.6, 29.55, 29.4, 29.3, 26.5 (2C), 22.7 (2C), 16.9, 14.1 (2C); MS (EI+) *m/z*: 408.06 (14.9%), 407.10 (100%). Calculated for $C_{20}H_{41}I$: 408.23 (100.0%), 409.23 (21.6%); $\nu_{max}$: 2955, 2921, 2852, 1458, 1377, 1193, 1056, 891, 721, 589 $cm^{-1}$.

**1,2-Didodecyldisulfide (2.19).**[32]

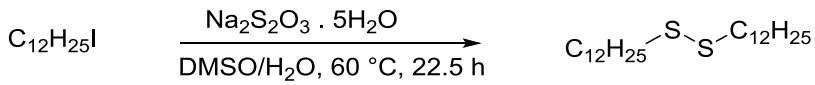


**2.18** **2.19**

A mixture of finely powdered $Na_2S_2O_3 \cdot 5H_2O$ (8.38g, 33.8 mmol), compound **2.18** (10.0 g, 33.8 mmol), DMSO (60 mL), and water (6 mL) were stirred at 60 °C. The progress of the reaction was examined by litmus paper. After stirring for 8 h, the colour of the litmus paper remained unchanged therefore the reaction was left to stir under the aforementioned conditions overnight. After 20 h, the colour of the litmus paper changed from yellow to red. The stirring was continued for a further 2.5 h under the same conditions, then the reaction mixture was worked up by adding water (30 mL) and extracting with PE (4 × 40 mL). The PE was evaporated, however only a small yield was obtained The aqueous layer was further

extracted with 1:1 PE and ethyl acetate (5 × 40 mL). The combined organic layers was dried over $MgSO_4$ and passed through a short column. The product (6.61 g, 97%) with ~99% purity (by $^1$H NMR) is a light orange solid (crystalline). The product was dissolved in PE and passed through a short column. The PE was evaporated to afford the target product **2.19** as a white, colourless, crystalline solid (6.26 g, 92%) with ~99% purity (by $^1$H NMR). The reaction was repeated on a large scale 16.3 g of **2.18** to afford (9.86 g, 89%) with ~99% purity (by $^1$H NMR), mp. 31 – 32 °C. Lit. [52] mp.31 – 33 °C, which showed $\delta_H$ (400 MHz, $CDCl_3$): 2.68 (t, *J* = 7.4 Hz, 4H), 1.67 (quintet, *J* = 7.4 Hz, 4H), 1.45 – 1.20 (m, 36H), 0.88 (t, *J* = 6.8 Hz, 6H); $\delta_C$ (100 MHz, $CDCl_3$): 39.3, 31.9, 29.7, 29.64, 29.6, 29.5, 29.4, 29.3, 28.6, 22.7, 14.1; MS (ESI+) *m/z*: 402.19 (100 %), 403.18 (26.0 %), 404.19 (7.0 %). Calculated for $(C_{12}H_{25})_2S_2$: 402.34 (100 %), 403.34 (26.0%), 404.33 (9.0 %); $\nu_{max}$: 2954, 2915, 2870, 2848, 1469, 718 cm$^{-1}$.

**1,2-Di(2-hexyldecyl)disulfide (2.20).**

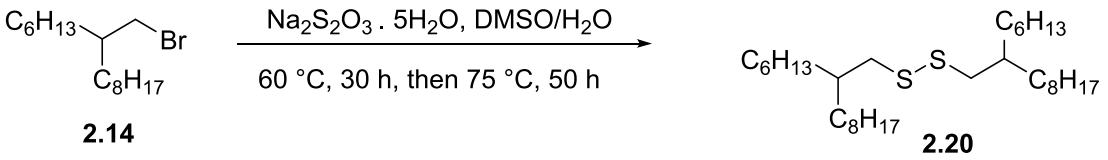


A mixture of finely powdered $Na_2S_2O_3 \cdot 5H_2O$ (8.12 g, 32.8 mmol), 2-hexyl-1-bromodecane **2.14** (10.0 g, 32.8 mmol), DMSO (60 mL) and water (6 mL) were stirred at 60 °C. The progress of the reaction was monitored by litmus paper. After stirring for 30 h, the colour of the litmus paper remained unchanged. Then the temperature was raised to 70 °C. After 21 h of stirring at 70 °C, the colour of the litmus paper changed from yellow to red. The reaction was worked up by adding water (20 mL). The crude product was extracted with PE (8 × 40 mL), and the solvent was evaporated to give a yellow solution with some semisolid on the walls. The solution was passed through silica using PE as eluent. The PE was evaporated again to afford a crude product as a light yellow liquid with 46 % purity (by $^1$H NMR). Using the crude product as a starting material the reaction was repeated at a higher temperature (75 °C) and longer time 50 h. The reaction was monitored by $^1$HNMR and after work up the reaction compound **2.20** was obtained as a colourless viscous liquid (4.73 g, 56%) with ~74% purity (by $^1$H NMR), which showed $\delta_H$ (400 MHz, $CDCl_3$): 2.69 (d, *J* = 6.3 Hz, 4H), 1.80 – 1.57 (m, 2H), 1.46 – 1.16 (m, 48H), 0.88 (t, *J* = 6.5, 12H); $\delta_C$ (100 MHz, $CDCl_3$):

44.6, 37.7, 32.9, 31.93, 31.9, 30.0, 29.6, 29.4, 26.6, 26.5, 22.7, 14.1; $\nu_{max}$: 2955, 2921, 2853, 1457, 1377, 1262, 1056, 892, 741, 722 $cm^{-1}$.

**1,2-Di(2-octyldodecyl)disulfide (2.21).**

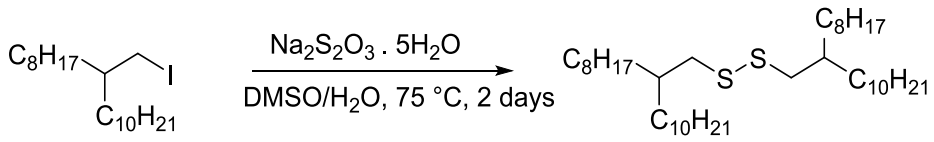


**2.17** **2.21**

A mixture of finely powdered $Na_2S_2O_3 \cdot 5H_2O$ (21.9 g, 88.2 mmol), 9-(iodomethyl)nonadecane **2.17** (36.0 g, 88.2 mmol), DMSO (216 mL) and water (22 mL) were stirred at 70 °C. The progress of the reaction was monitored by litmus paper. After stirring for 3 days, the colour of the litmus paper remained unchanged. Then the temperature was raised to 75 °C. After 2 days of stirring at 75 °C, the colour of the litmus paper changed from yellow to red. The reaction mixture was stopped and allowed to cool and the reaction product was then extracted with PE (10 × 50 mL). The solvent was evaporated and the crude product was purified by column chromatography using PE as eluent to afford the pure product **2.21**, as a clear oil, (26.9 g, 97%), which showed $\delta_H$ (400 MHz, $CDCl_3$): 2.69 (d, *J* = 6.3 Hz, 4H, S-$CH_2$), 1.69 – 1.62 (m, 2H), 1.44 – 1.19 (m, 64H, $CH_2$), 0.88 (t, *J* = 6.7 Hz, 12H, 4 × $CH_3$); $\delta_C$ (100 MHz, $CDCl_3$): 44.6, 37.7, 32.9, 31.9, 30.0, 29.7, 29.67, 29.6, 29.4, 26.6, 22.7, 14.1; MS (EI+) *m/z*: 626.44 (100%), 627.43 (45%). Calculated for $C_{36}H_{76}S_2$: 626.59 (100.0%), 627.59 (43.3%); $\nu_{max}$: 2955, 2919, 2850, 1467, 1377, 1263, 1056, 741, 719 $cm^{-1}$.

**1,2-Di(heptadecan-9-yl)disulfane (2.22).**

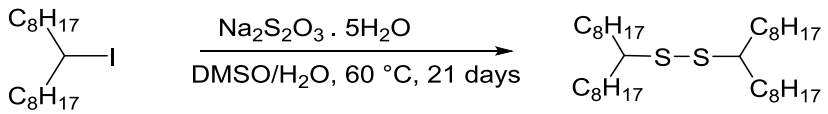


**2.16** **2.22**

A mixture of finely powdered $Na_2S_2O_3.5H_2O$ (15.8 g, 63.8 mmol), compound **2.16** (23.7 g, 63.8 mmol), DMSO (140 mL), and water (14 mL) were stirred at 60 °C. The progress of the reaction was examined by litmus paper and $^1H$ NMR spectroscopy. The reaction mixture

turned brown after 5 days. After 18 days, water (4 mL) was added and the temperature increased to 75 °C. After 21 days the reaction was stopped, water (10 mL) was added at room temperature and the reaction mixture was extracted by PE (10 × 50 mL). The organic layer was then passed through a short column and washed with PE (14 × 50 mL) and was dried under reduced pressure to give a pale yellow liquid. The alkene by-product was vacuum distilled at 100 °C and 46 μbar leaving the pure target product as a light orange liquid **2.22** (7.35 g, 42%), which showed $\delta_H$ (400 MHz, $CDCl_3$): 2.65 – 2.54 (m, 2H), 1.66 – 1.49 (m, 8H), 1.45 – 1.19 (m, 48H), 0.88 (t, *J* = 6.8 Hz, 12H); $\delta_C$ (100MHz, $CDCl_3$): 52.5, 34.2, 31.9, 29.6, 29.57, 29.3, 26.8, 22.7, 14.1; MS (EI+) *m/z:* 542.27 (100%), 543.26 (37%). Calculated for $C_{34}H_{70}S_2$: 542.49 (100.0%), 543.50 (36.8%); $\nu_{max}$: 2955, 2922, 2853, 1457, 1377, 1262, 1056, 907, 735, 649 $cm^{-1}$.

**1-Methylthio-3,7-dibromodibenzothiophene-*S*,*S*-dioxide (Br$_2$S-SMe).**

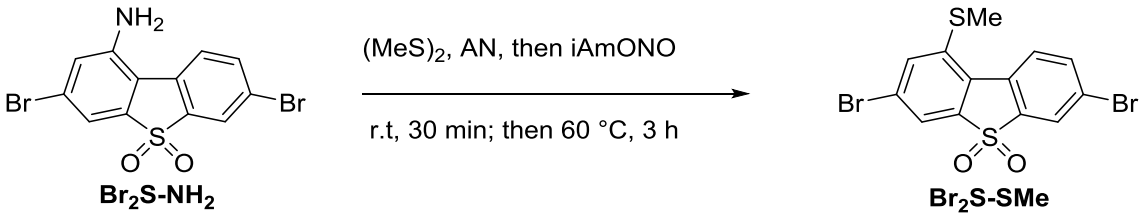


1-Amino-3,7-dibromodibenzothiophene-*S*,*S*-dioxide (**Br$_2$S-NH$_2$**) (750 mg, 1.94 mmol), acetonitrile (7.5 mL) and dimethyl disulfide (1.50 mL, 16.9 mmol) were charged in a 2-neck round bottom flask under a nitrogen atmosphere and stirred at room temperature for 30 min. To this, iso-amyl nitrite (2.25 mL, 35.9 mmol) was added dropwise over 25 min. The solution was brought to 60 °C and left to stir for 3 h. After this, the mixture was cooled to room temperature, the solid was filtered off, washed with water (3 × 10 mL) and dried *in vacuo* to afford the crude product. Further purification by flash chromatography using DCM as eluent and recrystallization from dioxane gave pure **Br$_2$S-SMe** (>98% purity by $^1$H NMR) (587 mg, 73%). The reaction was scaled up to a 5 g batch giving **Br$_2$S-SMe** in 53% yield (>99% purity by $^1$H NMR spectroscopy), mp. 300 – 301 °C, which showed $\delta_H$ (400 MHz, $CDCl_3$): 8.40 (d, *J* = 8.5 Hz, 1H), 7.96 (d, *J* = 1.9 Hz, 1H), 7.79 (dd, *J* = 8.5, 1.9 Hz, 1H), 7.72 (d, *J* = 1.6 Hz, 1H), 7.55 (d, *J* = 1.6 Hz, 1H), 2.67 (s, 3H); $\delta_C$ (100 MHz, $CDCl_3$): 140.0, 139.98, 138.6, 136.7, 133.0, 130.0, 127.7, 126.2, 125.4, 124.5, 124.0, 121.4, 16.2; MS (EI+): *m/z* 418.00 ($M^+$, $^{79}$Br/$^{79}$Br, 51%), 419.93 ($M^+$, $^{79}$Br/$^{81}$Br, 100%), 421.91 ($M^+$, $^{81}$Br/$^{81}$Br,

58%). Calculated for $C_{13}H_8Br_2O_2S_2$: 417.83 (49.1%) 419.83 (100%) 421.83 (55.4%); $\nu_{max}$: 3075, 2988, 1569, 1464, 1442, 1420, 1303, 1277, 1162, 1142, 1078, 1055, 821, 683, 601, 541, 523, 441 $cm^{-1}$.

**1-Dodecylthio-3,7-dibromodibenzothiophene-*S,S*-dioxide ($Br_2S$-$SC_{12}$).**

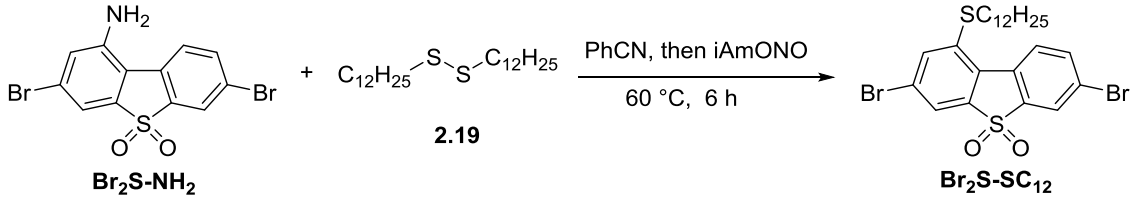


1-Amino-3,7-dibromodibenzothiophene-*S,S*-dioxide (**$Br_2S$-$NH_2$**) (2.26 g, 5.80 mmol), benzonitrile (20 mL, pre heated up to 160 °C for 30 minutes to remove water), and dialkyl disulfide **2.19** (14.1 g, 34.8 mmol) were charged into a 2-neck round bottom flask under a nitrogen atmosphere and stirred at room temperature for 30 min. To this, iso-amyl nitrite (3.9 mL, 29.0 mmol) was added dropwise over 25 min. The solution was heated to 60 °C and left to stir for 6 h. After this, the mixture was cooled to room temperature and the benzonitrile was evaporated under reduced pressure. The excess benzonitrile was removed under reduced pressure via freeze dryer with stirring and heated at 60 °C for two days. To separate the starting material compound **2.19** the product was passed through a short column using PE as eluent. The solvent was evaporated to afford the starting material **2.19** (12.0 g). Then the column was washed with DCM which was evaporated to dryness to afford a crude yellow solid. The reaction was repeated seven more times. All crude products were combined and purified by flash chromatography on silica gel using (PE: Tol, 1:1) as eluent, further purification was done *via* recrystallization from heptane to afford the pure target product (**$Br_2S$-$SC_{12}$**) as a light yellow/white fluffy solid (5.23 g, 43%) with ~100% purity (by $^1H$ NMR), mp. 124 – 125 °C, which showed $\delta_H$ (400 MHz, $CDCl_3$): 8.55 (d, *J* = 8.6 Hz, 1H), 7.95 (d, *J* = 1.9 Hz, 1H), 7.78 (dd, *J* = 8.5, 1.8 Hz, 1H), 7.73 (d, *J* = 1.5 Hz, 1H), 7.62 (d, *J* = 1.3 Hz, 1H), 3.08 (t, *J* = 7.2 Hz, 2H), 1.75 (quintet, *J* = 7.9 Hz, 2H), 1.52 – 1.2 (m, 18H), 0.88 (t, *J* = 6.5 Hz, 3H); $\delta_C$ (100 MHz, $CDCl_3$): 140.1, 139.0, 138.7, 136.8, 135.3, 130.2, 127.8, 127.1, 125.3, 124.2, 124.0, 121.9, 33.9, 31.9, 29.6 (2C), 29.55, 29.4, 29.3, 29.1, 28.8, 28.3, 22.7, 14.1; MS (ESI+) *m/z:* 572.18 ($M^+$, $^{79}Br/^{79}Br$, 49 %), 574.12 ($M^+$, $^{79}Br/^{81}Br$, 100 %), 576.04 ($M^+$, $^{81}Br/^{81}Br$, 57 %). Calculated For $C_{24}H_{30}Br_2O_2S_2$: 572.01

(51.4 %), 574.00 (100 %), 576.00 (48.6 %); $\nu_{max}$: 3050, 2964, 2916, 2849, 1567, 1536, 1463, 1417, 1403, 1377, 1304, 1164, 1144, 1080, 870, 826, 601, 573, 544, 525, 449 $cm^{-1}$.

**1-(2-Octyldodecyl)thio-3,7-dibromodibenzothiophene-*S*,*S*-dioxide (Br$_2$S-SEtC$_8$/C$_{10}$).**

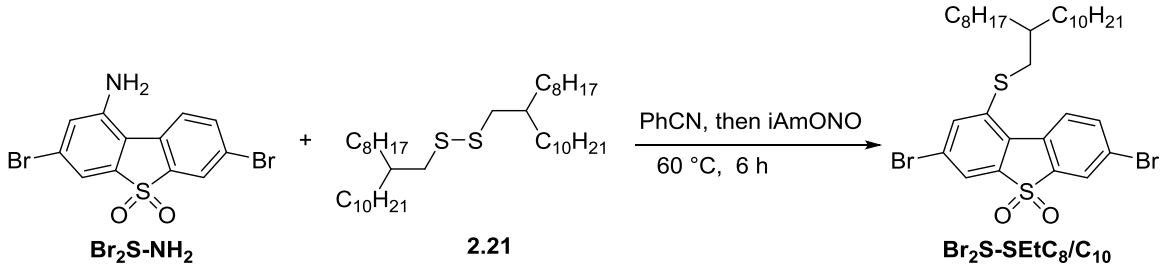


1-Amino-3,7-dibromodibenzothiophene-*S*,*S*-dioxide (**Br$_2$S-NH$_2$**) (2.40 g, 6.18 mmol), benzonitrile (33 mL, pre heated up to 160 °C for 30 minutes to remove water), and dialkyl disulfide **2.21** (31.0 g, 49.4 mmol) were charged into a 2-neck round bottom flask under a nitrogen atmosphere and stirred at room temperature for 30 min. To this, iso-amyl nitrite (4.2 mL, 30.9 mmol) was added dropwise over 25 min. The solution was heated to 60 °C and left to stir for 6 h. After this, the mixture was cooled to room temperature and the benzonitrile was evaporated under reduced pressure. The excess was removed via freeze dryer with stirring and heated at 60 °C for two days. To separate the starting material **2.21** the product was passed through a short column using PE as eluent. The solvent was evaporated to afford the starting material **2.21** (25.2 g). Then the column was washed with DCM and the solvent evaporated to afford a crude dark orange semi solid. The reaction was repeated one more time. Both crude products were combined and purified by flash chromatography on silica gel using (PE: Tol, 1:1) as eluent twice to afford the pure target product (**Br$_2$S-SEtC$_8$/C$_{10}$**) as a light yellow/white semi solid (3.10 g, 40%) with ~99% purity (by $^1$H NMR spectroscopy), mp. 59 – 60 °C, which showed $\delta_H$ (400 MHz, $CDCl_3$): 8.57 (d, *J* = 8.5 Hz, 1H), 7.95 (d, *J* = 1.8 Hz, 1H), 7.79 (dd, *J* = 8.5, 1.9 Hz, 1H), 7.72 (d, *J* = 1.6 Hz, 1H), 7.63 (d, *J* = 1.6 Hz, 1H), 3.04 (d, *J* = 6.1 Hz, 2H, S-$CH_2$), 1.79 – 1.67 (m, 1H, CH), 1.50 – 1.15 (m, 32H, $CH_2$), 0.88 (t, *J* = 6.8 Hz, 6H, 2 × $CH_3$); $\delta_C$ (100 MHz $CDCl_3$): 140.0, 139.6, 138.7, 136.8, 135.3, 130.2, 127.8, 127.1, 125.3, 124.2, 124.0, 121.8, 38.8, 37.3, 33.4, 31.92, 31.9, 29.9, 29.64, 29.6, 29.5, 29.4, 29.3, 26.6, 22.7, 22.67, 14.1; MS (EI+) *m/z*: 684.08 ($M^+$, $^{79}$Br/$^{79}$Br, 49%), 686.00 ($M^+$, $^{79}$Br/$^{81}$Br, 100%), 687.93 ($M^+$, $^{81}$Br/$^{81}$Br, 58%). Calculated for $C_{32}H_{46}Br_2O_2S_2$: 684.13 (51.4%), 686.13 (100.0%), 688.13 (48.6%); $\nu_{max}$:

2952, 2919, 2867, 2849, 1580, 1557, 1542, 1526, 1466, 1453, 1340, 1066, 851, 815, 760, 719, 686, 531, 427 $cm^{-1}$.

**1-(Heptadecan-9-ylthio)-3,7-dibromodibenzothiophene-*S*,*S*-dioxide ($Br_2$S-SMe$C_8$/$C_8$).**

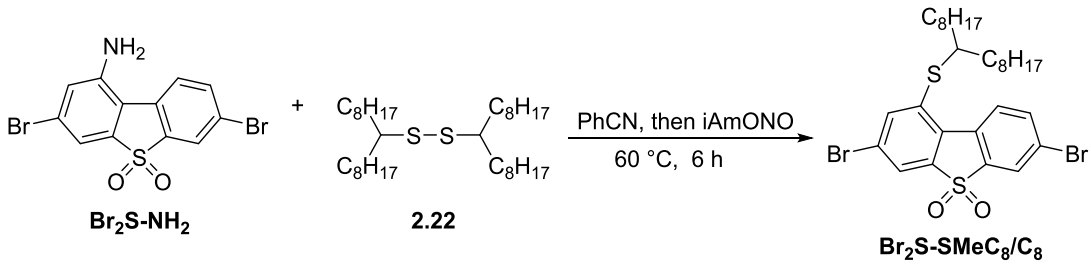


1-Amino-3,7-dibromodibenzothiophene-*S*,*S*-dioxide (**$Br_2$S-$NH_2$**) (0.879 g, 2.26 mmol), benzonitrile (28 mL, pre heated up to 160 °C for 30 minutes to remove water), and dialkyl disulfide **2.22** (7.35 g, 13.5 mmol), were charged into a 2-neck round bottom flask under nitrogen atmosphere and stirred at room temperature for 30 min. To this, iso-amyl nitrite (1.5 mL, 11.30 mmol) was added dropwise over 25 min. The solution was heated to 60 °C and left to stir for 6 h. After this, the mixture was cooled to room temperature and the benzonitrile was evaporated under reduce pressure. The excess of it was removed via freeze dryer with stirring and heated at 60 °C for two days. To separate the starting material compound **2.22** the product was passed through a short column using PE as eluent. The solvent was evaporated to afford the starting material **2.22** (7.19 g). Then the column was washed with DCM which was evaporated to afford a crude dark orange semi solid. The reaction was repeated four times. All crude products were combined and purified by flash chromatography on silica gel using (PE: Tol, 2:1) as eluent to afford the pure target product (**$Br_2$S-SMe$C_8$/$C_8$**) as a light yellow/white semi solid (1.89 g, 30%) with ~99% purity (by $^1$H NMR spectroscopy), mp. 87 – 88 °C, which showed $\delta_H$ (400MHz, $CDCl_3$): 8.73 (d, *J* = 8.5 Hz, 1H), 7.94 (d, *J* = 1.8 Hz, 1H), 7.77 (dd, *J* = 8.6, 1.8 Hz, 1H), 7.75 (d, *J* = 1.6 Hz, 1H), 7.68 (d, *J* = 1.6 Hz, 1H), 3.40 – 3.30 (m, 1H), 1.73 – 1.61 (m, 4H), 1.50 – 1.39 (m, 4H), 1.35 – 1.19 (m, 20H), 0.88 (t, *J* = 6.7 Hz, 6H); $\delta_C$ (100MHz, $CDCl_3$): 140.1, 138.7, 138.5, 138.0, 136.8, 130.3, 128.3, 128.0, 125.2, 124.1, 123.9, 122.5, 50.1, 34.1, 31.8, 29.5, 29.4, 29.2, 26.6, 22.7, 14.1; MS (EI+) *m/z:* 641.81 ($M^+$, $^{79}$Br/$^{79}$Br, 54%), 643.80 ($M^+$, $^{79}$Br/$^{81}$Br, 100%), 645.79 ($M^+$, $^{81}$Br/$^{81}$Br, 62%). Calculated for $C_{29}H_{40}Br_2O_2S_2$: 642.08 (51.4%), 644.08 (100.0%), 646.08 (48.6%).

Note: isolated pure byproduct dibromodibenzothiophene-*S*-oxide **2.23**, which showed $\delta_H$ (400MHz, $CDCl_3$): 8.41 (d, *J* = 8.4 Hz, 1H), 8.32 (d, *J* = 1.6 Hz, 1H), 7.97 (d, *J* = 1.8 Hz, 1H), 7.80 (dd, *J* = 8.5, 1.8 Hz, 1H), 7.77 (d, *J* = 1.6 Hz, 1H), 2.80 (quintet, *J* = 6.2 Hz, 1H), 1.65 – 1.49 (m, 4H), 1.48 – 1.35 (m, 4H), 1.35 – 1.19 (m, 20H), 0.88 (t, *J* = 6.8 Hz, 6H); MS (EI+) *m/z:* 625.41 ($M^+$, $^{79}Br/^{79}Br$, 54%), 626.36 ($M^+$, $^{79}Br/^{81}Br$, 100%), 627.40 ($M^+$, $^{81}Br/^{81}Br$, 49%). Calculated for $C_{29}H_{40}Br_2O_2S_2$: 626.09 (51.4%), 628.09 (100.0%), 630.08 (48.6%).

**1-Methylsulfonyl -3,7-dibromodibenzothiophene-*S*,*S*-dioxide ($Br_2S$-$SO_2Me$).**

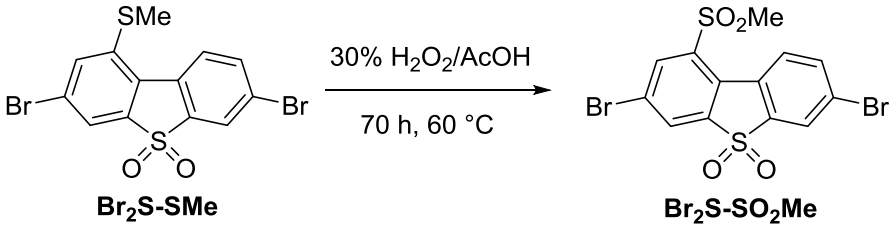


**$Br_2S$-SMe** **$Br_2S$-$SO_2Me$**

Compound **$Br_2S$-SMe** (2.50 g, 5.95 mmol) and glacial acetic acid (50 mL) were stirred at 60 °C for 10 min. Then 30% hydrogen peroxide (9.0 mL) was added dropwise over 50 minutes. The reaction progress was monitored by $^1$HNMR spectroscopy, and after 70 h the reaction was worked up by adding water (50 mL). The suspension was cooled to room temperature, the solid was filtered off and washed with water (7 × 5 mL). The crude product was purified by recrystallization from glacial acetic acid to afford the pure target product (**$Br_2S$-$SO_2Me$**) as an off white solid (2.25 g, 86%) with 100% purity (by $^1$H NMR), mp. 310 – 311 °C, which showed $\delta_H$ (400 MHz, $CDCl_3$): 8.77 (d, *J* = 8.6 Hz, 1H), 8.56 (d, *J* = 1.9 Hz, 1H), 8.21 (d, *J* = 1.9 Hz, 1H), 8.04 (d, *J* = 1.9 Hz, 1H), 7.88 (dd, *J* = 8.7, 1.9 Hz, 1H), 3.24 (s, 3H); $\delta_C$ (100 MHz, $CDCl_3$): 141.6, 139.1, 138.1, 138.0, 137.95, 130.4, 129.4, 127.8, 126.9, 126.6, 126.1, 125.2, 42.7; MS (ESI+) *m/z:* 449.99 ($M^+$, $^{79}Br/^{79}Br$, 51%), 451.92 ($M^+$, $^{79}Br/^{81}Br$, 100%), 453.98 ($M^+$, $^{81}Br/^{81}Br$, 49%). Calculated For $C_{13}H_8Br_2O_4S_2$: 449.82 (51.4%), 451.82 (100%), 453.82 (48.6%); $\nu_{max}$: 3094, 3072, 3030, 3009, 2929, 1583, 1466, 1432, 1383, 1187, 1155, 1107, 962, 816, 704, 682, 576, 554, 516, 451 $cm^{-1}$.

**1-Dodecylsufonyl-3,7-dibenzothiophene-*S*,*S*-dioxide ($Br_2S$-$SC_{12}$).**

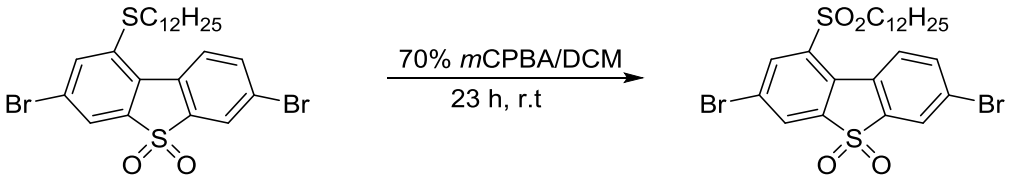


**$Br_2S$-$SC_{12}$** **$Br_2S$-$SO_2C_{12}$**

Compound **$Br_2S$-$SC_{12}$** (1.50g, 2.61 mmol) was dissolved in DCM (55 mL), and *m*CPBA (70%) (2.57 g, 10.4 mmol) was added to the reaction mixture which was then left to stir at room temperature. The reaction progress was monitored by TLC and $^1$HNMR spectroscopy, and after 23 h the reaction was worked up by washing with 5% $Na_2CO_3$ (6 × 20 mL) and water (3 × 25 mL). The organic layer was dried over $MgSO_4$ and the solvent was evaporated to give the crude product which was purified by flash chromatography using toluene as eluent to produce the pure target product (**$Br_2S$-$SO_2C_{12}$**) an off-white solid (1.48 g, 94%), mp. 137 – 138 °C, which showed $\delta_H$ (400 MHz, $CDCl_3$): 8.77 (d, *J* = 8.7 Hz, 1H), 8.52 (d, *J* = 1.9 Hz, 1H), 8.20 (d, *J* = 1.9 Hz), 8.03 (d, *J* = 2.0 Hz, 1H), 7.87 (dd, *J* = 8.7, 2.0 Hz, 1H), 3.25 (t, *J* = 8.0 Hz, 2H), 1.80 (quintet, *J* = 7.7 Hz, 2H), 1.42 – 1.15 (m, 18H), 0.88 (t, *J* = 6.8 Hz, 3H); $\delta_C$ (100 MHz, $CDCl_3$): 141.6, 139.1, 138.8, 137.8, 137.2, 130.3, 129.4, 128.0, 127.0, 126.5, 124.0, 125.1, 54.4, 31.9, 29.7, 29.5, 29.4, 29.3, 29.2, 28.9, 28.1, 22.7, 22.1, 14.1; MS (EI+) *m/z:* 603.95 (M+, $^{79}$Br/$^{79}$Br, 45%), 605.93 (M+, $^{79}$Br/$^{81}$Br, 100%), 607.90 (M+, $^{81}$Br/$^{81}$Br, 54%). Calculated for $C_{24}H_{30}Br_2O_4S_2$: 604.00 (51.4%), 605.99 (100.0%), 607.99 (48.6%); $\nu_{max}$: 3072, 2916, 2849, 1470, 1456, 1417, 1380, 1325, 1171, 1156, 1136, 1057, 996, 834, 818, 760, 684, 572, 544, 518, 498, 454 cm$^{-1}$.

**1-(2-Octyldodecyl)sulfonyl-3,7-dibromodibenzothiophene-*S*,*S*-dioxide ($Br_2S$-$SO_2EtC_8/C_{10}$).**

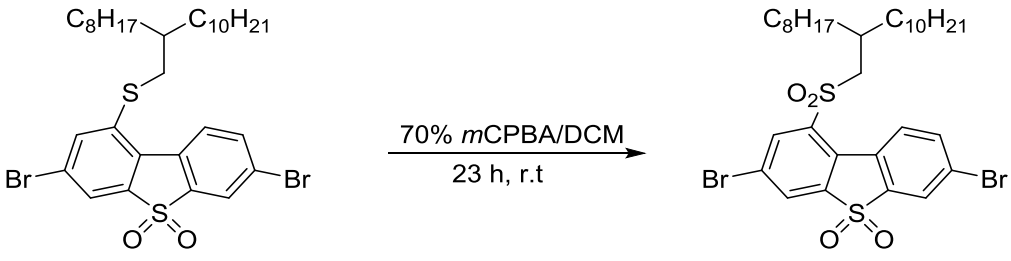


**$Br_2S$-$SEtC_8/C_{10}$** **$Br_2S$-$SO_2EtC_8/C_{10}$**

Compound **$Br_2S$-$SEtC_8/C_{10}$** (2.00 g, 2.91 mmol) was dissolved in DCM (50 mL), and *m*CPBA (70%) (2.87 g, 11.64 mmol) was added to the reaction mixture which was then left to stir at room temperature. The reaction progress was monitored by TLC and $^1$HNMR spectroscopy, and after 23 h the reaction was worked up by evaporating the solvent under reduced pressure. The remaining solid was purified by flash chromatography using toluene as eluent yielding the pure product (**$Br_2S$-$SO_2EtC_8/C_{10}$**) as a white crystalline solid (2.02 g, 97%), mp. 96 – 97 °C, which showed $\delta_H$ (400 MHz, $CDCl_3$): 8.79 (d, *J* = 8.7 Hz, 1H), 8.54 (d, *J* = 1.9 Hz, 1H), 8.19 (d, *J* = 1.9 Hz, 1H), 8.02 (d, *J* = 1.9 Hz, 1H), 7.85 (dd, *J* = 8.6, 1.9 Hz, 1H), 3.17 (d, *J* = 6.0 Hz, 2H, S-$CH_2$), 2.21 – 2.13 (m, 1H, CH), 1.46 – 1.38 (m, 4H), 1.35 – 1.10 (m, 28H), 0.88 (t, *J* = 6.8 Hz, 6H, $CH_3$); $\delta_C$ (100 MHz $CDCl_3$): 141.6, 139.1, 138.7, 138.2, 137.7, 130.1, 129.5, 127.8, 127.1, 126.6, 126.0, 125.2, 58.2, 33.3, 33.1, 31.9, 31.8, 29.6, 29.58, 29.56, 29.5, 29.47, 29.3, 29.2, 26.1, 22.7, 22.66, 14.1; MS ($EI^+$) m/z: 715.86 ($M^+$, $^{79}Br/^{79}Br$, 53%), 717.83 ($M^+$, $^{79}Br/^{81}Br$, 100%), 719.82 ($^{81}Br/^{81}Br$, 62%). Calculated for $C_{32}H_{46}Br_2O_4S_2$: 716.12 (51.4%), 718.12 (100.0%), 720.12 (48.6%); $\nu_{max}$: 3076, 2920, 2851, 1465, 1420, 1400, 1311, 1280, 1224, 1187, 1153, 903, 831, 759, 720, 706, 605, 577, 560, 544, 517, 425 $cm^{-1}$.

**1-(9-Heptadecanylsulfonyl)-3,7-dibromodibenzothiophene-*S,S*-dioxide (Br$_2$S-SO$_2$MeC$_8$/C$_8$).**

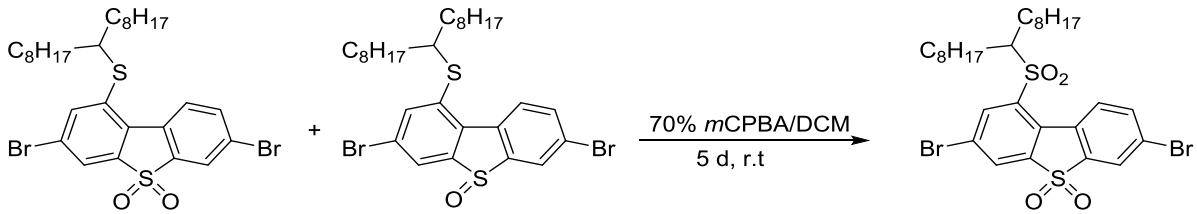


**$Br_2S$-$SMeC_8/C_8$** **2.23** **$Br_2S$-$SO_2MeC_8/C_8$**

A mixture of compounds **$Br_2S$-$SMeC_8/C_8$** and **2.23** (0.744 g, 1.15 mmol) was dissolved in DCM (30 mL), and *m*CPBA (70%) (1.70 g, 6.9 mmol) was added to the solution and the reaction mixture and left to stir at room temperature. The reaction progress was monitored by TLC and $^1$HNMR spectroscopy and after 5 days the reaction was worked up by evaporating the solvent under reduced pressure. The remaining solid was purified by flash chromatography using toluene as eluent yielding the pure product **$Br_2S$-$SO_2MeC_8/C_8$** as a white powder (0.640 g, 82%), mp. 110 – 111 °C, which showed $\delta_H$ (400 MHz, $CDCl_3$): 8.76

(d, *J* = 8.7 Hz, 1H), 8.51 (d, *J* = 1.8 Hz, 1H), 8.20 (d, *J* = 1.8 Hz, 1H), 8.02 (d, *J* = 1.8 Hz, 1H), 7.84 (dd, *J* = 8.6, 1.8 Hz, 1H), 3.20 – 3.10 (m, 1H), 1.84 – 1.67 (m, 4H), 1.50 – 1.19 m, 24H), 0.88 (t, *J* = 7.0 Hz, 6H); $\delta_C$ (100 MHz, $CDCl_3$): 141.6, 139.4, 139.1, 137.6, 136.8, 130.1, 129.5, 128.1, 127.2, 126.5, 125.9, 124.9, 62.6, 31.7, 29.4, 29.1, 27.3, 26.3, 22.6, 14.1; MS (EI+) *m/z:* 673.89 ($M^+$, $^{79}Br/^{79}Br$, 59%), 675.85 ($M^+$, $^{79}Br/^{81}Br$, 100%), 677.90 ($M^+$, $^{81}Br/^{81}Br$, 65%). Calculated for $C_{29}H_{40}Br_2O_4S_2$: 674.07 (51.4%), 676.07 (100.0%), 678.07 (48.6%).

**1-(2-Octyldodecyl)thio-3,7-dibromodibenzothiophene (2.24).**

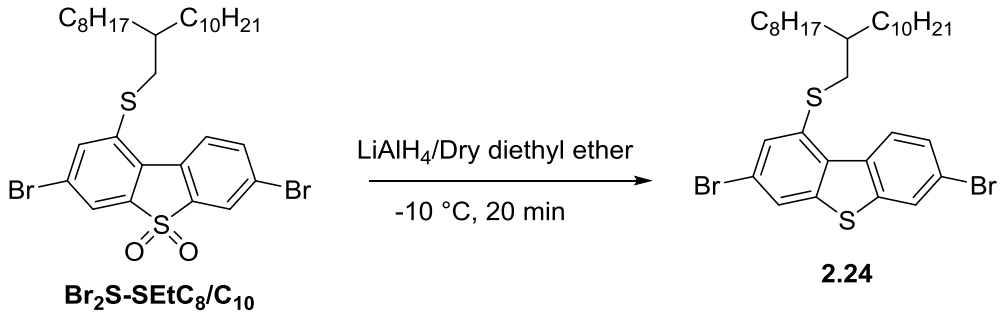


**$Br_2S$-$SEtC_8/C_{10}$** **2.24**

To a suspension of $LiAlH_4$ (0.354 g, 9.32 mmol) in dry diethyl ether (50 mL) cooled to –10 °C a solution of **$Br_2S$-$SEtC_8/C_{10}$** (1.60 g, 2.33 mmol) in dry diethyl ether (100 mL) was added. The mixture was stirred under a nitrogen atmosphere for 20 min at –10 °C. Ethyl acetate (50 mL) was then added to quench the reaction, and the solvent was removed under reduced pressure. The crude product was purified by flash column chromatography on silica gel eluting with PE to afford the desired product **2.24** as a colourless highly viscous liquid (0.900 g, 59%), which showed $\delta_H$ (400 MHz, $CDCl_3$): 8.92 (d, *J* = 8.8 Hz, 1H), 7.96 (d, *J* = 1.6 Hz, 1H), 7.78 (d, *J* = 1.2 Hz, 1H), 7.59 (dd, *J* = 8.8, 1.6 Hz, 1H), 7.46 (d, *J* = 1.1 Hz, 1H), 3.04 (d, *J* = 6.1 Hz, 2H, S-$CH_2$), 1.79 – 1.68 (m, 1H, CH), 1.51 – 1.15 (m, 32H), 0.88 (t, *J* = 6.7 Hz, 6H, 2 × $CH_3$); $\delta_C$ (100 MHz $CDCl_3$): 141.7, 140.9, 137.2, 134.2, 131.2, 127.7, 127.5, 127.4, 124.9, 122.3, 120.4, 120.1, 40.1, 38.8, 37.4, 33.4, 32.3, 31.92, 31.9, 29.9, 29.7, 29.6, 29.56, 29.4, 29.3, 28.6, 26.6, 22.7, 22.69, 14.1; MS (EI+) *m/z*: 652.27 ($M^+$, $^{79}Br/^{79}Br$, 52%), 654.22 ($M^+$, $^{79}Br/^{81}Br$, 100%), 656.15 ($M^+$, $^{81}Br/^{81}Br$, 56%). Calculated for $C_{32}H_{46}Br_2O_2S_2$: 652.14 (51.4%), 654.14 (100.0%), 656.14 (48.6%).

## References


1 I. I. Perepichka, I. F. Perepichka, M. R. Bryce, and L.-O. Pälsson, Dibenzothiophene-*S,S*-dioxide–fluorene co-oligomers. Stable highly-efficient blue emitters with improved electron affinity, *Chem. Commun.*, **2005**, 3397–3399. DOI: 10.1039/b417717g

2 K. T. Kamtekar, H. L. Vaughan, B. P. Lyons, A. P. Monkman, S. U. Pandya, and M. R. Bryce, Synthesis and spectroscopy of poly(9,9-dioctylfluorene-2,7-diyl-co-2,8-dihexyldibenzothiophene-*S*,*S*-dioxide-3,7-diyl)s: solution-processable, deep-blue emitters with a high triplet energy, *Macromolecules*, **2010**, *43*, 4481–4488. DOI: 10.1021/ma100566p

3 J. H. Cook, J. Santos, H. Li, H. A. Al-Attar, M. R. Bryce, and A. P. Monkman, Efficient deep blue fluorescent polymer light emitting diodes (PLEDs), *J. Mater. Chem. C*, **2014**, *2*, 5587–5592. DOI: 10.1039/c4tc00896k

4 H. Xiao, J. Miao, J. Cao, W. Yang, H. Wu, and Y. Cao, Alcohol-soluble polyfluorenes containing dibenzothiophene-*S*,*S*-dioxide segments for cathode interfacial layer in PLEDs and PSCs, *Org. Electronics*, **2014**, *15*, 758–774. DOI: 10.1016/j.orgel.2014.01.006

5 F. Mo, G. Dong, Y. Zhanga, and J. Wang, Recent applications of arene diazonium salts in organic synthesis, *Org. Biomol. Chem.*, **2013**, *11*, 1582–1593. DOI: 10.1039/c3ob27366k

6 N. Alessandro, L. Tonucci, M. Bonetti, M. Di Deo, M. Bressan, and A. Morvillo, Oxidation of dibenzothiophene by hydrogen peroxide or monopersulfate and metal–sulfophthalocyanine catalysts: an easy access to biphenylsultone or 2-(20-hydroxybiphenyl)sulfonate under mild conditions, *New J. Chem.*, **2003**, *27*, 989–993. DOI: 10.1039/b212152b

7 P. Ren, O. Vechorkin, K. von Allmen, R. Scopelliti, and X.e Hu, A structure_activity study of Ni-catalyzed alkyl_alkyl Kumada coupling. Improved catalysts for coupling of secondary alkyl halides, *J. Am. Chem. Soc.* **2011**, *133*, 7084–7095. DOI: 10.1021/ja200270k

8 S. Kommanaboyina, Conjuated Polymers Based on 4-Substituted Fluorenes and Fluorenones, PhD Thesis, Bangor University, **2016**.

9 L. Oldridge, M. Kastler, K. Müllen, Synthesis of a soluble poly(fluorenone), *Chem. Commun*., **2006**, *8*, 885–887. DOI: 10.1039/b516078b

10 F. B. Dias, S. King, A. P. Monkman, I. I. Perepichka, M. A. Kryuchkov, I. F. Perepichka, and M. R. Bryce, Dipolar stabilization of emissive singlet charge transfer excited states in polyfluorene copolymers, *J. Phys. Chem. B*, **2008**, *112*, 6557–6566. DOI**:** 10.1021/jp800068d

11 S. M. King, I. I. Perepichka, I. F. Perepichka, F. B. Dias, M. R. Bryce, and A. P. Monkman, Exploiting a dual-fluorescence process in fluorene dibenzothiophene-*S*,*S*-dioxide co-polymers to give efficient single polymer LEDs with broadened emission, *Adv. Funct. Mater.*, **2009**, *19*, 586–591. DOI: 10.1002/adfm.200801237

12 T. Cohen, A. G. Dietz, Jr., and J. R. Miser, A simple preparation of phenols from diazonium ions via the generation and oxidation of aryl radicals by copper salts, *J. Org. Chem.*, **1977**, *42*, 2053–2058.

13 F. E. Ray, and C. F. Hull, Fluorene oxazoles, *J. Org. Chem.*, **1949**, *14*, 39–396.

14 D. T. Mowry, The preparation of nitriles, *Chem. Rev.*, **1948**, *42*, 189–283.

15 H. H. Hodgson, The Sandmeyer reaction, *Chem. Rev.*, **1947**, *40*, 251–277.

16 W. M. Stanley, and R. Adams, Stereochemistry of diphenyls. Preparation and properties of 4,4'-dicarboxy-1,1'-dianthraquinoyl, *J. Am. Chem. Soc.*, **1931**, *53*, 2364–2368.

17 J. T. Repine, D. S. Johnson, A. D. White, D. A. Favor, M. A. Stier, J. Yip, T. Rankin, Q. Ding, and S. N. Maiti, Synthesis of monofluorinated 1-(naphthalen-1-yl)piperazines, *Tetrahedron Lett.*, **2007**, *48*, 5539–5541. DOI:10.1016/j.tetlet.2007.05.156

18 J. Jin, A. Morales-Ramos, P. Eidam, J. Mecom, Y. Li, C. Brooks, M. Hilfiker, D. Zhang, N. Wang, D. Shi, P. Tseng, K. Wheless, B. Budzik, K. Evans, J. Jaworski, J. Jugus, L. Leon, C. Wu, M. Pullen, B. Karamshi, P. Rao, E. Ward, N. Laping, C. Evans, C. Leach, D. Holt, X. Su, D. Morrow, H. Fries, K. Thorneloe, and R. Edwards, Novel 3-oxazolidinedione-6-aryl-pyridinones as potent, selective, and orally active EP3 receptor antagonists, *ACS Med. Chem. Lett.*, **2010**, *1*, 316–320. DOI: 10.1021/ml100077x

19 Y. Gao, K. J. Kellar, R. P. Yasuda, T. Tran, Y. Xiao, R. F. Dannals, and A. G. Horti, Derivatives of dibenzothiophene for positron emission tomography imaging of α7-nicotinic acetylcholine receptors, *J. Med. Chem.*, **2013**, *56*, 7574−7589. DOI: 10.1021/jm401184f

20 C. Lindenschmidt, D. Krane, S. Vortherms, L. Hilbig, H. Prinz, and K. Müller, 8-Halo-substituted naphtho[2,3-b]thiophene-4,9-diones as redoxactive inhibitors of keratinocyte hyperproliferation with reduced membrane-damaging properties, *European Journal of Medicinal Chemistry*, **2016**, *110*, 280–290. DOI: 10.1016/j.ejmech.2016.01.040

21 N. Cohen, C. G. Scott, C. Neukom, R. J. Lopresti, G. Weber, and G. Saucy, Total synthesis of all eight stereoisomers of α-tocopheryl acetate. Determination of their diastereoisomeric and enantiomeric purity by gas chromatography, *Helv. Chim. Acta*, **1981**, *64*, 1158–1173.

22 N. Blouin, A. Michaud, and M. Leclerc, A low-bandgap Poly(2,7-carbazole) derivative for use in high-performance solar cells, *Adv. Mater.*, **2007**, *19*, 2295–2300. DOI: 10.1002/adma.200602496

23 D. Patra, D. Sahu, H. Padhy, D. Kekuda, C. Chu, and H. Lin, Synthesis and applications of 2,7-carbazole-based conjugated main-chain copolymers containing electron deficient bithiazole units for organic solar cells, *J. Polym. Sci. Part A: Polym. Chem.*, **2010**, *48*, 5479–5489. DOI: 10.1002/pola.24356

24 M. Mathews, and N. Tamaoki, Planar chiral azobenzenophanes as chiroptic switches for photon mode reversible reflection color control in induced chiral nematic liquid crystals, *J. Am. Chem. Soc*., **2008**, *130*, 11409–11416. DOI**:** 10.1021/ja802472t

25 Z. Qiao, H. Liu, X. Xiao, Y. Fu, J. Wei, Y. Li, and X. Jiang, Efficient access to 1,4-benzothiazine: palladium-catalyzed double C–S bond formation using $Na_2S_2O_3$ as sulfurating reagent, *Org. Lett.*, **2013**, *15*, 2594–2597. DOI: 10.1021/ol400618k

26 Z. Qiao, J. Wei, and X. Jiang, Direct cross-coupling access to diverse aromatic sulfide: palladium-catalyzed double C−S bond construction using $Na_2S_2O_3$ as a sulfurating reagent, *Org. Lett.*, **2014**, *16*, 1212−1215. DOI: 10.1021/ol500112y

27 Y. Li, J. Pu, and X. Jiang, A highly efficient Cu-catalyzed S-transfer reaction: from amine to sulphide, *Org. Lett.*, **2014**, *16*, 2692−2695. DOI: 10.1021/ol5009747

28 F. Mo, G. Dong, Y. Zhanga, and J. Wang, Recent applications of arene diazonium salts in organic synthesis, *Org. Biomol. Chem.*, **2013**, *11*, 1582–1593. DOI: 10.1039/c3ob27366k

29 N. Cohen, C. G. Scott, C. Neukom, R. J. Lopresti, G. Weber, and G. Saucy, Total synthesis of all eight stereoisomers of α-tocopheryl acetate. Determination of their diastereoisomeric and enantiomeric purity by gas chromatography, *Helv. Chim. Acta*, **1981**, *64*, 1158–1173.

30 W. D. Jones, and F. J. Feher, Preparation and conformational dynamics of (C,Me,)Rh( PR’3)RX. Hindered rotation about rhodium-phosphorus and rhodium-carbon bonds, *Inorg. Chem.*, **1984**, *23*, 2376–2388.

31 F. Ferretti, E. Gallo, and F. Ragaini, Mineral Oil/Methanol: A Cheap Biphasic Reaction Medium with Thermomorphic Properties and Its Application to the Palladium-Catalyzed Carbonylation of Nitrobenzene to Methyl Phenylcarbamate, *ChemCatChem*, **2015**, *7*, 2241–2247. DOI: 10.1002/cctc.201500452

32 M. Abbasi, M. R. Mohammadizadeh, and N. Saeedi, The synthesis of symmetrical disulfides by reacting organic halides with $Na_2S_2O_3.5H_2O$ in DMSO, *New.J.Chem.*, **2016**, *40*, 89–92. DOI: 10.1039/c5nj01885d

33 J. Kim, H. J. Kim, and S. Chang, Synthesis of aromatic nitriles using nonmetallic cyano-group sources, *Angew. Chem. Int. Ed.*, **2012**, *51*, 11948–11959. DOI: 10.1002/anie.201206168

34 P. Anbarasan, T. Schareina, and M. Beller, Recent developments and perspectives in palladium-catalyzed cyanation of aryl halides: synthesis of benzonitriles, *Chem. Soc. Rev.*, **2011**, *40*, 5049–5067. DOI: 10.1039/c1cs15004a

35 J. I. G. Cadogan, D. A. Roy, and D. M. Smith, An alternative to the Sandmeyer reaction, *J. Chem. Soc. C*, **1966**, 1249–1250.

36 C. S. Giam, and K. Kikukawa, A simple preparation of aromatic or heteroaromatic sulphides, *J. Chem. Soc. Chem. Commun.*, **1980**, 756–757.

37 A. H. Ingall, J. Dixon, A. Bailey, M. E. Coombs, D. Cox, J. I. McInally, S. F. Hunt, N. D. Kindon, B. J. Teobald, P. A. Willis, R. G. Humphries, P. Leff, J. A. Clegg, J. A. Smith, and W. Tomlinson, Antagonists of the platelet $P_2T$ receptor: a novel approach to antithrombotic therapy, *J. Med. Chem.*, **1999**, *42*, 213–220. DOI: 10.1021/jm981072s

38 F. S. Allaire, and J. W. Lyga, Nonaqueous diazotization of arylamines in the presence of dimethyldisulfide; the convenient synthesis of arylmethylsulfides from anilines, *Synth. Commun.*, **2001**, *31*, 1857–1861. DOI:10.1081/SCC-100104335

39 G. Liu, J. Xu, K. C. Park, N. Chen, S. Zhang, Z. Ding, F. Wang, and H. Du, Novel synthesis approach and antiplatelet activity evaluation of 6-alkylamino-2,4-dialkyl(aryl)-thiopyrimidines, *Tetrahedron*, **2011**, *67*, 5156–5161. DOI:10.1016/j.tet.2011.05.056

40 O. V. Dolomanov, L. J. Bourhis, R. J. Gildea, J. A. K. Howard, and H. Puschmann, OLEX2: a complete structure solution, refinement and analysis program, *J. Appl. Cryst.*, **2009**, *42*, 339–341. DOI: 10.1107/S0021889808042726

41 G. M. Sheldrick, A short history of SHELX, *Acta Cryst.*, **2008**, *A64*, 112–122. DOI: 10.1107/S0108767307043930

42 B. Zhang, S. Li, S. Yue, M. Cokoja, M. Zhou, S. Zang, and F. E. Kühn, Imidazolium perrhenate ionic liquids as efficient catalysts for the selective oxidation of sulfides to sulfones, *Journal of Organometallic Chemistry*, **2013**, *744*, 108–112. DOI: 10.1016/j.jorganchem.2013.05.043

43 H. Sirringhaus, R. H. Friend, C. Wang, J. Leuninger, and K. Mu¨llen, Dibenzothienobisbenzothiophene–a novel fused-ring oligomer with high field-effect mobility, *J. Mater. Chem.*, **1999**, *9*, 2095–2101. DOI: 10.1039/A902679G

44 T. Fujisawa, T. Sato, T. Kawara, and K. Ohashi, A stereocontrolled total synthesis of optically active (R,R)-phytol, *Tetrahedron Letters*, **1981**, *22*, 4823–4826. DOI: 10.1016/S0040-4039(01)92354-8

45 S. Choi, G. E. Park, D. H. Lee, M. Godumala, M. J. Cho, and D. H. Choi, Quinoxaline-Based D-A Conjugated Polymers for Organic Solar Cells: Probing the Effect of Quinoxaline Side Chains and Fluorine Substitution on the Power Conversion Efficiency, *Polymer Chemistry*, **2017**, *55*, 1209–1218. DOI: 10.1002/pola.28483

46 T. Nakanishi, Y. Shirai, and L. Han, Synthesis and optical properties of photovoltaic materials based on the ambipolar dithienonaphthothiadiazole unit, *J. Mater. Chem. A*, **2015**, *3*, 4229–4238. DOI: 10.1039/c4ta05101g

47 G. Garbay, L. Muccioli, E. Pavlopoulou, A. Hanifa, G. Hadziioannou, C. Brochon, and E. Cloutet, Carbazole-based π-conjugated polyazomethines: Effects of catenation and comonomer insertion on optoelectronic features, *Polymer*, **2017**, *119*, 274–284. DOI: 10.1016/j.polymer.2017.05.039

48 G. Conboy, R. G. D. Taylor, N. J. Findlay, A. L. Kanibolotsky, A. R. Inigo, S. S. Ghosh, B. Ebenhoch, L. K. Jagadamma, G. K. V. V. Thalluri, M. T. Sajjad, I. D. W. Samuel, and P. J. Skabara, Novel 4,8-benzobisthiazole copolymers and their field-effect transistor and photovoltaic applications, *J. Mater. Chem. C*, **2017**, *5*, 11927–11936. DOI: 10.1039/c7tc03959j

49 G. Qian, J. Qi, J. A. Davey, J. S. Wright, and Z. Y. Wang, Family of Diazapentalene Chromophores and Narrow-Band-Gap Polymers: Synthesis, Halochromism, Halofluorism, and Visible−Near Infrared Photodetectivity, *Chem. Mater.*, **2012**, *24*, 2364−2372. DOI: 10.1021/cm300938s

50 Y. Chen, G. Ma, and H. Gong, Copper-Catalyzed Reductive Trifluoromethylation of Alkyl Iodides with Togni's Reagent, *Org. Lett.*, **2018**, *20*, 4677–4680. DOI: 10.1021/acs.orglett.8b02005

51 A. G. Gasanov, A. G. Azizov, S. R. Khalilova, I. G. Ayubov, M. M. Gurbanova, and S. T. Alieva, Synthesis of 8-Heptadecene by Decarboxylation of Oleic Acid in Various Catalyst Systems, *Russian Journal of Applied Chemistry*, **2014**, *87*, 214−216. DOI: 10.1134/S1070427214020153.

52 L. Bettanin, S. Saba, F. Z. Galetto, G. A. Mike, J. Rafique, and A. L. Braga, Solvent- and metal-free selective oxidation of thiols to disulfides using I2/DMSO catalytic system, *Tetrahedron Letters*, **2017**, *58*, 4713–4716. DOI: 10.1016/j.tetlet.2017.11.009

# CHAPTER 3

# Synthesis and Characterisation of 1-Functionalised Dibenzothiophene-*S,S*-dioxide Homopolymers

---

## 3.1 Introduction

The greatest number of semiconducting conjugated polymers are electron-rich structures (p-type), which have high HOMO energy levels for example polythiophenes,[1] poly(*p*-phenylenevinylenes)[2] and polyfluorenes.[3] They can be more straightforwardly p-doped to produce positive polarons relative to n-doped to get negative polarons, this is because they show higher hole mobility in the materials than electron mobility and their p-doped state is usually more stable. In the last decades, n-type semiconductors have been investigated less than p-type, even though a number of organic electronic applications need electron deficient n-type materials such as n-type transistors for full logic circuits, photovoltaics (plastic solar cells), cathode materials and charge-transfer materials *etc.*[4,5]

One of the challenges to research in the field of n-type semiconductors is to find a kind of special structure design capable of decreasing the energy of the LUMO. Many approaches are used to reduce the LUMO level particularly in conjugated polymers.[6] The first approach is utilizing electron-deficient heterocyclic units in the polymer chain such as oxadiazoles, benzothiadiazoles, pyridines,[7] quinoxalines, thiophene-*S,S*-dioxides[8] *etc*. The second approach is the construction of conjugated polymers based on electron-deficient heterocyclic building blocks, another approach is to use electron-withdrawing substituents on the side chains. Moreover, it is possible to use a combination of electron-withdrawing/electron-donating building blocks in the building of the polymer backbone to achieve a narrow band gap and a low LUMO level in the polymers.[9]

Barbarella *et. al.* first introduced thiophene-*S,S*-dioxide as an n-type electron deficient unit into conjugated oligomers and polymer backbones as materials for organic electronics.[10,11,12,13] HF/3-21G ab initio calculations on 2,2'-bithiophene (**3.1**) and on the corresponding mono **3.2** and *bis S,S*-dioxides **3.3** (see **Figure 3.1**) show that this kind of

chemical transformation of the thiophene ring has, in fact, a profound influence on the frontier orbital pattern. The calculations indicate that the formation of the *S,S*-dioxide decreases the energy of both the HOMO and the LUMO orbitals but that the latter is remarkably more affected than the former. Consequently, a decrease in the energy gap is also observed. According to the calculations, there is only a minor involvement of the orbitals of the SO group in the description of the frontier orbitals, which remain essentially of the π, π* type.[10]

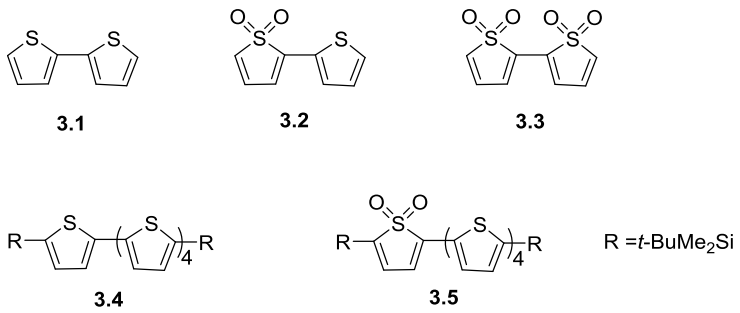


**Figure 3.1:** Structures of the thiophene-*S,S*-dioxide oligomers **3.1**–**3.5**.[10]

The cyclic voltammograms of the positive and the negative potentials of the pentamer having one terminal *S,S*-dioxide group (**3.5**), have anodic and cathodic peak potentials of 1.04 and –1.34, respectively. Comparison with the data reported for the oligothiophene (**3.4**) indicates that the oxidation potential of the *S,S*-dioxide has increased by 0.12 V while the reduction potential has become less negative by 0.79 V. Since the oxidation and reduction potentials are related to the HOMO and LUMO energies, the data shows that the LUMO of oligothiophene-*S,S*-dioxides lie at lower energies than those of the oligothiophenes, in agreement with the trend indicated by ab initio calculations.[10] Electron deficient conjugated polymers can improve the performance of OLED devices by two methods, by increased electron injection from the metal cathode and by blocking the holes in the emitting layer from a cathode thus balancing the electrons and holes in the material, hence increasing the chance of exciton formation.

Seki *et al.* in 2012 designed and synthesised a new series of n-type co-polymers based on the dicyanofluorene moiety.[14] Attaching two cyano groups made the dicyanofluorene segment a strong electron acceptor. Three co-polymers (**3.6–3.8**) were

investigated by incorporating various donor moieties with dicyanofluorene (see **Figure 3.2**). All co-polymers demonstrated strong absorption in the UV-visible region and the absorption maximum showed a bathochromic shift with an increasing number of thiophene moieties in the co-polymer backbone (see **Figure 3.3**). A space-charge-limited current (SCLC) study demonstrated that the electron mobility of the materials in the bulk state were 1 to 2 orders greater than that of the corresponding hole mobility, which proved the n-type nature of the polymers.

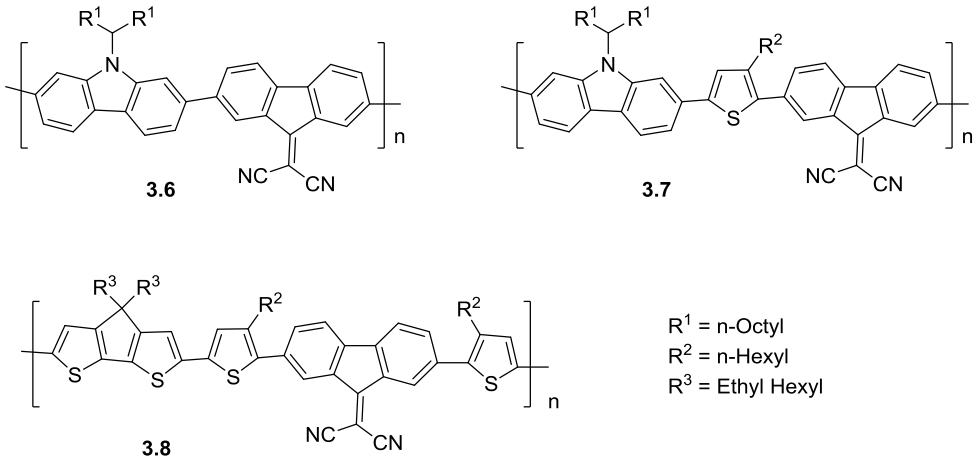


**Figure 3.2:** Structures of co-polymers **3.6–3.8**.[14]

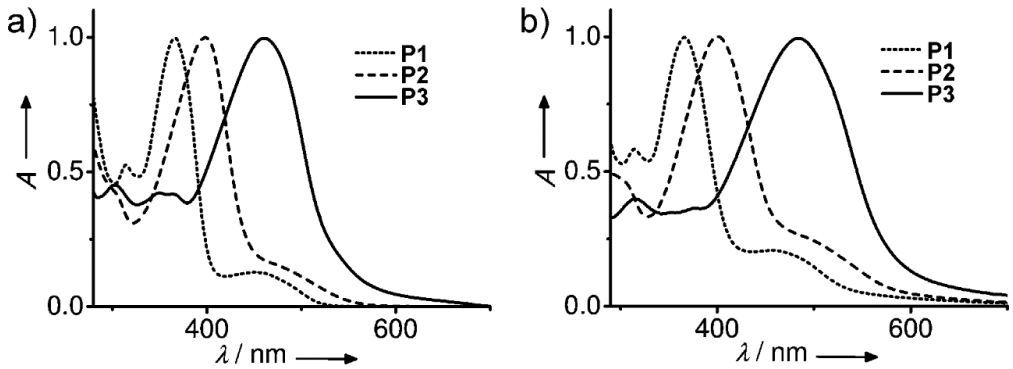


**Figure 3.3:** Absorption spectrum of **3.6–3.8** (P1–P3) in a) tetrahydrofuran and b) the thin-film state.[14]

Dibenzothiophene-*S*,*S*-dioxide, in contrast to fluorene, is an electron-deficient moiety because of the electron-withdrawing character of the sulfonyl group and as a result it is an interesting building block for the building of conjugated materials. In 2005, Perepichka and Bryce introduced dibenzothiophene-*S*,*S*-dioxide as an electron deficient building block for organic electronic applications.[15] The idea was that dibenzothiophene-*S*,*S*-dioxide was topologically similar to the fluorene unit, in which the $C(R_2)$ bridge between the phenylene moieties is replaced by an electron-withdrawing $SO_2$ bridge, thus reducing the LUMO energy and giving the materials a higher electron affinity. Since this first seminal research, over 400 papers have been published in the literature which use dibenzothiophene-*S*,*S*-dioxide in organic electronic materials as an electron-deficient building block, particularly for the design of new light-emitting co-polymers.[16,17,18,19,20,21] (*Yet, to date of writing this thesis, no dibenzothiophene-S,S-dioxide homopolymers have been reported. This is one of the aims of the present studies in our PhD program of research*).

### 3.1.1 Aims of the chapter

Since the first influential paper presenting dibenzothiophene-*S*,*S*-dioxide as a useful building block for conjugated organic molecular and polymeric materials for organic electronics,[15] numerous papers have been published reporting different variations in structures, studies of their optoelectronic properties and testing the materials in various devices (mainly in OLEDs, but applications in other devices have also been studied).

The main aim of this chapter is the synthesis of the first (yet unknown as a class) soluble conjugated dibenzothiophene-*S*,*S*-dioxide homopolymers as n-type electron deficient homopolymers by using a Ni-mediated coupling polymerisation method. To reach this goal, synthetic methods for the introduction of solubilising groups (alkoxy, alkylthio and alkylsulfonyl) at position 1 of the dibenzothiophene-*S*,*S*-dioxide moiety as described in Chapter 2, were utilised to prepare and study conjugated polymers based on this structural moiety (**Scheme 3.1**). A full characterisation and identification of the photo physical, cyclic voltammetry, and thermal stability properties of the synthesised homopolymers, using different techniques (e.g. $^1$H NMR, GPC, TGA, CV, UV, PL, PLQY *etc.*) will then be presented, to understand their perspectives as light-emitting and electron-transporting materials for organic electronics.

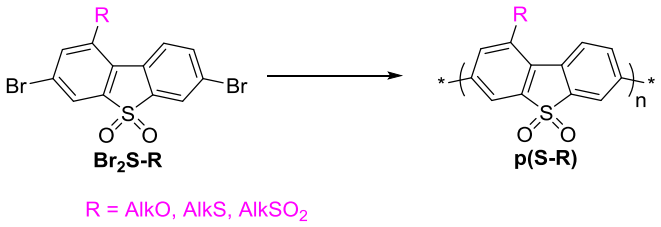


**Scheme 3.1:** General scheme showing the synthetic route to soluble 1-substituted dibenzothiophene-*S*,*S*-dioxide homopolymers.

## 3.2 Results and Discussion

### 3.2.1 Nickel-mediated Yamamoto polycondensation of $Br_2$S-R and characterisation of the first soluble dibenzothiophene-*S,S*-dioxide homopolymers, p(S-R)

The first polymerisation of dibenzothiophene-*S,S*-dioxide monomers by Ni-mediated dehalogenative Yamamoto coupling polycondensation[22,23,24,25,26,27,28,29,30,31,32,33,34,35,36] was done for linear 1-dodecyloxy derivative **$Br_2$S-$OC_{12}$** on a small scale (200 mg) to investigate the polymerisation process, the solubility and the spectral properties of the formed **p(S-$OC_{12}$)** polymer. The reaction was performed with $Ni(COD)_2$ in dry DMF-toluene under an argon atmosphere for 4 days at 85 °C and the polymer formed was then end-capped with phenyl groups (**Scheme 3.2**).

After precipitation into MeOH:$H_2O$:HCl, the crude greenish yellow polymer was extracted using a soxhlet apparatus with methanol to remove any low-molecular weight oligomers and other by-products. It was then extracted with acetone, THF and chloroform to collect **p(S-$OC_{12}$)** polymer fractions of different molecular weights. As substantial amounts of insoluble materials remained in the extraction thimble, this was further extracted with chlorobenzene and anisole (at temperatures close to the boiling points of these solvents in the extractor). Finally, an insoluble fraction of **p(S-$OC_{12}$)** was collected from the thimble. The results of these extractions are collated in **Table 3.1**.

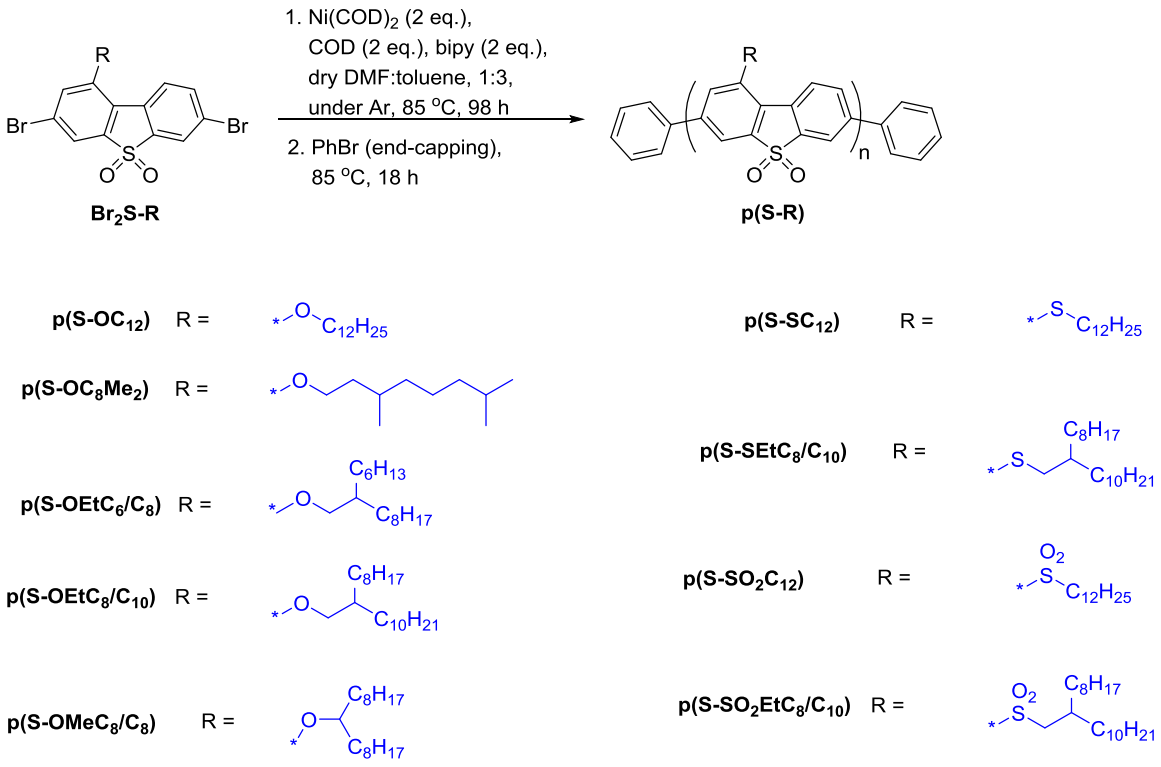


**Scheme 3.2:** Synthesis of homopolymers **p(S-R)** by Ni-mediated Yamamoto polycondensation of **Br2S-R** monomers.

**Table 3.1** Weights and yields of extracted fractions of polymer **p(S-OC12)**.[a]

| Fraction | Weight (mg) | % yield | Appearance (solid material |
|---|---|---|---|
| Methanol-soluble[b] | 16 | 11.2 | Yellow |
| Acetone-soluble[c] | 9 | 6.3 | Greenish-yellow |
| THF-soluble[c] | 20 | 14.0 | Greenish-yellow |
| Chloroform-soluble[c] | 9 | 6.3 | Greenish-yellow |
| Chlorobenzene-soluble[c] | 23 | 16.1 | Greenish-yellow |
| Anisole-soluble[b] | 29 | 20.3 | Greenish-yellow |
| Insoluble fraction[b] | 32 | 22.4 | Light brown |

[a]Theoretical yield of **p(S-OC12)** is 143 mg (from 200 mg of **Br2S-OC12**). [b]Weakly fluorescent or non-fluorescent. [c]Fluorescent.

Considering the successful synthesis of the first soluble electron-deficient high bandgap dibenzothiophene-*S*,*S*-dioxide conjugated polymer with a linear alkoxy long-chain solubilising group, and the observation of bright emission from it (deep blue in solution and green-yellow in the solid state), as will be discussed in the next pages, the polymerisation of other dibenzothiophene-*S*,*S*-dioxide monomers **$Br_2$S-R** was carried out. These polymerisations were performed with linear and branched alkoxy, alkylthio, and alkylsulfonyl groups on a 1 mmol scale under similar reaction conditions (amount of $Ni(COD)_2$ was decreased from 2.2 eq. to 2.0 eq.) (**Scheme 3.2**).[d] Polymers **p(S-R)** with different alkoxy, alkylthiol, and alkylsulfonyl solubilising groups were successfully obtained and the crude materials underwent consequent extraction with different solvents in a similar manner to that described above for **p(S-$OC_{12}$)**. THF was not used for extraction in these experiments, as previous studies showed very close spectral characteristics (see Section 3.2.6.1) of the THF and chloroform fractions of **p(S-$OC_{12}$)** (**Figure 3.5, Table 3.4**). Instead, a longer extraction with acetone (36 h instead of 24 h) was used for total removal of low molecular weight polymer fractions. The results for **p(S-$OC_{12}$)** reproduced well as in the previous synthesis of this polymer, giving 28.3% from the chloroform fraction (20.3% for THF + $CHCl_3$ in the previous run) and 30% of insoluble polymer (22.4% in the previous run). Despite the presence of branched groups in the **p(S-R)** polymers, they also showed a substantial amount of insoluble polymer fractions (17–71%) and 10–52% yields of chloroform-soluble polymers (see **Table 3.9**, Section 3.4.10).

So, it seems that the Yamamoto polymerisation works well for dibenzothiophene-*S*,*S*-dioxide, but the solubilising effect of a linear or branched chain is not enough to give polymers with good solubility in common organic solvents (THF, chloroform, toluene, *etc.*). Thus, molecular weights of the homopolymers have been estimated by gel permeation chromatography (GPC) as shown in the next section. In conclusion, nine novel dibenzothiophene-*S*,*S*-dioxide homopolymers with different solubilising alkyl groups were successfully synthesised, which emit bright deep blue light in solution and green/yellow in the solid (or aggregated) state as will be discussed in the next sections.

[d] *Polymerisation of **$Br_2$S-$OC_{12}$** was also repeated at this scale.*

### 3.2.1.1 Attempted nickel-mediated Yamamoto polymerisation of $Br_2S$-$SMeC_8/C_8$, $Br_2S$-$SO_2MeC_8/C_8$, and 2.24 monomers

It was attempted to polymerise the **$Br_2S$-$SMeC_8/C_8$**, **$Br_2S$-$SO_2MeC_8/C_8$**, and **2.24** monomers in the same way, as was described in the previous Section 3.2.1 (see **Scheme 3.3**). However, the polymerisations failed and all the materials obtained from the reaction mixtures were soluble in the methanol and acetone fractions, which means only short oligomers (dimers or trimers) were formed. This is not surprising, as these types of reactions are extremely sensitive to oxygen and water, therefore they should be carried out under an argon atmosphere and using nitrogen gloves. Unfortunately, the nitrogen gloves, which were available in the laboratory, were very old and have a lot of holes so it was very hard to control the reaction. Three trails for each monomer were carried out, however none of them gave polymers with sufficient molecular weights. Due to all the starting monomers being consumed no further trials were attempted.

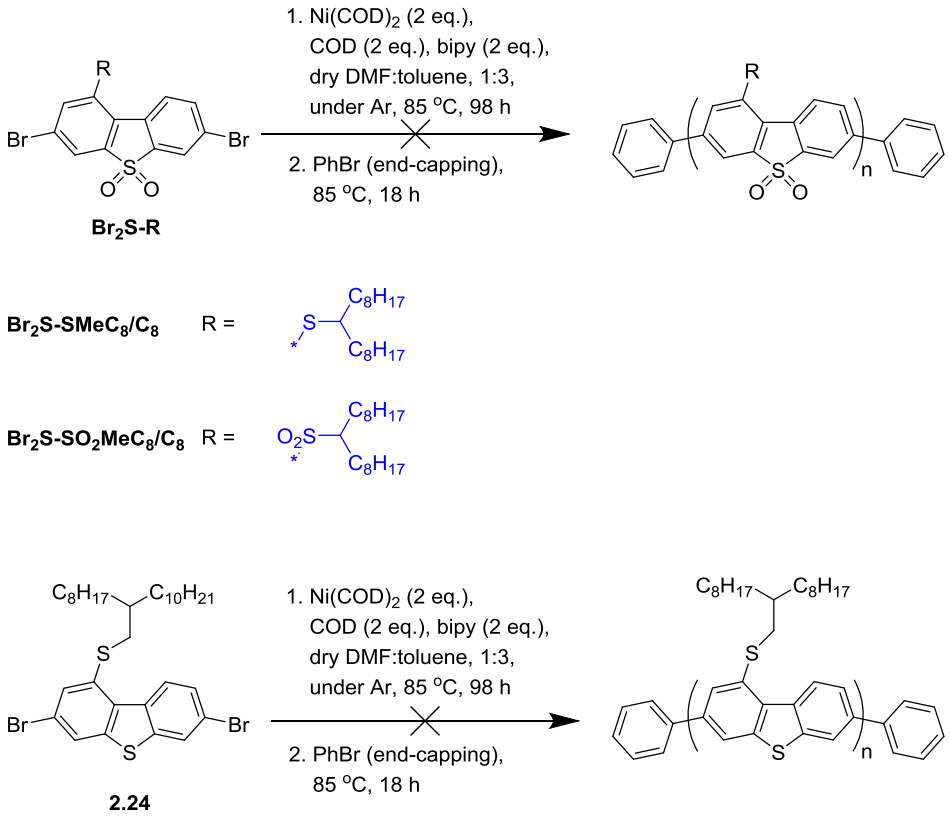


**Scheme 3.3:** Reaction scheme of attempted polymerisation of **$Br_2S$-$SMeC_8/C_8$**, **$Br_2S$-$SO_2MeC_8/C_8$**, and **2.24** monomers.

### 3.2.2 Characterisation of 1-substituted poly(dibenzothiophene-*S*,*S*-dioxide) p(S-OR), p(S-SR), and p(S-$SO_2$R) by GPC method

Molecular weights of the synthesised homopolymers have been estimated by gel permeation chromatography (GPC) in THF solutions, with the column calibrated versus polystyrene standards. Estimates of their weight average molecular weight (Mw), number average molecular weight (Mn) and polydispersity index PDI = Mw/Mn were obtained. An example of a GPC trace is shown in **Figure 3.4** for the **p(S-OEt$C_8$/$C_{10}$)** chloroform fraction. The GPC traces for all the other polymers can be seen in Appendix 6.8.

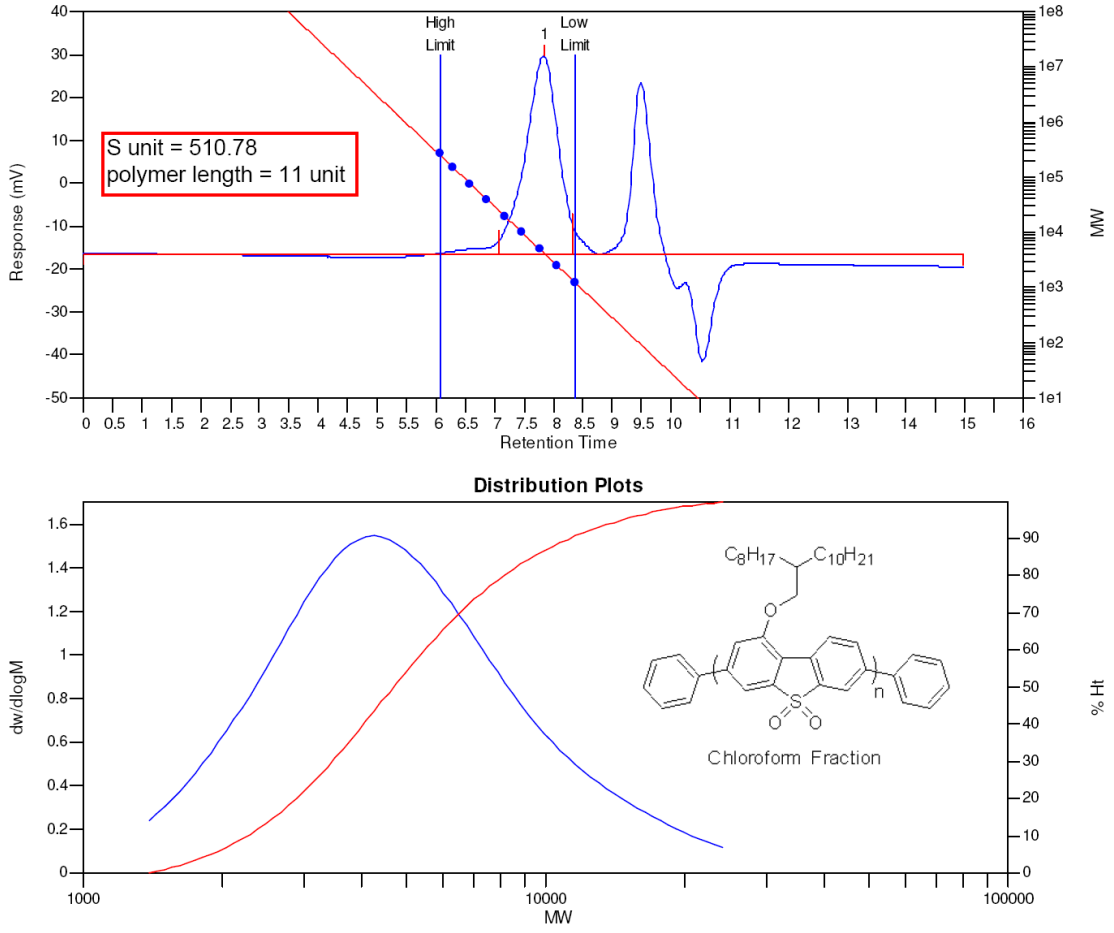


**MW Averages**

| Peak No | Mp | Mn | Mw | Mz | Mz+1 | Mv | PD |
|---|---|---|---|---|---|---|---|
| 1 | 4249 | 4054 | 5803 | 8543 | 11868 | 5474 | 1.43143 |

**Figure 3.4:** GPC trace for **p(S-OEt$C_8$/$C_{10}$)** chloroform fraction in THF.

GPC analysis of the acetone fractions of 1-substituted poly(dibenzothiophene-*S*,*S*-dioxide) homopolymers showed molecular weights less than 2000 Daltons which indicate very short oligomers, between 2 – 4 units, but with a very narrow peak (PDI < 1.5 in all cases). However, the chloroform fractions showed higher molecular weights (Mw = 3,443 – 17,605 Da; Mn = 2,496 – 6,769 Da; PDI = 1.23 – 2.60), see **Table 3.2**, from which the average chain length can be estimated as n = 9 – 14. Thus, in all the cases, the molecular weight is somewhat equal or a bit higher or lower than the conjugation length in polyfluorenes (estimated in the literature as n = 11 – 12).[37] It seems that the polymerisations were successful; however, the highest molecular weight material remained in the thimble as an insoluble fraction due to the poor solubility of these types of homopolymers in the solvents used.

Another important conclusion from the GPC measurements is that the polymers **p(S-R)** with branched alkyl chains have higher molecular weights compared to those with linear alkyl chains for both the acetone and chloroform fractions. This is due to the better solubility of the polymers with branched alkyl chains in common solvents (acetone, chloroform, chlorobenzene, *etc*.) relative to the linear ones.

**Table 3.2** GPC data for 1-substituted poly(dibenzothiophene-*S*,*S*-dioxide) homopolymers.

| homopolymer | $M_{w,}$[a] (Da) | $M_{n,}$[b] (Da) | PDI[c] |
|---|---|---|---|
| **p(S-OC$_{12}$)** acetone fraction | 1457 | 1188 | 1.23 |
| **p(S-OC$_{12}$)** chloroform fraction | 4560 | 2474 | 1.84 |
| **p(S-OC$_8$Me$_2$)** acetone fraction | 1842 | 1419 | 1.30 |
| **p(S-OC$_8$Me$_2$)** chloroform fraction | 4921 | 3623 | 1.36 |
| **p(S-OEtC$_6$/C$_8$)** acetone fraction | 1958 | 1499 | 1.31 |
| **p(S-OEtC$_6$/C$_8$)** chloroform fraction | 6252 | 4331 | 1.44 |
| **p(S-OEtC$_8$/C$_{10}$)** acetone fraction | 2066 | 1628 | 1.27 |
| **p(S-OEtC$_8$/C$_{10}$)** chloroform fraction | 5803 | 4054 | 1.43 |
| **p(S-OMeC$_8$/C$_8$)** acetone fraction | 1918 | 1540 | 1.25 |
| **p(S-OMeC$_8$/C$_8$)** chloroform fraction | 5367 | 4054 | 1.32 |
| **p(S-SC$_{12}$)** acetone fraction | 1475 | 1199 | 1.23 |
| **p(S-SC$_{12}$)** chloroform fraction | 3443 | 2496 | 1.38 |

| | | | |
|---|---|---|---|
| **p(S-SEtC$_8$/C$_{10}$)** acetone fraction | 1901 | 1538 | 1.24 |
| **p(S-SEtC$_8$/C$_{10}$)** chloroform fraction | 13506 | 5542 | 2.44 |
| **p(S-SO$_2$C$_{12}$)** acetone fraction | 2533 | 1787 | 1.42 |
| **p(S-SO$_2$C$_{12}$)** chloroform fraction | 4664 | 2911 | 1.60 |
| **p(S-SO$_2$EtC$_8$/C$_{10}$)** acetone fraction | 1851 | 1344 | 1.38 |
| **p(S-SO$_2$EtC$_8$/C$_{10}$)** chloroform fraction | 17605 | 6769 | 2.60 |

[a] $M_w$:weight average molecular weight. [b] $M_n$: number average molecular weights, [c] Polydispersity index, PDI = $M_w/M_n$.

### 3.2.3 Thermal Analyses of 1-substituted poly(dibenzothiophene-*S*,*S*-dioxide) p(S-OR), p(S-SR), and p(S-SO$_2$R) chloroform fractions

The thermal stabilities of the chloroform fractions of all **p(S-OR)**, **p(S-SR)**, and p**(S-SO$_2$R)** polymers have been studied by thermogravimetric analysis (TGA). Estimating their thermal decomposition in a nitrogen atmosphere at a level of 5% mass loss with a heating rate of 10 °C/min. All polymers showed good stability, with decomposition temperatures of $T_d$ = 340–388 °C (**Figure 3.5**, **Table 3.3**), typical for polyfluorenes (e.g. for **PF8** it was reported as $T_d$ = 385 °C).[38] From the TGA data in the region of ~330–450 °C with *ca* 55–65% mass loss, it seems that major mass losses on decomposition are due to cleavage of the alkoxy, alkyl thio or alkyl sulfonyl groups in the **p(S-OR)**, **p(S-SR)**, and **p(S-SO$_2$R)** polymer units.

**Table 3.3:** TGA data for the **p(S-OR)**, **p(S-SR)**, and **p(S-SO$_2$R)** chloroform fraction polymers.

| Polymer | $T_{d,}$[a] (°C) | Polymer | $T_{d,}$[a] (°C) |
|---|---|---|---|
| **p(S-OC$_{12}$)** | 388 | **p(S-SC$_{12}$)** | 350 |
| **p(S-OEtC$_6$/C$_8$)** | 383 | **p(S-SEtC$_8$/C$_{10}$)** | 363 |
| **p(S-OC$_8$Me$_2$)** | 380 | **p(S-SO$_2$C$_{12}$)** | 343 |
| **p(S-OEtC$_8$/C$_{10}$)** | 388 | **p(S-SO$_2$EtC$_8$/C$_{10}$)** | 355 |
| **p(S-OMeC$_8$/C$_8$)** | 340 | | |

[a] $T_d$ is the decomposition temperature measured at 5% weight loss under $N_2$.

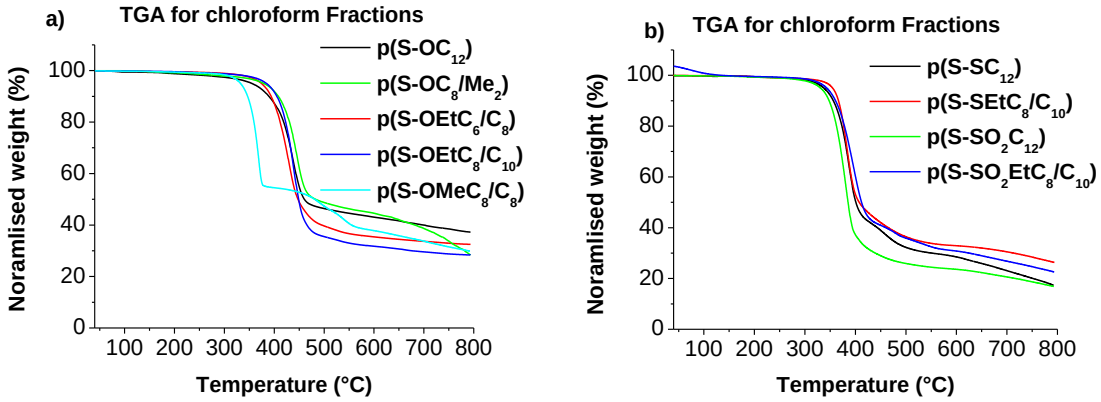


**Figure 3.5:** Thermogravimetric analysis (TGA) curves of a) **p(S-OR)**, b) **p(S-SR)** and **p(S-SO2R)** chloroform fraction polymers under a nitrogen atmosphere at a heating rate of 10 °C/min.

### 3.2.4 DFT calculations of electronic properties of 1-substituted dibenzothiophene-*S,S*-dioxide

Density functional theory (DFT) B3LYP/6-31G(d) calculations were carried out to investigate the HOMO and LUMO energy levels and the HOMO-LUMO gaps of a variety of different oligomers of 1-substituted dibenzothiophene-*S,S*-dioxide units to determine the optical properties of their polymer analogies from trends in the increase in oligomer chain length.

**Figures 3.6 a-c** show the differences in the energy levels of a variety of different monomer units. Comparing all the values to unsubstituted dibenzothiophene-*S,S*-dioxide (H), the expected trend can be seen, with the electron donating groups expressing higher HOMO and LUMO energy levels and the electron withdrawing groups expressing a lower HOMO and LUMO energy level. For the HOMO energy levels, there is a maximum energy difference of 1.13 eV between $NMe_2$ (-5.83 eV) and $SO_2CF_3$ (-6.96 eV). The same is true for the LUMO energy levels, with a maximum difference in energy of 1.03 eV between $NMe_2$ (-2.63 eV) and $SO_2CF_3$ (-3.66 eV). This similarity in the change of HOMO/LUMO energy levels is reflected in the band gap energy values, with small variations between each different substitution (~0.2 eV), showing that all of these polymers will express similar optical properties, but the small variances allow optical devices to be finely tuned for specific applications. It should also be noted that the band gap for the unsubstituted analogue

is higher than all of the substituted analogues. This shows a red-shift for all of the polymers, which is the desired property for co-polymerisation with fluorene.

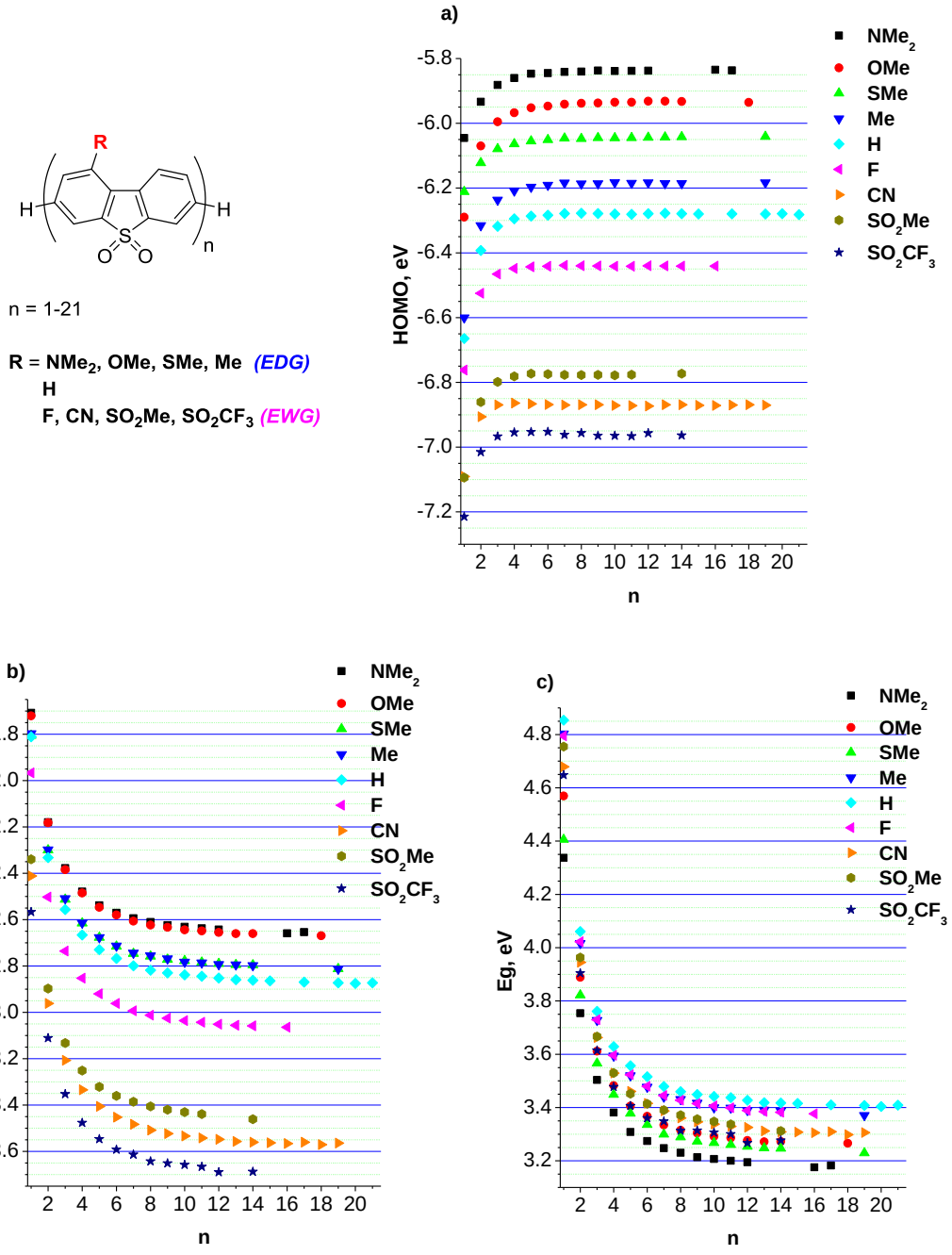


**Figure 3.6:** DFT B3LYP/6-31G(d) calculation of energy levels of 1-substituted dibenzothiophene-*S*,*S*-dioxide oligomers (for n = 1–20) in the gas phase: (a) HOMO energy levels, (b) LUMO energy levels, (c) HOMO-LUMO energy gaps ($E_g$) of oligomers.

### 3.2.5 Electrochemical studies of 1-substituted polydibenzothiophene-*S*,*S*-dioxide p(S-OR), p(S-SR), and p(S-$SO_2$R) chloroform fractions

The electrochemical behaviour of the **p(S-OR)**, **p(S-SR)**, and **p(S-$SO_2$R)** series of polymers was studied by cyclic voltammetry (CV) in films drop-cast from chloroform solution onto glassy carbon electrodes. Measurements have been done in acetonitrile with 0.1 M $Bu_4NPF_6$ as a supporting electrolyte at a scan rate of 100 mV/s. The results of the CV experiments are shown in **Figures 3.7, 3.8** demonstrating that all the polymers are electroactive and undergo oxidation (p-doping) with onsets in the region of +(1.18–1.51) V and reduction (n-doping) with onsets in the region of –(0.94–1.33) V (see **Table 3.4**). **Figure 3.7b** shows how the reduction onset of **p(S-OEtC$_8$/C$_{10}$)** polymer was calculated, as an example. The same procedure was followed to calculate the oxidation and reduction onset for all other polymers described in this thesis. From these CV measurements, it was estimated the HOMO/LUMO energy levels of the **p(S-OR)**, **p(S-SR)**, and **p(S-$SO_2$R)** polymers using general formulas (1 and 2), where 4.8 eV is an estimation of the potential of the $Fc/Fc^+$ couple versus vacuum.[39]

$$E_{HOMO} = -e(E^{ox}_{onset} + 4.8)\ eV, \quad (1)$$

$$E_{LUMO} = -e(E^{red}_{onset} + 4.8)\ eV, \quad (2)$$

$$E_g = E_{LUMO} - E_{HOMO}, \quad (3)$$

The **p(S-OR)** polymers showed similar results when measuring both the reduction and the oxidation which is expected because the difference between the polymer series is only the alkyl groups which have no direct involment with oxidation and reduction (see **Figure 3.7**). A pronounced effect was observed for the EWG $–SO_2$ on the oxidation, reduction and $E_g^{CV}$, even in the presence of the alkoxy group which is an EDG compared to polyfluorene (**PF8**) (**Table 3.4**).[40] Due to the EWG ($-SO_2$) the reduction was easier to carry out as the polymer wasn't as easy to oxidise. Also the reduction was easy to repeat multiple times so a uniform spectrum could be obtained. Due to the properties of the polymer the oxidation process was harder to reproduce as the groups present within the polymers are not very compliant with losing electrons.

The results of the CV experiments of the **p(S-R)** series of polymers demonstrated that the HOMO/LUMO energy levels can be efficiently tuned by alternating the functional group at the 1- position (see **Figure 3.8**). Thus, from the strongest EDG (**R** = **OEtC$_8$/C$_{10}$**)

to the strongest EWG (**R** = **$SO_2EtC_8/C_{10}$**), HOMO and LUMO energy levels can be tuned by 0.21 eV and 0.35 eV, respectively. These tunings of frontier orbital energies are somewhat lower than those obtained from DFT calculations for isolated molecules in the gas phase (tuning both HOMO and LUMO by ~0.8 eV, **Figure 3.6**), which can be expected as DFT calculations do not take into account solvation and solid state effects. Nevertheless, the strong effect itself and the trends are in good agreement with DFT predictions.

Another important conclusion from the CV measurements is that the band gap of polymers, $E_g^{CV}$, reduced by ~ 1.1 eV compared to polyfluorene **PF8** and the effect of the functional group at the 1- positon, is pretty weak. **Table 3.4** also presents optical band gaps, $E_g^{opt}$, estimated from the red edge of the absorption spectra of the studied polymers (see next section for detailed studies). These values are a little different to the electrochemical band gaps ($E_g^{CV}$) estimated from the CV experiments. This is not surprising as optical and electrochemical energy gaps are due to different physical processes. Even though, similar to the $E_g^{CV}$ values, $E_g^{opt}$ are reduced compared to polyfluorene **PF8** and the effect of the functional group at the 1- positon, is also very weak.

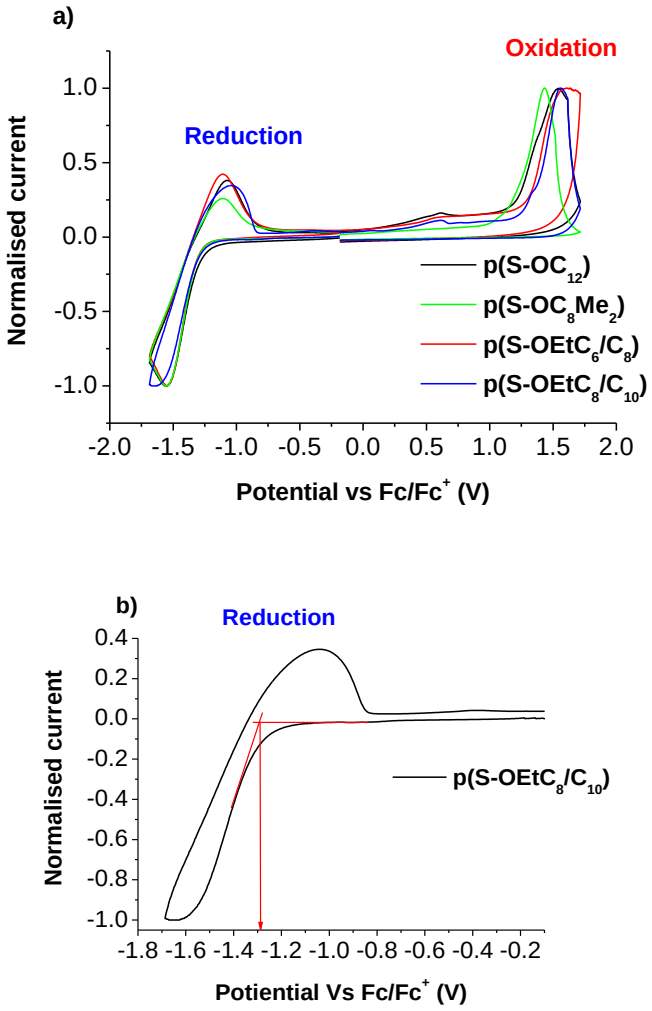


**Figure 3.7:** a) Cyclic voltammetry of **p(S-OR)** polymer films on glassy carbon electrode in 0.1 M of $Bu_4NPF_6$ / $CH_3CN$, scan rate 100 mV/s. For convenience, CV data are presented with normalisation to the current maximum of an oxidation / reduction processes. b) Method of calculation of the reduction onset of **p(S-OEtC8/C10)** polymer as an example.

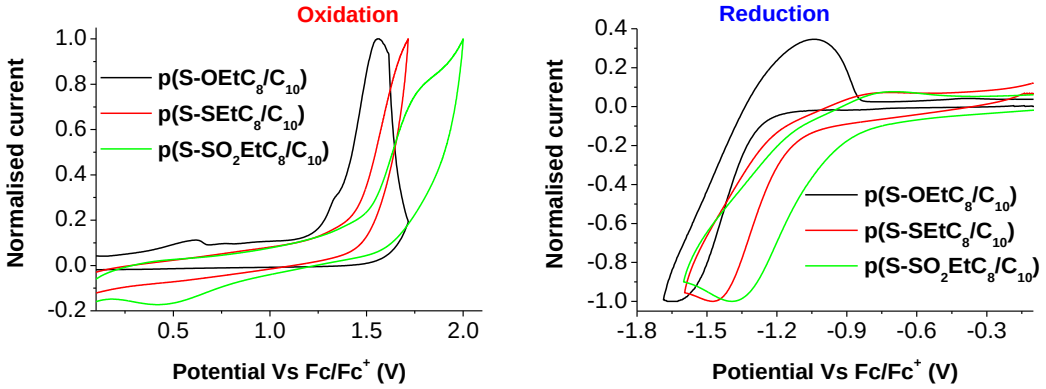


**Figure 3.8:** Cyclic voltammetry of **p(S-R)** (**R** = **OEtC8/C10**, **SEtC8/C10** and **SO2EtC8/C10**) polymer films on glassy carbon electrode in 0.1 M of $Bu_4NPF_6$ / $CH_3CN$, scan rate 100 mV/s. For convenience, CV data are presented with normalisation to the current maximum of an oxidation / reduction processes.

**Table 3.4:** Cyclic voltammetry data, HOMO/LUMO energy levels and band gaps of **p(S-OR)**, **p(S-SR)**, and **p(S-SO2R)** polymers.

| Polymer | $E_g^{opt}$,[a] (eV)[a] | $E^{ox}_{onset}$,[b] (V) | $E^{red}_{onset}$,[b] (V) | HOMO[c] (eV) | LUMO[c] (eV) | $E_g^{CV}$,[d] (eV) |
|---|---|---|---|---|---|---|
| **PF8**[40] | 2.82 | 0.97[e] | –2.64[e] | –5.77 | –2.16 | 3.61 |
| **p(S-OC12)** | 2.64 | 1.18 | –1.28 | –5.98 | –3.52 | 2.46 |
| **p(S-OMe2C8)** | 2.61 | 1.19 | –1.31 | –5.99 | –3.49 | 2.50 |
| **p(S-OEtC6/C8)** | 2.55 | 1.29 | –1.33 | –6.09 | –3.47 | 2.62 |
| **p(S-OEtC8/C10)** | 2.57 | 1.30 | –1.29 | –6.10 | –3.51 | 2.59 |
| **p(S-SEtC8/C10)** | 2.58 | 1.44 | –1.15 | –6.24 | –3.65 | 2.59 |
| **p(S-SO2EtC8/C10)** | 2.61 | 1.51 | –0.94 | –6.31 | –3.86 | 2.45 |

[a] $E_g^{opt}$ are optical band gaps estimated from the red edge of UV–Vis spectra of polymer films. [b] $E^{ox}_{onset}$ and $E^{red}_{onset}$ are the onset potentials of oxidation and reduction of polymer films measured versus $Fc/Fc^+$ couple. [c] $E_{HOMO}$ and $E_{LUMO}$ energies calculated from empirical formulas (1) and (2): $E_{HOMO}$ (eV) = –e($E^{ox}_{onset}$ + 4.8) and $E_{LUMO}$ = –e($E^{red}_{onset}$ + 4.8). [d] Electrochemical band gap $E_g^{CV} = E_{LUMO} - E_{HOMO}$. [e] CV data in ref.[40] are given versus Ag/AgCl electrode; we have recalculated them to $Fc/Fc^+$ as $E(Fc/Fc^+) = E(Ag/AgCl) - 0.4$ V.

### 3.2.6 Photophysical studies of 1-substituted poly(dibenzothiophene-*S*,*S*-dioxide) p(S-OR), p(S-SR), and p(S-$SO_2$R)

#### 3.2.6.1 Electron absorption and photoluminescence spectra of p(S-$OC_{12}$) homopolymer

Initially, the **p(S-$OC_{12}$)** polymer was synthesised on a small scale, as mentioned in the previous section, to study the polymerisation process, the solubility and spectral properties. The different fractions of the **p(S-$OC_{12}$)** polymer that were isolated were characterised by UV-Vis electron absorption and photoluminescence (PL) spectroscopy. The UV-Vis and PL spectra are shown in **Figure 3.9** and the data are summarised in the **Table 3.5**.

UV-Vis spectra demonstrate clear bathochromic shifts of $\lambda_{abs}$ values (by 43 nm, from the acetone to the chlorobenzene fraction), in accordance with the expected increase in molecular weights of the fractions from the "poor solvent" acetone to "good solvents" chloroform and chlorobenzene.[e] For the less soluble (and presumably higher molecular weight) chlorobenzene fraction (as well as for the anisole fraction), the UV-Vis spectrum becomes structured indicating the rigidification of the system (and possibly an aggregation of polymer chains) (**Figure 3.9**). Photoluminescence spectra of **p(S-$OC_{12}$)** polymer fractions show a bathochromic shift from the acetone ($\lambda_{PL}$ = 400sh, 425 nm) to the THF fraction and then it remains almost unchanged for the other fractions ($\lambda_{PL}$ = 434 nm) see **Figure 3.9**, **Table 3.5**. Moreover, pronounced vibronically resolved PL spectra are observed for the higher molecular weight fractions, a typical feature of rigid-rod conjugated polymers (see e.g. **Figure 1.13** for PL spectrum of poly(9,9-dioctylfluorene), **PF8** Chapter 1).[41] An increase in short-wavelength absorption and an increased PL intensity in the 500–600 nm region of the anisole fraction might indicate partial decomposition of this material (possibly due to the high boiling point of this solvent, 154 °C, which was used for 24 h during extraction of this fraction).

[e] *As proven in the previous section by measuring the molecular weights of the polymer fractions by gel-permeation chromatography (GPC).*

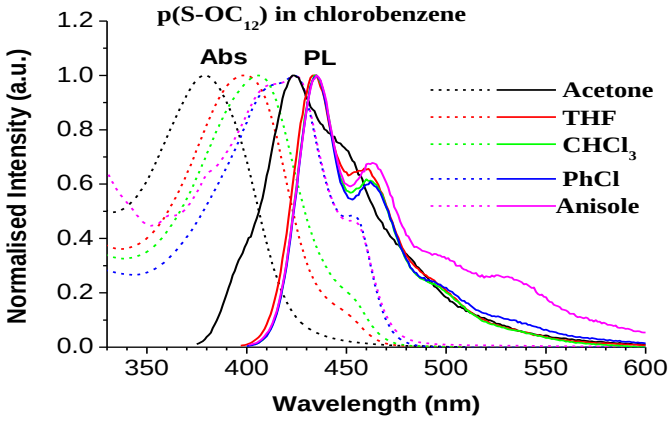


**Figure 3.9** UV-Vis electron absorption and photoluminescence spectra of different fractions of polymer **p(S-OC$_{12}$)** in chlorobenzene.

**Table 3.5:** UV-Vis electron absorption ($\lambda_{abs}$) and photoluminescence ($\lambda_{PL}$) maxima for extracted fractions of polymer **p(S-OC$_{12}$)** in chlorobenzene solution.

| **Polymer fraction**[a] | $\lambda_{abs}$ (nm)[b] | $\lambda_{PL}$ (nm)[b,c] |
|---|---|---|
| **Acetone-soluble** | 380 | 400sh, 425, 450sh |
| **THF-soluble** | 397 | 434, 460sh |
| **Chloroform-soluble** | 405 | 434, 461sh |
| **Chlorobenzene-soluble** | 410sh, 423 | 434, 462sh |
| **Anisole-soluble** | 410sh, 423 | 434, 463sh, 500sh, 525sh |

[a]Extraction time for each fraction was ~ 24 h. [b]sh – Shoulder. [c]For PL measurements, the excitation wavelengths, $\lambda_{exc}$, of 10 nm shorter than their absorption maxima $\lambda_{abs}$ have been used for all fractions.

The low solubility of the presumably high molecular weight chlorobenzene fraction and the appearance of a structured feature in its absorption spectrum might indicate an increased tendancy of the dibenzothiophene-*S*,*S*-dioxide polymer to aggregate, compared to poly(dialkylfluorenes), which are well-soluble in chloroform and toluene even for very high molecular weight polymers of $M_w$ > 300,000 Da.[42] This can be understood by taking into account that linear solubilising **OC$_{12}$H$_{25}$** lies in the plane of the aromatic moiety allowing close π-π interactions between neighbouring polymer chains (in contrast to polyfluorenes, in which two alkyl groups are orthogonal to the fluorene moiety preventing such inter-chain interactions).

The emission colours of different polymer fractions at different concentrations of polymers in chlorobenzene under UV irradiation (laboratory UV-lamp, 360 nm) have been investigated. **Figure 3.10 a** shows emissions of the different fractions (from acetone-soluble to anisole-soluble) at low (Abs ~ 0.1 a.u., bottom photos in **Figure 3.10 a**) and high (Abs. ~ 1.0 a.u., top photos in **Figure 3.10 a**) concentrations in chlorobenzene. It can be clearly seen, that at low concentrations, all fractions emit blue light, in accordance with their PL spectra in **Figure 3.9**. However, at ~10-times higher concentrations, the emission of the high molecular weight fractions (chloroform to anisole) are bathochromically shifted from a deep-blue to a bluish colour (**Figure 3.10 a**, top). This effect becomes even more pronounced when high concentrations of chloroform solutions of the polymer fractions were irradiated with 360 nm UV lamp (**Figure 3.10 b**): the colour emission of the chlorobenzene and anisole fractions is further shifted to the red region and they emit a green-yellow colour (PhCl and PhOMe fractions were slightly opaque, which is an indication on nano/microaggregation of the polymers). A similar, and even more pronounced change in the emission is observed for solid samples: an intense green emission for solids of the THF fraction and a greenish-yellow colour for the chlorobenzene fraction (**Figure 3.10 c**).

This is in agreement with what we expect to see, as the higher molecular weight polymers have longer wavelengths, thus resulting in a bathochromic shift. The appearance of a bright green emission in the solid state can also be seen with high concentrations of the polymer (**Figure 3.10 c**), this can be attributed to the yellow colour of the polymer material mixing with the blue emission, causing an appearance of green photoluminescence. These observations are all in agreement with the obtained UV/Vis absorption and PL emission data (**Figure 3.9**), and confirm that the **p(S-OC$_{12}$)** homopolymer is indeed a blue-fluorescent emitter. These outcomes might also indicate that strong intermolecular interactions exist for the high molecular weight soluble 1-dodecyloxydibenzothiophene-*S*,*S*-dioxide polymer. These π-π interactions lead to decreasing the polymer solubility and formation of excimers (excited state dimers of polymer chains), which emit at longer wavelengths compared to an isolated polymer chain.[f]

[f] *Further, more detailed studies on this matter are presented in the next sections to clarify the origin of this phenomenon.*

Fractions (from the left to the right):
Acetone / THF / $CHCl_3$ / PhCl / PhOMe

**a)** **b)** **c)**

**Figure 3.10:** Emission of different fractions of polymer **p(S-OC$_{12}$)** under UV-light irradiation (360 nm): **a)** emission in chlorobenzene solutions at low concentrations (Abs. ~ 0.1 a.u; bottom) and high concentrations (Abs. ~ 1. a.u., top). **b)** emission in chloroform solutions at very high concentrations. **c)** Solid state emission of **p(S-OC$_{12}$)**: THF-soluble fraction (on left) and chlorobenzene fraction (on right).

### 3.2.6.2 Electron absorption and photoluminescence spectra of p(S-OR) homopolymers

The different fractions of the **p(S-OR)** polymers that were isolated were characterised by UV-Vis electron absorption and photoluminescence (PL) spectroscopy in chlorobenzene and chloroform. The UV-Vis and PL spectra are shown in **Figures 3.11, 3.12** and the data are summarised in **Table 3.6**.

UV-Vis spectra demonstrate clear bathochromic shifts of $\lambda_{abs}$ values (by 32 nm, from acetone to chlorobenzene fraction) for the **p(S-OC$_{12}$)** and **p(S-OC$_8$Me$_2$)** polymers (see **Table 3.6**, **Figure 3.11 a**), in accordance with the expected increase in molecular weights of the fractions from a "poor solvent" acetone to "good solvents" chloroform and chlorobenzene. However, a bigger bathochromic shift of $\lambda_{abs}$ values was observed (by 55 nm, and 60 nm, from the acetone to chlorobenzene fraction) for **p(S-OEtC$_6$/C$_8$)** and **p(S-OEtC$_8$/C$_{10}$)** polymers (see **Table 3.6**, **Figure 3.11 b**) which indicates better solubility of the branched alkyl substituted polymers compared to the linear ones. For the less soluble (and presumably higher molecular weight) chlorobenzene fraction, the UV-Vis spectra become structured indicating rigidification of the system (and possibly an aggregation of polymer chains).

PL spectra of the **p(S-OC$_{12}$)** and **p(S-OC$_8$Me$_2$)** polymer fractions show a bathochromic shift by 11 nm from the acetone to the chloroform fractions and then they remain almost unchanged for the chlorobenzene fraction (see **Table 3.6**, **Figure 3.11 a**).

However, for the **p(S-OEtC$_6$/C$_8$)** and **p(S-OEtC$_8$/C$_{10}$)** polymers, a bathochromic shift from the acetone ($\lambda_{PL}$ = 423 nm) to the chloroform fractions ($\lambda_{PL}$ = 434 nm) was observed and then a further shift ($\lambda_{PL}$ = 540 nm) to the chlorobenzene fractions (see **Figure 3.11 b**). Moreover, pronounced vibronically resolved PL spectra are observed for higher molecular weight fractions, a typical feature of rigid-rod conjugated polymers. Low solubility of the (presumably high molecular weight) polymers from the chlorobenzene fraction and the appearance of a structured feature in their absorption spectra might indicate an increased tendency of the dibenzothiophene-*S*,*S*-dioxide polymers to aggregation (compared to poly((dialkylfluorenes), which have good solubility in chloroform and toluene even for very high molecular weight polymers of $M_w$ > 300,000 Da).

As shown in **Table 3.6** and **Figures 3.12** there is no effect from the solvent polarity on the absorption and photoluminescence spectra when changing the solvent from chlorobenzene to chloroform. UV-Vis spectra demonstrate bathochromic shifts of $\lambda_{abs}$ values (by 33 nm, from the acetone to the chloroform fraction) for the **p(S-OMeC$_8$/C$_8$)** polymer see **Table 3.6**, in accordance with the expected increase in molecular weights from the acetone fraction to the chloroform fraction. PL spectra of **p(S-OMeC$_8$/C$_8$)** polymer fractions show a bathochromic shift by 8 nm from the acetone to chloroform fraction (**Figure 3.12**). Moreover, pronounced vibronically resolved PL spectra are observed for higher molecular weight fractions, a typical feature of rigid-rod conjugated polymers.

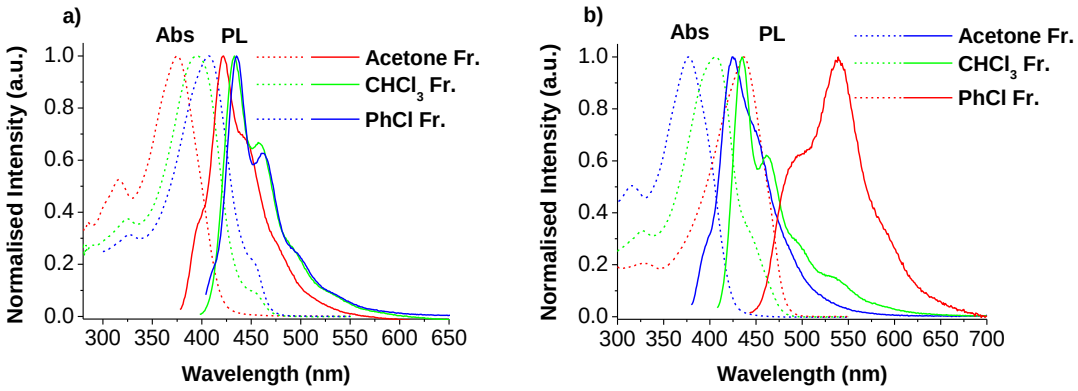


**Figure 3.11:** UV-Vis electron absorption and photoluminescence spectra of acetone, chloroform, and chlorobenzene fractions in chlorobenzene of a) polymers **p(S-OC$_{12}$)**. b) polymers **p(S-OEtC$_8$/C$_{10}$)**.

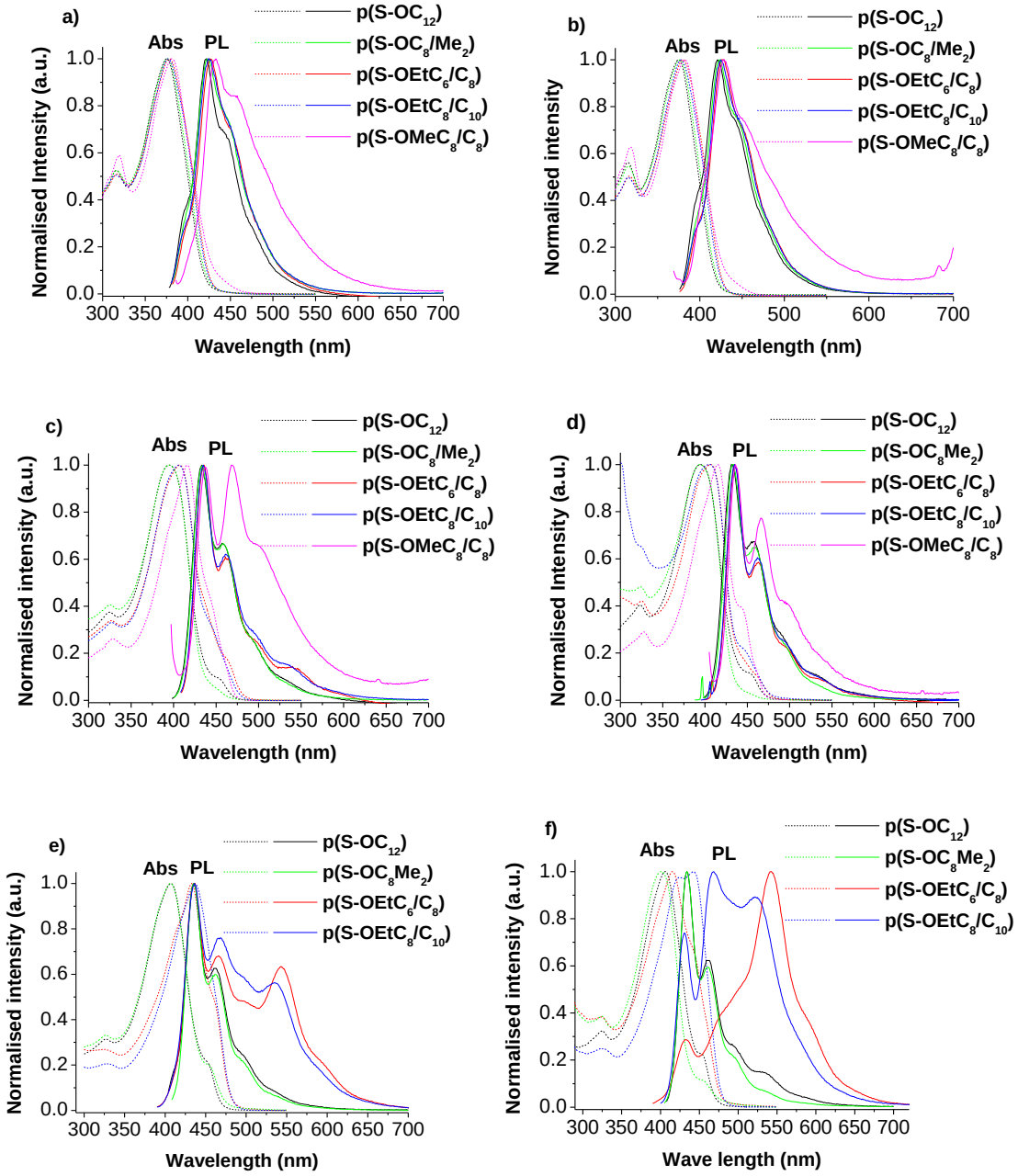


**Figure 3.12:** UV-Vis electron absorption and photoluminescence spectra of polymers **p(S-OR)** a) acetone fractions in chlorobenzene b) acetone fractions in chloroform c) $CHCl_3$ fractions in chlorobenzene d) $CHCl_3$ fractions in chloroform e) PhCl fractions in chlorobenzene f) PhCl fractions in chloroform.

**Table 3.6:** UV-Vis electron absorption ($\lambda_{abs}$), and photoluminescence ($\lambda_{PL}$) maxima of polymers **p(S-OR)** in chloroform and chlorobenzene solutions and PLQY (photoluminescence quantum yield) for acetone chloroform, and chlorobenzene fractions.

| Polymer fraction | Solvent[a] | Parameter | **p(S-OC$_{12}$)** [b,c,d] | **p( S-OC$_8$Me$_2$)** [b,c,d] | **p(S-OEtC$_6$/C$_8$)** [b,c,d] | **p(S-OEtC$_8$/C$_{10}$)** [b,c,d] | **p(S-OMeC$_8$/C$_8$)** [b,c,d] |
|---|---|---|---|---|---|---|---|
| Acetone | $CHCl_3$ | $\lambda_{abs}$ (nm) | 315, **375** | 315, **376** | 317, **380** | 315, **378** | 319, **382** |
| Acetone | PhCl | $\lambda_{abs}$ (nm) | 288, **375** | 286, **376** | 285, **378** | 286, **377** | 320, **381** |
| Acetone | $CHCl_3$ | $\lambda_{PL}$ (nm), *($\lambda_{exc}$)* nm | 400sh, **421**, 451sh, *(376)* | 395sh, **424**, 453sh, *(377)* | 395sh, **429**, 456sh, *(380)* | 393sh, **425**, 454sh, *(377)* | **429**, 459sh, *(382)* |
| Acetone | PhCl | $\lambda_{PL}$ (nm), *($\lambda_{exc}$)* nm | **422**, 437sh, *(375)* | **423**, 446sh, *(376)* | **426**, 447sh, *(379)* | **424**, 447sh, *(377)* | **433**, 453sh, *(381)* |
| Acetone | PhCl | $\Phi_{PL}^{abs}$ (%), *($\lambda_{exc}$)* nm | 93.8, *(375)* | 93.1, *(375)* | 93.4, *(390)* | 98.9, *(375)* | 61.0, *(381)* |
| Acetone | PhCl | CIE (x, y) | 0.15, 0.04 | 0.15, 0.05 | 0.15, 0.05 | 0.15, 0.05 | 0.16, 0.09 |
| $CHCl_3$ | $CHCl_3$ | $\lambda_{abs}$ (nm) | 324, **395** | 324, **393** | 325, **407** | 324, **405** | 328, **415**, sh450 |
| $CHCl_3$ | PhCl | $\lambda_{abs}$ (nm) | 324, **395** | 324, **394** | 325, **407** | 325, **406** | 328, **416** |
| $CHCl_3$ | $CHCl_3$ | $\lambda_{PL}$ (nm), *($\lambda_{exc}$)* nm | **433**, 459, 496sh, *(395)* | **433**, 459, 495sh, *(396)* | **435**, 463, 502sh, *(408)* | **435**, 462, 502sh, *(405)* | **436**, **466**, 505sh, *(415)* |
| $CHCl_3$ | PhCl | $\lambda_{PL}$ (nm), *($\lambda_{exc}$)* nm | **433**, 457, 505sh, *(395)* | **434**, 458, 505sh, *(396)* | **436**, 462, 500sh, 545sh, *(406)* | **435**, 461, 500sh, 540sh, *(405)* | **437**, **468**, 496sh, *(416)* |
| $CHCl_3$ | PhCl | $\Phi_{PL}^{abs}$ (%), *($\lambda_{exc}$)* nm | 97.9, *(400)* | 81.8, *(400)* | 94.4, *(400)* | 88.3, *(400)* | 54.7, *(416)* |
| $CHCl_3$ | PhCl | CIE (x, y) | 0.15, 0.06 | 0.15, 0.06 | 0.15, 0.06 | 0.15, 0.07 | 0.16, 0.15 |
| PhCl | $CHCl_3$ | $\lambda_{abs}$ (nm) | 326, **406** | 324, **401** | 325, **416** | 324, **443** | - |
| PhCl | PhCl | $\lambda_{abs}$ (nm) | 327, **407** | 326, **407** | 325, **433** | 327, **437** | - |
| PhCl | $CHCl_3$ | $\lambda_{PL}$ (nm), *($\lambda_{exc}$)* nm | **434**, 463, 490sh, 535sh, *(405)* | **434**, 462, 495sh, 530sh, *(402)* | **436**, 465, 500sh, 535sh, *(415)* | **528**, 494, *(444)* | - |
| PhCl | PhCl | $\lambda_{PL}$ (nm), *($\lambda_{exc}$)* nm | **435**, 463, 500sh, *(401)* | **436**, 463, 500sh, *(405)* | 480sh, **544**, 590sh, *(433)* | 490sh, **539**, 590sh, *(437)* | - |
| PhCl | PhCl | $\Phi_{PL}^{abs}$ (%), *($\lambda_{exc}$)* nm | 92.4, *(440)* | 90.3, *(410)* | 68.1, *(400)* | 79.8, *(400)* | - |
| PhCl | PhCl | CIE (x, y) | 0.15, 0.07 | 0.15, 0.07 | 0.17, 0.14 | 0.21, 0.53 | - |

[a]solvent which used for the measurements. [b]$\Phi_{PL}^{abs}$ is an absolute PLQY in chlorobenzene measured using an integrated sphere. [c]sh – Shoulder. [d]For PL measurements, the excitation wavelengths in Italic *($\lambda_{exc}$)*, and the bold numbers are the absorption maxima $\lambda_{abs}$.

The electron absorption spectra of 1-substituted **p(S-OR)** polymers in the solid state were also carried out for the acetone, chloroform, and chlorobenzene fractions (see **Figures 3.13, 3.14**). These demonstrated an absorption with peaks in the region of 383–435 nm, which can be assigned to the $\pi$-$\pi^*$ transition of delocalised electrons on the backbone of the polymer (**Figures 3.13, 3.14**), which is close to the typical region of polyfluorenes. When looking at the UV-Vis values for the acetone fractions, they are very uniform as they all share almost the exact same maxima $\lambda_{abs}$ value **Figure 3.13 a**. This could indicate that all polymers have the same or close molecular weights. In comparison to the chloroform fractions, there is a clear bathochromic shift of 26–36 nm (see **Figures 3.13 b**). The chlorobenzene fractions also show a red shift when compared to the acetone fractions by 38–49 nm (see **Figures 3.13 c**) in accordance with the expected increase in molecular weights of the fractions from a "poor solvent" acetone to "good solvents" chloroform and chlorobenzene. However, larger bathochromic shifts of $\lambda_{abs}$ values (by 46 nm, and 49 nm, from acetone to chlorobenzene fraction) were observed for the **p(S-OEtC$_6$/C$_8$)** and **p(S-OEtC$_8$/C$_{10}$)** polymers respectively (**Table 3.6**), which indicates better solubility of polymers with branched alkyl substituents compared to linear ones, as was proven by GPC measurements (see Section 3.2.2).

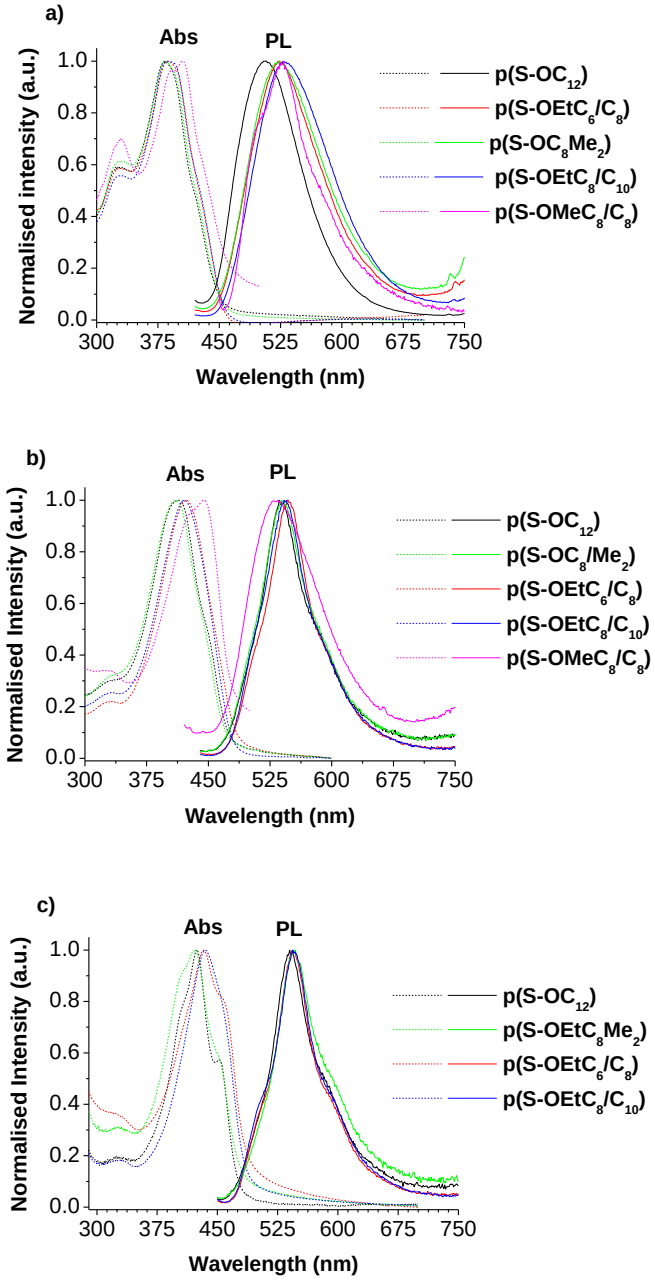


**Figure 3.13:** UV-Vis electron absorption and photoluminescence spectra of polymers **p(S-OR)** in the solid state a) acetone fractions b) $CHCl_3$ fractions c) PhCl fractions.

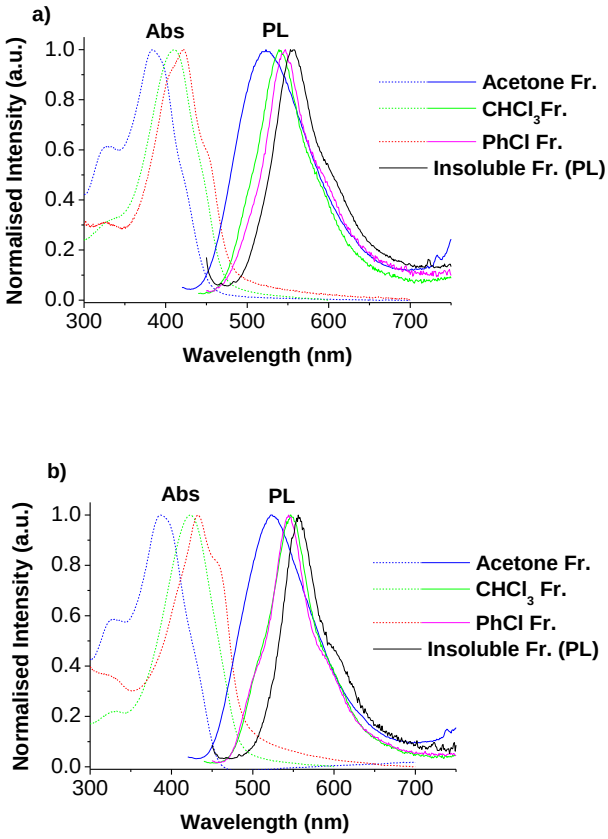


**Figure 3.14:** UV-Vis electron absorption and photoluminescence spectra in films of a) polymer fractions **p(S-OC$_8$Me$_2$)** b) polymer fractions **p(S-OEtC$_6$/C$_8$)**.

Surprisingly, the emission spectra of the 1-substituted **p(S-OR)** polymers in the solid state for the acetone, chloroform, and chlorobenzene fractions are in the green region with peaks in the region of 522–547 nm which was unexpected (see **Figures 3.13, 3.14**). The dibenzothiophene-*S*,*S*-dioxide unit is topographically similar to the fluorene unit, however polyfluorenes emit in the blue region in the solid state which we do not observe for 1-substituted polydibenzothiophene-*S*,*S*-dioxide. Moreover, their PL spectra (in films) do not show separate vibronic transitions, but some shoulders and non-symmetry of PL indicate weakly-resolved vibronics and a very pronounced bathochromic shift by ~115 nm compared to in solution. Thus, they emit in the blue region in solution and in the green yellowish region in the solid state as shown in the **Figure 3.15**. The reason for this phenomenon is not fully clear and requires more studies; in the next sections, this phenomenon will be investigated.

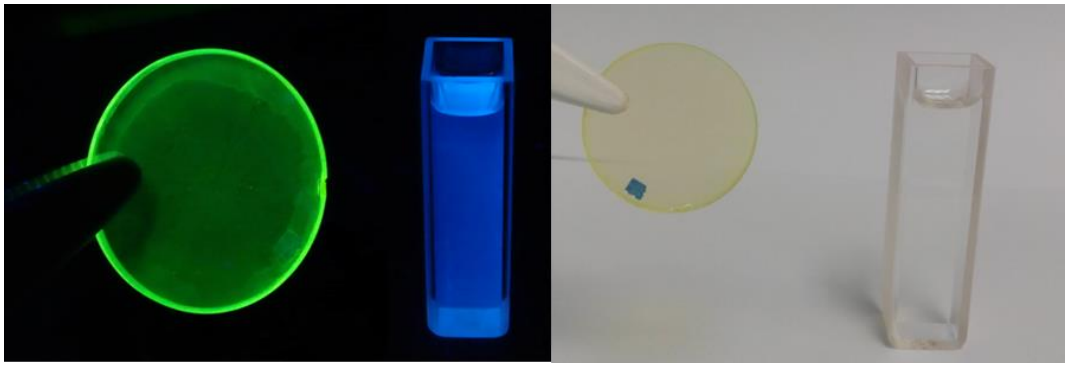

**a)** **b)**

**Figure 3.15:** Emission of **p(S-OEtC$_8$/C$_{10}$)** chloroform fraction in thin film and in chlorobenzene solvent. a) under UV-light irradiation (360 nm): b) under ambient light

**Table 3.7:** UV-Vis electron absorption ($\lambda_{abs}$), photoluminescence ($\lambda_{PL}$) maxima and PLQY for acetone, chloroform, and chlorobenzene fractions of polymers **p(S-OR)** in solid state.

| Polymer fraction | Parameter | **p(S-OC$_{12}$)**[a,b,c] | **p( S-OC$_8$Me$_2$)**[a,b,c] | **p(S-OEtC$_6$/C$_8$)**[a,b,c] | **p(S-OEtC$_8$/C$_{10}$)**[a,b,c] | **p(S-OMeC$_8$/C$_8$)**[a,b,c] |
|---|---|---|---|---|---|---|
| Acetone | $\lambda_{abs}$ (nm) | 326, **383** | 325, **384** | 326, **387** | 326, **386** | 332, **406** |
| Acetone | $\lambda_{PL}$ (nm), ($\lambda_{exc}$) nm. | **522**, *(383)* | **523**, *(384)* | **522**, *(387)* | **528**, *(386)* | **529**, *(406)* |
| Acetone | $\Phi_{PL}^{abs}$ (%), ($\lambda_{exc}$) nm. | 5.1, *(383)* | 11.3, *(384)* | 12.2, *(387)* | 11.6, *(386)* | 10.8, *(406)* |
| Acetone | CIE (x, y) coordinates, film | 0.18, 0.51 | 0.23, 0.53 | 0.22, 0.56 | 0.25, 0.57 | 0.29, 0.60 |
| $CHCl_3$ | $\lambda_{abs}$ (nm) | 326, **412** | 327, **410** | 326, **423** | 326, **420** | 335sh, **444** |
| $CHCl_3$ | $\lambda_{PL}$ (nm), ($\lambda_{exc}$) nm. | **536**, *(412)* | **539**, *(410)* | **546**, *(423)* | **545**, *(420)* | **535**, *(444)* |
| $CHCl_3$ | $\Phi_{PL}^{abs}$ (%), ($\lambda_{exc}$) nm. | 19.1, *(412)* | 15.0, *(410)* | 28.5, *(423)* | 30.3, *(420)* | 26.5, *(444)* |
| CHCL3 | CIE (x, y) coordinates, film | 0.29, 0.61 | 0.30, 0.61 | 0.32, 0.61 | 0.31, 0.62 | 0.25, 0.58 |
| PhCl | $\lambda_{abs}$ (nm) | 324, **425**, 452, 411sh | 324, **422**, 409sh, 461sh | 322, **433**, 483sh | 323, **435** | - |
| PhCl | $\lambda_{PL}$ (nm), ($\lambda_{exc}$) nm. | **540**, *(425)* | **547**, *(422)* | **544**, *(433)* | **544**, *(435)* | - |
| PhCl | $\Phi_{PL}^{abs}$ (%), ($\lambda_{exc}$) nm. | 19.3, *(425)* | 14.9, *(422)* | 20.9, *(433)* | 30.2, *(435)* | - |
| PhCl | CIE (x, y) coordinates, film | 0.30, 0.62 | 0.32, 0.62 | 0.31, 0.62 | 0.31, 0.61 | - |

[a]$\Phi_{PL}^{abs}$ is an absolute PLQY in film measured using an integrated sphere. [b]sh – Shoulder. [c]For PL measurements, the excitation wavelengths in Italic ($\lambda_{exc}$), and the bold numbers are the absorption or emitting maxima $\lambda_{abs}$, $\lambda_{PL}$.

### 3.2.7 Explanation of the huge bathochromic shifts from blue light (in solution) to green light (in the solid state) of PL spectra for 1-alkoxydibenzothiophene-*S,S*-dioxide homopolymers p(S-OR)

The first soluble homopolymers were synthesised by a Yamamoto coupling reaction of dibenzothiophene-*S,S*-dioxide by substituting long liner and branched alkoxy chains at the 1- **p(S-OR)** as shown in **Scheme 3.2**. It was observed that **p(S-OR)** homopolymers absorb light in the region of around $\lambda_{abs}$ = 381–409 nm in solution (**Figure 3.12**) typically like polyfluorene ($\lambda_{abs}$ = 380–390 nm). Moreover, in solid state they show absorption peaks in the region of ($\lambda_{abs}$ = 396–421 nm) (**Figure 3.13**).

The photoluminescence spectra of **p(S-OR)** homopolymers in solution showed emission in the blue region ($\lambda_{PL}$ = 423–447 nm), which is typical for polyfluorene. However, a clear bathochromic shift showed a change in the solid state by ~ 115 nm ($\lambda_{PL}$ = 523–562 nm) (see **Figure 3.15**), which does not consign with the polyfluorene results. Therefore, to understand this phenomenon, many experiments were carried out as will be discussed in the next pages.

#### 3.2.7.1 Investigation of two new series of dibenzothiophene-*S,S*-dioxide homopolymers p(S-SR), and p(S-$SO_2$R)

Initially, it was believed that the red shift was due to intramolecular charge transfer (ICT) between the donating group (alkoxy **OR**) at the 1- position and the electron withdrawing group (-$SO_2$-) which forms a bridge between the two phenyl rings of the **p(S-OR)** homopolymers. This ICT state showed a clear appearance in the solid state and a very weak signal in solution. Therefore, it was decided to synthesise more homopolymers with different substituents at the 1- position (**SR, $SO_2$R**) (**Scheme 3.2**), using the same procedure, as was used for the synthesis of the **p(S-OR)** polymers.

The absorption spectra of **p(S-OEt$C_8$/$C_{10}$)**, **p(S-SEt$C_8$/$C_{10}$)** and **p(S-$SO_2$Et$C_8$/$C_{10}$)** in solution and thin films are shown in **Figures 3.16 a-d**. The polymers showed bathochromic shifts in their absorption spectra from 397 to 409 nm. This could be due to the charge-transfer character of the absorption, see **Figure 3.16 a**. However, no obvious changes in the PL spectra were noted in **Figure 3.16 b**. In contrast to its solid state, there was a small

red shift in absorption, however, all homopolymer films emitted in the region of 520–533 nm, see **Tables 3.8, 3.9**. The absorption spectra of **p(S-$SO_2C_{12}$)** and **p(S-$SC_{12}$)** from solution and solid state showed absorption peaks in the region from 382–396 nm and 402–416 nm, see **Tables 3.8, 3.9** (**Figure 3.16 e-f**). These homopolymers are blue emitting in solution when between the range of 425–462 nm and green emitting in thin films when between the range of 523–562 nm, see **Figure 3.16** and **Tables 3.8, 3.9**.

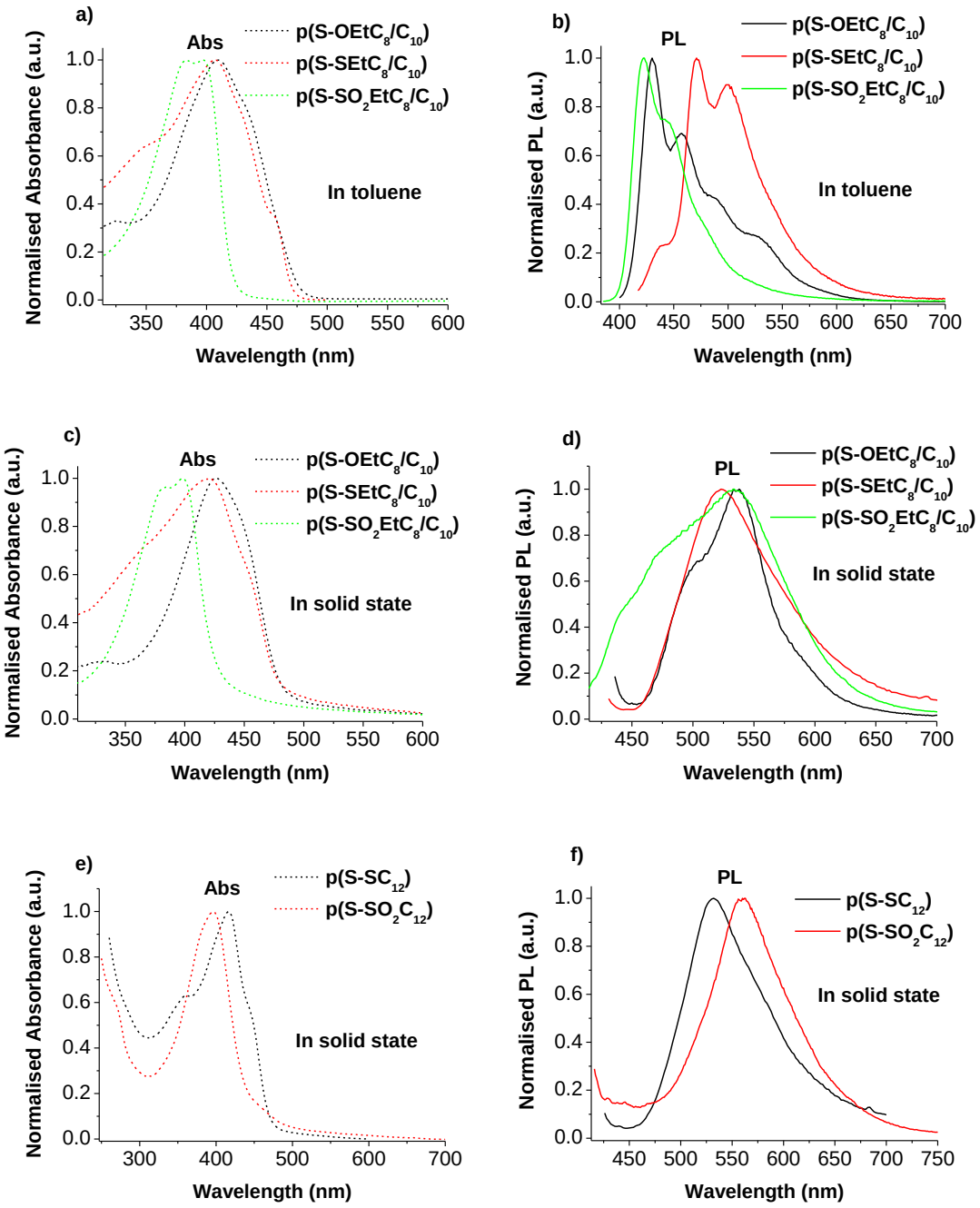


**Figure 3.16:** UV-Vis and PL spectra of **p(S-R)** homopolymers in toluene solution (a-b) and in the solid state (c–f). The excitations for PL spectra ($\lambda_{exc}$) are at the corresponding maxima of the absorption spectra.

**Figure 3.17** shows the electron absorption, emission and excitation spectra of **p(S-SO2EtC8/C10)** in chloroform and in the solid state, which demonstrates the same bathochromic shift from blue to green, as was seen for the **p(S-OR)** polymers. Even with having the **SO2R** group (EWG) at the 1-position this huge red shift by ~ 115 nm can be

observed. Therefore, from **Figures 3.16, 3.17**, we can conclude that this red shift is not due to charge transfer (CT) between the alkoxy group at the 1-position and the sulfonyl group. Another supposition was raised that this bathochromic shift was due to the polarity of the polymer structure and to clarify that more photophysical studies in different solvents were done as shown in the next section.

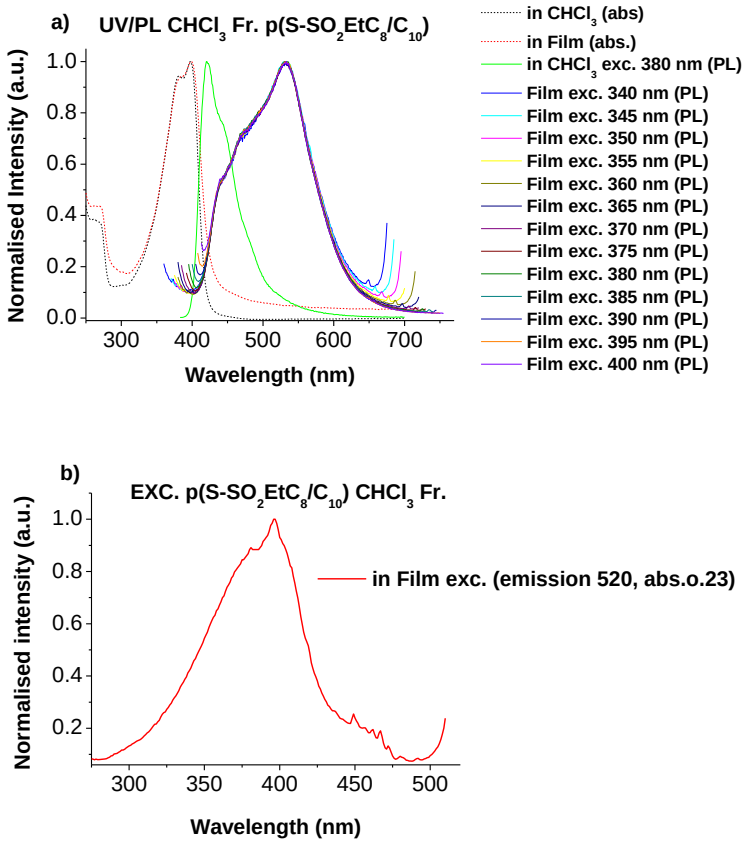


**Figure 3.17:** a) UV-Vis electron absorption and photoluminescence spectra of chloroform fraction in chloroform and film of **p(S-SO2EtC8/C10)**. b) Excitation spectrum in film using emission at 520 nm.

### 3.2.7.2 Solvent polarity effect on absorption and PL spectra of 1-substituted p(S-R)

Further studies were carried out because of the assumptions that this bathochromic shift was due to the polarity of the polymer. The UV and PL characterisation of **p(S-R)** in different solvent polarity (toluene (ε = 2.38), chloroform (ε = 4.81), chlorobenzene (ε = 5.62), and benzonitrile (ε = 25.20) were used to investigate this supposition. As shown in **Figure 3.18** there was almost no change in red shift with a change in solvent polarity. Small

bathochromic shifts were observed in both the UV (2–11 nm) and PL (4–11 nm) spectra whilst maintaining the same vibronic structure (**Table 3.8**). This could be due to the polarity of the excited state as it is more polar than the ground state. To conclude, it is difficult to say, from this experiment, whether the solid state bathochromic shifts of ~ 115 nm are due to the polarity of the polymers.

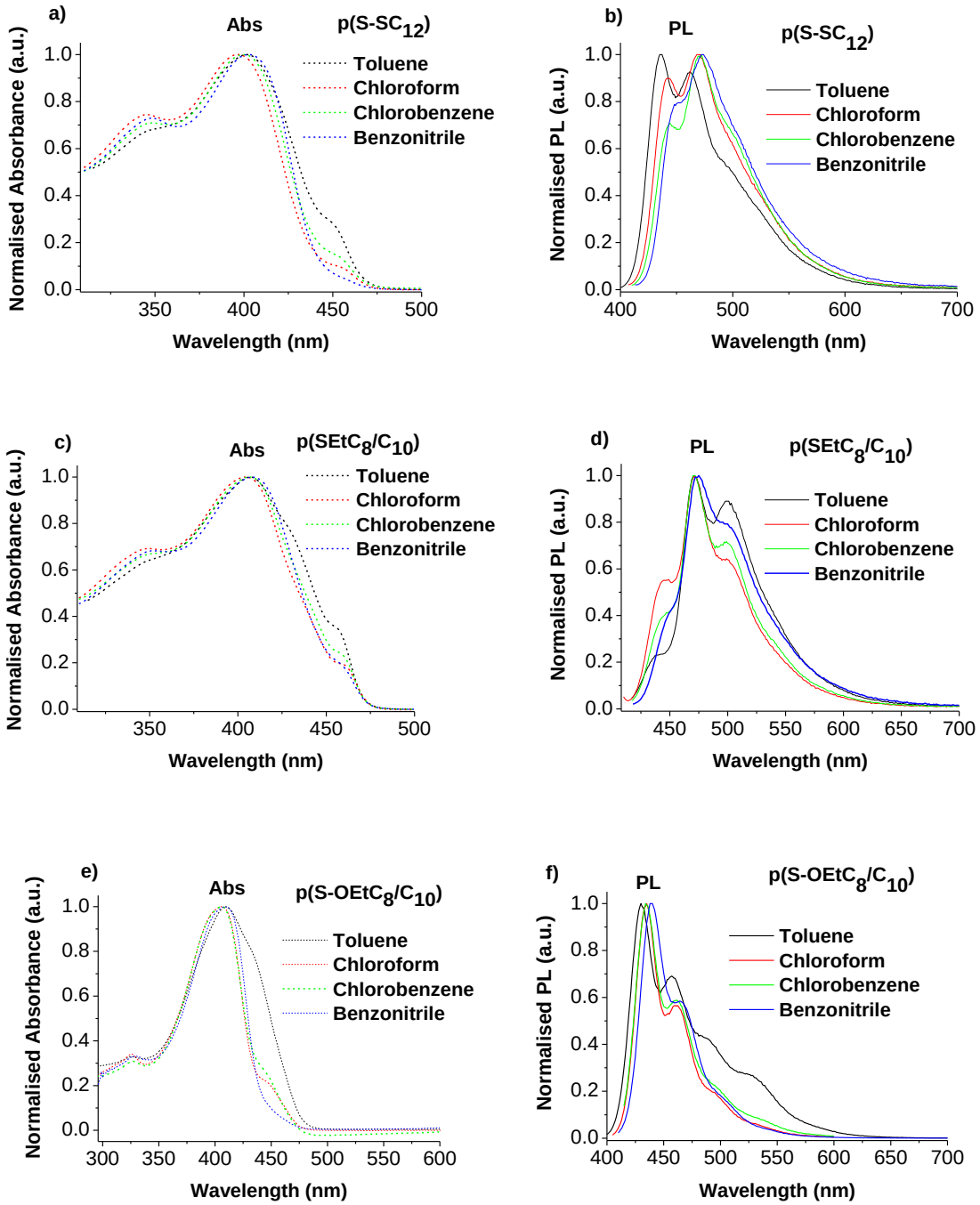

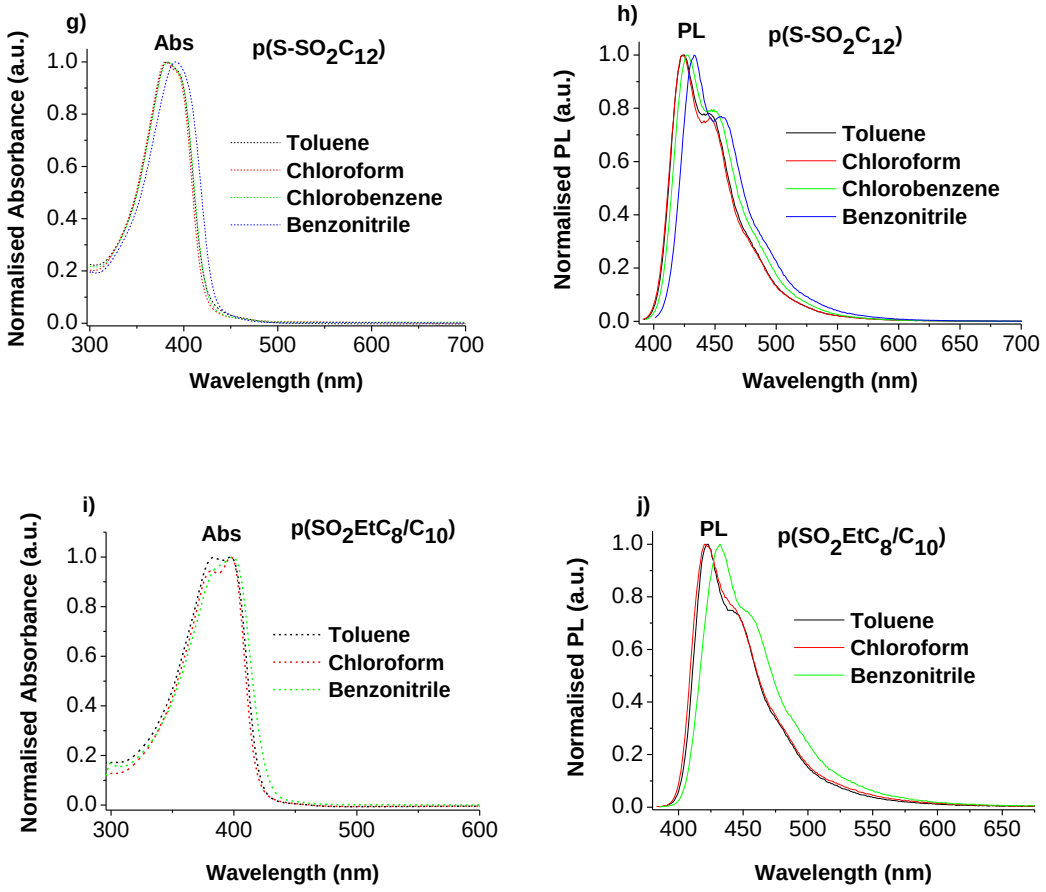


**Figure 3.18:** Solvent effects on UV-Vis absorption and PL spectra of 1-substituted dibenzothiophene-*S*,*S*-dioxide homopolymers **p(S-R)**. The excitations for PL spectra ($\lambda_{exc}$) are at the maxima of the absorption spectra.

UV/PL measurements for **p(S-OR)** chlorobenzene fractions in different solvents was also carried out. **Figure 3.19 b, c** show a clear hypsochromic shift from green (in toluene) to blue (in benzonitrile) emission and actually these blue shifts are not due to the polarity of the solvents but only due to the solubility of the polymer chains. The chlorobenzene fraction polymers have higher molecular weights than the chloroform fractions and it seems that these polymers are more soluble in benzonitrile compared to toluene. **Figure 3.19 c** shows that the **p(S-OEtC$_8$/C$_{10}$)** polymer emits green light in toluene in the same region as the solid state, this may be due to nano aggregation because of poor solubility. Actually, this result is in agreement with what has previously been regarding the huge bathochromic shift from solution to solid state.

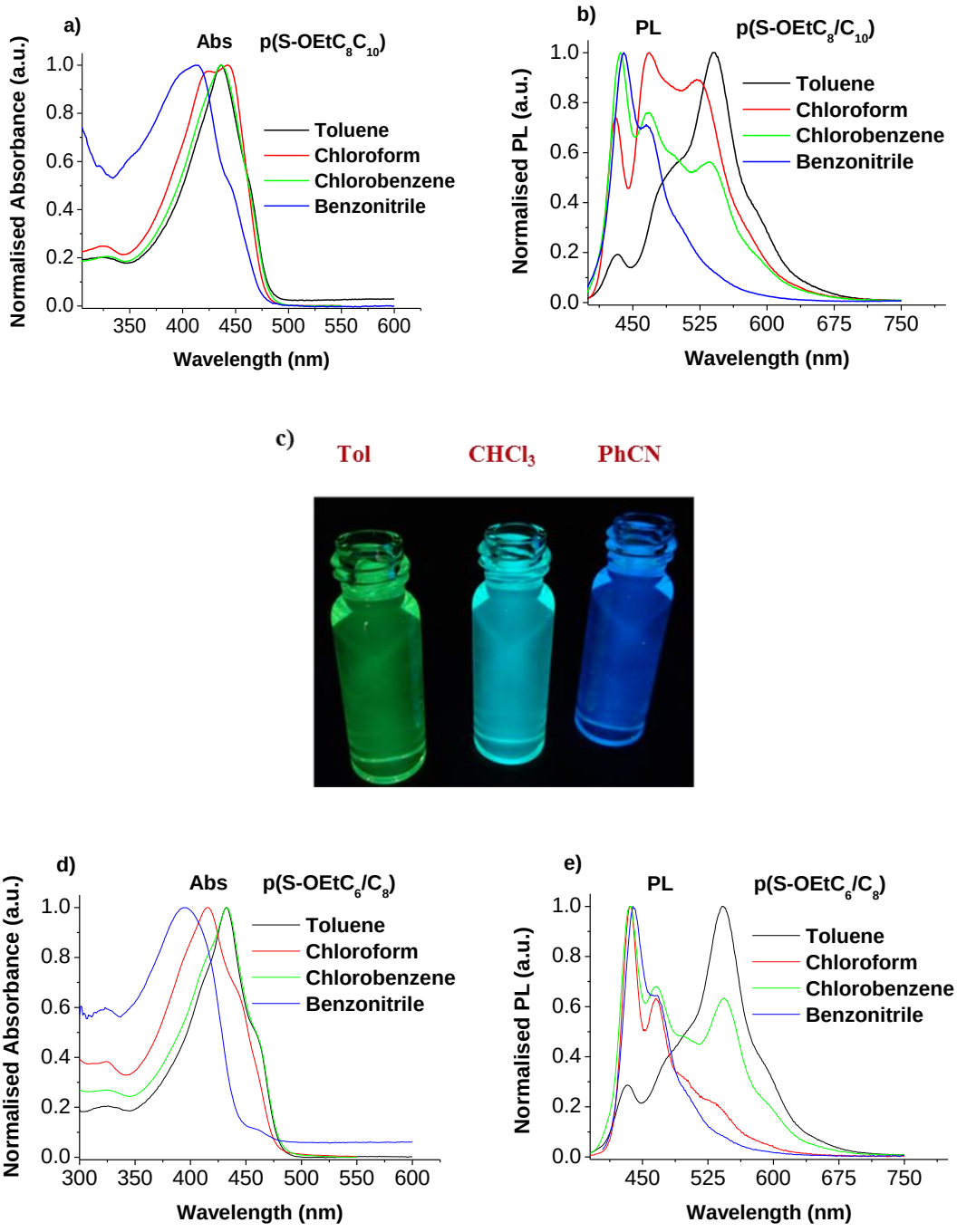


**Figure 3.19:** a), d) UV-Vis electron absorption b), e) photoluminescence spectra, of chlorobenzene fractions in different solvents of **p(S-OEtC8/C10)** and **p(S-OEtC6/C8)** homopolymers respectively. c) Emission of polymer **p(S-OEtC8/C10)** chlorobenzene fraction in Tol, $CHCl_3$, and PhCN from left to right under UV-light irradiation (360 nm).

**Table 3.8:** Absorption and photoluminescence spectral data for **p(S-SC$_{12}$), p(S-SEtC$_8$/C$_{10}$), p(S-OEtC$_8$/C$_{10}$), p(S-SO$_2$C$_{12}$), p(S-SO$_2$EtC$_8$/C$_{10}$)** homopolymers in different solvents.

| **Polymer** | $\lambda_{abs}$ (nm)[a,b] Tol | $\lambda_{abs}$ (nm)[a,b] $CHCl_3$ | $\lambda_{abs}$ (nm)[a,b] PhCl | $\lambda_{abs}$ (nm)[a,b] PhCN | $\lambda_{PL}$ (nm), ($\lambda_{exc}$) (nm)[a,b,c] Tol | $\lambda_{PL}$ (nm), ($\lambda_{exc}$) (nm)[a,b,c] $CHCl_3$ | $\lambda_{PL}$ (nm), ($\lambda_{exc}$) (nm)[a,b,c] PhCl | $\lambda_{PL}$ (nm), ($\lambda_{exc}$) (nm)[a,b,c] PhCN |
|---|---|---|---|---|---|---|---|---|
| **p(S-SC$_{12}$)** | (345sh), **402,** (450sh) | (344 sh),**397**, (455 sh) | (346sh),**400 ,**(451sh) | (347sh),**403** | 436, **462,**(*402*) | 442, **470**,(*397*) | 442, **472**,(*400*) | 450sh, **473**,(*403*) |
| **p(S-SEtC$_8$/C$_{10}$)** | (350sh), **407,** (457sh) | (348sh), **405**, (461sh) | (350sh)**, 406**, (459sh) | (350sh), **407,** (460sh) | 438, **471**, 500sh (*407*) | 445, **471**, 500sh, (*405*) | 447sh, **472**, 500sh, (*406*) | 450, **475**, 500sh, (*407*) |
| **p(S-OEtC$_8$/C$_{10}$)** | **409**, (450sh) | **406**, (448sh) | **406**, (449sh) | **409** | **430,** (457sh, 490sh, 530sh) **,**(*409*) | **435**, (463sh), (*406*) | **434**, (461sh) **,**(*406*) | **439**, (468sh) **,**(*409*) |
| **p(S-SO$_2$C$_{12}$)** | **382**, (394 sh) | **381**, (394 sh) | **383** (395 sh) | **392** | **425**, (448sh) **,**(*382*) | **423**, (446 sh) **,**(*409*) | **427** ,(453 sh),(*409*) | **433**, (456 sh)**,**(*409*) |
| **p(S-SO$_2$EtC$_8$/C$_{10}$)** | 384, **397** | 380, **398** | - | (385sh) **399,** | **423**, (442sh), **,**(*397*) | **421**, (444sh) **,**(*398*) | - | **432**, (457sh), **,**(*399*) |

[a] sh–Shoulders. [b] Bold numbers are the strongest absorption or emission peaks. [c] Excitation wavelengths used for PL measurements ($\lambda_{exc}$) are given in italic in brackets.

**Table 3.9:** CIE and $\Phi_{PL}^{abs}$ (%) spectral data for **p(S-R)** homopolymers in chlorobenzene solution and solid state. $\lambda_{abs}$ and $\lambda_{PL}$ for **p(S-R)** homopolymers in solid state.

| **Polymer** | CIE (x, y) PhCl | $\Phi_{PL}^{abs}$ (%) PhCl | $\lambda_{abs}$ (nm)[a,b] | $\lambda_{PL}$ (nm), ($\underline{\lambda_{exc}}$) (nm)[a,b,c] | CIE (x, y) film | $\Phi_{PL}^{abs}$ (%) film |
|---|---|---|---|---|---|---|
| **p(S-SC$_{12}$)** | 0.15, 0.16 | 47.1% | 358, **416,** 444sh | **532**, (*416*) | 0.28, 0.66 | 12% |
| **p(S-SEtC$_8$/C$_{10}$)** | 0.14, 0.17 | 51.1% | 356, **421**, 455sh | **523**, (*421*) | 0.25, 0.58 | 15% |
| **p(S-SO$_2$C$_{12}$)** | 0.15, 0.07 | 80.8% | **396** | **562,** (*396*) | 0.45, 0.54 | 6.1% |
| **p(S-SO$_2$EtC$_8$/C$_{10}$)** | 0.16, 0.08 | 58.8% | 382, **398** | 437,470, **533,** (*398*) | 0.27, 0.44 | 12.4% |

[a] sh–Shoulders. [b] Bold numbers are the strongest absorption or emission peaks. [c] Excitation wavelengths used for PL measurements ($\underline{\lambda_{exc}}$) are given in italic in brackets.

### 3.2.7.3 Thermal annealing studies of homopolymers

Fortunately, it was thought that this large red shift in the solid state was caused by the packing and organisation of the monomer units within the polymer chains. To prove this, annealing studies were carried out at temperatures between 80 °C and 260 °C monitoring the change of their absorption and PL spectra (in film) with time intervals (heating 30 min). In these experiments, we were trying to keep the polymer film in a Teflon holder during all the measurements to avoid misinterpretation of the results to analyse the effect on the UV and PL spectra of **p(S-SO$_2$EtC$_8$/C$_{10}$)**, **p(S-SEtC$_8$/C$_{10}$)** and **p(S-OEtC$_8$/C$_{10}$)** in the solid state, see **Figure 3.20 a-f**, to observe at what temperature the homopolymers decomposed. It showed that these polymers were thermally stable up to 220 °C. The homopolymers were fluorescent until 220 °C, which indicates the decomposition of the polymer. The thermal annealing of **p(S-SO$_2$EtC$_8$/C$_{10}$)**, **p(S-SEtC$_8$/C$_{10}$)**, and **p(S-OEtC$_8$/C$_{10}$)** films showed almost no change in their absorption spectra, see **Figure 3.20 a, c, e**.

**Figure 3.20 b** shows the PL spectra of the **p(S-SO$_2$EtC$_8$/C$_{10}$)** polymer after annealing at different temperatures, and it shows a broad unsymmetrical peak with a shoulder in the blue region at room temperature. The amplitude of the shoulder gradually decreases as the temperature is increased and the PL shoulders for **p(S-SO$_2$EtC$_8$/C$_{10}$)** disappeared after 120 °C and the PL spectra showed red shifts of 533–556 nm, see **Figure 3.20 b**. Actually, this study is quite interesting because it gives a key to explain the huge bathochromic shifts of the dibenzothiophene-*S*,*S*-dioxide homopolymers PL spectrum from

solution to the solid state. Therefore, at room temperature when the polymer chains are not packed and organized, there is some emission in the blue region (shoulder) and with an increase in the temperature due to the flexibility of the polymer chains, they become more ordered. At temperature of +160 °C the PL spectrum becomes narrow and featureless and is shifted to the green region. To conclude, it seems that these homopolymers emit in the blue region but in the solid state when all the polymer chains are packed together there is some loss of the energy due to a non-radiative process. This might be the reason for the disappearance of the shoulder in the spectrum shown in **Figure 3.20 b** with an increase in the temperature.

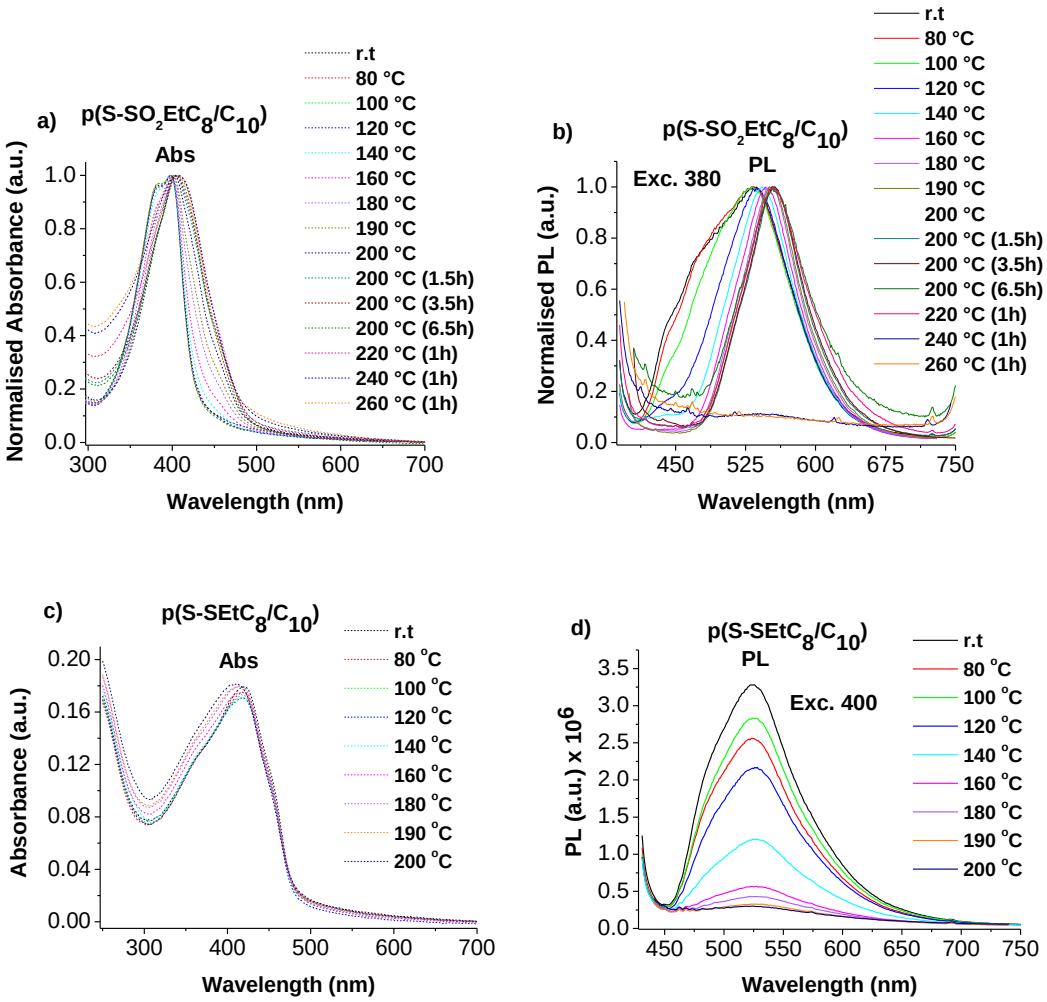

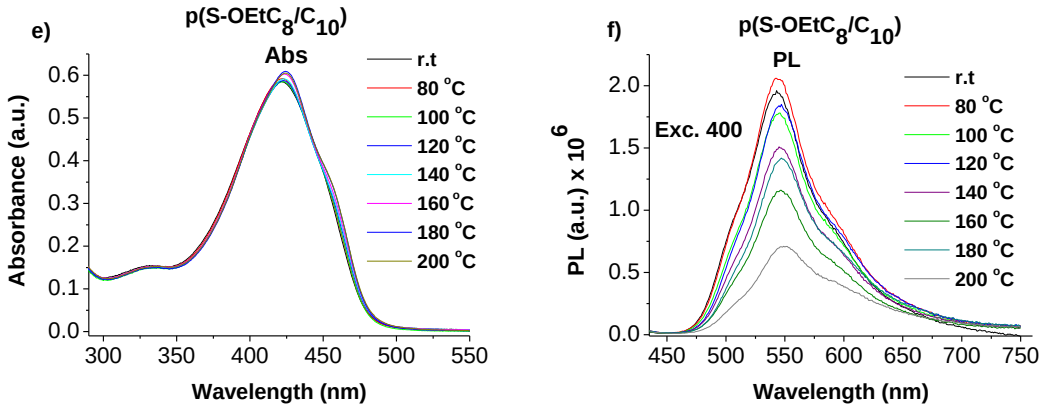


**Figure 3.20:** Effect of different temperatures on a) UV-Vis absorption b) PL spectra of **p(S-SO$_2$EtC$_8$/C$_{10}$)**, c) UV-Vis absorption d) PL spectra of **p(S-SEtC$_8$/C$_{10}$)**, e) UV-Vis absorption f) PL spectra of **p(S-OEtC$_8$/C$_{10}$)** polymers. The excitations for PL spectra ($\lambda_{exc}$) are at the maxima of the absorption spectra ($\lambda_{max}$). Graphs (a,b) showing the normalised, and (c-f) showing the normal spectra in thin films. Annealing was carried out at range of 80 – 260 °C.

As the temperature increased there was a clear decrease in emission intensities, see **Figure 3.20 d, f**. The annealing studies of **p(S-SEtC$_8$/C$_{10}$)** and **p(S-OEtC$_8$/C$_{10}$)** showed small bathochromic shifts in the UV and PL spectra with broadening towards the green region in the PL spectrum, see **Figure 3.20**. This could be due to the polymer chains being reordered at a higher temperature. Part of the investigation was to look at why there was a decreased intensity of the PL spectra of **p(S-SEtC$_8$/C$_{10}$)** and **p(S-OEtC$_8$/C$_{10}$)** during annealing. Possible reasons for this were polymer decomposition or solid state quench emission. The PL spectra of the **p(S-OEtC$_8$/C$_{10}$)** film showed a gradual decrease in emission intensities as the duration increased, see **Figure 3.20 f**. The thermal annealing of **p(S-OEtC$_8$/C$_{10}$)** showed almost no change in its absorption spectra, see **Figure 3.20 e**. At room temperature, the maximum of the PL spectra was at 538 nm, and as the temperature increased it got red shifted by 5 nm. However, after annealing and once the film was remade, the PL was blue shifted to 529 nm (**Figure 3.21 b**). The full methodology of film formation is shown in the experimental section. This is clear evidence that the polymer does not decompose but it is only solid state quench emission that is observed.

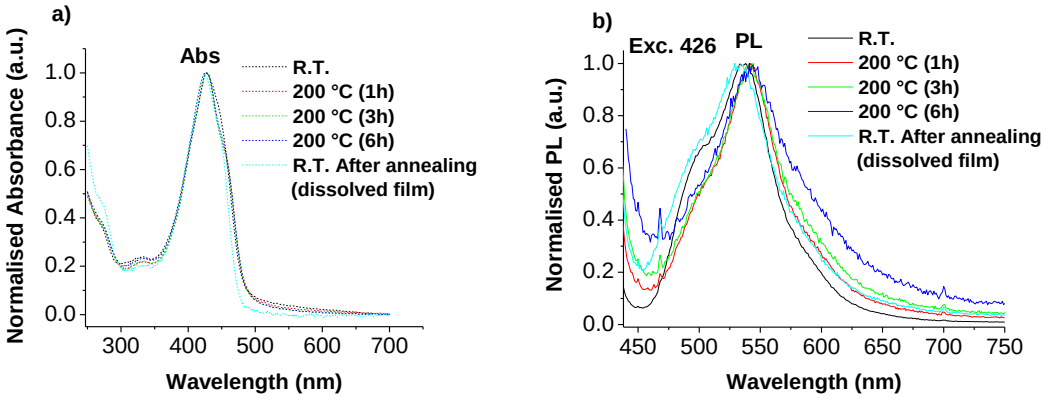


**Figure 3.21:** Annealing on UV-Vis absorption (a) and photoluminescence spectra (b) of **p(S-OEtC$_8$/C$_{10}$)** polymers. The excitations for PL spectra ($\lambda_{exc}$) are at the maximum of the absorption spectra ($\lambda_{max}$). Graphs showing the normalised spectra in thin films. Annealing was carried out at 200 °C.

A comparison of the **p(S-OEtC$_8$/C$_{10}$)** homopolymer in solution before and after annealing was carried out at room temperature (see **Figure 3.22**). Both UV and PL show the same spectra structure before and after annealing. This is further evidence about the stability of these polymers. Experiment carried out by measuring the homopolymer under room temperature, followed by sample being put in the oven at 200 °C and then measured again when it is cooled down.

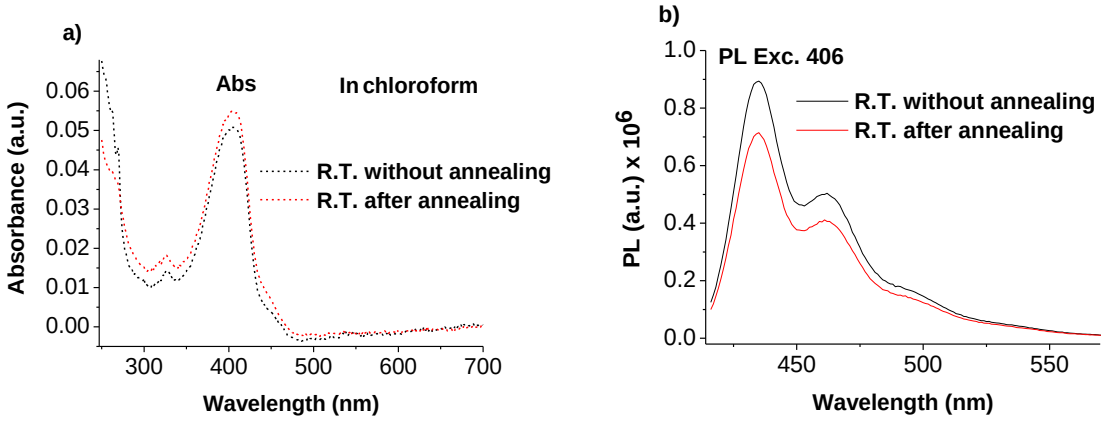


**Figure 3.22:** a) Annealing on UV-Vis absorption and b) PL spectra of **p(S-OEtC$_8$/C$_{10}$)** polymers. The excitations for PL spectra ($\lambda_{exc}$) are at the maximum of the absorption spectra ($\lambda_{max}$). Graphs showing the actual measurements in chloroform solutions.

### 3.2.8 Photoluminescence quantum yields (PLQY) of p(S-R) homopolymers

The acetone, chloroform, and chlorobenzene fractions of **p(S-R)**, show bright blue emission in solution and green light in the solid state as demonstrated in previous sections. Estimating their photoluminescence quantum yields (PLQY, $\Phi_{PL}$) in solution by an absolute method in chlorobenzene by using an integrated sphere and all polymer fractions demonstrate very high PLQY values of $\Phi_{PL}^{abs}$ ~ 68–99% (**Table 3.6**) comparable to the values reported in the literature for other polyfluorenes.[42,43] Solid state PLQY has been measured for spin coated films on a quartz substrate (from chloroform solution) for all fractions by an absolute method using an integrating sphere. The values are expectedly lower (as is usual for solid state PLQY compared to the solution) but still reasonably high, 5–30% see **Table 3.7, 3.9**. Acetone fractions gave the lowest PLQY between 5-12% but chloroform and chlorobenzene fractions demonstrate higher values 15-30% (values of 25–40% are reported in the literature for many 9,9-disubstituted polyfluorenes).[42,43]

### 3.3 Conclusion

The first soluble dibenzothiophene-*S*,*S*-dioxide homopolymers with various electron-donating and electron-withdrawing alkyl groups have been successfully synthesised by using a Ni-mediated coupling polymerisation method. Extractions of the homopolymers display part solubility in chloroform with average yields of ~25%. They showed excellent thermal stabilities ($T_d$ = 380–388 °C). Cyclic voltammetry studies of polymer films showed that they can be electrochemically oxidised and reduced (p-doped and n-doped) and from their redox potential onsets, the HOMO and LUMO energies of these polymers have been estimated (HOMO = –6.31 to –5.98 eV, LUMO = –3.86 to –3.47 eV). DFT calculations at the B3LYP/6-31G(d) level of theory have been performed for model 1-substituted polydibenzothiophene-*S*,*S*-dioxide (from 1 to 20 repeating dibenzothiophene-*S*,*S*-dioxide units). The HOMO and LUMO energy levels derived for 1-substituted polydibenzothiophene-*S*,*S*-dioxide, fit well with the CV data showing the pronounced effect of the substitution at the 1- position on the frontier orbital energies of polydibenzothiophene-*S*,*S*-dioxide.

These novel homopolymers are highly fluorescent, displaying clear blue-light emission with absorption and emission studies in chlorobenzene solutions ($\lambda_{abs}$ = 380–420 nm, $\lambda_{PL}$ = 425–435 nm). Solid-state emission of these homopolymers exhibits a shift to a highly fluorescent greenish-yellow colour. A variety of experiments were carried out to see why there was such a big red shift between the solution and solid state. The initial thoughts were that it was due to the polarity effect but upon further analysis it became apparent that it was the result of a vibronic effect only. Annealing experiments were carried out to investigate whether the results of the experiment were due to the reorganisation of the polymer chain. The experiment showed that it is thermally stable and that it does in fact red shift with an increase in temperature.

Finally, as we only managed to obtain ~25% chloroform soluble polymer material, there is still potential to further investigate and improve the solubility of these 1-substituted dibenzothiophene-*S*,*S*-dioxide homopolymers, perhaps by incorporating longer branched alkyl chains, which could lead to the use of these electron deficient polymers as major building blocks in conjugated polymer materials.

## 3.4 Experimental Section

### 3.4.1 Chemicals and instruments

All the solvents and commercial chemicals, which were used without further purifications, were supplied from Aldrich, Fisher, Acros, AlfaAesar, and Apollo Scientific chemical companies. Dry solvents for water-sensitive reactions or measurements were either commercially dry solvents or were been dried in a still (reflux over Na for THF and toluene). Details on $^{1}$H NMR measurements are the same as mentioned in Chapter 2.

### 3.4.2 GPC measurements

The polymers weight average molecular weights ($M_w$), number average molecular weights ($M_n$) and polydispersity indices (PDI) were measured on a Varian PL-GPC 50 plus gel permeation chromatograph (GPC) at room temperature in THF solution with calibration of the column by polystyrene standards. In a typical procedure, the polymer sample in THF (3 mg/mL) was stirred for 24 hrs until full dissolution, filtered through a 0.2 μm membrane filter and used for GPC analysis.

### 3.4.3 Thermogravimetry analysis (TGA)

The thermal stabilities of polymers (5–7 mg samples) were measured by thermogravimetric analysis (TGA). When measuring the TGA on TA-SDT-Q600 instrument, the solid polymer was used. A small crucible was filled with ~5 mg of the solid polymer and was heated at 10 ºC/min from ambient temperature to 800 ºC. The decomposition temperatures ($T_d$) of the samples were estimated at the level of 5% mass loss.

### 3.4.4 Computational procedures

DFT computations of the geometries of studied 1-substituted poly (dibenzothiophene-*S*,*S*-dioxide) were carried out with the Gaussian 09 package[44] of programs using Pople's 6-31G split valence basis set supplemented by d-polarization functions and diffusion functions for the heavy atoms. Becke's three parameter hybrid exchange functional[45,46] with the Lee–

Yang–Parr gradient-corrected correlation functional (B3LYP)[47] were employed. The restricted Hartree-Fock formalism was used and calculations were performed for the isolated molecules in the gas phase. No constraints of bonds/angles/dihedral angles were applied in the calculations and all the atoms were free to optimise. Generally, for decreasing the time of calculations, the first optimisation was performed for the longest oligomers (n = 16–20), then shorter oligomer structures have been generated by removal of one to "n–1" dibenzothiophene-*S*,*S*-dioxide moieties and obtained structures have been used as input <*.gjf> files for the re-optimisation. Thus, the geometries of all oligomers were optimised at the B3LYP/6-31G(d) level of theory and the electronic structures were calculated at the same level of theory for the estimation of frontier orbital energies (HOMO and LUMO). The treatment of the calculated data and plotting the graphs of energies versus the size of the molecules were done with Origin Pro7.0 software.

### 3.4.5 Cyclic voltammetry

The cyclic voltammetry experiments of the polymer films were taken using a Metrohm Autolab PGSTAT-302N potentiostat/galvanostat. The measurements have been done on three electrodes in spectroscopic grade acetonitrile (dry acetonitrile for CV reduction measurements) with a supporting electrolyte of 0.1 M $Bu_4NPF_6$ and a reference electrode of $Ag/Ag^+$ (0.01 M $AgNO_3$ with 0.1 M $Bu_4NPF_6$ in dry acetonitrile). A polymer thin film was formed on the end of the glassy carbon working electrode (d = 2 mm). A solution was made up of 5 mg/mL for each of the polymers. The polymer solution was applied dropwise and then dried *in vacuo* to evaporate any and all solvent left in order to form a solid film. The measurements were done at ambient temperature under an argon atmosphere using a scan rate of 100 mV/s. A background was taken initially and then the polymer was measured along with ferrocene as a control for all of the measurements. The potentials measured versus Ag/Ag+ were then calibrated against ferrocene/ferrocenium redox couple (Fc/Fc+) as an internal standard, and recalculated to Fc/Fc+ scale.

### 3.4.6 Electron absorption and photoluminescence spectra measurements

UV-Vis electron absorption spectra were recorded on a Shimadzu UV-3600 spectrophotometer in 10 mm quartz cells in different solvents at ambient temperature. For

measurements of UV-Vis spectra the concentrations were prepared to give an absorbance in the range of ~0.6–1.0 a.u.

Photoluminescence spectra were recorded on a Horiba Jobin Yvon Fluoromax-4 spectrofluorimeter. Solution measurements for PL were performed in fluorescence 10 mm path length quartz cells in chlorobenzene or chloroform. The samples were excited at their longest wavelength absorption maxima ($\lambda_{max}$) or 10–20 nm below those values. Typical concentrations of solutions for PL measurements were ~0.05–0.1 a.u.

Data analysis and graphical representations of the results of spectral measurements were performed using Origin Pro 7.0 or 8.5 softwares.

### 3.4.7 Spin-coating of polymer films for UV-Vis and PL studies

Programmed spin coater Laurell Technologies model WS-650Mz-23NPP/LITE was used for polymer thin films preparation (in air). Thin polymer films were prepared by spin-coating from chloroform solutions. The concentrations of *ca.* 1.0 mg/mL were for the absorption spectra measurements to have optical densities of the samples of ~0.2–0.6 a.u. The same films were used to measure the PL. Thin films were prepared from these solutions by dropping their solutions on d = 12.5 or 25 mm quartz ring windows placed on the spin-coater and rotating at 3000 rpm for 30 seconds. After that, the polymer films were dried in vacuo (~20–50 μbar) for 0.5–2 h before the measurements.

### 3.4.8 Photoluminescence quantum yields (PLQY) measurements

Measurements of absolute PLQY values in the solution and solid state were done using an integrating sphere Horiba F-3018 on Horiba Jobin Yvon Fluromax-4 spectrofluorimeter. For solution measurements, the concentrations were verified between OD ~ 0.02-0.1 a.u. while for solid state, the film thickness for these measurements was varied to have OD ~ 0.2–0.6 a.u. The integrated sphere was tested by measuring the PLQY for standard compounds such as 9,10-diphenylanthracene (DPA) (PLQY = 90%), and anthracene (PLQY = 27%).[48,49] The $\lambda_{max}$ from the UV measurement was used for the excitation value during the experiment. An empty/blank cell was used for the reference in all measurements. Values given were in a specific range for each fraction.

### 3.4.9 Thermal annealing experiments

Homopolymers **p(S-OEtC$_8$/C$_{10}$)**, **p(S-SEtC$_8$/C$_{10}$)** and **p(S-SO$_2$EtC$_8$/C$_{10}$)** films were made by spin coating from the chloroform solution. The film has been prepared by dropping the solution on d = 12.5 or 25 mm quartz ring windows in a spin coater and rotating it for 3000 rpm for 30 seconds. The films were then placed in a preheated oven at 80, 100, 120, 140, 160, 180, 190, 200, 220, 240, 260 °C at 30 minute intervals. During the intervals, they were measured by UV-Vis and PL characterisation to track the absorbance and emission of light. The film was kept in a Teflon holder during all the measurements to decrease the percentage of error.

### 3.4.10 Synthesis

**Parallel synthesis of poly(1-R-dibenzothiophene-*S*,*S*-dioxides) p(S-R) on Radleys Carousel Reaction Station 12+**

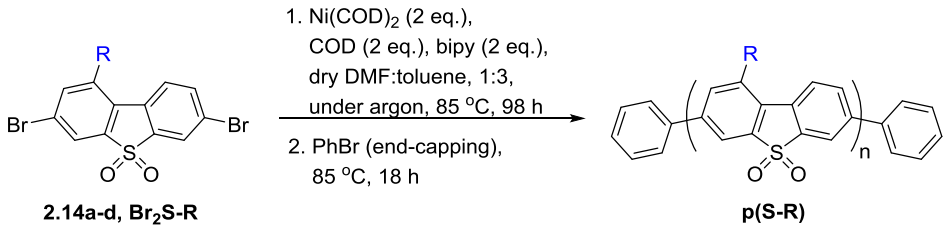


**2.14a-d, Br$_2$S-R** **p(S-R)**

**p(S-OC$_{12}$)** R = 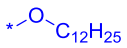

**p(S-OC$_8$Me$_2$)** R = 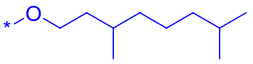

**p(S-OEtC$_6$/C$_8$)** R = 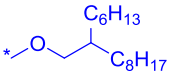


**p(S-OEtC$_8$/C$_{10}$)** R = 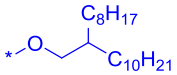


**p(S-OMeC$_8$/C$_8$)** R = 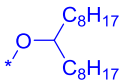


**p(S-SC$_{12}$)** R = 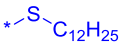

**p(S-SEtC$_8$/C$_{10}$)** R = 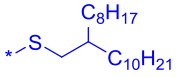


**p(S-SO$_2$C$_{12}$)** R = 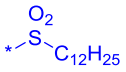

**p(S-SO$_2$EtC$_8$/C$_{10}$)** R = 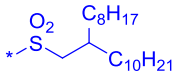


**p(S-OC$_{12}$), p(S-OC$_8$Me$_2$), p(S-OEtC$_6$/C$_8$), p(S-OEtC$_8$/C$_{10}$), p(S-OMeC$_8$/C$_8$), p(S-SC$_{12}$), p(S-SEtC$_8$/C$_{10}$), p(S-SO$_2$C$_{12}$), p(S-SO$_2$EtC$_8$/C$_{10}$)** homopolymers were produced on the same scale. Under an argon atmosphere, 8 reactions of *bis*(1,5-cyclooctadiene)nickel(0),

$Ni(COD)_2$ (550 mg, 2.00 mmol), 1,5-cyclooctadiene (216 mg, 2.00 mmol), and 2,2'-bipyridyl (312 mg, 2.00 mmol) in dry DMF (4.0 mL) were stirred at 85 °C for 1 hour to form a dark violet coloured solution. To this solution the dibromo monomer (0.558 g, 0.530 g, 0.614 g, 0.671 g, 0.629 g, 0.574 g, 0.606, 0.719 g, 1 mmol) in dry toluene (10 mL) was added slowly and the mixture was stirred at 85 °C for 98 hours. Then bromobenzene (3 drops) was added as an end capper and the mixture was stirred for an additional 18 hours.

The solvent was evaporated, and the residue was dissolved in a minimal amount of chloroform and transferred dropwise into a solution of acetone:methanol:HCl conc. 1:1:1 (150 mL) to form a precipitate. The precipitate was then filtered off washed with a minimal amount of water and methanol and was then dried under vacuum. The solid was extracted using soxhlet extraction in methanol for 24 h. The methanol was then removed and replaced with acetone and left to extract for 24 h and the process was then repeated using chloroform, then chlorobenzene. Each polymer fraction was collected separately after solvent evaporation. When the extractions were finished, there was still some solid insoluble material left in the extraction thimble.

**p(S-SEtC$_8$/C$_{10}$),** was produced by the same method using *bis*(1,5-cyclooctadiene)nickel(0) $Ni(COD)_2$ (0.825 g, 3mmol), 5-cyclooctadiene (0.325 g, 3 mmol), 2,2'-bipyridyl (0.469 g, 3 mmol), dry DMF (6 mL), dibromo monomer (1.030 g, 1.5 mmol) and dry toluene (18 mL).

**Table 3.9** The results of extractions

| Homopolymer | Acetone fraction[a] | Chloroform fraction[a] | Chlorobenzene fraction[a] | Insoluble fraction |
|---|---|---|---|---|
| **p(S-OC$_{12}$)** | 51 mg (12.8%) | **113 mg (28.3%)** | 32 mg (8.0%) | 120 mg, (30.0%) |
| **p(S-OC$_8$Me$_2$)** | 90 mg (24.3%) | **74 mg, (19.9%)** | 6 mg (1.6%) | 117 mg (31.5%) |
| **p(S-OEtC$_6$/C$_8$)** | 206 mg ( 45.3%) | **95 mg (20.9%)** | 6 mg (0.6%) | 76 mg (17.0%) |
| **p(S-OEtC$_8$/C$_{10}$)** | 142 mg (27.8%) | **127 mg (24.9%)** | 4 mg (0.8%) | 173 mg (33.9%) |
| **p(S-OMeC$_8$/C$_8$)** | 70 mg, 15 % | **145 mg, (30.9%)** | 3 mg (0.6%) | 0 |
| **p(S-SC$_{12}$)** | 115 mg (28%) | **60 mg (14.4%)** | 3 mg (0.7%) | 85 (20%) |
| **p(S-SEtC$_8$/C$_{10}$)** | 49 mg (6%) | **413 mg (52%)** | 5 mg (0.6%) | 202 mg (25%) |
| **p(S-SO$_2$C$_{12}$)** | 30 mg (6.7%) | **45 mg (10.1%)** | 17 mg (3.8%) | 320 mg (71%) |

| | | | | |
|---|---|---|---|---|
| **p(S-$SO_2EtC_8/C_{10}$)** | 30 mg, (5.4%) | **159 mg, (28.4%)** | 13 mg (2.3%) | 343 mg (61.4%) |

[a]Extraction time was ~ 24 h.

## References


1 A. Mishra, C. Ma, and P. Bauerle, Functional Oligothiophenes: Molecular Design for Multidimensional Nanoarchitectures and Their Applications, *Chem. Rev.*, **2009**, *109*, 1141–1276. DOI: 10.1021/cr8004229

2 A. J. Blayney, I. F. Perepichka, F. Wudl, and D. F. Perepichka, Advances and Challenges in the Synthesis of Poly(*p*-phenylene vinylene)-Based Polymers, *Isr. J. Chem.*, **2014**, 54, 674–688. DOI: 10.1002/ijch.201400067

3 A. C. Grimsdale, K. L. Chan, R. E. Martin, P. G. Jokisz, and A. B. Holmes, Synthesis of Light-Emitting Conjugated Polymers for Applications in Electroluminescent Devices, *Chem. Rev.* **2009**, *109*, 897–1091. DOI: 10.1021/cr000013v

4 Y. Olivier, D. Niedzialek, V. Lemaur, W. Pisula, K. Müllen ,U. Koldemir, J. R. Reynolds, R. Lazzaroni, J.Cornil, and D. Beljonne, High-Mobility Hole and Electron Transport Conjugated Polymers: How Structure Defines Function, *Adv. Mater.*, **2014**, *26*, 2119–2136. DOI: 10.1002/adma.201305809

5 J. Choi, K.-H. Kim, H. Yu, C. Lee, H. Kang, I. Song, Y. Kim, J. H. Oh, and B. J. Kim, Importance of Electron Transport Ability in Naphthalene Diimide Based Polymer Acceptors for High-Performance, Additive-Free, All Polymer Solar Cells, *Chem. Mater.*, **2015**, *27*, 5230−5237. DOI: 10.1021/acs.chemmater.5b01274

6 J. Choi, H. Song, N. Kim, and F. S. Kim, Development of n-type polymer semiconductors for organic field-effect transistors, *Semicond. Sci. Technol.*, **2015**, *30*, 1–16. DOI: 10.1088/0268-1242/30/6/064002

7 H. Chen, M. Nikolka, A. Wadsworth, W. Yue, A. Onwubiko, M. Xiao, A. J. P. White, D. Baran, H. Sirringhaus, and I. McCulloch, A Thieno[*2,3*‑*b*]pyridine-Flanked Diketopyrrolopyrrole Polymer as an n‑Type Polymer Semiconductor for All-Polymer Solar Cells and Organic Field-Effect Transistors, *Macromolecules*, **2018**, *51*, 71–79. DOI: 10.1021/acs.macromol.7b00934

8 F. Mariano, M. Mazzeo, Y. Duan, G. Barbarella, L. Favaretto, S. Carallo, R. Cingolani, and G. Gigli, Very low voltage and stable *p–i–n* organic light-emitting diodes using a linear *S,S*-dioxide oligothiophene as emitting layer, *Appl. Phys. Lett.*, **2009**, *94*, 1–3. DOI: 10.1063/1.3072798

9 W. Li, L. Yan, H. Zhou, and W. You, A General Approach toward Electron Deficient Triazole Units to Construct Conjugated Polymers for Solar Cells, *Chem. Mater.*, **2015**, *27*, 6470–6476. DOI: 10.1021/acs.chemmater.5b03098

10 C. Arbizzani, G. Barbarella, A. Bongini, L. Favaretto, M. Mastragostino, P. Ostoja, O. Pudova, and M. Zambianchi, Oligothiophene-*S,S*-dioxides: towards n-type semiconductor oligothiophenes?, *Optical Materials*, **1998**, *9*, 43–45. DOI: 10.1016/S0925-3467(97)00064-5

11 G. Barbarella, L. Favaretto, G. Sotgiu, M. Zambianchi, A. Bongini, C. Arbizzani, M. Mastragostino, M. Anni,| G. Gigli,| and R. Cingolani, Tuning Solid-State Photoluminescence Frequencies and Efficiencies of Oligomers Containing One Central Thiophene-*S,S*-dioxide Unit, *J. Am. Chem. Soc.* **2000,** *122*, 11971–11978. DOI: 10.1021/ja002037p

12 E. Tedesco, B. M. Kariuki, K. D. M. Harris, R. L. Johnston, O. Pudova, G. Barbarella, E. A. Marseglia, G. Gigli, and R. Cingolani, Structural Aspects of High-Efficiency Blue-Emitting 2,5-Bis(trimethylsilyl)thiophene-*S,S*-dioxide and Related Materials, *Journal of Solid State Chemistry*, **2001**, *161*, 121–128. DOI:10.1006/jssc.2001.9298

13 N. Camaioni, G. Ridolfi, V. Fattori, L. Favaretto, and G. Barbarella, Oligothiophene-*S,S*-dioxides as a class of electron-acceptor materials for organic Photovoltaics, *Appl. Phys. Lett.*, **2004**, *84*, 1901–1903. DOI: 10.1063/1.1682681

14 C. Vijayakumar, A. Saeki, and S. Seki, Optoelectronic Properties of Dicyanofluorene-Based n-Type Polymers, *Chem. Asian J.*, **2012**, *8*, 1845–1852. DOI: 10.1002/asia.201200082

15 I. I. Perepichka, I. F. Perepichka, M. R. Bryce, and L.-O. Pälsson, Dibenzothiophene-*S,S*-dioxide–fluorene co-oligomers. Stable, highly-efficient blue emitters with improved electron affinity, *Chem. Commun.*, **2005**, 3397–3399. DOI: 10.1039/b417717g

16 C. Li, Y. Wang, D. Sun, H. Li, X. Sun, D. Ma, Z. Ren, and S. Yan, Thermally Activated Delayed Fluorescence Pendant Copolymers with Electron- and Hole-Transporting Spacers, *ACS Appl. Mater. Interfaces*, **2018**, *10*, 5731−5739. DOI: 10.1021/acsami.8b00136

17 F. Yang, K. Sun, Z. J. Cao, Z. Hui Li, and M. S. Wong, Synthesis and functional properties of oligofluorenyl-dibenzothiophene-*S,S*-dioxides end-capped by diphenylamine moieties, *Synth. Metals*, **2008**, *158*, 391–395. DOI: 10.1016/j.synthmet.2008.02.012

18 S. Fujii, Z. Duan, T. Okukawa, Y. Yanagi, A. Yoshida, T. Tanaka, G. Zhao, Y. Nishioka, and H. Kataura, Synthesis of novel thiophenephenylene oligomer derivatives with a dibenzothiophene-5,5-dioxide core for use in organic solar cells, *Phys. Status Solidi*, **2012**, *B249*, 2648–2651. DOI: 10.1002/pssb.201200439

19 F. B. Dias, K. N. Bourdakos, V. Jankus, K. C. Moss, K. T. Kamtekar, V. Bhalla, J. Santos, M. R. Bryce, and A. P. Monkman, triplet harvesting with 100% efficiency by way of thermally activated delayed fluorescence in charge transfer OLED emitters, *Adv. Mater.*, **2013**, *25*, 3707–3714. DOI: 10.1002/adma.201300753

20 X. Zhan, Z. Wu, Y. Lin, S. Tang, J. Yang, J. Hu, Q. Peng, D. Ma, Q. Lia, and Z. Li, New AIEgens containing dibenzothiophene-*S,S*-dioxide and tetraphenylethene moieties: similar structures but very different hole/electron transport properties, *J. Mater. Chem. C*, **2015**, *3*, 5903–5909. DOI: 10.1039/c5tc01028d

21 C. Fan, C. Duan, Y. Wei, D. Ding, H. Xu, and W. Huang, dibenzothiophene-based phosphine oxide host and electron-transporting materials for efficient blue thermally activated delayed fluorescence diodes through compatibility optimization, *Chem. Mater.*, **2015**, *27*, 5131−5140. DOI: 10.1021/acs.chemmater.5b02012

22 T. Yamamoto, Ni-catalyzed dehalogenation polycondensation of dihaloaromatic compounds with NaH, *Macromol. Chem. Phys.*,**1997** *198*,341–351.

23 M. Kreyenschmidt, G. Klaerner, T. Fuhrer, J. Ashenhurst, S. Karg, W. D. Chen, V. Y. Lee, J. C. Scott, and R. D. Miller, thermally stable blue-light-emitting copolymers of poly(alkylfluorene), *Macromolecules*, **1998**, *31*, 1099–1103.

24 G. Klaerner, and R. D. Miller, Polyfluorene derivatives: effective conjugation lengths from well-defined oligomers, *Macromolecules*, **1998**, *31*, 2007–2009.

25 G. Klärner, J.-I. Lee, V. Y. Lee, E. Chan, J.-P. Chen, A. Nelson, D. Markiewicz, R. Siemens, J. C. Scott, and R. D. Miller, Cross-linkable polymers based on dialkylfluorenes, *Chem. Mater.*, **1999**, *11*, 1800–1805. DOI: 10.1021/cm990027l

26 D. Marsitzky, J. Murray, J. C. Scott, and K. R. Carter, Amorphous poly-2,7-fluorene networks, *Chem. Mater.*, **2001**, *13*, 4285–4289. DOI: 10.1021/cm010282h

27 C. Ego, D. Marsitzky, S. Becker, J. Zhang, A. C. Grimsdale, K. Müllen, J. D. MacKenzie, C. Silva, and R. H. Friend, Attaching perylene dyes to polyfluorene: three simple, efficient methods for facile color tuning of light-emitting polymers, *J. Am. Chem. Soc.*, **2003**, *125*, 437–443. DOI: 10.1021/ja0205784

28 J. Jacob, S. Sax, T. Piok, E. J. W. List, A. C. Grimsdale, and K. Müllen, Ladder-type pentaphenylenes and their polymers: efficient blue-light emitters and electron-accepting materials via a common intermediate, *J. Am. Chem. Soc.*, **2004**, *126*, 6987–6995. DOI: 10.1021/ja0398823

29 F. Dierschke, A. C. Grimsdale, K. Müllen, Novel carbazole-based ladder-type polymers for electronic applications, *Macromol. Chem. Phys.*, **2004**, *205*, 1147–1154. DOI: 10.1002/macp.200300219

30 M. Heeney, C. Bailey, M. Giles, M. Shkunov, D. Sparrowe, S. Tierney, W. Zhang, and I. McCulloch, *Macromolecules*, **2004**, *37*, 5250–5256. DOI: 10.1021/ma049798n

31 G. Tu, C. Mei, Q. Zhou, Y. Cheng, Y. Geng, L. Wang, D. Ma, X. Jing, and F. Wang, Highly efficient pure-white-light-emitting diodes from a single polymer: polyfluorene with naphthalimide moieties, *Adv. Funct. Mater.*, **2006**, *16*, 101–106. DOI: 10.1002/adfm.200500028

32 C. Mei, G. Tu, Q. Zhou, Y. Cheng, Z. Xie, D. Ma, Y. Geng, L. Wang, Green electroluminescent polyfluorenes containing 1,8-naphthalimide moieties as color tuner, *Polymer*, **2006**, *47*, 4976–4984. DOI:10.1016/j.polymer.2006.03.085

33 S. K. Lee, T. Ahn, N. S. Cho, J.-I. Lee, Y. K. Jung, J. Lee, H. K. Shim, Synthesis of new polyfluorene copolymers with a comonomer containing triphenylamine units and their applications in white-light-emitting diodes, *J. Polym. Sci., Pt A: Polym. Chem.*, **2007**, *45*, 1199–1209. DOI: 10.1002/pola.21892

34 F. Galbrecht, T. W. Bünnagel, U. Scherf, T. Farrell, microwave-assisted preparation of semiconducting polymers, *Macromol. Rapid Commun.*, **2007**, *28*, 387–394. DOI: 10.1002/marc.200600778

35 T. Yamamoto, R. Tokimitsu, T. Asao, T. Iijima, H. Fukumoto, T.-A. Koizumi, T. Fukuda, H. Ushijima, π -Conjugated polymers consisting of 9,10-dihydrophenanthrene units, *Macromol. Chem. Phys.*, **2011**, *212*, 2406−2416. DOI: 10.1002/macp.201100310

36 W.-J. Li, B. Liu, Y. Qian, L.-H. Xie, J. Wang, S.-B. Li, and W. Huang, Synthesis and characterization of diazafluorene-based oligofluorenes and polyfluorene, *Polym. Chem.*, **2013**, *4*, 1796–1802. DOI: 10.1039/c2py20971c

37 G. Klaerner, and R. D. Miller, polyfluorene derivatives: effective conjugation lengths from well-defined oligomers, *Macromolecules,* **1998**, *31*, 2007–2009. DOI: 10.1021/ma971073e

38 E. Wang, C. Li, Y. Mo, Y. Zhang, G. Ma, W. Shi, J. Peng, W. Yang, and Y. Cao, Poly(3,6-silafluorene-co-2,7-fluorene)-based high-efficiency and color-pure blue light-emitting polymers with extremely narrow band-width and high spectral stability, *Mater. Chem.*, **2006**, *16*, 4133–4140. DOI: 10.1039/B609250K

39 C. M. Cardona, W. Li, A. E. Kaifer, D. Stockdale, and G. C. Bazan, Electrochemical Considerations for Determining Absolute Frontier Orbital Energy Levels of Conjugated Polymers for Solar Cell Applications, *Adv. Mater*., **2011**, *23*, 2367–2371. DOI: 10.1002/adma.201004554

40 W. Yang, J. Huang, C. Liu, Y. Niu, Q. Hou, R. Yang, and Y. Cao, Soluble eggshell membrane protein: Preparation, characterization and biocompatibility, *Polymer*, **2004**, *45*, 865–872. DOI: 10.1016/j.polymer.2003.11.052

41 X. Gong, P. K. Iyer, D. Moses, G. C. Bazan, A. J. Heeger, and S. S. Xiao, Stabilized blue emission from polyfluorene-based light-emitting diodes: elimination of flourenone defects, *Adv. Funct. Mater.*, **2003**, *13*, 325–330. DOI: 10.1002/adfm.200304279

42 S. Kommanaboyina, Conjuated Polymers Based on 4-Substituted Fluorenes and Fluorenones, PhD Thesis, Bangor University, **2016**.

43 C. Xia, and R. C. Advincula, Decreased Aggregation Phenomena in Polyfluorenes by Introducing Carbazole Copolymer Units, *Macromolecules*, **2001**, *34*, 5854–5859. DOI: 10.1021/ma002036h

44 Gaussian 09, Revision **E.01**, M. J. Frisch, G. W. Trucks, H. B. Schlegel, G. E. Scuseria, M. A. Robb, J. R. Cheeseman, G. Scalmani, V. Barone, B. Mennucci, G. A. Petersson, H. Nakatsuji, M. Caricato, X. Li, H. P. Hratchian, A. F. Izmaylov, J. Bloino, G. Zheng, J. L. Sonnenberg, M. Hada, M. Ehara, K. Toyota, R. Fukuda, J. Hasegawa, M. Ishida, T. Nakajima, Y. Honda, O. Kitao, H. Nakai, T. Vreven, J. A. Montgomery, Jr., J. E. Peralta, F. Ogliaro, M. Bearpark, J. J. Heyd, E. Brothers, K. N. Kudin, V. N. Staroverov, R. Kobayashi, J. Normand, K. Raghavachari, A. Rendell, J. C. Burant, S. S. Iyengar, J. Tomasi, M. Cossi, N. Rega, J. M. Millam, M. Klene, J. E. Knox, J. B. Cross, V. Bakken, C. Adamo, J. Jaramillo, R. Gomperts, R. E. Stratmann, O. Yazyev, A. J. Austin, R. Cammi, C. Pomelli, J. W. Ochterski, R. L. Martin, K. Morokuma, V. G. Zakrzewski, G. A. Voth, P. Salvador, J. J. Dannenberg, S. Dapprich, A. D. Daniels, Ö. Farkas, J. B. Foresman, J. V. Ortiz, J. Cioslowski, and D. J. Fox, Gaussian, Inc., Wallingford CT, **2009**.

45 A. D. Becke, Density-functional exchange-energy approximation with correct asymptotic behavior, *Phys. Rev. A*, **1988**, *38*, 3098–3100. DOI: org/10.1103/PhysRevA.38.3098

46 A. D. Becke, Density-functional thermochemistry. The role of exact exchange *J. Chem. Phys.*, **1993**, *98*, 5648–5652. DOI: 10.1063/1.464913

47 C. Lee, W. Yang, and R. G. Parr, Development of the Colle-Salvetti correlation-energy formula into a functional of the electron density, *Phys. Rev. B*, **1988**, *37*, 785–789. DOI: org/10.1103/PhysRevB.37.785

48 Yvon, and Horiba Jobin, A guide to recording fluorescence quantum yields, *HORIBA, Jobin Yvon Ltd., Stanmore, Middlesex, UK*, **2012**.

49 C. Würth, M. Grabolle, J. Pauli, M. Spieles, and U. R.-Genger**,** Relative and absolute determination of fluorescence quantum yields of transparent samples, *Nature Protocols*, **2013**, *8 NO.8*, 1535–1550. DOI:10.1038/nprot.2013.087

# CHAPTER 4

# Synthesis and Characterisation of 9,9-Dioctylfluorene / 1-Functionalised Dibenzothiophene-*S,S*-dioxide Co-polymers

---

## 4.1 Introduction

Polyfluorenes (**PF**) are a group of molecules that have emerged as a leading electroluminescent material to be used as part of an OLED device (**Figure 4.1**). These molecules express a bright blue emission, have a high hole mobility and have easily tuneable properties through chemical modification and co-polymerisation.[1,2] Dibenzothiophene-*S,S*-dioxide (**S**) is an alternative conjugated building block (see **Figure 4.1**) for electroluminescent and other organic electronics applications. The addition of the electron accepting $SO_2$ group to the rings decreases the LUMO energy level, improving the electron transport properties of the material, increasing the conversion efficiency compared to a fluorene unit.[3]

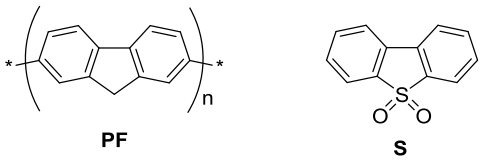


**Figure 4.1:** Examples of semiconducting polymers (**PF**) and dibenzothiophene-*S,S*-dioxide (**S**) structure.

### 4.1.1 Intramolecular charge transfer

In both the fields of photochemistry and biochemistry, the Intramolecular charge transfer (ICT) process is well studied,[4] especially for organic π-conjugated molecules, which contain a donor (D) and an acceptor (A) unit or group. When such types of molecules are excited by

photoexcitation, the charge transfer happens from the donor (D) unit to the acceptor (A) unit. The ICT process is more efficient when the D and A moieties are linked by a π-conjugated bridge. The geometry and the electronic configuration of both the ground and the excited states could be affected by the ICT, for example, some of the molecules become emissive in the excited ICT state. One of the famous examples is *N*,*N*-dimethylaminobenzonitrile (**DMABN**, see **Figure 4.2**) when Lippert *et al.* demonstrated the dual emission from the local excited state (LE) and the ICT state of the **DMABN**.[5] A number of other emissive (donor-acceptor) molecules were investigated to explain the mechanism of ICT emission for example 4-(dicyanomethylene)-2-methyl-6-(*p*-dimethylaminostyryl)-4*H*-pyran (**DCMP**) which was also widely studied (see **Figure 4.2**).[6]

Perepichka and Bryce *et al.* published a paper in 2008, which described the synthesis and properties of statistic (random) 9,9-dioctylfluorene/dibenzothiophene-*S*,*S*-dioxide co-polymers **p(F/S)-y** incorporating different amounts of dibenzothiophene-*S*,*S*-dioxide units into the main polymer chain (2, 5, 15, and 30%) as shown in **Figure 4.2**.[7] It was demonstrated that the **p(F/S)-y** co-polymers show broadened photo- and electroluminescence spectra due to dual emission from the local excited state (LE) and the intramolecular charge transfer state (ICT) throughout the visible spectrum from a blue colour to the green region and emitted greenish-white light (see Chapter 1, **Figure 1.23**), and as such can be used as materials for white-light emission OLEDs (WPLEDs).[8]

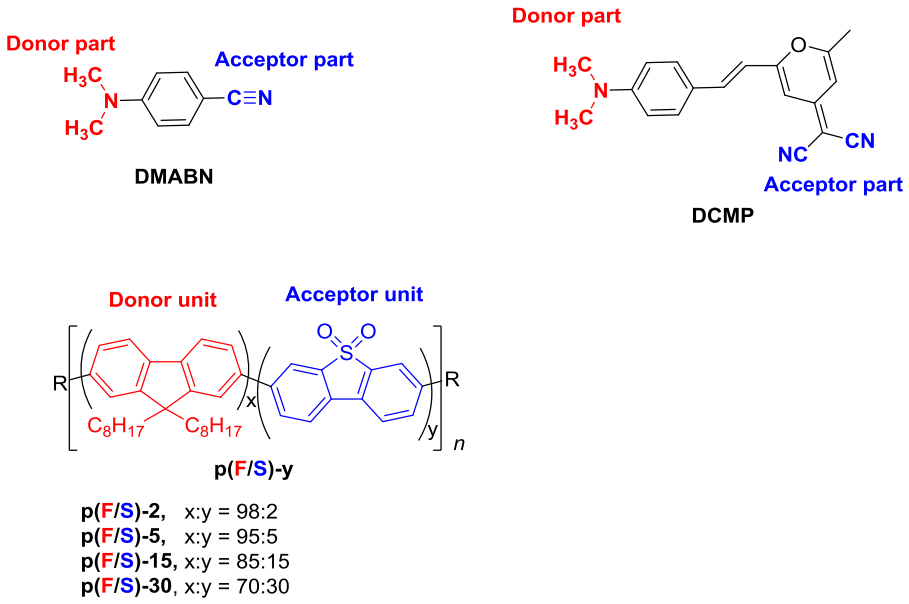


**Figure 4.2:** Examples of intramolecular charge transfer (ICT) molecule structures **DMABN**, **DCMP** and **p(F/S)-y** co-polymers.

### 4.1.2 Aims of the chapter

The aim of the work in this chapter is the development of novel light-emitting co-polymers incorporating 1-substituted dibenzothiophene-*S*,*S*-dioxide moieties. The goal of this task is to achieve efficient tuning of the electronic and optical properties of the co-polymers by electronic effects from electron donating groups (EDG) or electron withdrawing groups (EWG) at the 1- position. It has already been shown that **p(F/S)-y** co-polymers (**Figure 4.2**) are efficient electroluminescent materials showing broad photo/electroluminescence spectra due to a combination of LE/ICT emission (see Chapter 1, **Figure 1.23**) with a change in colour of their emission from blue to greenish-white with an increase in the proportion of dibenzothiophene-*S*,*S*-dioxide units incorporated into the co-polymer.[8] An increase of electron accepting strength of the dibenzothiophene-*S*,*S*-dioxide moiety by functionalisation with EDG/EWG groups (e.g. **OMe**, **$SO_2$Me**, **CN**, **SMe**, **F**, **$NO_2$**) at the 1- position (see **Scheme 4.1**) should increase the donor-acceptor interactions in the main chain and change the colour of the emission from the materials and change the electronic properties of the materials. Thus, the aims from this chapter are to investigate how changing the functional group from an EDG to an EWG and changing the ratio between the **F** and **S** units within the co-polymer chains can affect the optical and electronic properties of these materials.

After elaboration of synthetic methods to obtain a range of monomers, they can also be used for developing other classes of co-polymers with other (not only fluorene) conjugated building blocks.

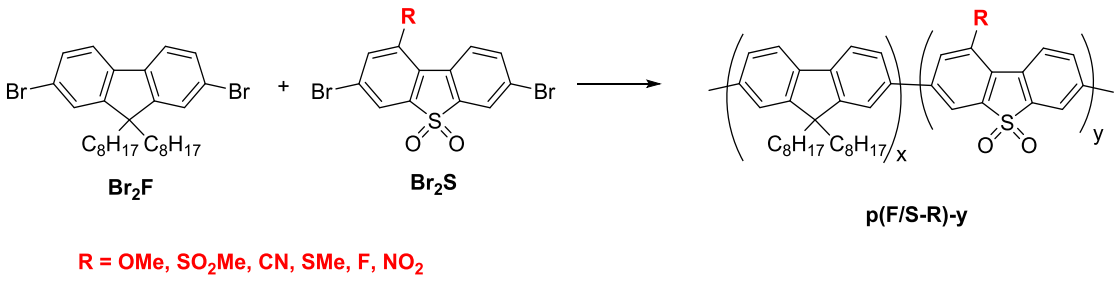


**Scheme 4.1:** General scheme describing the synthesis of co-polymers **p(F/S-R)-y**.

## 4.2 Results and Discussion

### 4.2.1 Synthesis of random (9,9-dioctylfluorene)-(1-substituted-dibenzothiophene-*S*,*S*-dioxide) p(F/S-R)-y co-polymers

The synthesis of random (9,9-dioctylfluorene)-(1-substitued-dibenzothiophene-*S*,*S*-dioxide) co-polymers **p(F/S-R)-y** was carried out using a Pd catalysed Suzuki coupling reaction as shown in **Scheme 4.2**. The procedure followed is the same as the one reported by Dias *et al.*[7] The 1-R-3,7-dibromodibenzothionphene-*S*,*S*-dioxide monomers were synthesised as shown in Chapter 2. The polymerisation was performed using a Suzuki coupling of dibromides **Br$_2$F** and **Br$_2$S-R** in the presence of diboronic ester **4.1** with the molar ratio of 0.50 (total for **Br$_2$F** and **Br$_2$S-R** ) : 0.50 (**4.1**) (**Scheme 4.2**). The synthesis was performed in a toluene/dioxane/2 M aqueous $K_2CO_3$ mixture with aliquat 336 as a phase transfer reagent and $Pd(Ph_3P)_4$ as catalyst under reflux for 72 h. The polymer was then end-capped with a phenyl group.

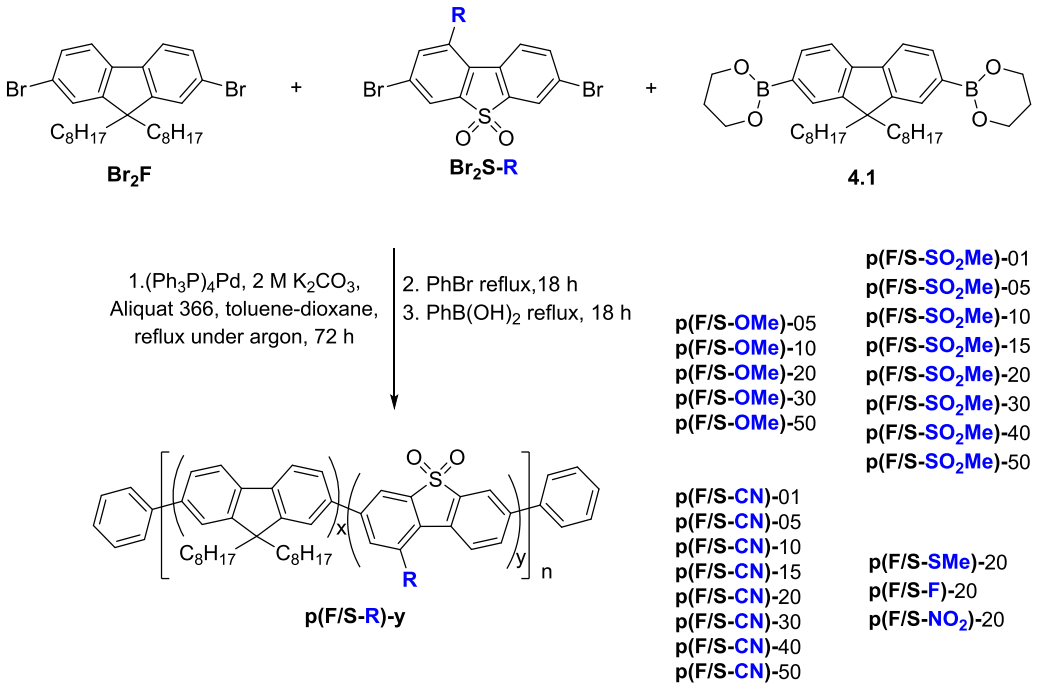


**Scheme 4.2:** The reaction scheme for the synthesis of **p(F/S-R)-y** co-polymers**.**

After precipitation into MeOH:$H_2O$:HCl, the crude dark green polymer was extracted in a Soxhlet apparatus with methanol to remove any monomers and other by-products then acetone to remove low-molecular weight oligomers. Extraction with

chloroform was then carried out to collect the **p(F/S-R)-y** co-polymers. Co-polymers **p(F/S-OMe)-y** were soluble in chloroform, as were the **p(F/S-$SO_2$Me)-1** to **p(F/S-$SO_2$Me)-40** co-polymers, however the **p(F/S-$SO_2$Me)-50** co-polymer was extracted twice in chloroform; the first extraction was carried out for 6 hours and as all the polymer was not extracted it was extracted again for a longer time, 24 hours. In the case of the **p(F/S-CN)-1** to **p(F/S-CN)-30** co-polymers, they were soluble in chloroform, however the **p(F/S-CN)-40** and **p(F/S-CN)-50** co-polymers again needed to be extracted twice with chloroform. Despite carrying out two extractions, there was about 46% of insoluble material still remaining in the extraction thimble for **p(F/S-CN)-50**. These experiments were carried out to study the effect of functionalisation, with different EDG/EWG at position 1 of the **S** unit, and the use of a different ratio of the **F** and **S** monomers, on the dual emission from LE/ICT and the electronic properties of the materials. From the above experiments it was found that the **p(F/S-R)-20** polymers had the highest ICT among the others as will be described in detail in Section 4.2.6. Therefore, it was decided to synthesise a range of other co-polymers using a 20% ratio of the **S-R** monomers containing different functional groups (**SMe**, **F**, **$NO_2$**). For **p(F/S-$NO_2$)-20**, although it was still soluble in chloroform, it needed to be extracted twice. Nevertheless, there was about 63% of insoluble material remaining in an extraction thimble.

### 4.2.2 Characterisation of random (9,9-dioctylfluorene)-(1-substituted-dibenzothiophene-*S*,*S*-dioxide) p(F/S-R)-y co-polymers by $^1$H NMR spectroscopy

The synthesised co-polymers **p(F/S-R)-y** were characterised by $^1$H NMR spectroscopy. $^1$H NMR spectroscopy gives limited information about the polymer structure relative to the smaller monomer molecules, because of the slightly non-equivalent protons in the polymer building blocks so the peaks appear broader. Therefore, the polymer spectra were compared to those of the corresponding monomers in order to look for similar patterns of peaks to be sure that the structure of the co-polymer matched with what was expected. Interestingly, the NMR spectra were also useful to calculate the ratio between the **F** and **S-R** units in the co-polymer backbone. The result showed the complete assignment of observed signals to the corresponding protons as shown in **Figure 4.3 a**, which shows the $^1$H NMR spectra of the monomer **$Br_2$S-OMe** and the corresponding polymer **p(F/S-OMe)-30**. When comparing the monomer **$Br_2$S-OMe** with the polymer **p(F/S-OMe)-30**, a relatable pattern of proton signals

was found. In the aromatic region, protons were shifted downfield with the largest shift being observed for the H-9 proton (8.40 ppm) whilst the others were shifted by 0.20–0.23 ppm.

Another example, **Figure 4.3 b** shows the $^{1}$H NMR spectra for the **(Br$_2$S-SO$_2$Me)** monomer and the corresponding co-polymer **p(F/S-SO$_2$Me)-30**, with complete assignments of the observed signals in the aromatic region. The percentages of the **F** to **S-R** moieties in the co-polymer were calculated using the integrated value of the last peak H-9 for the co-polymer, because it does not overlap with any other signals, by using the general formula (1). The $^{1}$H NMR spectra for all the other polymers can be seen in Appendix 6.8.

$$y = \frac{\text{integrated value}}{1+\text{integrated value}} \cdot 100\% \qquad (1)$$

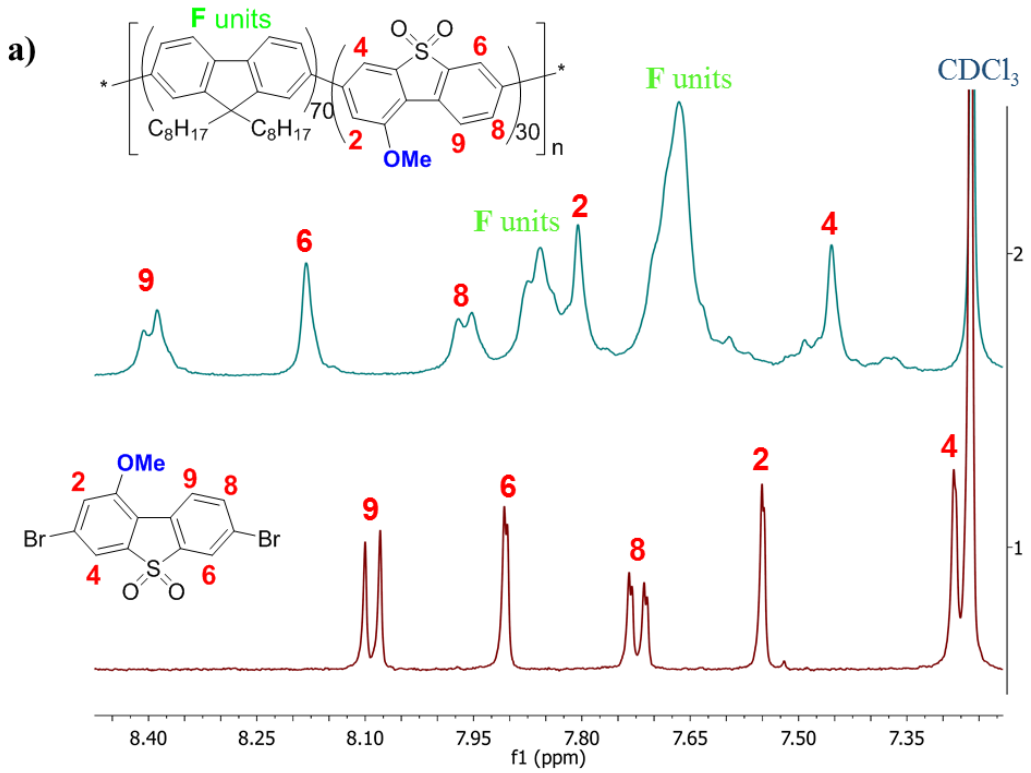

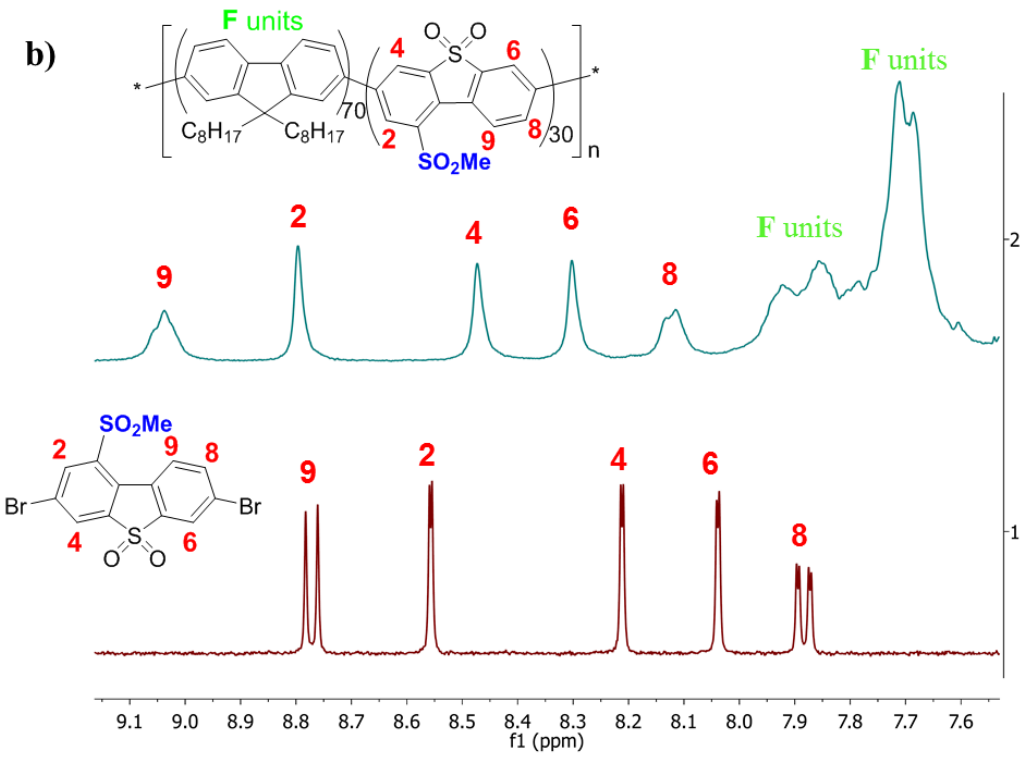


**Figure 4.3:** Expanded view of the aromatic region of the $^{1}$H NMR spectra of a) the **Br$_2$S-OMe** monomer (bottom) and the **p(F/S-OMe)-30** co-polymer (top); and b) the **Br$_2$S-SO$_2$Me** monomer (bottom) and the **p(F/S-SO$_2$Me)-30** co-polymer (top), with signal assignments.

### 4.2.3 Characterisation of (9,9-dioctylfluorene)-(1-substituted-dibenzothiophene-*S*,*S*-dioxide) p(F/S-R)-y co-polymers by GPC method

Molecular weights of the synthesised co-polymers **p(F/S-R)-y** have been estimated by gel permeation chromatography (GPC) in THF solutions with the column calibrated versus polystyrene standards, estimating their weight average molecular weight ($M_w$), number average molecular weight ($M_n$) and polydispersity index PDI = $M_w/M_n$. An example of a GPC trace is shown in **Figure 4.4** for the **p(F/S-SO$_2$Me)-50** co-polymer. The GPC traces for all the other polymers can be seen in Appendix 6.8.

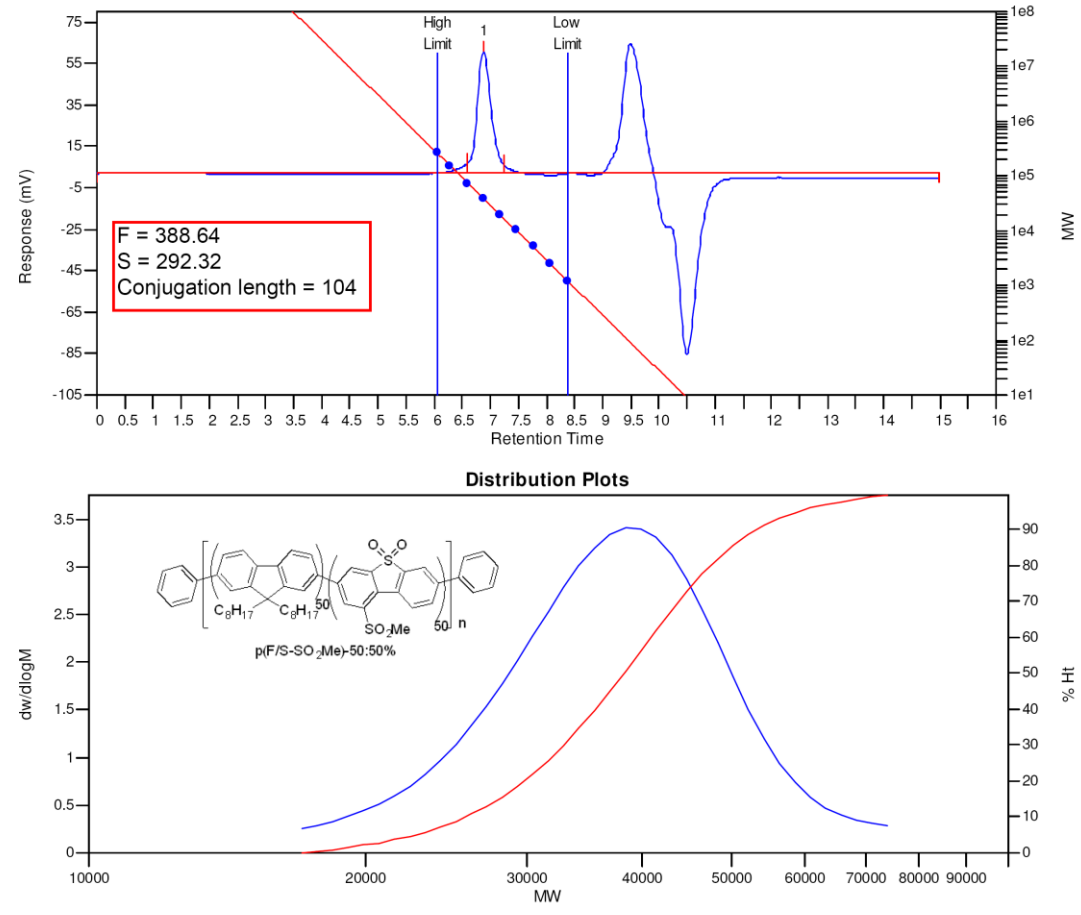


**MW Averages**

| Peak No | Mp | Mn | Mw | Mz | Mz+1 | Mv | PD |
|---|---|---|---|---|---|---|---|
| 1 | 38320 | 35352 | 38315 | 41319 | 44340 | 37871 | 1.08381 |

**Figure 4.4:** GPC trace for the **p(F/S-SO$_2$Me)-50** co-polymer in THF.

All the synthesised **p(F/S-SO$_2$Me)-y** co-polymers showed high molecular weights ($M_w$ = 10,869 – 76,642 Da; $M_n$ = 7,158 – 35,352 Da; PDI = 1.08 – 2.86), from which the average chain length can be estimated as n = 19 – 104. For the **p(F/S-OMe)-y**, **p(F/S-CN)-y**, **p(F/S-F)-20**, **p(F/S-SMe)-20**, and **p(F/S-NO$_2$)-20** co-polymers, the molecular weights were somewhat lower ($M_w$ = 9,656 – 45,962 Da; $M_n$ = 5,320 – 22,008 Da), but still quite high, with a narrower polydispersity PDI = 1.39 – 2.25. Estimations from their molecular weights give average lengths of the polymer chains of n = 17 – 58. Thus, in all the cases, the molecular weight is substantially higher than the conjugation length in polyfluorenes (estimated in the literature as n = 11 – 12).[9]

**Table 4.1:** GPC data for **p(F/S-R)-y** co-polymers.

| Co-polymer | $M_{w,}$[a] (Da) | $M_{n,}$[b] (Da) | PDI[c] |
|---|---|---|---|
| **p(F/S-OMe)-5** | 9656 | 5320 | 1.82 |
| **p(F/S-OMe)-10** | 11920 | 7613 | 1.57 |
| **p(F/S-OMe)-20** | 11526 | 7168 | 1.61 |
| **p(F/S-OMe)-30** | 15679 | 10372 | 1.51 |
| **p(F/S-OMe)-50** | 14397 | 10323 | 1.39 |
| **p(F/S-$SO_2$Me)-1** | 10869 | 7158 | 1.52 |
| **p(F/S-$SO_2$Me)-5** | 62186 | 24592 | 2.53 |
| **p(F/S-$SO_2$Me)-10** | 71780 | 25095 | 2.86 |
| **p(F/S-$SO_2$Me)-15** | 50058 | 21391 | 2.34 |
| **p(F/S-$SO_2$Me)-20** | 59327 | 24185 | 2.45 |
| **p(F/S-$SO_2$Me)-30** | 76642 | 26871 | 2.85 |
| **p(F/S-$SO_2$Me)-40** | 64938 | 27298 | 2.38 |
| **p(F/S-$SO_2$Me)-50** | 38315 | 35352 | 1.08 |
| **p(F/S-CN)-1** | 9786 | 6633 | 1.48 |
| **p(F/S-CN)-5** | 45962 | 22008 | 2.09 |
| **p(F/S-CN)-10** | 33598 | 15319 | 2.19 |
| **p(F/S-CN)-15** | 22198 | 12407 | 1.79 |
| **p(F/S-CN)-20** | 25100 | 13280 | 1.89 |
| **p(F/S-CN)-30** | 25799 | 13519 | 1.91 |
| **p(F/S-CN)-40** | 28090 | 16325 | 1.72 |
| **p(F/S-CN)-50** | 20814 | 12536 | 1.66 |
| **p(F/S-F)-20** | 37507 | 16682 | 2.25 |
| **p(F/S-SMe)-20** | 25662 | 13614 | 1.88 |
| **p(F/S-$NO_2$)-20** | 18777 | 10431 | 1.80 |

[a] $M_w$ is weight average molecular weight. [b] $M_n$ is number average molecular weights, [c] Polydispersity index, PDI = $M_w/M_n$.

### 4.2.4 Thermal analyses of (9,9-dioctylfluorene)-(1-substituted-dibenzothiophene-*S*,*S*-dioxide) p(F/S-R)-y co-polymers by TGA method

The thermal stabilities of the **p(F/S-R)-y** co-polymers have been studied by thermogravimetric analysis (TGA). Estimating their thermal decomposition in a nitrogen atmosphere at a level of 5% mass loss with a heating rate of 10 °C/min. All the co-polymers showed good stability, with decomposition temperatures of $T_d$ = 377–423 °C (**Figure 4.5**, **Table 4.2**), typical for polyfluorenes (e.g. for **PF8** it was reported as $T_d$ = 385 °C).[10] From the TGA data in the region of ~380–500 °C with *ca* 55–65% mass loss, it seems that major mass losses on decomposition are due to cleavage of alkyl groups from both the fluorene and dibenzothiophene-*S*,*S*-dioxide units in the **p(F/S-R)-y** co-polymers. While in the region of ~500–800 °C, it seems that decomposition of the aromatic system of the **p(F/S-R)-y** co-polymers occurs.

**Table 4.2:** TGA data for the **p(F/S-R)-y** co-polymers.

| Polymer | $T_{d,}$[a] (°C) | Polymer | $T_{d,}$[a] (°C) |
|---|---|---|---|
| **p(F/S-OMe)-5** | 417 | **p(F/S-CN)-1** | 392 |
| **p(F/S-OMe)-10** | 417 | **p(F/S-CN)-20** | 412 |
| **p(F/S-OMe)-20** | 421 | **p(F/S-CN)-30** | 388 |
| **p(F/S-OMe)-50** | 423 | **p(F/S-CN)-40** | 382 |
| **p(F/S-$SO_2$Me)-1** | 395 | **p(F/S-F)-20** | 415 |
| **p(F/S-$SO_2$Me)-20** | 397 | **p(F/S-SMe)-20** | 418 |
| **p(F/S-$SO_2$Me)-40** | 384 | **p(F/S-$NO_2$)-20** | 397 |
| **p(F/S-$SO_2$Me)-50** | 377 | | |

[a] $T_d$ is the decomposition temperature measured at 5% weight loss under $N_2$.

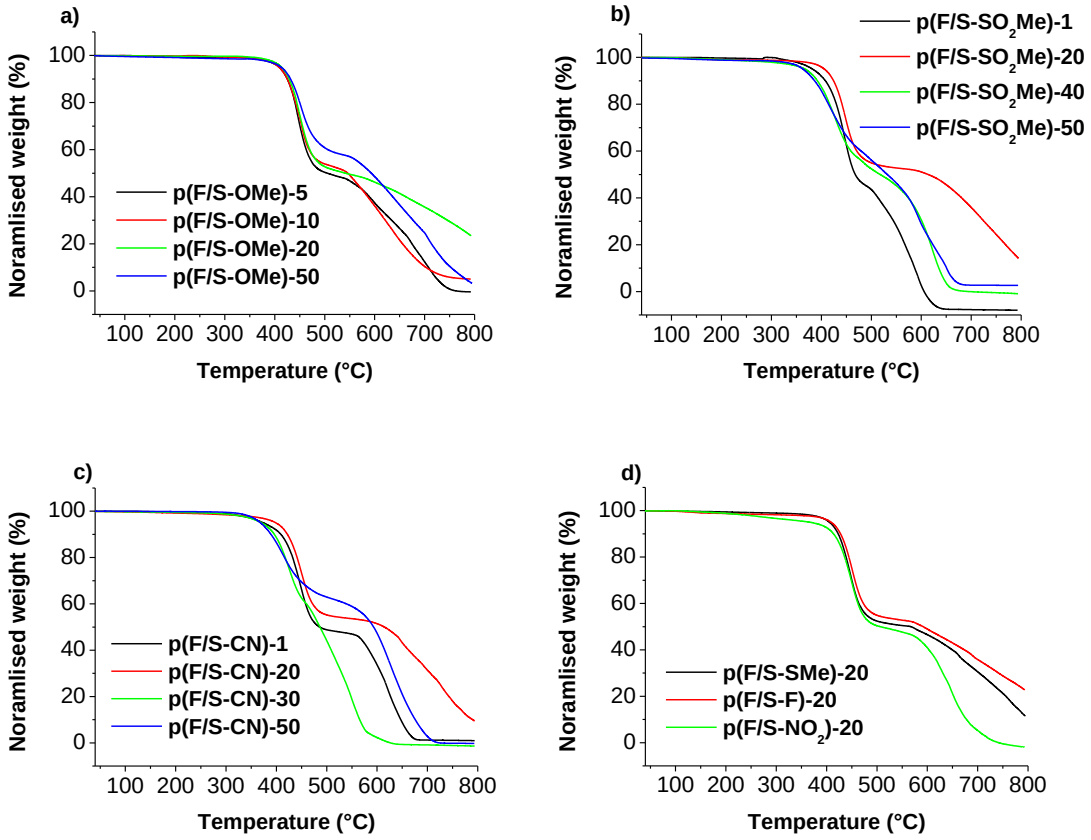


**Figure 4.5:** Thermogravimetric analysis (TGA) curves of a) **p(F/S-OMe)-y**, b) **p(F/S-SO$_2$Me)-y**, c) **p(F/S-CN)-1**, and d) **p(F/S-R)-20** co-polymers under a nitrogen atmosphere at a heating rate of 10 °C/min.

### 4.2.5 Electrochemical studies of (9,9-dioctylfluorene)/(1-substituted-dibenzothiophene-*S*,*S*-dioxide) p(F/S-R)-y co-polymers

The electrochemical behaviour of the **p(F/S-R)-y** co-polymers has been studied by cyclic voltammetry (CV) in films drop-cast from chloroform solution onto glassy carbon electrodes. Measurements were carried out in acetonitrile with 0.1 M $Bu_4NPF_6$ as the supporting electrolyte at a scan rate of 100 mV/s. The results of the CV experiments are shown in **Figure 4.6 a-h**, demonstrating that all polymers are electroactive and undergo oxidation (p-doping) with onsets in the region of +(0.96 – 1.33) V and reduction (n-doping) with onsets in the region of – (1.10–2.32) V as shown in **Table 4.3**. From these CV measurements, the HOMO/LUMO energy levels of the **p(F/S-SO$_2$Me)-y** co-polymers have been estimated using the general formulae (2, 3), where 4.8 eV is an estimation of the potential of $Fc/Fc^+$ couple versus vacuum.[11]

$$E_{HOMO} = -e(E^{ox}_{onset} + 4.8)\ ev \quad (2)$$

$$E_{LUMO} = -e(E^{red}_{onset} + 4.8)\ ev \quad (3)$$

$$E_g = E_{LUMO} - E_{HOMO}, \quad (4)$$

Onsets of redox potentials ($E^{ox}_{onset}$ and $E^{red}_{onset}$), together with frontier orbital energies (HOMO and LUMO) and electrochemical band gaps ($E_g^{CV}$) are collated in **Table 4.3**. The results of the CV experiments show that the HOMO/LUMO energy levels of **p(F/S-R)-y** co-polymers can be efficiently tuned by changing the ratio of **S-R** units in the polyfluorene backbone. Thus, from the **p(F/S-SO$_2$Me)-1** co-polymers to the **p(F/S-SO$_2$Me)-50** co-polymers, HOMO and LUMO energy levels can be tuned by 0.26 eV and 1.16 eV, respectively. The results also proved that the HOMO/LUMO energy levels can be efficiently tuned by changing the functional group at the 1- position of the dibenzothiophene-*S*,*S*-dioxide ring. Thus for the **p(F/S-R)-20** co-polymer series, from the strongest EDG (R = **OMe**) to the strongest EWG (R = **CN**, **SO$_2$Me**), HOMO and LUMO energy levels can be tuned by 0.29 eV and 0.12 eV, respectively.

The aim of measuring the CV for those polymers is to study how they react to an applied potential, as they are intended to be part of electronic components. By calculating $E_g^{CV}$, the difference between the HOMO and LUMO energy levels, the approximate energy needed to excite the polymer can be calculated; the smaller the difference between those energies, the less energy that is needed for the compound to reach an excited state. Another important conclusion from the CV measurements is that the effect of substituents on the band gap of the polymers, $E_g^{CV}$, is strong. Polyfluorene is among the highest band gap polymers in the series and the introduction of 1-substituted-dibenzothiophene-*S*,*S*-dioxide units (either EDG or EWG) generally results in band gap contraction as shown in **Table 4.3**.

**Figure 4.6** demonstrates the effect of the incorporation of **S-R** units into the polyfluorene backbone on the electrochemical behaviour of the co-polymers even at a low ratio of this unit. For example, the **p(F/S-SO$_2$Me)-1** co-polymer can be reversibly p- and n-doped in cyclic voltammetry (CV) experiments. The oxidation potential is almost the same with respect to the polyfluorene **PF8** homopolymer and the reduction potential is shifted positively, by 0.32 V, with respect to the **PF8** homopolymer. It is obvious from **Table 4.3** that increasing the ratio of **S-R** moieties in the co-polymer backbone cause a positive shift in both the oxidation and reduction potentials of the **p(F/S-R)-y** co-polymers compared with

the **PF8** homopolymer with a more pronounced shift in the reduction wave compared to the oxidation wave.

The **p(F/S-SO$_2$Me)-30** co-polymer oxidation and reduction potentials are shifted positively with respect to the **PF8** homopolymer, with a more pronounced shift in the reduction wave compared to the oxidation wave (by onsets: 1.16 V and 0.11 V, respectively). Moreover in comparison with the unsubstituted **p(F/S)-30** co-polymer[8] see **Table 4.3**, the oxidation potential is almost unchanged but there is a clear positive shift in the reduction potential by 0.65 V. The enhanced electron acceptor properties and easier reduction of **p(F/S-SO$_2$Me)-30** are shown in a positive shift in its reduction potential (by 1.16 V compared to **PF8**), thus better electron injection and electron transport properties are expected for this co-polymer.

**Table 4.3** also presents optical band gaps, $E_g^{opt}$, estimated from the red edge of the absorption spectra of the studied co-polymers. These values are lower than the electrochemical band gaps ($E_g^{CV}$) estimated from CV experiments for the **p(F/S-R)-1** co-polymers and higher for the other co-polymers. It is not surprising as optical and electrochemical energy gaps belong to different physical processes, and such differences are well documented in the literature.[12]

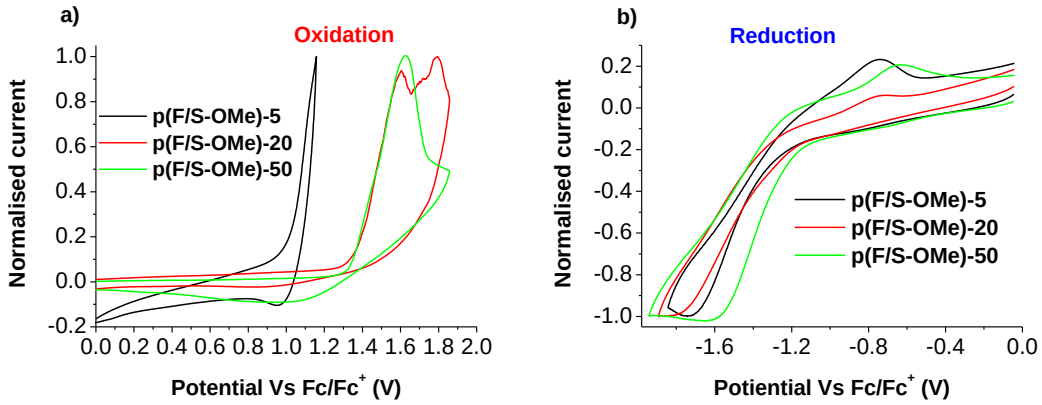

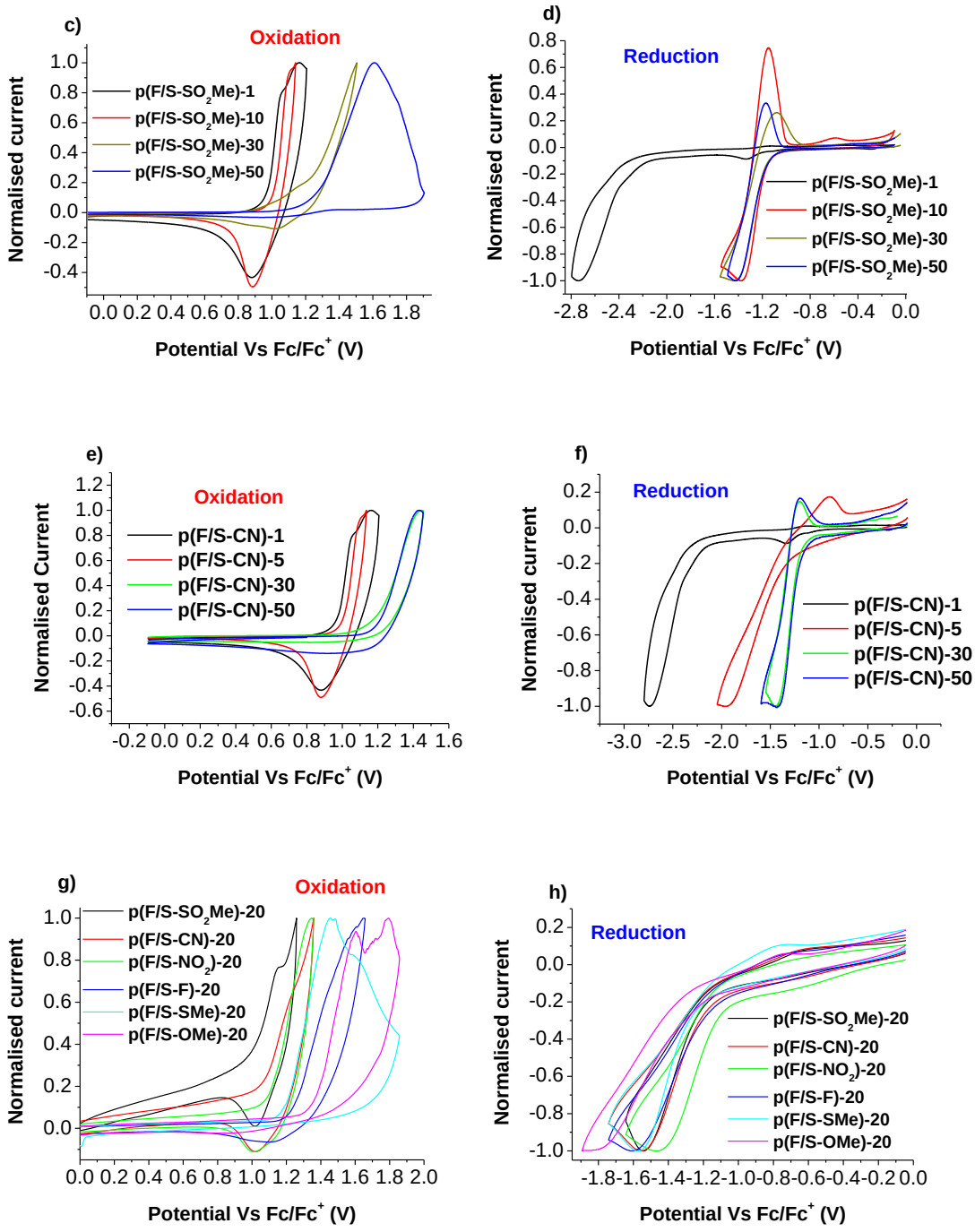


**Figure 4.6:** Cyclic voltammetry of **p(F/S-R)-y** polymer films on a glassy carbon electrode in 0.1 M of $Bu_4NPF_6$ / $CH_3CN$, scan rate 100 mV/s. For convenience, CV data are presented with normalisation to the current maximum of an oxidation / reduction processes.

**Table 4.3:** Electrochemical study of **p(F/S-SO$_2$Me)-y** co-polymers

| Polymer | $E_g^{opt}$, [a] (eV) | $E^{ox}_{onset}$, [b] (V) | $E^{red}_{onset}$, [b] (V) | HOMO[c] (eV) | LUMO[c] (eV) | $E_g^{CV}$, [d] (eV) |
|---|---|---|---|---|---|---|
| **PF8**[13] | - | 0.97[e] | -2.64[e] | -5.77 | -2.16 | 3.61 |
| **p(F/S)-30**[8] | 2.77 | 1.10 | -1.81 | -5.90 | -2.99 | 2.91 |
| **p(F/S-OMe)-5** | 2.81 | 1.02 | -1.33 | -5.82 | -3.46 | 2.36 |
| **p(F/S-OMe)-20** | 2.76 | 1.31 | -1.29 | -6.11 | -3.51 | 2.60 |
| **p(F/S-OMe)-50** | 2.73 | 1.33 | -1.25 | -6.13 | -3.55 | 2.58 |
| **p(F/S-SO$_2$Me)-1** | 2.92 | 0.96 | -2.32 | -5.76 | -2.49 | 3.27 |
| **p(F/S-SO$_2$Me)-10** | 2.67 | 1.03 | -1.18 | -5.83 | -3.63 | 2.21 |
| **p(F/S-SO$_2$Me)-20** | 2.64 | 1.02 | -1.21 | -5.82 | -3.59 | 2.23 |
| **p(F/S-SO$_2$Me)-30** | 2.60 | 1.08 | -1.16 | -5.88 | -3.64 | 2.24 |
| **p(F/S-SO$_2$Me)-50** | 2.63 | 1.22 | -1.15 | -6.02 | -3.65 | 2.37 |
| **p(F/S-CN)-1** | 2.92 | 0.96 | -2.31 | -5.76 | -2.49 | 3.27 |
| **p(F/S-CN)-5** | 2.75 | 0.99 | -1.39 | -5.79 | -3.41 | 2.38 |
| **p(F/S-CN)-20** | 2.61 | 1.06 | -1.17 | -5.86 | -3.63 | 2.23 |
| **p(F/S-CN)-30** | 2.67 | 1.15 | -1.19 | -5.95 | -3.61 | 2.34 |
| **p(F/S-CN)-50** | 2.61 | 1.19 | -1.17 | -6.02 | -3.63 | 2.39 |
| **p(F/S-NO$_2$)-20** | 2.58 | 1.07 | -1.10 | -5.87 | -3.70 | 2.17 |
| **p(F/S-F)-20** | 2.71 | 1.21 | -1.15 | -6.01 | -3.65 | 2.36 |
| **p(F/S-SMe)-20** | 2.73 | 1.19 | -1.22 | -5.99 | -3.58 | 2.41 |

[a] $E_g^{opt}$ are optical band gaps estimated from the red edge of UV–Vis spectra of polymer films. [b] $E^{ox}_{onset}$ and $E^{red}_{onset}$ are the onset potentials of oxidation and reduction of polymer films measured versus $Fc/Fc^+$ couple. [c] $E_{HOMO}$ and $E_{LUMO}$ energies calculated from empirical formulas (1) and (2): $E_{HOMO}$ (eV) = –e($E^{ox}_{onset}$ + 4.8) and $E_{LUMO}$ = –e($E^{red}_{onset}$ + 4.8). [d] Electrochemical band gap $E_g^{CV} = E_{LUMO} - E_{HOMO}$. [e] CV data in ref.[13] are given versus Ag/AgCl electrode; we have recalculated them to $Fc/Fc^+$ as $E(Fc/Fc^+) = E(Ag/AgCl) - 0.4$ V.

### 4.2.6 Photophysical studies of (9,9-dioctylfluorene)-(1-substituted-dibenzothiophene-*S*,*S*-dioxide) p(F/S-R)-y co-polymers

#### 4.2.6.1 Electron absorption and photoluminescence (PL) spectra of p(F/S-OMe)-y co-polymers

The isolated **p(F/S-OMe)-y** co-polymers were characterised by UV-Vis and PL spectroscopy in different solvents and in the solid state. The absorption spectra of **p(F/S-OMe)-5** to **p(F/S-OMe)-50** in toluene and chloroform solutions showed a small red shift of 25–30 nm, see **Figures 4.7 a, c** and the data in **Table 4.4**. The increased **S**-unit moiety (20–50%) led to the appearance of shoulders in the range of 342–347 nm. In accordance with the expected increase in ratio of **S-OMe** in the co-polymer backbone, the **p(F/S-OMe)-5** showed a typical spectra region of polyfluorene.[14] Nevertheless, there was a clear bathochromic shift for **p(F/S-OMe)-30** in chloroform solution **(**$\lambda_{abs}$ = 407 nm) compared to the unsubstituted **p(F/S)-30** co-polymer **(**$\lambda_{abs}$ = 392 nm).[8] The PL spectra of the **p(F/S-OMe)-y** polymers showed a bathochromic shift of 2–12 nm in toluene and chloroform solutions. **Figure 4.7 e, f** shows CIE diagram of colours being emitted under excitation, **p(F/S-OMe)-y** emitted blue light typically like polyfluorene.

**Table 4.4:** $\lambda_{abs}$, $\lambda_{PL}$, CIE and $\Phi_{PL}$ spectral data for **p(F/S-OMe)-y** co-polymers in solution and solid state.

| **Parameter** | **p(F/S-OMe)-5** | **p(F/S-OMe)-10** | **p(F/S-OMe)-20** | **p(F/S-OMe)-30** | **p(F/S-OMe)-50** |
|---|---|---|---|---|---|
| $\lambda_{abs}$ (nm)[a,b] Tol | **379** | **380** | **388**, 342sh | **396**, 345sh | **404**,342sh |
| $\lambda_{abs}$ (nm)[a,b] $CHCl_3$ | **380** | **381** | **390**, 347sh | **407**, 347sh | **410**, 345sh |
| $\lambda_{abs}$ (nm)[a,b] film | **381** | **385** | **390**, 345sh | **399**, 350sh | **401**, 351sh |
| $\lambda_{PL}$ (nm), ($\underline{\lambda_{exc}}$) (nm)[a,b,c] Tol | 415,**436,**464sh,(*379*) | 413,**435**,463sh,(*380*) | **434**,462sh,(*388*) | **434**,462sh.(*396*) | **434**,460sh,(*404*) |
| $\lambda_{PL}$ (nm), ($\underline{\lambda_{exc}}$) (nm)[a,b,c] $CHCl_3$ | 417, **444**, 478sh, (*380*) | 416, **446**, 473sh, (*381*) | **445**, 477sh,(*390*) | **442**, 471sh, (*407*) | **441**, 464sh, (*410*) |
| $\lambda_{PL}$ (nm), ($\underline{\lambda_{exc}}$) (nm)[a,b,c] film | 448, **473**, (*381*) | 450, **476**, (*385*) | **477**, 457sh, (*390*) | **479**, 459sh, (*399*) | **480**, 460sh, (*401*) |
| CIE (x, y) Tol | 0.154, 0.056 | 0.153, 0.064 | 0.157, 0.062 | 0.154, 0.063 | 0.157, 0.065 |
| CIE (x, y) $CHCl_3$ | 0.157, 0.101 | 0.155, 0.116 | 0.153, 0.112 | 0.157, 0.105 | 0.158, 0.091 |
| CIE (x, y) film | 0.153, 0.145 | 0.144, 0.158 | 0.151, 0.215 | 0.146, 0.204 | 0.165, 0.262 |
| $\Phi_{PL}$ (%) Tol | 89 | 81 | 72 | 75 | 65 |
| $\Phi_{PL}$ (%) $CHCl_3$ | 67 | 71 | 66 | 57 | 60 |
| $\Phi_{PL}$ (%) film | 13.3 | 12.7 | 7.4 | 9.2 | 8.4 |

[a] sh-shoulders. [b] Bold numbers are the absorption maxima $\lambda_{abs}$. [c] For PL measurements, the excitation wavelengths are in italic ($\underline{\lambda_{exc}}$).

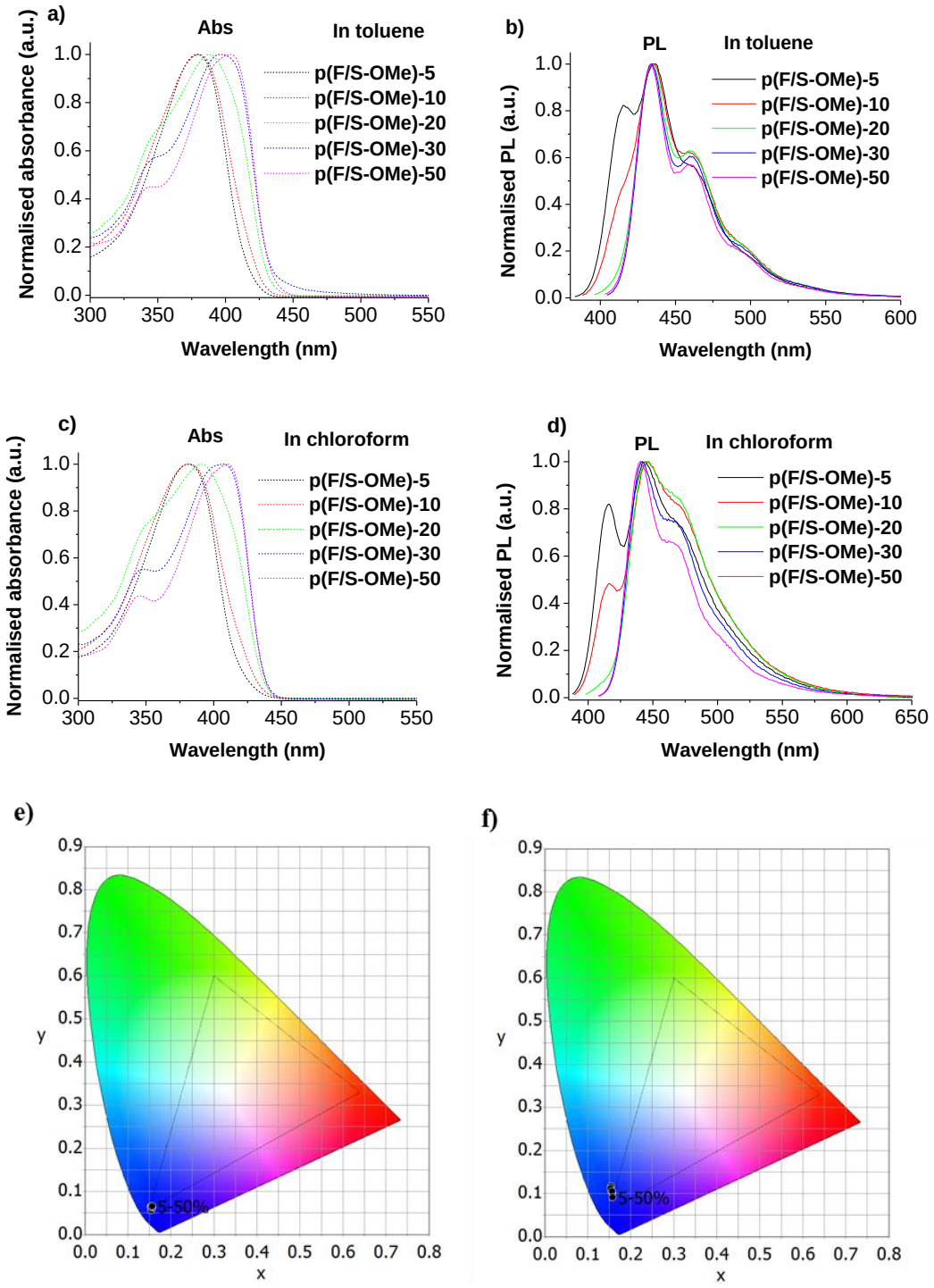


**Figure 4.7:** (a,c) Normalised UV-Vis absorption spectra and (b,d) normalised PL spectra of **p(F/S-OMe)-y** moiety in toluene and chloroform solutions. CIE colour diagrams in toluene (e) and chloroform (f) showing colours emitted by **p(F/S-OMe)-y** under excitation, based on PLQY data (see **Table 4.4**). The excitations for PL spectra ($\lambda_{exc}$) are at the maxima of their absorption spectra.

The thin-film absorption spectra of **p(F/S-OMe)-y** co-polymers showed red shifts of 20 nm for **p(F/S-OMe)-5** to **p(F/S-OMe)-50**, see **Figure 4.8 a**. The increased **S**-unit moiety between **p(F/S-OMe)-5** to **p(F/S-OMe)-50** led to an appearance of shoulders in the range of 345–351 nm. The PL spectra of the **p(F/S-OMe)-y** polymers showed a red shift of 7 nm with an increase in the **S**-unit moiety in the chain. The EDG (**OMe**) showed a weaker interplay dual emission between the LE and ICT state, (see **Figure 4.8 a**), compared to the unsubstituted **p(F/S)-y** co-polymers.[8] The EDG (**OMe**) has not affected the co-polymer dramatically as the LE state remained around the same in both solution and the solid state with a small red shift. However, the LE disappeared in the solid state with the EWG (**$SO_2$Me**, **CN**) co-polymers, even with 1% moiety (see next Section 4.2.6.2). **Figure 4.8 b** shows CIE diagrams of colours being emitted under excitation with increased ratios of **S-OMe** units. As a conclusion, the **p(F/S-OMe)-y** co-polymers in thin films are highly emissive materials emitting a blue colour.

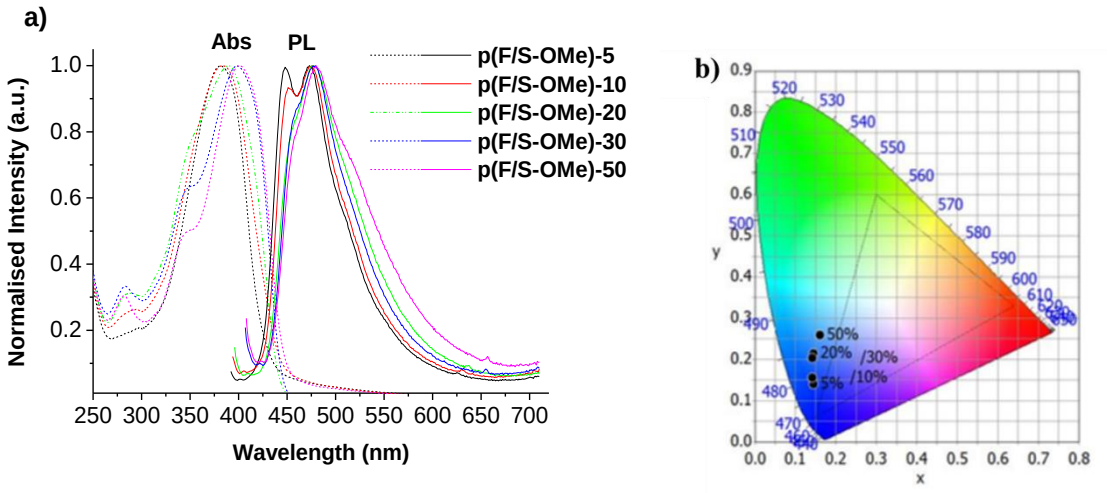


**Figure 4.8:** (a) Normalised UV-Vis absorption spectra and PL spectra of **p(F/S-OMe)-y** co-polymers in thin films. (b) CIE diagram inset showing colours emitted by **p(F/S-OMe)-y** under excitation, based on PLQY data (see **Table 4.4**).

### 4.2.6.2 Electron absorption and photoluminescence spectra, of p(F/S-$SO_2$Me)-y and p(F/S-CN)-y co-polymers

Both the **p(F/S-$SO_2$Me)-y** and **p(F/S-CN)-y** series of co-polymers were characterised by UV-Vis electron absorption and PL spectroscopy in solutions and in the solid state. The

electron absorption spectra of the **p(F/S-$SO_2$Me)-y** co-polymers in toluene solution show peaks between 380–430 nm, which can be assigned to the $\pi$-$\pi^*$ transition due to the delocalisation of electrons on the conjugated polymer, and any shoulders which appear occur between 425–430 nm as shown in **Figure 4.9 a**. UV-Vis spectra demonstrate clear bathochromic shifts of $\lambda_{abs}$ values by 43 nm, from the **p(F/S-$SO_2$Me)-1** to **p(F/S-$SO_2$Me)-50** co-polymers, in accordance with the expected increase in the ratio of the **S-$SO_2$Me** moiety in the co-polymer backbone. The **p(F/S-$SO_2$Me)-1** co-polymer shows a typical spectra region of polyfluorene[14] then it starts to become red shifted with an increase in the percentage of the **S-$SO_2$Me** unit. In toluene solution, **p(F/S-$SO_2$Me)-1** to **p(F/S-$SO_2$Me)-15** co-polymers show almost no shifts in $\lambda_{abs}$ maxima compared to the corresponding unsubstituted co-polymers **p(F/S)-y** however it was noticed that there is a clear bathochromic shift in **p(F/S-$SO_2$Me)-30** ($\lambda_{abs}$ = 410 nm) compared to the unsubstituted **p(F/S)-30** co-polymer ($\lambda_{abs}$ = 392 nm).[8] The UV-Vis spectra are shown in **Figure 4.9 a** and the data are summarised in the **Table 4.5**.

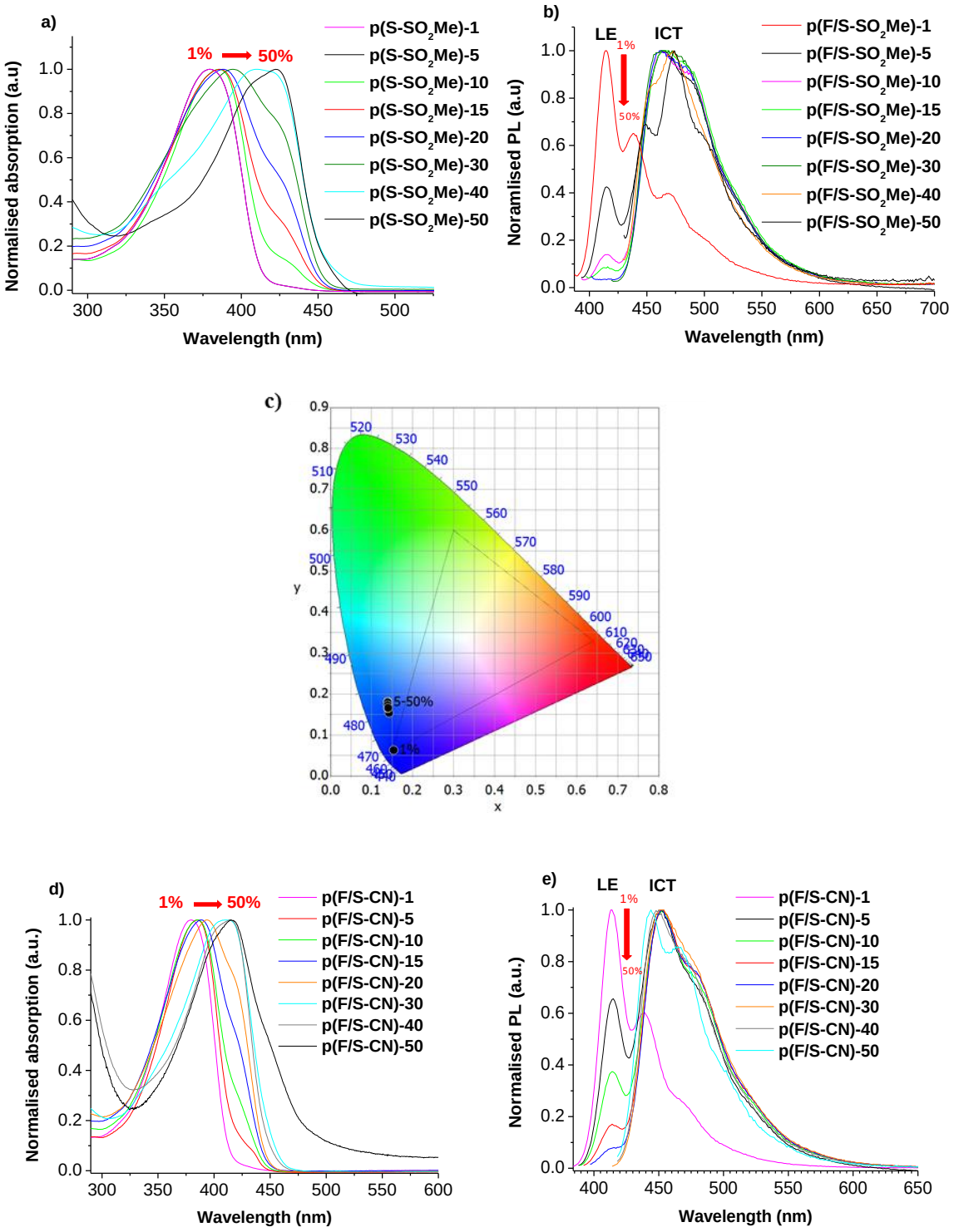


**Figure 4.9:** a) Normalised UV-Vis absorption spectra b) Normalised PL spectra. c) CIE diagram inset showing colours emitted under excitation of **p(F/S-SO2Me)-y** in toluene solution. d) Normalised UV-Vis absorption spectra. e) Normalised PL spectra of **p(F/S-CN)-y** in toluene solution.

All the prepared **p(F/S-$SO_2$Me)-y** co-polymers are highly emissive materials in toluene solution, emitting a deep blue colour to a bright blue colour. For example **Figure 4.9 c** shows a CIE diagram of colours emitted under excitation, and as can be seen the **p(F/S-$SO_2$Me)-1** co-polymer emits a bright blue light typical of polyfluorene,[14] while there is a small change in the colour emitted with an increasing feed ratio of the **S-$SO_2$Me** moiety in the co-polymer backbone. However, PL spectra of **p(F/S-$SO_2$Me)-y** show pronounced interplay dual emission between the local excited state (LE) and the intramolecular charge transfer state (ICT) as shown in **Figure 4.9 b**. The **p(F/S-$SO_2$Me)-1** co-polymer shows vibronically well-resolved PL spectra and majorly emits from the LE, as a typical feature of polyfluorene as a rigid-rod conjugated polymer.[14] While the **p(F/S-$SO_2$Me)-5** co-polymer has clearly dual emission from both LE and ICT and it is obvious from PL spectra that the intensity of the LE emission decreases in comparison to the ICT emission with an increase of the **S-$SO_2$Me** moiety ratio in the co-polymer chain (see **Figure 4.9 b**). In toluene solution, the **p(F/S-$SO_2$Me)-y** co-polymers show a pronounced difference in structure of PL spectra compared to unsubstituted co-polymers **p(F/S)-y**[8] with the existence of a new excited state band (ICT) and this can be explained due to the effectiveness of the EWG (**-$SO_2$Me**) substituted on the 1- position of the dibenzothiophene-*S*,*S*-dioxide moiety.

The **p(F/S-CN)-y** co-polymers show almost the same behaviour in UV/PL spectra as **p(F/S-$SO_2$Me)-y** co-polymers due to both the **$SO_2$Me** and **CN** groups being strong EWG's, as shown in **Figures 4.9 d, e** and **Table 4.5**.

**Table 4.5:** Absorption and PL spectral data for **p(F/S-SO$_2$Me)-y** and **p(F/S-CN)-y** co-polymers in different solvents.

| **Co-polymer** | $\lambda_{abs}$ (nm)[a,b] Toluene | $\lambda_{abs}$(nm)[a,b] THF | $\lambda_{abs}$ (nm)[a,b] $CHCl_3$ | $\lambda_{PL}$ (nm), ($\lambda_{exc}$) (nm)[a,b,c] Toluene | $\lambda_{PL}$, ($\lambda_{exc}$) (nm)[a,b,c] THF | $\lambda_{PL}$, ($\lambda_{exc}$) (nm)[a,b,c] $CHCl_3$ | CIE (x, y), $CHCl_3$ |
|---|---|---|---|---|---|---|---|
| **p(F/S-SO$_2$Me)-1** | **380** | **383** | **379** | **414**, 438, 469,(*380*) | **416**,440,475sh,(*383*) | **496**, (*379*) | 0.16, 0.07 |
| **p(F/S-SO$_2$Me)-5** | **386** | **390** | **388**, 430sh | **415**, **464**, (*386*) | **416**,**442**,512,(*390*) | **416**, 441, **518**, (*387*) | 0.20, 0.33 |
| **p(F/S-SO$_2$Me)-10** | **386**, 430sh | **392** | **388**, 430sh | **416**, **463**, (*386*) | **416**,448sh, **512**, (*392*) | **415**, **519**, (*387*) | 0.22, 0.44 |
| **p(F/S-SO$_2$Me)-15** | **389**, 429sh | **394** | **388**, 425sh | **416**, **466**, (*389*) | **416**, **515**, (*394*) | **417**, **518**, (*389*) | 0.24, 0.49 |
| **p(F/S-SO$_2$Me)-20** | **395**,426sh | **397** | **393**, 425sh | **463**, (*395*) | **416**, **512**, (*397*) | **521**, (*394*) | 0.24, 0.52 |
| **p(F/S-SO$_2$Me)-30** | **410**, 425sh | **408**, 420sh | **417** | **465**, (*410*) | **508**, (*408*) | **519**, (*412*) | 0.23, 0.50 |
| **p(F/S-SO$_2$Me)-40** | 350sh, **423** | 410sh, **422** | **426** | 453sh, **473**, (*423*) | 460sh, **454**, (*422*) | 415sh, **508**, (*426*) | 0.20, 0.39 |
| **p(F/S-SO$_2$Me)-50** | **423** | 407sh, **425** | **428** | 449, **474**, 500sh, (*423*) | **456**, 482sh, (*425*) | **457**, 531sh, (*428*) | 0.14, 0.17 |
| **p(F/S-CN)-1** | **379** | **383** | **382** | **414**, 439, 470sh, (*379*) | **416**, 440, 475sh, (*383*) | **416**, 440, 475sh, (*382*) | 0.16, 0.07 |
| **p(F/S-CN)-5** | **385,** 435sh | **390**, 435sh | **387**, 425 sh | 415, **452**, 473sh, (*485*) | **416**, 442, 504, (*390*) | 416, 447, **501**, (*387*) | 0.18, 0.27 |
| **p(F/S-CN)-10** | **386**, 425sh | **390**, 430sh | **387**, 427 sh | 414, **453**, 475sh, (*485*) | 417, 443, **505**, (*390*) | 416, 442, **506**, (*387*) | 0.18, 0.32 |
| **p(F/S-CN)-15** | **388**, 425sh | **393**, 430sh | **390**, 425 sh | 414, **453**, 473sh, (*488*) | 417, **510**, (*393*) | 415, **507**, (*389*) | 0.19, 0.38 |
| **p(F/S-CN)-20** | **394**, 420sh | **393**, 420sh | **395**, 425 sh | 415, **453**, 477sh, (*493*) | 415, **507**, (*393*) | 416, **504**, (*395*) | 0.20, 0.41 |
| **p(F/S-CN)-30** | **410** | **413** | **418** | **454**, 472sh, (*410*) | 455sh, **508**, (*413*) | **501**, (*417*) | 0.18, 0.36 |
| **p(F/S-CN)-40** | **415** | 405sh, **422** | **422** | **450**, 470sh, (*415*) | 455sh, **493**, (*422*) | **488**, (*420*) | 0.17, 0.30 |
| **p(F/S-CN)-50** | **415** | 404sh, **423** | **422** | **444**, 465, (*415*) | **453**, 425sh, (*423*) | **454**, 477sh, (*420*) | 0.14, 0.14 |

[a] sh–Shoulders. [b] Bold numbers are the strongest absorption or emission peaks. [c] Excitation wavelengths used for PL measurements ($\lambda_{exc}$) are given in italic in brackets.

In the solid state (spin-coated films from chloroform solution), the isolated chloroform fractions of both the **p(F/S-SO$_2$Me)-y** and **p(F/S-CN)-y** series of co-polymers were characterised by UV-Vis electron absorption and PL spectroscopy. Overall the electron absorption spectra of the **p(F/S-SO$_2$Me)-y** and **p(F/S-CN)-y** co-polymers in the solid state show peaks between 380–420 nm, which can be assigned to the $\pi$-$\pi^*$ transition due to the delocalisation of electrons on the conjugated polymer, and any shoulders which appear occur between 430–433 nm as shown in **Figures 4.10 a, c**. UV-Vis spectra demonstrate clear bathochromic shifts of $\lambda_{abs}$ 30 nm, from the **p(F/S-SO$_2$Me)-1** to **p(F/S-SO$_2$Me)-50** co-polymers, and by 36 nm, from the **p(F/S-CN)-1** to **p(F/S-CN)-50** co-polymers in accordance with the expected increase in the ratio of the **S-R** moiety in the co-polymer backbone. The **p(F/S-R)-1** co-polymer shows a typical spectra region of polyfluorene[14] (see **Figure 1.13**, Chapter 1) then it starts to become red shifted as the percentage of the **S-R** unit is increased. The **p(F/S-SO$_2$Me)-1** to **p(F/S-SO$_2$Me)-15** co-polymers show almost no shifts in $\lambda_{abs}$ maxima compared to the corresponding unsubstituted co-polymers **p(F/S)-y** however it was noticed that there was a bathochromic shift in **p(F/S-SO$_2$Me)-30** ($\lambda_{abs}$ = 407 nm) compared to the unsubstituted **p(F/S)-30** co-polymer ($\lambda_{abs}$ = 398 nm).[8]

All the prepared **p(F/S-SO$_2$Me)-y** and **p(F/S-CN)-y** co-polymers, are highly emissive materials in the solid state, emitting greenish to pure green light under excitation. **Figures 4.10 b, d** show CIE diagrams of the colours emitted under excitation, and it can be seen how the substitution with an EWG (**SO$_2$Me** or **CN**) can affect the colour emission of the co-polymers **p(F/S-R)-y**. For example, increasing the ratio of **S-SO$_2$Me** by 1% (from 0% to 1%) changes the colour emitted from pure bright blue to greenish and there is a change in the colour emitted with an increase in the feed ratio of **S-SO$_2$Me** in the co-polymer backbone to reach a pure green colour with a feed ratio of **p(F/S-SO$_2$Me)-15-40**. The PL spectra of **p(F/S-R)-y** show a pronounced domain of emission from the intramolecular charge transfer state (ICT) as shown in **Figures 4.10 a, c**. The ICT band of **p(F/S-R)-y** becomes broadened covering the region between (450-700 nm) compared to unsubstituted **p(F/S)-y** co-polymers which cover the region between (400-590 nm) for both bands LE/ICT.[8] The LE band does not appear even with **p(F/S-R)-1**, therefore it could be possible to obtain this if 0.5% or less of the **S-R** unit was used to reach the white emitting colour for the whole region between (400-700 nm). The UV-Vis/PL spectra are shown in **Figure 4.10** and the data are summarised in **Table 4.6**.

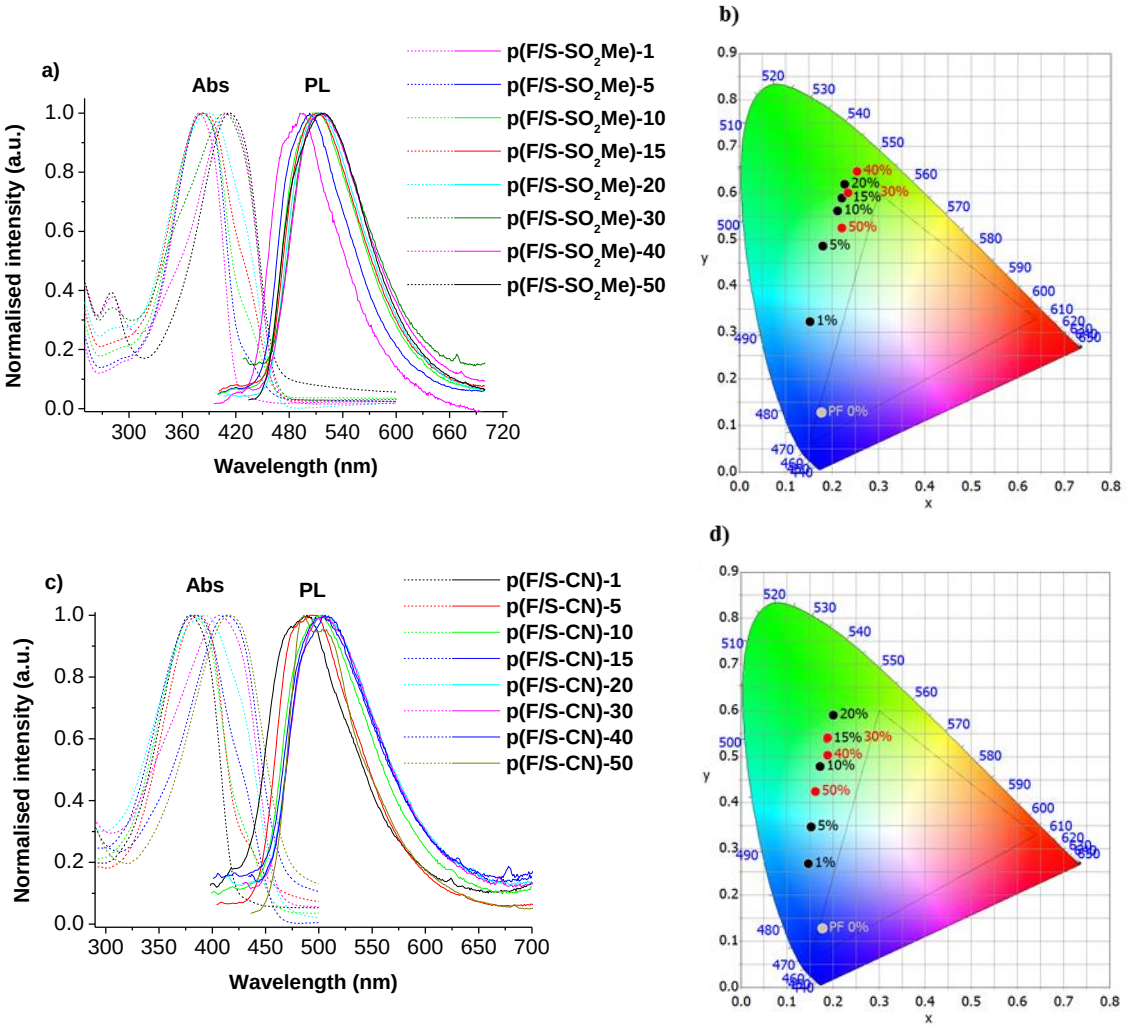


**Figure 4.10:** a) UV-Vis absorption and PL spectra. b) CIE diagram inset showing colours emitted under excitation of **p(F/S-SO$_2$Me)-y** co-polymers in thin films. c) UV-Vis absorption and PL spectra. d) CIE diagram inset showing colours emitted under excitation of **p(F/S-CN)-y** co-polymers in thin films.

**Table 4.6:** $\lambda_{abs}$, and $\lambda_{PL}$ for **p(F/S-SO$_2$Me)-y** and **p(F/S-CN)-y** co-polymers in solid state.

| **Co-polymer** | **$\lambda_{abs}$ (nm)** film[a,b] | **$\lambda_{PL}$ (nm),** ($\underline{\lambda_{exc}}$) (nm)[c] film |
|---|---|---|
| **p(F/S-SO$_2$Me)-1** | **383** | **496** *(383)* |
| **p(F/S-SO$_2$Me)-5** | **383**, 433sh | **503** *(383)* |
| **p(F/S-SO$_2$Me)-10** | **383**, 430sh | **510** *(383)* |
| **p(F/S-SO$_2$Me)-15** | **384** | **512** *(384)* |
| **p(F/S-SO$_2$Me)-20** | **390** | **514** *(390)* |
| **p(F/S-SO$_2$Me)-30** | **407** | **516** *(407)* |

| | | |
|---|---|---|
| **p(F/S-$SO_2$Me)-40** | **410** | **515** *(410)* |
| **p(F/S-$SO_2$Me)-50** | **413** | **516** *(413)* |
| **p(F/S-CN)-1** | **380** | 417sh, **489**, 624, (*380*) |
| **p(F/S-CN)-5** | **386**, 437sh | **495**, (*386*) |
| **p(F/S-CN)-10** | **381**, 437sh | 419, **503**, (*381*) |
| **p(F/S-CN)-15** | **384**, 428sh | **504**, 630, (*384*) |
| **p(F/S-CN)-20** | **393**, 430sh | 414, **505**, (*393*) |
| **p(F/S-CN)-30** | **408** | 432sh, **503**, (*408*) |
| **p(F/S-CN)-40** | **413** | 437, **506**, 678, (*413*) |
| **p(F/S-CN)-50** | **416** | **486**, 507, (*416*) |

[a] sh-shoulders. [b] Bold numbers are the absorption maxima $\lambda_{abs}$. [c] For PL measurements, the excitation wavelengths are in italic ($\lambda_{exc}$).

#### 4.2.6.3 Solvent polarity effect on the electron absorption and photoluminescence spectra, of p(F/S-$SO_2$Me)-y and p(F/S-CN)-y co-polymers

Experiments were carried out to study the effect of solvent polarity on the UV/PL spectra, in chloroform solution, of both the **p(F/S-$SO_2$Me)-y** and **p(F/S-CN)-y** series of co-polymers. **Figures 4.11 a, c** show the electron absorption spectra of **p(F/S-$SO_2$Me)-y** and **p(F/S-CN)-y** co-polymers in chloroform solution (dielectric permitivity $\varepsilon = 4.89$), which demonstrated almost the same absorption spectra as those in toluene solution (dielectric permitivity $\varepsilon = 2.43$). There is a slightly larger bathochromic shift of maxima $\lambda_{abs}$ values by 49 nm, from the **p(F/S-$SO_2$Me)-1** to **p(F/S-$SO_2$Me)-50** co-polymers, compared to those in toluene solution (43 nm), while the shift was 40 nm from the **p(F/S-CN)-1** to **p(F/S-CN)-50** co-polymers, compared with those in toluene solution, where the shift was 35 nm.

In chloroform solution, all the prepared co-polymers **p(F/S-$SO_2$Me)-y** and **p(F/S-CN)-y** are highly emissive materials, and the light emitted is tuneable from bright blue to blueish white, greenish white, green then back to blue light with an increase in the feed ratio of the **S-R** unit in the co-polymer chain from 1% to 50%, as shown in the CIE diagrams (**Figures 4.11 e, f**). PL spectra of **p(F/S-$SO_2$Me)-y** and **p(F/S-CN)-y** show pronounced interplay dual emission between the local excited state (LE) and the intramolecular charge transfer state (ICT) (**Figures 4.11 b, d**) as was the case in toluene solution. **Figure 4.11 g** shows emission from a chloroform solution of the **p(F/S-$SO_2$Me)-1, 20,** and **50** co-polymers

under UV-light irradiation, which shows how it is possible to tune the colour emitted with a change in the ratio of the co-polymer units. For the **p(F/S-SO$_2$Me)-1** and **p(F/S-CN)-1** co-polymers the emission is only from the LE state due to 99% of the units in the co-polymer backbone being **F** units, so that the polymer is not very polar. While in the **p(F/S-SO$_2$Me)-20** and **p(F/S-CN)-20** co-polymers the emission is from the ICT state at the maximum due to the excitation being localized on both the electron-donating group (**F** units) and the electron-accepting group (**S** unit). This is due to the **S-R** acceptor units being stronger relative to the **F** donor unit therefore each **S-SO$_2$Me** or **S-CN** unit is statistically equal to four **F** units to make the charge transfer in the excited state. With an increase in the ratio of the **S-SO$_2$Me** or **S-CN** units in the polymer backbone up to 50% (**p(F/S-SO$_2$Me)-50** and **p(F/S-CN)-50**), a hypsochromic shift was observed. This might be because lowering the HOMO (which is located on the **F** unit) results in an increase in the HOMO-LUMO band gap.[15, 16, 17, 18]

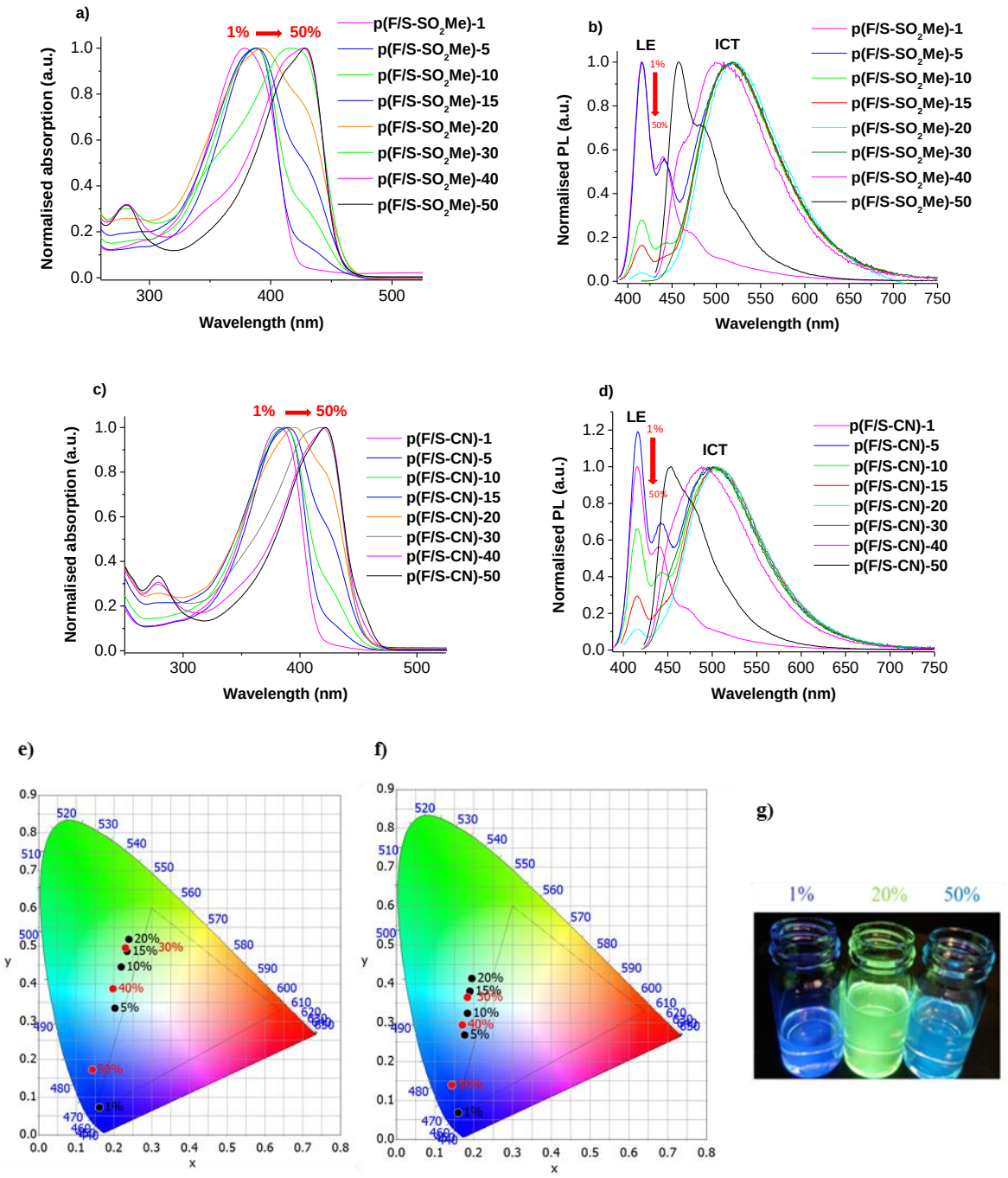


**Figure 4.11:** a, c) Normalised UV-Vis absorption spectra; b, d) Normalised PL spectra; e, f) CIE diagram, inset showing colours emitted under excitation of **p(F/S-SO$_2$Me)-y**, and **p(F/S-CN)-y** respectively in chloroform solution; g) Emission of polymer **p(F/S-SO$_2$Me)1, 20, 50** from left to right in chloroform solution under UV-light irradiation (360 nm).

**Figure 4.12 a** shows the normalised UV/PL spectra of the **p(F/S-$SO_2$Me)-5** co-polymer in both toluene (dielectric permitivity ε = 2.43) and chloroform (dielectric permitivity ε = 4.89) solution. The electron absorption spectra show almost the same spectra in both cases for toluene and chloroform due to the absorption spectra being less sensitive to solvent polarity relative to the emission spectra. This is because the polymer is exposed to the same local environment in the ground and excited states, absorption of light occurs in about $10^{-15}$ s (Franck-Condon principle), a time that is too short for motion of the fluorophore (co-polymer) or solvent. In contrast, the emitting polymer is exposed to the relaxed environment, which contains solvent molecules orientated around the dipole moment of the excited state this is because the fluorescence lifetimes (1–10 ns) are usually much longer than the time required for solvent relaxation. For fluid solvents at room temperature, solvent relaxation occurs in 10–100 ps, therefore, the PL spectra of **p(F/S-$SO_2$Me)-5** gave a pronounced positive solvatochromic effect, and a clear bathochromic shift is observed, by 54 nm, with a broadened ICT band in chloroform compared with toluene. This is because the ICT is more stabilised in polar solvents, which leads to a reduced band gap between the ground and excited state which will cause a red shift in the ICT spectra (**Figure 4.12 c**). Even though the LE state $\lambda_{max}$ = 416 nm stayed the same with no shifts in both solvents this is due to the excitation being localised on the fluorene (**F**) unit rings, so that the polymer is not polar then it is affected less by the solvent polarity. Also, the intensity of the LE band becomes higher (1.00 a.u) compared to that in toluene (0.41 a.u.) and the PL spectra become more structured with three peaks (**Figure 4.12 a**). **Figure 4.12 b** shows the emission from chloroform and toluene solutions of the **p(F/S-$SO_2$Me)-5, 10, 15,** and **30** co-polymers under UV-light irradiation, and as can be seen changing the solvent from low polarity, i.e. toluene to a high polarity, i.e. chloroform, the colour of the light emitted from the co-polymers is affected.

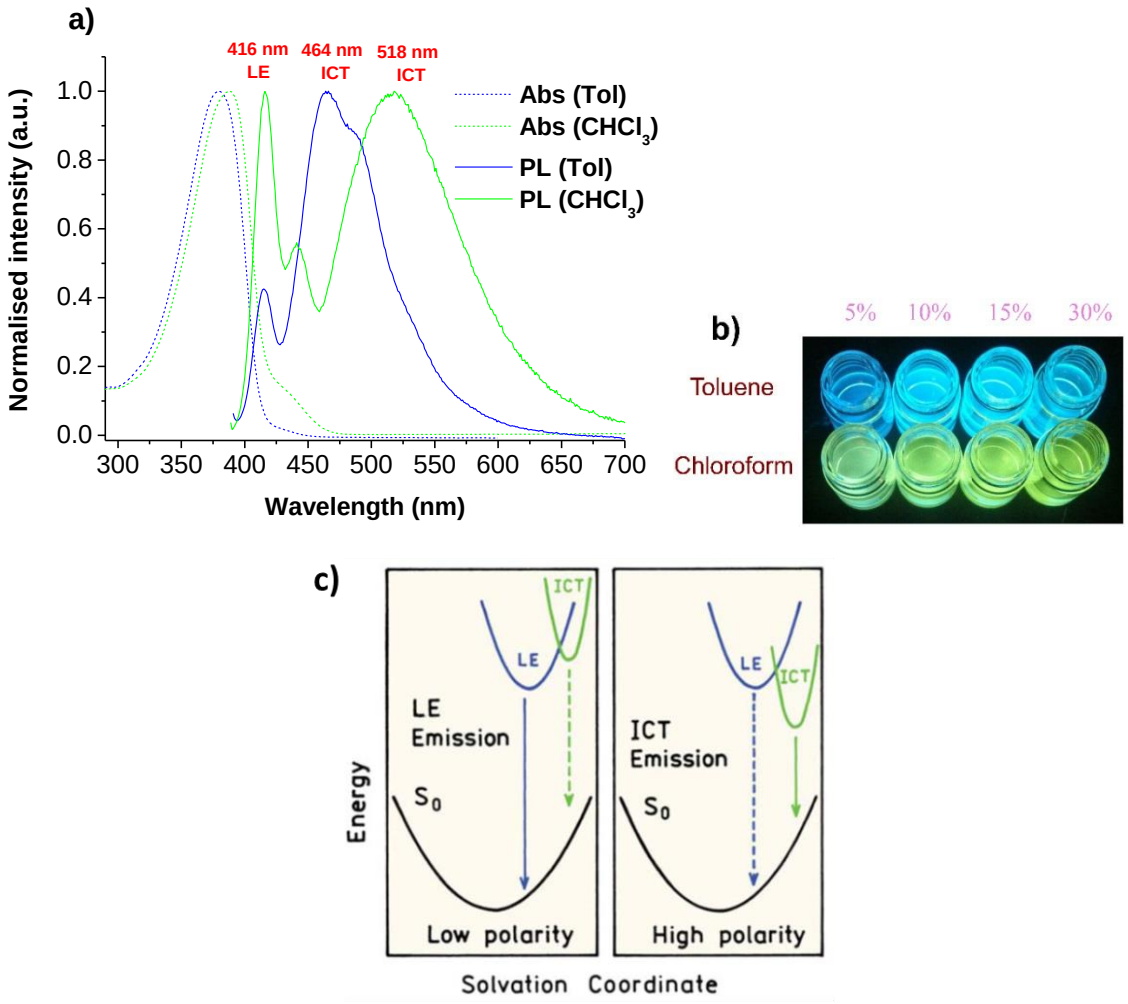


**Figure 4.12:** a) UV-Vis absorption and PL spectra of **p(F/S-SO$_2$Me)-5** co-polymers in solution. b) Emission of **p(F/S-SO$_2$Me)-5, 10, 15,** and **30** co-polymers in solution under UV-light irradiation (360 nm). c) Effect of solvent polarity on the energies of LE and ICT states in different polarity solvents.[19]

In tetrahydrofuran solution, both the **p(F/S-SO$_2$Me)-y** and **p(F/S-CN)-y** series of co-polymers were studied by UV-Vis electron absorption and PL spectroscopy. Both series show the same results as in chloroform solution with very small shifts in the UV and PL spectra, sometimes there is a hypsochromic shift and sometimes a bathochromic shift, but there is no significant difference. This could be due to the accuracy of measurements (**Table 4.5**). The UV-Vis/PL spectra are shown in **Figure 4.13** and the data are summarised in the **Table 4.5**.

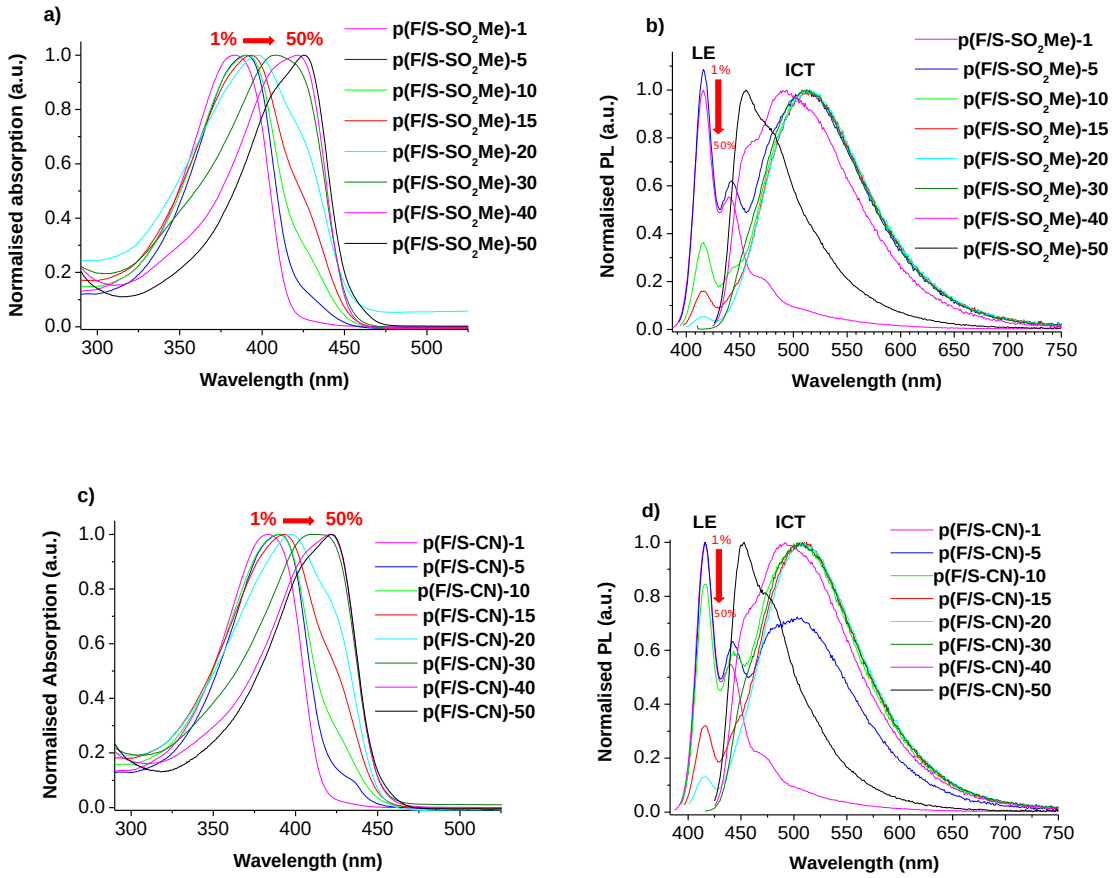


**Figure 4.13:** a) Normalised UV-Vis absorption spectra and b) Normalised PL spectra of **p(F/S-SO$_2$Me)-y** in THF solution; c) Normalised UV-Vis absorption spectra and d) Normalised PL spectra of **p(F/S-CN)-y** in THF solution.

### 4.2.6.4 Electron absorption and photoluminescence spectra of p(F/S-R)-20 with different side groups and solvent effect

After noticing that **p(F/S-SO$_2$Me)-20** and **p(F/S-CN)-20** have the highest bathochromic shift in their PL spectra, thus the strongest ICT among the polymers, it was decided to synthesise more co-polymers with the same ratio but with different functional groups, as described in Section 4.2.1 and study their electro and optical properties.

The absorption spectra of **p(F/S-R)-20** in toluene and chloroform solutions showed a bathochromic shift of 13 nm, see **Figure 4.14 a, c**. Shoulders began to appear for the least polar groups in the range of 342–350 nm and 427–432 nm, but as polarity increased the shoulders disappeared. The PL spectra of the **p(F/S-R)-20** polymers showed a red shift of

28 nm in toluene and 76 nm in chloroform, see **Figure 4.14 b, d**. The co-polymers with different groups were ICT pronounced and showed a weaker LE state emission. With an increased solvent polarity, the EWGs showed a stronger bathochromic shift, for example **p(F/S-CN)-20** (453 to 504 nm) and **p(F/S-SO$_2$Me)-20** (463 to 521 nm). This can be explained by the different properties of the attached EWGs (**S-R** units) and how they co-operate within the conjugated system of the co-polymer chain. In toluene solution, all **p(F/S-R)-20** polymers are highly emissive materials emitting a blue colour whereas in chloroform solution the **p(F/S-CN)-20** and **p(F/S-SO$_2$Me)-20** polymers emitted a green colour, see **Figures 4.14 e, f, g** and **Table 4.7**.

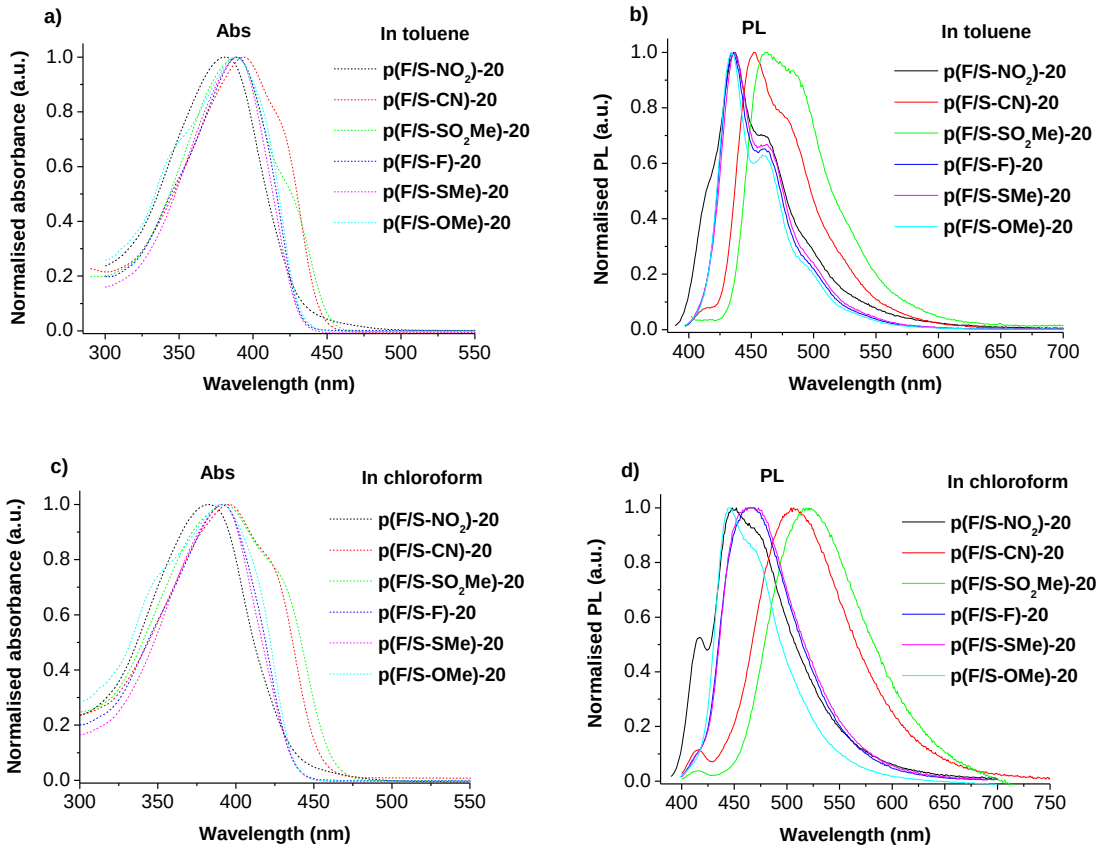

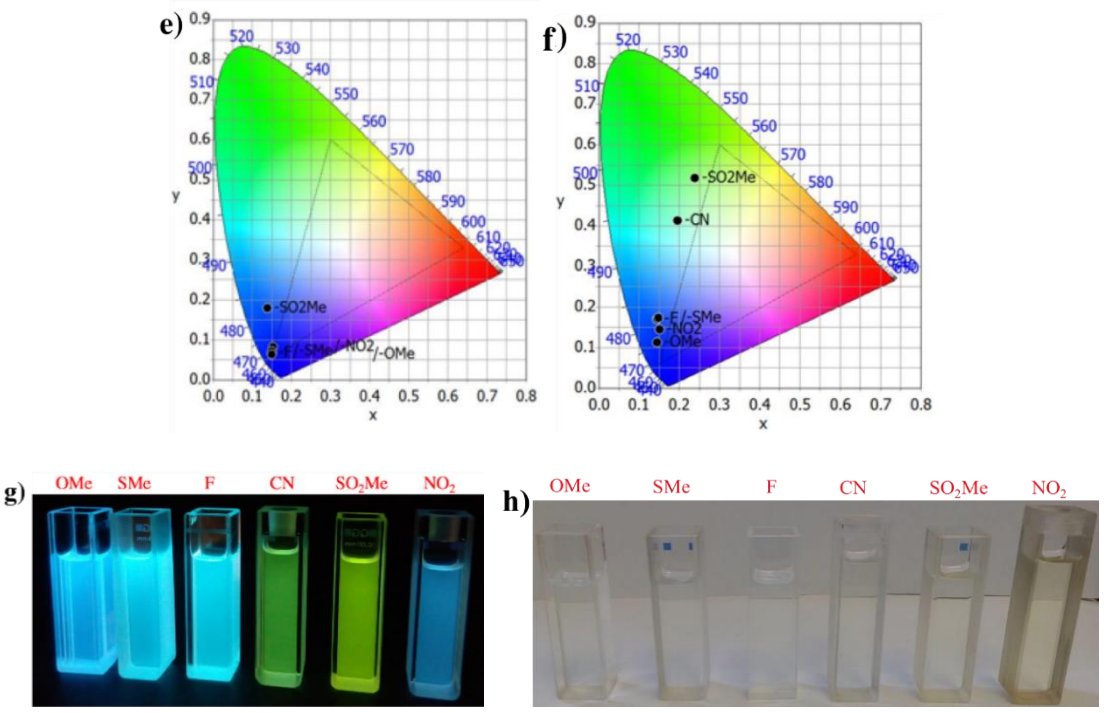


**Figure 4.14:** (a, c) Normalised UV-Vis absorption spectra and (b, d) normalised PL spectra of **p(F/S-R)-20** in toluene and chloroform solutions respectively. CIE colour diagrams of **p(F/S-R)-20** in toluene (e) and chloroform (f) showing colours emitted under excitation. (g, h) Emission of polymer **p(F/S-R)-20** from left to right in chloroform solution under UV-light irradiation and without. The excitations for PL spectra ($\lambda_{exc}$) are at the maxima of the absorption spectra ($\lambda_{max}$).

The absorption spectra of the **p(F/S-R)-20** polymers in the solid state had a red shift of 14 nm and the PL spectra of **p(F/S-R)-20** showed a red shift of 59 nm, see **Figure 4.15 a**. The EWGs are red shifted and emitted a green colour, while the EDGs were blue shifted and emitted a blue colour. EDGs had a small red shift of 11–30 nm between the solution and solid state but the major change was with **p(F/S-NO$_2$)-20**. For this polymer, there was a shift of 84 nm with a change in the structure of the spectrum with very weak emissive light, which is due to quench emission by the nitro group, which is known in the literature.[20] When in the solid state the **p(F/S-R)-20** co-polymers are highly emissive materials which emit blue and green colours, see **Figure 4.15 b** and **Table 4.7**.

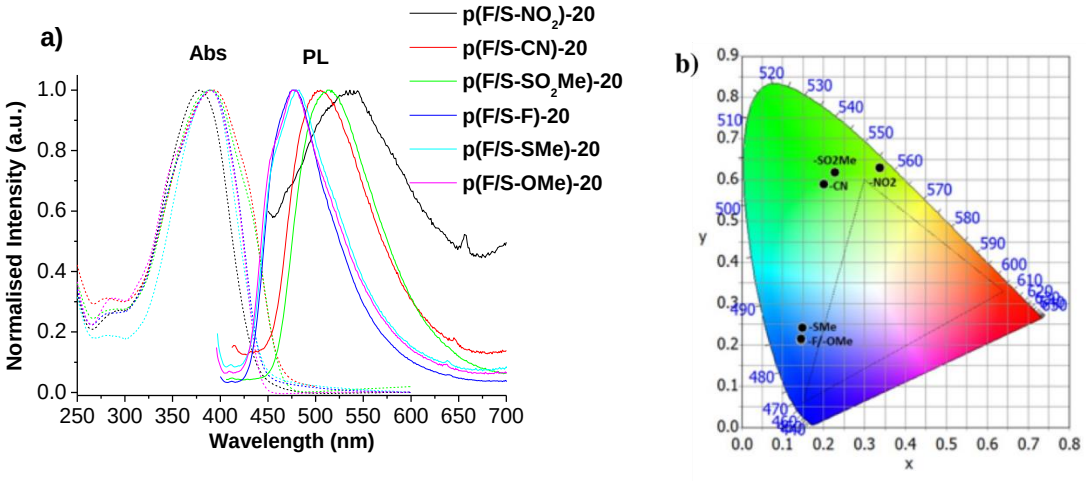


**Figure 4.15:** a) Normalised UV-Vis absorption spectra and PL spectra of **p(F/S-R)-20** co-polymers in thin films. b) CIE diagram inset showing colours emitted under excitation, based on PLQY data (see **Table 4.7**).

**Table 4.7:** $\lambda_{abs}$, $\lambda_{PL}$, CIE and $\Phi_{PL}$ spectral data for **p(F/S-R)-20** co-polymers in solution and solid state.

| Parameters | p(F/S-NO2)-20 | p(F/S-F)-20 | p(F/S-SMe)-20 |
|---|---|---|---|
| $\lambda_{abs}$ (nm)[a,b] Tol | **381** | **390**, 350sh | **389** |
| $\lambda_{abs}$ (nm)[a,b] $CHCl_3$ | **382** | **392**, 350sh | **391** |
| $\lambda_{abs}$ (nm) [a,b] film | 290 ,**378** | 285, **390** | 280, **389** |
| $\lambda_{PL}$, ($\underline{\lambda_{exc}}$) (nm)[a,b,c] Tol | 414sh, **437**, 464sh,(*381*) | **436**, 463sh, (*390*) | **437**, 463sh, (*389*) |
| $\lambda_{PL}$, ($\underline{\lambda_{exc}}$) (nm)[a,b,c] $CHCl_3$ | 417, **452**, 478sh (*382*) | **466**, (*392*) | **467**, (*391*) |
| $\lambda_{PL}$, ($\underline{\lambda_{exc}}$) (nm)[a,b,c] film | 450, **536**, (*378*) | **477**, 458sh (*390*) | **483**, 456sh (*389*) |
| CIE (x, y) Tol | 0.153, 0.083 | 0.158, 0.073 | 0.152, 0.074 |
| CIE (x, y) $CHCl_3$ | 0.159, 0.143 | 0.156, 0.177 | 0.154, 0.174 |
| CIE (x, y) film | 0.344, 0.635 | 0.155, 0.213 | 0.154, 0.246 |

[a] sh–Shoulders. [b] Bold numbers are the strongest absorption or emission peaks. [c] Excitation wavelengths used for PL measurements ($\underline{\lambda_{exc}}$) are given in italic in brackets.

### 4.2.6.5 Photoluminescence quantum yields (PLQY) of p(F/S-R)-y co-polymers

Every series of co-polymers, **p(F/S-R)-y**, show bright emission colours in solution (**Figures 4.7–4.15**). The photoluminescence quantum yields (PLQY, $\Phi_{PL}$) in solution have been estimated by an absolute method using an integrating sphere. The integrated sphere used was tested by measuring the PLQY for standard compounds such as 9,10-diphenylanthracene (DPA) (PLQY = 90%), and anthracene (PLQY = 27%).[21,22] In chloroform and also in toluene, all polymers demonstrate very high PLQY values of $\Phi_{PL}^{abs}$ ~58–95%, comparable to the values reported in the literature for other polyfluorenes.[14] The PLQY values are also comparable to the values of unsubstituted co-polymers **p(F/S)-y**.[8] Solid state PLQY has been measured for spin coated films on a quartz substrate (from chloroform solution) by an absolute method using an integrating sphere. The values are expectedly lower (as is usual for solid state PLQY compared to that in solution) but still reasonably high, 5–27% (values of 8–21% are reported in the literature for unsubstituted co-polymers **p(F/S)-y**).[8] All the PLQY values are summarised in **Table 4.8**.

**Table 4.8:** PLQY of **p(F/S-R)-y** co-polymers in solutions and solid state.

| Co-polymer | $\Phi_{PL}^{abs}$ (%) toluene[a] | $\Phi_{PL}^{abs}$ (%) $CHCl_3$[a] | $\Phi_{PL}^{abs}$ (%) film[a] |
|---|---|---|---|
| **p(F/S-OMe)-5** | 89 | 67 | 13.3 |
| **p(F/S-OMe)-10** | 81 | 71 | 12.7 |
| **p(F/S-OMe)-20** | 72 | 66 | 7.4 |
| **p(F/S-OMe)-30** | 75 | 57 | 9.2 |
| **p(F/S-OMe)-50** | 65 | 60 | 8.4 |
| **p(F/S-$SO_2$Me)-1** | 94 | 95 | 20 |
| **p(F/S-$SO_2$Me)-5** | 81 | 69 | 23 |
| **p(F/S-$SO_2$Me)-10** | 80 | 67 | 18 |
| **p(F/S-$SO_2$Me)-15** | 75 | 59 | 14 |
| **p(F/S-$SO_2$Me)-20** | 76 | 60 | 13 |
| **p(F/S-$SO_2$Me)-30** | 75 | 60 | 13 |
| **p(F/S-$SO_2$Me)-40** | 70 | 58 | 09 |
| **p(F/S-$SO_2$Me)-50** | 61 | 74 | 12 |
| **p(F/S-CN)-1** | - | 94 | 18 |
| **p(F/S-CN)-5** | - | 80 | 18 |

| | | | |
|---|---|---|---|
| **p(F/S-CN)-10** | - | 70 | 8 |
| **p(F/S-CN)-15** | - | 66 | 7 |
| **p(F/S-CN)-20** | - | 63 | 5 |
| **p(F/S-CN)-30** | - | 59 | 6 |
| **p(F/S-CN)-40** | - | 65 | 9 |
| **p(F/S-CN)-50** | - | 73 | 27 |
| **p(F/S-$NO_2$)-20** | 50 | 47 | 0.1 |
| **p(F/S-F)-20** | 80 | 73 | 26 |
| **p(F/S-SMe)-20** | 76 | 64 | 8 |

$^{a}\Phi_{PL}^{abs}$ is an absolute PLQY in film measured using an integrated sphere.

#### 4.2.6.6 Lippert-Mataga equation studies of p(F/S-$SO_2$Me)-20 and p(F/S-$SO_2$Me)-50, solvents effects

After noticing a clear positive solvatochromic effect from toluene to chloroform on the light emitted by the co-polymers, it was decide to expand this study with more solvents. The solvents are classed in polarity order, from the least to the most polar and the co-polymer **p(F/S-$SO_2$Me)-20** was used for these studies because it is the one which has the highest red shift (ICT) to study the Lippert-Mataga equation.

From **Figure 4.16** and **Table 4.9**, it can be seen that the solvent polarity has almost no effect on the absorption spectrum, from methyl cyclohexane (dielectric permitivity $\varepsilon$ = 2.02) $\lambda_{max}$ = 384 nm to benzonitrile (dielectric permitivity $\varepsilon$ = 25.20) $\lambda_{max}$ = 400 nm and this is known due to the Franck-Condon principle. In contrast, there is a pronounced bathochromic shift in the PL spectrum by 122 nm from methyl cyclohexane to benzonitrile.

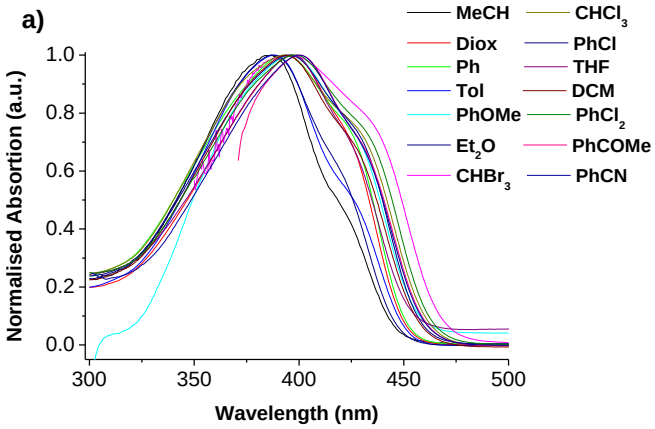


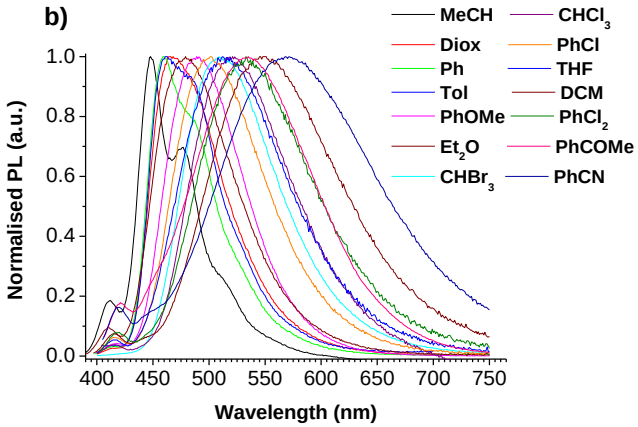


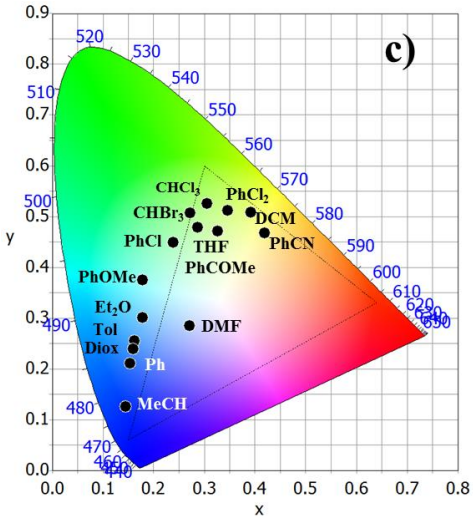


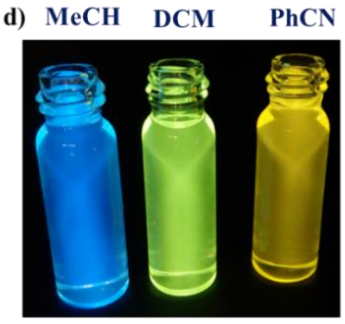


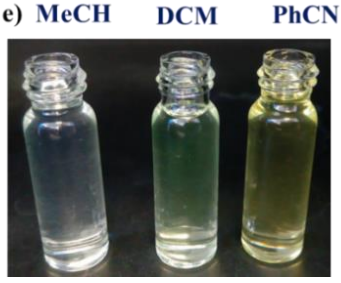


**Figure 4.16:** a) Normalised UV-Vis absorption spectra b) Normalised PL spectra. c) CIE diagram inset showing colours emitted under excitation of **p(F/S-SO$_2$Me)-20** in different solvents. d) Emission of polymer **p(F/S-SO$_2$Me)-20** in MeCH, DCM, and PhCN from left to right in chloroform solution under UV-light irradiation (360 nm) e) without UV-light.

**Table 4.9:** $\lambda_{abs}$ and $\lambda_{PL}$ for **p(F/S-$SO_2$Me)-20** co-polymers in solvents.

| **Solvent**[a] | **$\lambda_{abs}$ (nm)** [b, c] | **$\lambda_{PL}$ (nm),** ($\underline{\lambda_{exc}}$) (nm) [b, c, d] |
|---|---|---|
| **Methylcyclohexane** | **384**, 425sh | 412, **448**, 477, 510sh, (*384*) |
| **Dioxane** | **397,** 425sh | 414, **468**, (*397*) |
| **Benzene** | **394**, 421sh | 414, **460**, 485sh, (*394*) |
| **Toluene** | **395,** 426sh | **462,** (*395*) |
| **Anisole** | **396**, 430sh | 418, **489**, (*396*) |
| **$Et_2O$** | **387**, 422sh | 411, **480**, (*387*) |
| **Bromoform** | **394,** 440 sh | **510,** (*394*) |
| **Chloroform** | **394**, 425sh | **521**, (*394*) |
| **PhCl** | **396**, 433sh | 415, **501**, (*396*) |
| **THF** | **397** | 416, **514**, (*397*) |
| **DCM** | **394**, 424sh | 415, **549**, (*394*) |
| **$PhCl_2$** | **398**, 440sh | 417, **533**, (*398*) |
| **Acetophenone** | **401**, 450sh | 421, **534**, (*401*) |
| **PhCN** | **400**, 436sh | 420, 450sh, **570**, (*400*) |

[a] Solvent which used for the measurements. [b] sh-shoulders. [c] Bold numbers are the absorption maxima $\lambda_{abs}$. [d] For PL measurements, the excitation wavelengths are in italic ($\underline{\lambda_{exc}}$).

The Lippert-Mataga equation (5) is a plot, which permits how the solvent affects the energy difference between the ground state and the exited state to be calculated. This difference is called the Stokes shift, in $cm^{-1}$, and it depends on the refractive index (*n*), and the dielectric constant (ε) of the solvent.[23,24]

$$\bar{\nu}_A - \bar{\nu}_F = \frac{2}{hc}\left(\frac{\varepsilon - 1}{2\varepsilon + 1} - \frac{n^2 - 1}{2n^2 + 1}\right)\frac{(\mu_E - \mu_G)^2}{a^3} + constant \qquad (5)$$

In this equation *h* (= 6.6256 x $10^{-27}$ ergs) is Planck's constant, *c* (= 2.9979 x $10^{10}$ cm/s) is the speed of light, and *a* is the radius of the cavity in which the fluorophore resides. $\bar{\nu}_A$ and $\bar{\nu}_F$ are the wavenumbers ($cm^{-1}$) of the absorption and emission, respectively. Equation (5) is only an approximation, but there is reasonable correlation between the observed and calculated energy losses in non-protic solvents. The Lippert-Mataga equation (5) is an approximation in which the polarizability of the fluorophore and higher-order terms

are neglected. The polarizability of the solvent is a result of both the mobility of electrons in the solvent and the dipole moment of the solvent molecules. Each of these components has a different time dependence. Reorientation of the electrons in the solvent is essentially instantaneous. The high frequency polarizability $f(n)$ is a function of the refractive index ($n$). The polarizability of the solvent also depends on the dielectric constant (ε), which includes the effect of molecular orientation of the solvent molecules. Because of the slower timescale of molecular reorientation, this component is called the low frequency polarizability of the solvent. The difference between these two terms is the orientation polarizability equation (6).

$$\Delta f = \left(\frac{\varepsilon - 1}{2\varepsilon + 1} - \frac{n^2 - 1}{2n^2 + 1}\right) \qquad (6)$$

The dielectric constant (ε) is the basis for the orientation polarizability ($\Delta f$) and is used in the form of the Kirkwood functions $p = \frac{\varepsilon-1}{2\varepsilon+1}$.[25] **Table 4.10** shows the Lippert-Mataga parameters in different solvents. **Figures 4.17, 4.18** demonstrated clearly that changing the solvent polarity does not have an effect on the absorption of the fluorophore but it does affect the emission and Stokes shift values. Therefore, with increasing the orientation polarizability ($\Delta f$) or the Kirkwood parameter (p) the energy of emission decreases and the Stokes shift increases. The linearity of plots is often regarded as evidence for the dominant importance of general solvent effects in the spectral shifts. Specific solvent effects lead to nonlinear Lippert-Mataga plots.

**Table 4.10:** Lippert-Mataga and Kirkwood coefficients for **p(F/S-$SO_2$Me)-20.**

| **Solvent**[a] | **ε** [b] | **$n_D^{20}$** [c] | **p** [d] | **Δf** [e] | **$\lambda_{abs}$**[f]**(nm)** | ***E*$_{abs}$**[g]**(eV)** | **$\lambda_{PL}$**[f]**(nm)** | ***E*$_{PL}$**[g]**(eV)** | **Stokes shift (nm)** | **Stokes shift ($cm^{-1}$)** | **Stokes shift (eV)** |
|---|---|---|---|---|---|---|---|---|---|---|---|
| **Methyl cyclohexane** | 2.02 | 1.422 | 0.20238 | -0.00025 | 384 | 3.229 | 448 | 2.768 | 64 | 3720.2 | 0.461 |
| **Dioxane** | 2.25 | 1.4224 | 0.22727 | 0.024512 | 397 | 3.123 | 468 | 2.650 | 71 | 3821.4 | 0.474 |
| **Benzene** | 2.27 | 1.5011 | 0.22924 | 0.001642 | 394 | 3.147 | 460 | 2.696 | 66 | 3641.6 | 0.452 |
| **Toluene** | 2.38 | 1.4969 | 0.23958 | 0.013235 | 395 | 3.139 | 462 | 2.684 | 67 | 3671.4 | 0.455 |
| **Anisole** | 4.33 | 1.517 | 0.34472 | 0.112454 | 396 | 3.131 | 489 | 2.536 | 93 | 4802.6 | 0.596 |
| **Diethyl ether** | 4.33 | 1.3524 | 0.34472 | 0.166749 | 387 | 3.204 | 480 | 2.583 | 93 | 5006.5 | 0.621 |
| **Bromoform** | 4.39 | 1.584 | 0.34663 | 0.09587 | 394 | 510 | 510 | 3.147 | 2.431 | 5772.9 | 0.716 |
| **Chloroform** | 4.81 | 1.4458 | 0.35876 | 0.148295 | 394 | 3.147 | 521 | 2.380 | 127 | 6186.9 | 0.767 |
| **Chlorobenzene** | 5.62 | 1.524 | 0.37745 | 0.143166 | 396 | 3.131 | 501 | 2.475 | 105 | 5292.4 | 0.656 |
| **Tetrahydrofuran** | 7.58 | 1.4072 | 0.40718 | 0.209572 | 397 | 3.123 | 514 | 2.412 | 117 | 5733.7 | 0.711 |
| **Dichloromethane** | 8.93 | 1.4241 | 0.42047 | 0.217137 | 394 | 3.147 | 549 | 2.259 | 155 | 7165.8 | 0.889 |
| **Dichlorobenzene** | 9.93 | 1.5514 | 0.42809 | 0.186104 | 398 | 3.116 | 533 | 2.326 | 135 | 6363.9 | 0.789 |
| **Acetophenone** | 17.89 | 1.532 | 0.45922 | 0.22265 | 401 | 3.092 | 534 | 2.322 | 133 | 6211.1 | 0.770 |
| **Benzonitrile** | 25.20 | 1.528 | 0.47082 | 0.235388 | 400 | 3.100 | 570 | 2.175 | 170 | 7456.1 | 0.925 |

[a] Solvent used for the measurements. [b] Dielectric constant. [c] refractive index .[d] The Kirkwood p = $\frac{\varepsilon-1}{2\varepsilon+1}$. [e] Δf = $\frac{\varepsilon-1}{2\varepsilon+1} - \frac{n^2-1}{2n^2+1}$ . [f] Absorption maxima. [g] $E = \frac{1240}{\lambda}$

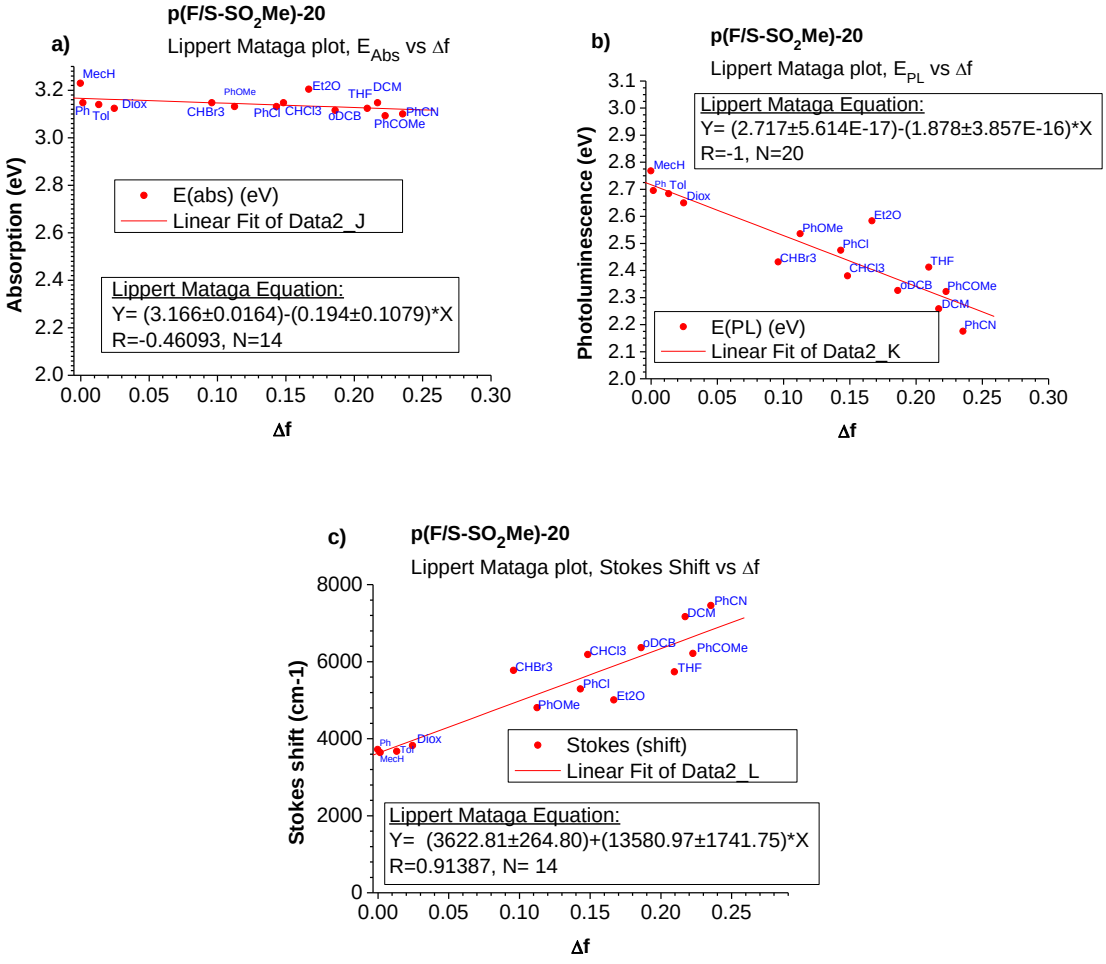


**Figure 4.17:** Lippert-Mataga plots for **p(F/S-SO2Me)-20** in different solvents. a) the orientation polarizability (Δ*f*) versus energy of absorption. b) the orientation polarizability (Δ*f*) versus energy of emission. c) the orientation polarizability (Δ*f*) versus Stokes shift.

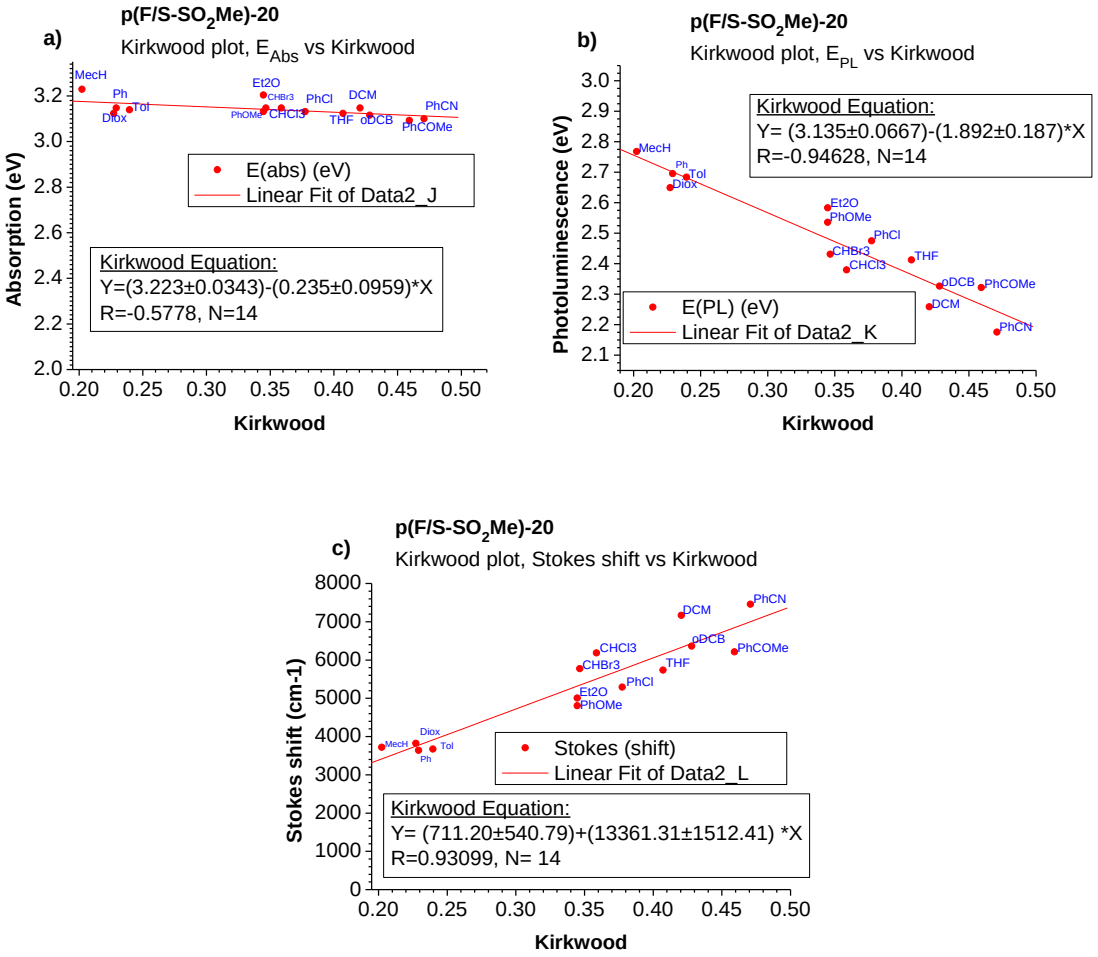


**Figure 4.18:** Kirkwood plots for **p(F/S-SO2Me)-20** in different solvents. a) The Kirkwood (p = $\frac{\varepsilon-1}{2\varepsilon+1}$) versus energy of absorption. b) The Kirkwood (p = $\frac{\varepsilon-1}{2\varepsilon+1}$) versus energy of emission. c) The Kirkwood (p = $\frac{\varepsilon-1}{2\varepsilon+1}$) versus Stokes shift.

After a clear hypsochromic shift was demonstrated for the **p(F/S-SO2Me)-50** co-polymer, it was decided to study this phenomenen in more detail by measuring the UV/PL of this polymer in different solvents and investigating the Lippert-Mataga, and Kirkwood equations. From **Figures 4.19–4.21** and **Tables 4.11, 4.12** it can be seen that the solvent polarity has almost no effect on the absorption spectrum of the **p(F/S-SO2Me)-50** polymer in toluene (dielectric permitivity ε = 2.43) $\lambda_{max}$ = 423 nm or benzonitrile (dielectric permitivity ε = 25.20) $\lambda_{max}$ = 429 nm, and this is known due to the Franck-Condon principle. In addition, the PL spectra also shows no change in maximum wavelength, which is because the **p(F/S-SO2Me)-50** co-polymer is a regular co-polymer between **S-SO2Me** and **F** units and also because the distance is too short between the units, thus the polarity of the co-

polymer is reduced compared to the **p(F/S-SO$_2$Me)-20** co-polymer, which leads to a decrease in the effectiveness of the solvent polarity on the light emitted and Stokes shift of the polymer.

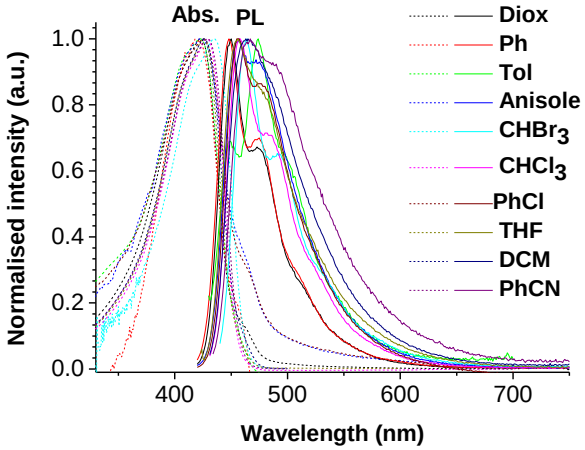


**Figure 4.19:** UV-Vis electron absorption and PL spectra of **p(F/S-SO$_2$Me)-50** in different solvents.

**Table 4.11:** $\lambda_{abs}$ and $\lambda_{PL}$ for **p(F/S-SO$_2$Me)-50** co-polymer in solutions.

| **Solvent**[a] | **$\lambda_{abs}$ (nm)** [b, c] | **$\lambda_{PL}$ (nm), ($\lambda_{exc}$) (nm)** [b, c, d] |
|---|---|---|
| **Dioxane** | **423** | **450**, 473, *(410)* |
| **Benzene** | **418** | 448, 475, *(410)* |
| **Toluene** | 405sh, **423** | **449**, 474, 500sh, (*423*) |
| **Anisole** | **422** | **457**, 501sh, *(410)* |
| **Bromoform** | 414sh, **435** | **463**, 493 |
| **Chloroform** | 410sh, **428** | **457**, 531sh, (*428*) |
| **PhCl** | **424** | **456**, 475, *(410)* |
| **THF** | 407sh, **425** | **456**, 482sh, (*425*) |
| **DCM** | 407sh, **426** | **464**, 486sh |
| **PhCN** | 406sh, **429** | **467**, 495sh |

[a] Solvent which used for the measurements. [b] sh-shoulders. [c] Bold numbers are the absorption maxima $\lambda_{abs}$. [d] For PL measurements, the excitation wavelengths are in italic ($\lambda_{exc}$).

**Table 4.12:** Lippert-Mataga coefficients for **p(F/S-$SO_2$Me)-50**

| Solvent[a] | ε[b] | $n_D^{20}$[c] | p [d] | Δf [e] | $\lambda_{abs}$[f] (nm) | $E_{abs}$[g] (eV) | $\lambda_{PL}$[f] (nm) | $E_{PL}$[g] (eV) | Stokes shift (nm) | Stokes shift ($cm^{-1}$) | Stokes shift (eV) |
|---|---|---|---|---|---|---|---|---|---|---|---|
| **Dioxane** | 2.25 | 1.4224 | 0.22727 | 0.20276 | 0.02451 | 423 | 450 | 27 | 2.931 | 2.756 | 1418.4 |
| **Benzene** | 2.27 | 1.5011 | 0.22924 | 0.2276 | 0.00164 | 418 | 448 | 30 | 2.967 | 2.768 | 1602.0 |
| **Toluene** | 2.38 | 1.4969 | 0.23958 | 0.22635 | 0.01324 | 423 | 474 | 51 | 2.931 | 2.616 | 2543.6 |
| **Anisole** | 4.33 | 1.517 | 0.34472 | 0.23227 | 0.11245 | 422 | 457 | 35 | 2.938 | 2.713 | 1814.8 |
| **Bromoform** | 4.39 | 1.584 | 0.34663 | 0.25075 | 0.09587 | 435 | 463 | 28 | 2.851 | 2.678 | 1390.2 |
| **Chloroform** | 4.81 | 1.4458 | 0.35876 | 0.21046 | 0.14829 | 428 | 457 | 29 | 2.897 | 2.713 | 1482.6 |
| **Chlorobenzene** | 5.62 | 1.524 | 0.37745 | 0.23429 | 0.14317 | 424 | 456 | 32 | 2.925 | 2.719 | 1655.1 |
| **Tetrahydrofuran** | 7.58 | 1.4072 | 0.40718 | 0.19761 | 0.20957 | 423 | 456 | 33 | 2.931 | 2.719 | 1710.8 |
| **Dichloromethane** | 8.93 | 1.4241 | 0.42047 | 0.20333 | 0.21714 | 426 | 464 | 38 | 2.911 | 2.672 | 1922.5 |
| **Benzonitrile** | 25.2 | 1.528 | 0.47082 | 0.23543 | 0.23539 | 429 | 467 | 38 | 2.890 | 2.655 | 1896.7 |

[a] Solvent which used for the measurements. [b] Dielectric constant. [c] refractive index .[d] $p = \frac{\varepsilon-1}{2\varepsilon+1}$. [e] $\Delta f = \frac{\varepsilon-1}{2\varepsilon+1} - \frac{n^2-1}{2n^2+1}$ . [f] Absorption maxima.

[g] $E = \frac{1240}{\lambda}$

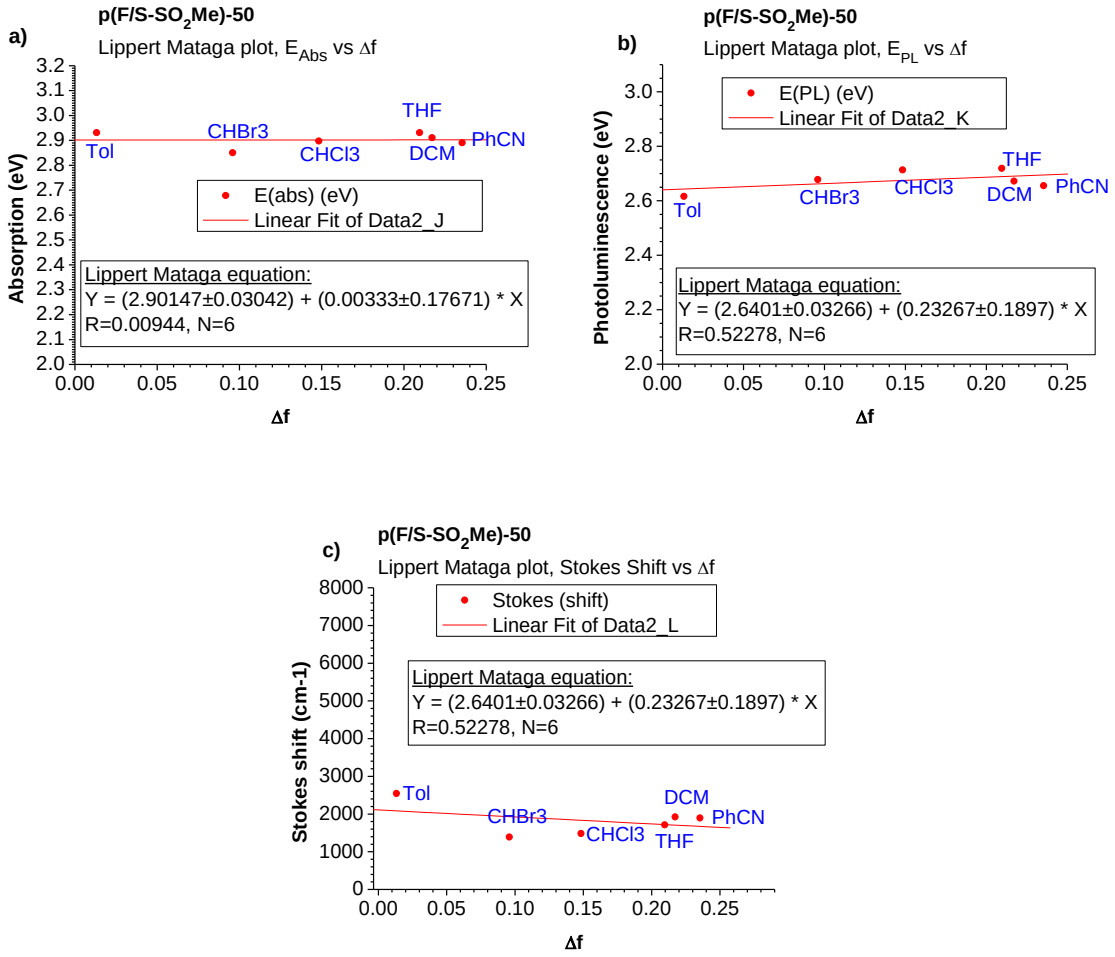


**Figure 4.20:** Lippert-Mataga plots for **p(F/S-SO2Me)-50** in different solvents. a) the orientation polarizability (Δ*f*) versus energy of absorption. b) the orientation polarizability (Δ*f*) versus energy of emission. c) the orientation polarizability (Δ*f*) versus Stokes shift.

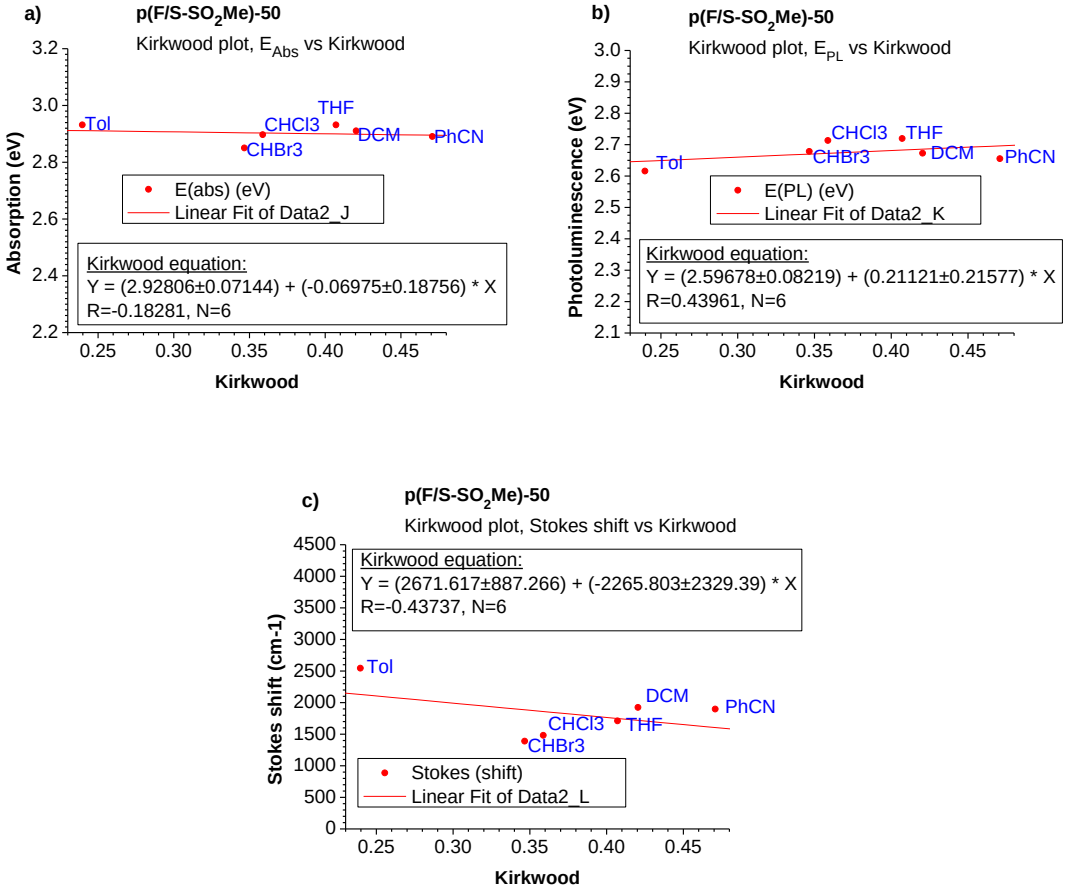


**Figure 4.21:** Kirkwood plots for **p(F/S-SO2Me)-50** in different solvents. a) The Kirkwood ($p = \frac{\varepsilon-1}{2\varepsilon+1}$) versus energy of absorption. b) The Kirkwood ($p = \frac{\varepsilon-1}{2\varepsilon+1}$) versus energy of emission. c) The Kirkwood ($p = \frac{\varepsilon-1}{2\varepsilon+1}$) versus Stokes shift.

### 4.3 Conclusion

Four novel families of statistical donor-acceptor poly(fluorene/1-substituted dibenzothiophene-*S*,*S*-dioxide) co-polymers **p(F/S-R)-y**, functionalised with various electron-donating (**R = OMe, SMe**) and electron-withdrawing (**R = CN, $SO_2$Me, F, $NO_2$**) groups on the dibenzothiophene-*S*,*S*-dioxide moiety have been successfully synthesised by a Suzuki coupling polymerisation of the corresponding monomers. The co-polymers were obtained with high molecular weights ($M_w$ = 9,656–71,780 Da, $M_n$ = 5,320–35,352 Da) and showed excellent thermal stabilities ($T_d$ = 377–423 °C). Cyclic voltammetry studies of co-polymer films showed that they can be electrochemically oxidised and reduced (p-doped and n-doped) and from their redox potential onsets, the HOMO and LUMO energies of these polymers have been estimated (HOMO = –6.13 to –5.76 eV; LUMO = –3.27 to –2.17 eV). Analysis of this data clearly shows the strong effect of the 1-substituents and feed ratio of the dibenzothiophene-*S*,*S*-dioxide moiety on the energy levels of the synthesised co-polymers: the introduction of an EDG results in an increase and the introduction of an EWG results in a decrease of both the HOMO and LUMO, respectively. UV-Vis electron absorption and PL spectral data have been obtained for the **p(F/S-R)-y** co-polymers in both solution and the solid state. The co-polymers are highly fluorescent in both solution (PLQY = 58-95%) and the solid state (PLQY = 9-23%). Their excitation leads to formation of local excited and intramolecular charge transfer state (which are in equilibrium) and fluorescence occurs with simultaneous emission from both excited states broadening the emission. The solvent polarity, solid state packing and the contents of the dibenzothiophene-*S*,*S*-dioxide moieties in the polymer chains change the contribution of LE and ICT emission and change the emission of the co-polymers from blue to bluish, greenish-white and a purely green colour.

## 4.4 Experimental Section

### 4.4.1 Chemicals and instruments

All the solvents and commercial chemicals, were used without further purification, and were supplied from Aldrich, Fisher, Acros, AlfaAesar, and Apollo Scientific chemical companies. Dry solvents for water-sensitive reactions or measurements were either commercially dried solvents or were dried in a still (reflux over Na for THF and toluene). Details of NMR and MS spectrometers, UV-Vis and PL spectrophotometers, PLQY measurements, GPC and flash chromatographs, freeze dryer, and TGA instruments are described in Chapters 2 and 3.

### 4.4.2 Synthesis

**Synthesis of tetrakis(triphenylphosphine)palladium(0).**[26]

$2\ PdCl_2 + 8\ PPh_3 + 5\ NH_2NH_2{\cdot}H_2O \longrightarrow 2\ Pd(PPh_3)_4 + 4\ NH_2NH_2{\cdot}HCl + N_2 + 5\ H_2O$

Under a nitrogen atmosphere, palladium dichloride (3.04g, 17.0 mmol), triphenylphosphine (22.3 g, 85.0 mmol), and DMSO (200 mL) were added to a two-necked, 500 mL, round-bottomed flask and the suspension was stirred and heated to 140 °C until complete solution occurred. Stirring was then continued for 15 minutes without the heat source, before hydrazine monohydrate (3.5 mL, 68.0 mmol) was added dropwise over approximately 1 minute. Upon the addition of hydrazine monohydrate, the solution turned a deep red colour with a beige-yellow foam sitting on top; nitrogen was also produced. The solution was then cooled using a water bath, during which time sand coloured crystals formed, and the mixture was allowed to cool to room temperature. The solution was then filtered under nitrogen, through a coarse sintered glass funnel. The product was then washed with methylated spirits (2 × 20 mL) and diethyl ether (6 × 20 mL). The $Pd(Ph_3P)_4$ formed was then left to dry under a slow stream of nitrogen for 6 h, freeze dried for 7 days and stored in a freezer, resulting in a brown/yellow coloured powder (16.3 g, 83%).

**Synthesis of random (9,9-dioctylfluorene)-(1-substituted-dibenzothiophene-*S*,*S*-dioxide) co-polymers (p(F/S-R)-y.**

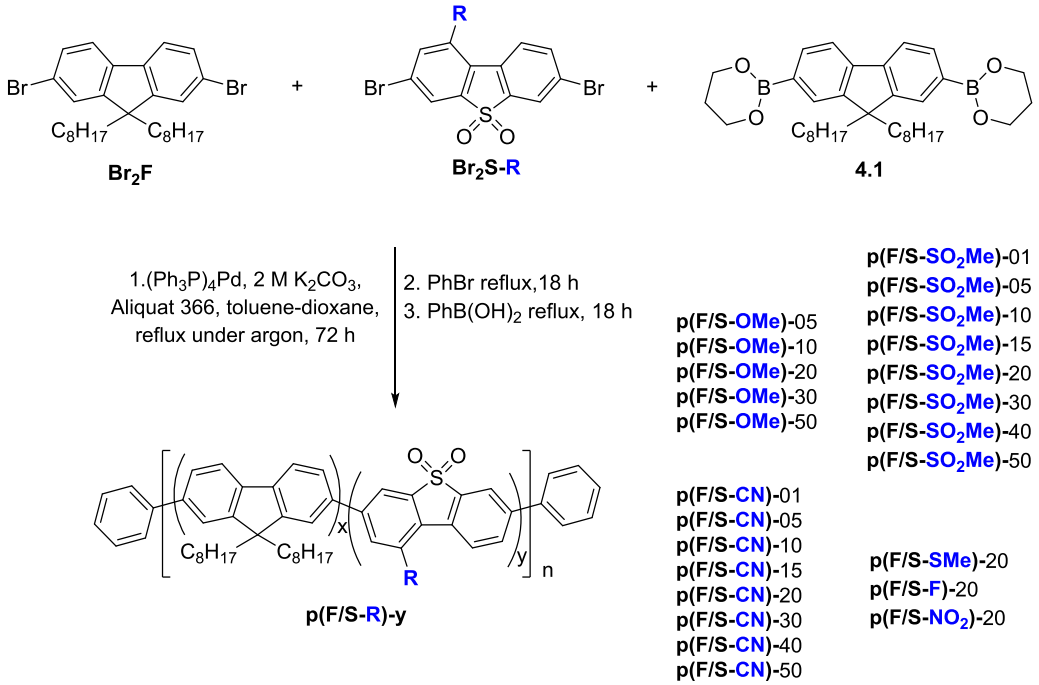


**Scheme 4.3:** The reaction scheme for the synthesis of **p(F/S-R)-y**.

**Table 4.13:** The ratio of monomers for **p(F/S-R)-y**.

| Co-polymers | compound **$Br_2F$** | | compound **$Br_2S$-R** | | Theo. Yield |
|---|---|---|---|---|---|
| **p(F/S-$SO_2$Me)-y** | **mmol** | **mg** | **mmol** | **mg** | **mg** |
| **p(F/S-$SO_2$Me)-1**[a] | 0.49 | 269 | 0.01 | 3 | 272 |
| **p(F/S-$SO_2$Me)-5** | 0.45 | 247 | 0.05 | 23 | 386 |
| **p(F/S-$SO_2$Me)-10** | 0.40 | 219 | 0.10 | 45 | 381 |
| **p(F/S-$SO_2$Me)-15** | 0.35 | 193 | 0.15 | 68 | 376 |
| **p(F/S-$SO_2$Me)-20** | 0.30 | 166 | 0.20 | 91 | 371 |
| **p(F/S-$SO_2$Me)-30** | 0.20 | 110 | 0.30 | 137 | 361 |
| **p(F/S-$SO_2$Me)-40** | 0.10 | 55 | 0.40 | 181 | 351 |
| **p(F/S-$SO_2$Me)-50** | 0.00 | 0 | 0.50 | 226 | 341 |
| **p(F/S-CN)-1**[a] | 0.49 | 269 | 0.01 | 3 | 272 |
| **p(F/S-CN)-5** | 0.45 | 247 | 0.05 | 21 | 338 |

| | | | | | |
|---|---|---|---|---|---|
| **p(F/S-CN)-10** | 0.40 | 219 | 0.10 | 42 | 376 |
| **p(F/S-CN)-15** | 0.35 | 193 | 0.15 | 62 | 370 |
| **p(F/S-CN)-20** | 0.30 | 166 | 0.20 | 83 | 363 |
| **p(F/S-CN)-30** | 0.20 | 110 | 0.30 | 125 | 350 |
| **p(F/S-CN)-40** | 0.10 | 55 | 0.40 | 166 | 336 |
| **p(F/S-CN)-50** | 0.00 | 0 | 0.50 | 208 | 323 |
| **p(F/S-OMe)-5**[a] | 0.315 | 173 | 0.035 | 14 | 0.267 |
| **p(F/S-OMe)-10**[a] | 0.28 | 154 | 0.07 | 28 | 0.262 |
| **p(F/S-OMe)-20**[a] | 0.21 | 115 | 0.14 | 57 | 0.252 |
| **p(F/S-OMe)-30**[a] | 0.14 | 77 | 0.21 | 85 | 0.242 |
| **p(F/S-OMe)-50**[a] | 0.00 | 0 | 0.35 | 141 | 0.222 |
| **p(F/S-SMe)-20**[a] | 0.21 | 115 | 0.14 | 59 | 0.254 |
| **p(F/S-F)-20**[a] | 0.21 | 115 | 0.14 | 55 | 0.250 |
| **p(F/S-$NO_2$)-20**[a] | 0.21 | 115 | 0.14 | 59 | 0.254 |

[a] Polymerisation was carried out on a smaller scale, 70% of the molar amount of the following polymerisations.

9,9-Dioctylfluorene-2,7-diboronic acid *bis*(1,3-propanediol) ester (**4.1**) (0.280 g, 0.50 mmol) was placed in the vials of a Radleys Carousel Reaction Station 12+. Different amounts of 9,9-Dioctyl-2,7-dibromofluorene (**$Br_2$F**) and the 1-*R*-3,7-dibromodibenzothiophene-*S*,*S*-dioxide (**$Br_2$S-R**) monomers (**Table 4.13**) were then added to each vial, along with $Pd(Ph_3P)_4$ (0.012 g, 2 mol%). Dioxane (1 mL), toluene (3 mL) and 2 M potassium carbonate (1 mL) were then added along with Aliquat 366 (~0.080 g, ~0.2 mmol). The resulting mixtures were heated to reflux under argon with stirring. Reflux began once the reaction had reached 85 °C and the solids gradually dissolved from the mixture containing 1% (**$Br_2$S-R**) to that containing 50%.

At this point there was a dark yellow/greenish fluorescence from all the reaction mixtures. The reactions were left to reflux under argon for 72 h. Phenylboronic acid (~0.047 g, ~$2.14\times10^{-3}$ mmol) in dioxane (0.2 mL) was then added, and the mixtures were heated under reflux, under an argon atmosphere for 18 h. After this time bromobenzene (~0.025 g, ~0.16 mmol) was added, and reflux was continued under argon for a further 18 h. The reactions were then stopped and the solvents were evaporated off under a stream of nitrogen. The resulting products were dissolved in chloroform (5 mL) and pipetted into a mixture of

rapidly stirring methanol : water : concentrated hydrochloric acid (100 mL : 50 mL : 10 mL). The products formed dark green precipitates, and upon precipitation the mixtures were gentley stirred for approximately 1 h. The precipitates were then collected by filtration using a fine glass sinter and washed with water (150 mL) and methanol (150 mL), and then dried under vacuum. The polymers were extracted with methanol (~100 mL, 24 h), to remove inorganic impurities, monomers, and other low molecular impurities using a Soxhlet extractor. The polymers were again extracted using acetone (~100 mL, 24 h), to remove low molecular weight co-polymers, and then chloroform (~100 mL, 2 h), and the products obtained at this stage were concentrated down to a small volume and precipitated out into rapidly stirring methanol. The precipitates were left to stir (1 h), then filtered and washed with methanol (~20 mL) and dried in a freeze dryer to give **p(F/S-R)-y** co-polymers ranging from a light yellow powder to a light green powder and dark green fibrous strands (see **Table 4.14**).

**Table 4.14:** Weights and yields of extracted fractions of **p(S-R)-y** co-polymers.

| **Co-polymer** | Acetone Fraction[a] | **Chloroform Fraction[b]** | Appearance[c] |
|---|---|---|---|
| **p(F/S-$SO_2$Me)-01** | 80 mg, 29% | **178 mg, 65%** | green |
| **p(F/S-$SO_2$Me)-05** | 30 mg, 8% | **339 mg, 88%** | green |
| **p(F/S-$SO_2$Me)-10** | 43 mg,11.3% | **307 mg, 81%** | green yellowish |
| **p(F/S-$SO_2$Me)-15** | 74 mg, 19.7% | **264 mg, 70%** | green yellowish |
| **p(F/S-$SO_2$Me)-20** | 57 mg, 15.4% | **313 mg, 84%** | green yellowish |
| **p(F/S-$SO_2$Me)-30** | 70 mg, 19.4% | **273 mg, 76%** | green yellowish |
| **p(F/S-$SO_2$Me)-40** | 30 mg, 8.5% | **297 mg, 85%** | green yellowish |
| **p(F/S-$SO_2$Me)-50[d]** | 4 mg, 1.2% | **243 mg, 71%** | green |
| **p(F/S-CN)-01** | 84 mg, 31% | **173 mg, 64%** | green |
| **p(F/S-CN)-05** | 38 mg, 9.9% | **320 mg, 86%** | green |
| **p(F/S-CN)-10** | 71 mg, 18.9% | **290 mg, 77%** | green |
| **p(F/S-CN)-15** | 149 mg, 40.0% | **218 mg, 59%** | green yellowish |
| **p(F/S-CN)-20** | 114 mg, 31.4% | **241 mg, 66%** | green yellowish |
| **p(F/S-CN)-30** | 102 mg, 29.1% | **246 mg, 70%** | green yellowish |
| **p(F/S-CN)-40** | 50 mg, 14.9% | **206 mg, 61%** | green |
| **p(F/S-CN)-50[e]** | 4 mg, 1.2% | **147 mg, 46%** | yellow |
| **p(F/S-OMe)-05** | 124 mg, 46% | **129 mg, 48%** | dark green |
| **p(F/S-OMe)-10** | 131 mg, 50% | **126 mg, 48%** | dark green |
| **p(F/S-OMe)-20** | 97 mg, 39% | **134 mg, 53%** | dark green |
| **p(F/S-OMe)-30** | 157 mg, 65% | **75 mg, 31%** | dark green |
| **p(F/S-OMe)-50** | 98 mg, 44% | **116 mg, 52%** | dark green |
| **p(F/S-SMe)-20** | 50 mg, 20% | **205 mg, 81%** | green |
| **p(F/S-F)-20** | 50 mg, 20% | **196 mg, 78%** | green yellowish |
| **p(F/S-$NO_2$)-20[f]** | 54 mg, 21% | **32 mg, 13%** | orange |

[a] Extraction time was ~ 24 h. [b] Extraction time was ~ 2 h. [c] Solid material for chloroform fraction. [d] 2nd chloroform fraction 75 mg (22%). [e] Insoluble fraction 148 mg (46%). [f] Insoluble fraction 159 mg (63%).

**p(F/S-$SO_2$Me)-01**

$\delta_H$ (400 MHz, $CDCl_3$): 7.93–7.76 (m, 2H), 7.76–7.52 (m, 4H), 2.26–1.80 (m, 4H), 1.41–1.00 (m, 20H), 0.95–0.61 (m, 10H).

**p(F/S-$SO_2$Me)-50**

$\delta_H$ (400 MHz, $CDCl_3$): 9.05 (d, *J* = 7.6 Hz, 1H), 8.80 (s, 1H), 8.47 (s, 1H), 8.30 (s, 1H), 8.13 (d, *J* = 7.6 Hz, 1H), 7.93–7.76 (m, 2H), 7.76–7.52 (m, 4H), 3.39 (s, 3H, $CH_3$) 2.27–1.90 (m, 4H), 1.42–1.01 (m, 20H), 0.90–0.59 (m, 10H).

**p(F/S-CN)-01**

$\delta_H$ (400 MHz, $CDCl_3$): 7.93–7.76 (m, 2H), 7.76–7.52 (m, 4H), 2.26–1.80 (m, 4H), 1.41–1.00 (m, 20H), 0.95–0.61 (m, 10H).

**p(F/S-CN)-50**

$\delta_H$ (400 MHz, $CDCl_3$): 8.78 (d, *J* = 7.8 Hz 1H), 8.39 (s, 1H), 8.29–8.18 (m, 2H), 8.11 (d, *J* = 8.0 Hz, 1H), 8.04–7.85 (m, 2H), 7.79–7.54 (m, 4H), ), 2.26–1.80 (m, 4H), 1.41–1.00 (m, 20H), 0.95–0.61 (m, 10H).

## References


1 U. Scherf, and E. J. W. List, Semiconducting polyfluorenes-towards reliable structure-property relationships, *Adv. Mater.*, **2002**, *14*, 477–487. DOI: 10.1002/1521-4095(20020404)14:7<477

2 A. J. Cadby, P. A. Lane, M. Wohlgenannt, C. An, Z. V. Vardeny, and D. D. C. Bradley, Optical studies of photoexcitations of poly(9,9-dioctylfluorene), *Synth. Metals*, **2000**, *111*, 515–518. DOI: 10.1016/S0379-6779(99)00409-9

3 I. I. Perepichka, I. F. Perepichka, M. R. Bryce, and L.-O. Pälsson, Dibenzothiophene-*S,S*-dioxide–fluorene co-oligomers. Stable, highly-efficient blue emitters with improved electron affinity, *Chem. Commun.*, **2005**, *1*, 3397–3399. DOI: 10.1039/b417717g

4 Z. R. Grabowski, and K. Rotkiewicz, Structural Changes Accompanying Intramolecular Electron Transfer: Focus on Twisted Intramolecular Charge-Transfer States and Structures, *Chem. Rev.*, **2003,** *103,* 3899–4031. DOI: 10.1021/cr940745l

5 E. Lippert, W. Lìder, F. Moll, W. Nogele, H. Boos, H. Prigge, and I. Seibold-Blankenstein, Umwandlung von Elektronenanregungsenergie, *Angew. Chem*. **1961**, *73*, 695–706. DOI: 10.1002/ange.19610732103

6 C. Zhong, The driving forces for twisted or planar intramolecular charge transfer, *Phys. Chem. Chem. Phys.*, **2015**, *17*, 9248–9257. DOI: 10.1039/c4cp02381a

7 F. B. Dias, S. King, A. P. Monkman, I. I. Perepichka, M. A. Kryuchkov, I. F. Perepichka, and M. R. Bryce, Dipolar stabilization of emissive singlet charge transfer excited states in polyfluorene co-polymers, *J. Phys. Chem. B*, **2008**, *112*, 6557–6566. DOI: 10.1021/jp800068d

8 S. M. King, I. I. Perepichka, I. F. Perepichka, F. B. Dias, M. R. Bryce, and A. P. Monkman, Exploiting a dual-fluorescence process in fluorene dibenzothiophene-*S,S*-dioxide co-polymers to give efficient single polymer LEDs with broadened emission, *Adv. Funct. Mater.*, **2009**, *19*, 586–591. DOI: 10.1002/adfm.200801237

9 G. Klaerner, and R. D. Miller, Polyfluorene derivatives: effective conjugation lengths from well-defined oligomers, *Macromolecules*, **1998**, *31*, 2007–2009. DOI: 10.1021/ma971073e

10 E. Wang, C. Li, Y. Mo, Y. Zhang, G. Ma, W. Shi, J. Peng, W. Yang, and Y. Cao, Poly(3,6-silafluorene-co-2,7-fluorene)-based high-efficiency and color-pure blue light-emitting polymers with extremely narrow band-width and high spectral stability, *Mater. Chem.*, **2006**, *16*, 4133–4140. DOI: 10.1039/B609250K

11 C. M. Cardona, W. Li, A. E. Kaifer, D. Stockdale, and G. C. Bazan, Electrochemical Considerations for Determining Absolute Frontier Orbital Energy Levels of Conjugated Polymers for Solar Cell Applications, *Adv. Mater*., **2011**, *23*, 2367–2371. DOI: 10.1002/adma.201004554

12 R. Holze, Optical and Electrochemical Band Gaps in Mono-, Oligo-, and Polymeric Systems: A Critical Reassessment, *Organometallics*, **2014**, *33*, 5033−5042. DOI: 10.1021/om500604z

13 W. Yang, J. Huang, C. Liu, Y. Niu, Q. Hou, R. Yang, and Y. Cao, Soluble eggshell membrane protein: Preparation, characterization and biocompatibility, *Polymer*, **2004**, *45*, 865–872. DOI: 10.1016/j.polymer.2003.11.052

14 M. Kreyenschmidt, G. Klaerner, T. Fuhrer, J. Ashenhurst, S. Karg, W. D. Chen, V. Y. Lee, J. C. Scott, and R. D. Miller, Thermally stable blue-light-emitting co-polymers of poly(alkylfluorene), *Macromolecules*, **1998**, *31*, 1099–1103. DOI: 10.1021/ma970914e

15 J. Cornil, I. Gueli, A. Dkhissi, J. C. Sancho-Garcia, E. Hennebicq, J. P. Calbert, V. Lemaur, D. Beljonne, and J. L. Bre´das, Electronic and optical properties of polyfluorene and fluorene-based copolymers: A quantum-chemical characterization, *Journal of Chemical Physics*, **2003**, *18*, 6615–6623. DOI: 10.1063/1.1561054

16 F. Ji-kang, Z. Jing-hua, R. Ai-min, R. Xue-qin, and L. Yuan-yuan, Theoretical Investigation on the Luminescent Properties of Polyfluorene and Poly(fluorene-co-thiophene), *Chem. Res. Chinese Universities,* **2009**, *25(5)*, 711–718. DOI: 1005-9040(2009)-05-711-08

17 N. A. Sánchez-Bojorge, L. M. Rodríguez-Valdez, and N. Flores-Holguín, DFT calculation of the electronic properties of fluorene-1,3,4-thiadiazole oligomers, *J. Mol. Model*, **2013**, *19*, 3537–3542. DOI 10.1007/s00894-013-1878-9

18 R. Holze, Optical and Electrochemical Band Gaps in Mono⁻, Oligo⁻, and Polymeric Systems: A Critical Reassessment, *Organometallics*, **2014**, *33*, 5033–5042. DOI: 10.1021/om500604z

19 M. K. Singh, H. Pal, A. C. Bhasikuttan, and A. V. Sapre, Dual Solvatochromism of Neutral Red, *Photochemistry and Photobiology*, **1998**, *68(1)*, 32–38. DOI: 10.1111/j.1751-1097.1998.tb03249.x

20 P. E. Shaw, and P. L. Burn, Real-time fluorescence quenching-based detection of nitro-containing explosive vapours: what are the key processes?, *Phys. Chem. Chem. Phys.*, **2017**, *19*, 29714–29730. DOI: 10.1039/c7cp04602b

21 Yvon, Horiba Jobin, A guide to recording fluorescence quantum yields, *HORIBA, Jobin Yvon Ltd., Stanmore, Middlesex, UK*, **2012**.

22 C. Würth, M. Grabolle, J. Pauli, M. Spieles, and U. R.-Genger**,** Relative and absolute determination of fluorescence quantum yields of transparent samples, *nature protocols*, **2013**, *8 NO.8*, 1535–1550. DOI:10.1038/nprot.2013.087

23 V. E. Lippert, Spektroskopische bistimmung des dipolmomentes aromatischer verbindungen im ersten angeregten singulettzustand, *Z. Electrochem*, **1957**, *61*, 962–975.

24 N. Mataga, Y. Kaifu, and M. Kolzumi, Solvent Effects upon Fluorescence Spectra and the Dipolemoments of Excited Molecules, *Bull Chem. Soc. Jpn*, **1956**, *29*, 465–470.

25 C. Reichardt, Empirical Parameters of Solvent Polarity as Linear Free-Energy Relationships, *Angew. Chem. Lnt. Ed. Engl.*, **1979**, *18*, 98–110.

26 D. R. Coulson, L. C. Satek, and S. O. Grim, Tetrakis (triphenylphosphine) palladium (0), *Inorganic Syntheses*, **2007**, *13*, 121–124. DOI: 10.1002/9780470132593.ch28

# CHAPTER 5
# Conclusions and Future Work

## 5.1 Conclusions

In this project novel classes of light-emitting polydibenzothiophene-*S*,*S*-dioxide based homopolymers and co-polymers, functionalised with different groups at position 1 of the dibenzothiophene-*S*,*S*-dioxide moieties, with tuneable optical and electronic properties, have been successfully developed.

Synthetic methodologies to introduce a wide range of both electron-donating and electron-withdrawing substituents onto position 1 of the 3,7-dibromodibenzothiophene-*S*,*S*-dioxide monomers were elaborated (see **Figure 5.1**). 1-Amino-3,7-dibromodibenzothiophene-*S*,*S*-dioxide (**$Br_2S$-$NH_2$**) was considered a useful synthon for this work, which was then converted into a wide range of 1-substituted dibenzothiophene-*S*,*S*-dioxide monomers *via* diazonium chemistry. The multistep reaction route to the key intermediate, **$Br_2S$-$NH_2$**, started from commercially available dibenzothiophene, followed by oxidation, bromination, nitration, and reduction. Attention was also paid to scaling up the reactions and optimisation of the conditions, to elaborate convenient and efficient methods for their synthesis and purification. Having the **$Br_2S$-$NH_2$** monomer in hand, the amino group was converted (*via* diazonium salts) into four different groups (OH, CN, I and F). A series of 1-alkoxy-3,7-dibromodibenzothiophene-*S*,*S*-dioxide **$Br_2S$-OR** monomers were then synthesised by alkylation of **$Br_2S$-OH** with alkyl halides and alkyl tosylates.

Replacement of the $NH_2$ group in **$Br_2S$-$NH_2$** by an SR group by classical reaction *via* a diazonium salt ($-N_2^+$) was not possible as diazonium salts oxidise thiols or disulfides instead of a nucleophilic substitution reaction occuring. This transformation was, therefore performed by other methods under milder conditions using iso-amyl nitrite as a nitrosation reagent in organic solvents. After obtaining the **$Br_2S$-SR** monomers, they were then successfully oxidised to obtain **$Br_2S$-$SO_2R$** monomers.

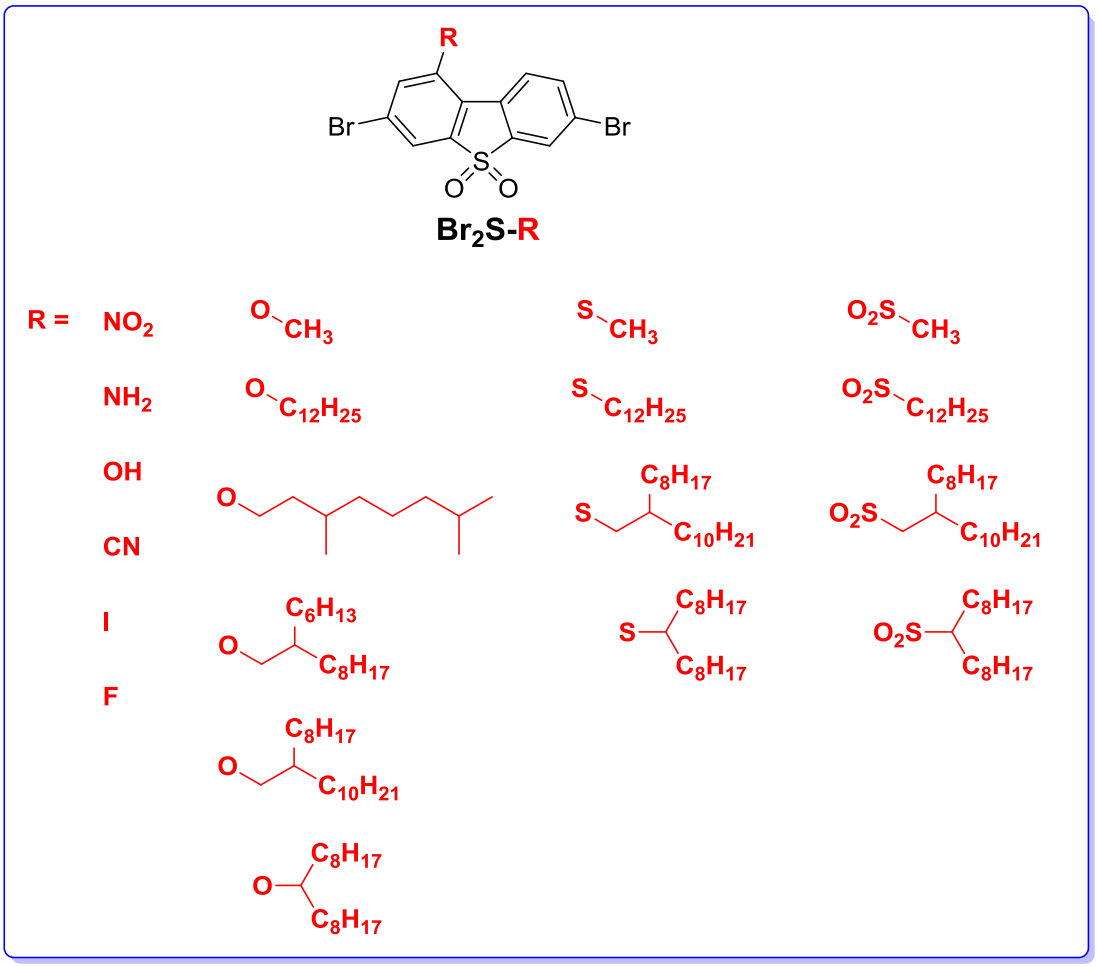


**Figure 5.1:** Structures of 1-functionalised dibenzothiophene-*S*,*S*-dioxide **Br$_2$S-R** monomers.

The first, yet unknown as a class, soluble conjugated dibenzothiophene-*S*,*S*-dioxide homopolymers as n-type electron deficient polymers with various electron-donating and electron-withdrawing alkyl groups have been successfully synthesised by using a Ni-mediated coupling polymerisation method (see **Figure 5.2**). Extractions of the homopolymers display part solubility in chloroform with average yields of ~25%. They showed excellent thermal stabilities ($T_d$ = 380–388 °C). Cyclic voltammetry studies of polymer films showed that they can be electrochemically oxidised and reduced (p-doped and n-doped) and from their redox potential onsets, the HOMO and LUMO energies of these polymers have been estimated (HOMO = –6.31 to –5.98 eV, LUMO = –3.86 to –3.47 eV). DFT calculations at the B3LYP/6-31G(d) level of theory have been performed for model 1-substituted polydibenzothiophene-*S*,*S*-dioxide (from 1 to 20 repeating dibenzothiophene-

*S*,*S*-dioxide units). The HOMO and LUMO energy levels derived for 1-substituted polydibenzothiophene-*S*,*S*-dioxide, fit well with the CV data showing the pronounced effect of the substitution at the 1-position on the frontier orbital energies of polydibenzothiophene-*S*,*S*-dioxide.

These novel homopolymers are highly fluorescent, displaying clear blue-light emission with absorption and emission studies in chlorobenzene solutions ($\lambda_{abs}$ = 380–420 nm, $\lambda_{PL}$ = 425–435 nm). Solid-state emission of these homopolymers exhibits a shift to a highly fluorescent greenish-yellow colour. A variety of experiments were carried out to see why there was such a big red shift between the solution and solid state. The initial thoughts were that it was due to the charge transfer effect, but upon further analysis it became apparent that it was the result of a molecular packing of polymer chains in the solid state. Annealing experiments were carried out to investigate whether the results of the experiment were due to the reorganisation of the polymer chain. The experiment showed that they are thermally stable and they do in fact red shift with an increase in temperature.

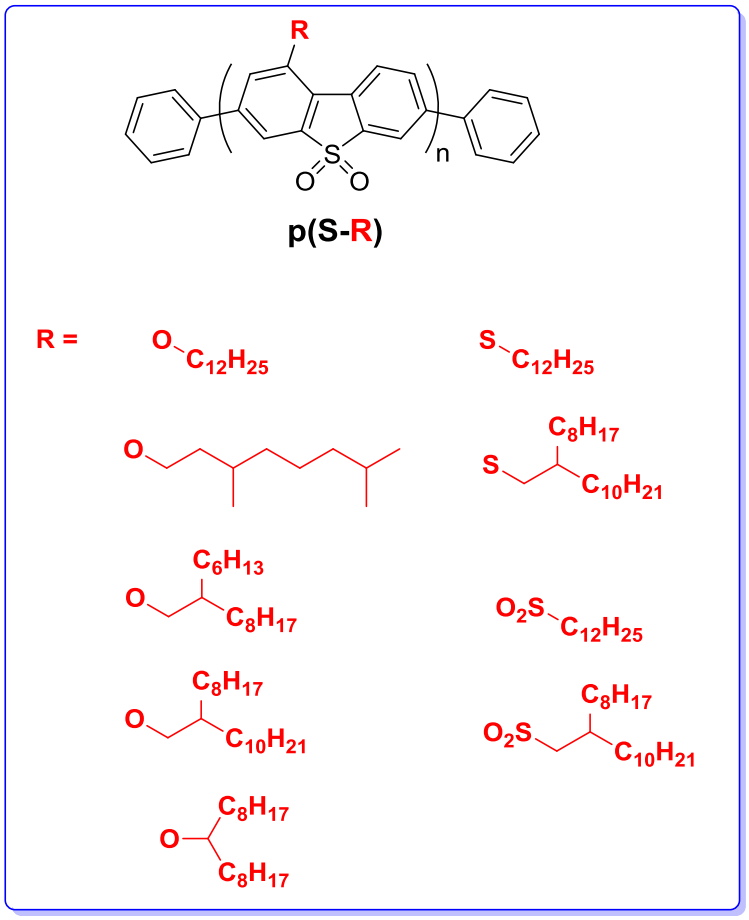


**Figure 5.2:** Structures of 1-functionalised dibenzothiophene-*S*,*S*-dioxide **p(S-R)** homo polymers.

Four novel families of statistical donor-acceptor poly(fluorene/1-substituted dibenzothiophene-*S*,*S*-dioxide) co-polymers **p(F/S-R)-y**, functionalised with various electron-donating (**R = OMe, SMe**) and electron-withdrawing (**R = CN, $SO_2$Me, F, $NO_2$**) groups on the dibenzothiophene-*S*,*S*-dioxide moiety have also been successfully synthesised using a Suzuki coupling polymerisation of the corresponding monomers (see **Figure 5.3**). The co-polymers were obtained with high molecular weights ($M_w$ = 9,656–71,780 Da, $M_n$ = 5,320–35,352 Da) and showed excellent thermal stabilities ($T_d$ = 377–423 °C). Cyclic voltammetry studies of the co-polymer films showed that they can be electrochemically oxidised and reduced (p-doped and n-doped) and from their redox potential onsets, the HOMO and LUMO energies of these polymers have been estimated (HOMO = –6.13 to –5.76 eV; LUMO = –3.27 to –2.17 eV). Analysis of this data clearly shows the strong effect of the 1-substituents and feed ratio of the dibenzothiophene-*S*,*S*-dioxide moiety on the

energy levels of the synthesised co-polymers: the introduction of an EDG results in an increase and the introduction of an EWG results in a decrease of both the HOMO and LUMO, respectively.

UV-Vis electron absorption and PL spectral data have been obtained for the **p(F/S-R)-y** co-polymers in both solution and the solid state. The co-polymers are highly fluorescent in both solution (PLQY = 58-95%) and the solid state (PLQY = 9-23%). Their excitation leads to formation of a local excited and intramolecular charge transfer state (which are in equilibrium) and fluorescence occurs with simultaneous emission from both excited states broadening the emission. The solvent polarity, solid state packing and the contents of the dibenzothiophene-*S*,*S*-dioxide moieties in the polymer chains change the contribution of LE and ICT emission and change the emission of the co-polymers from blue to bluish, greenish-white and a purely green colour. An interesting phenomenon was observed, in that for the **p(F/S-$SO_2$Me)-20** and **p(F/S-CN)-20** co-polymers the emission is from the ICT state at the maximum due to the excitation being localized on both the electron-donating group (**F** units) and the electron-accepting group (**S-R** unit). This is due to the **S-R** acceptor units being stronger relative to the **F** donor unit therefore each **S-$SO_2$Me** or **S-CN** unit is statistically equal to four **F** units to make the charge transfer in the excited state. With an increase in the ratio of the **S-$SO_2$Me** or **S-CN** units in the polymer backbone up to 50% (**p(F/S-$SO_2$Me)-50** and **p(F/S-CN)-50**), a hypsochromic shift was observed. This might be because lowering the HOMO (which is located on the **F** unit) results in an increase in the HOMO-LUMO band gap.

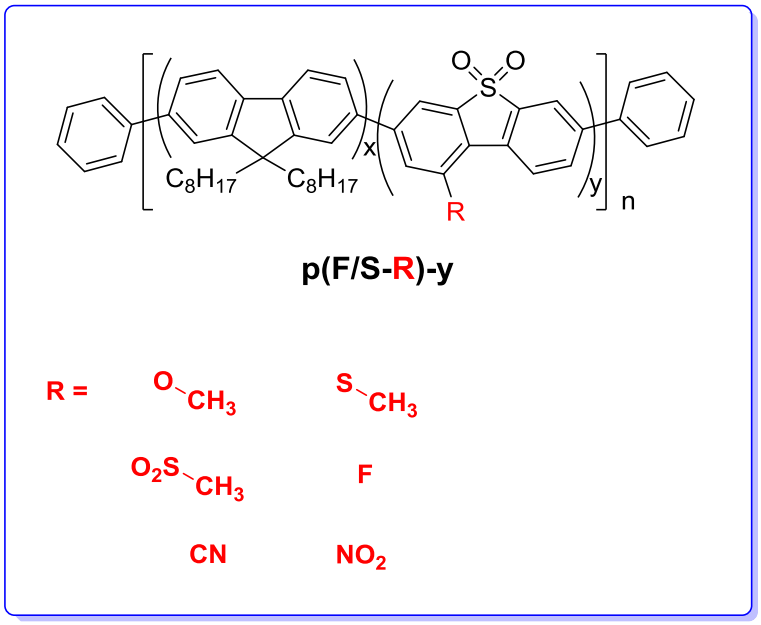


**Figure 5.3:** Structures of fluorene/1-functionalised dibenzothiophene-*S*,*S*-dioxide **p(F/S-R)-y** co-polymers.

## 5.2 Future work

### 5.2.1 Synthesis of fully soluble dibenzothiophene-*S*,*S*-dioxide homopolymers

In this project, only 25% of the homo polymers **p(S-R)** were soluble in the chloroform fraction (with reasonable molecular weights). However, a lot of material remained insoluble (as an insoluble fraction) in the extraction thimble, which have higher molecular weights compared to the chloroform fraction. This occurs because the solubilising groups (**OR**, **SR**, and **$SO_2$R**) do not have enough of an effect to obtain fully soluble polymers in common organic solvents (chloroform, toluene, DCM, THF, *etc*). Therefore, other ways could be investigated in future work to obtain polymers with improved solubility. Firstly, by trying to change the functional group e.g. using a longer alkyl chain or have a benzene ring linked to the alkyl chain (see **Figure 5.4**).

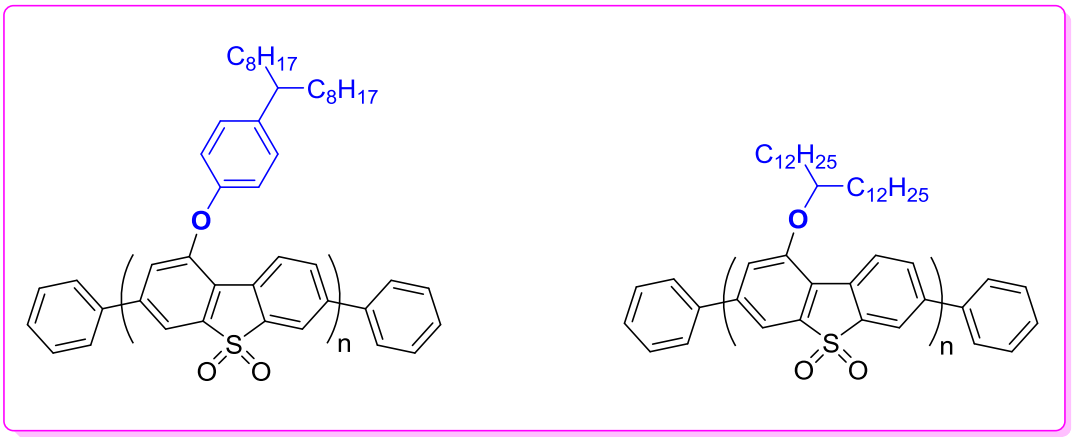


**Figure 5.4:** Suggested structures of 1-functionalised dibenzothiophene-*S*,*S*-dioxide **p(S-R)** homo polymers to achieve better solubility.

Secondly, by functionalising both the 1- and 9-positions as both are symmetrical, this will not affect the conjugation system of the polymer backbone. At the same time, good synthetic methodology has already been developed in this project to substitute the 1-position. Hence, **Br$_2$S** could be used as the starting compound then the nitration reaction for both positions 1 and 9. Because both positions have the same activation energy for electrophilic substitution reaction, it should be straightforward to get di-substitution with a good percentage yield by only increasing the time of the reaction from 24 h to maybe 48 h. Once di-substitution had been achieved the modification of the $NO_2$ group to prepare various monomers could then be carried out as before (see **Scheme 5.1**).

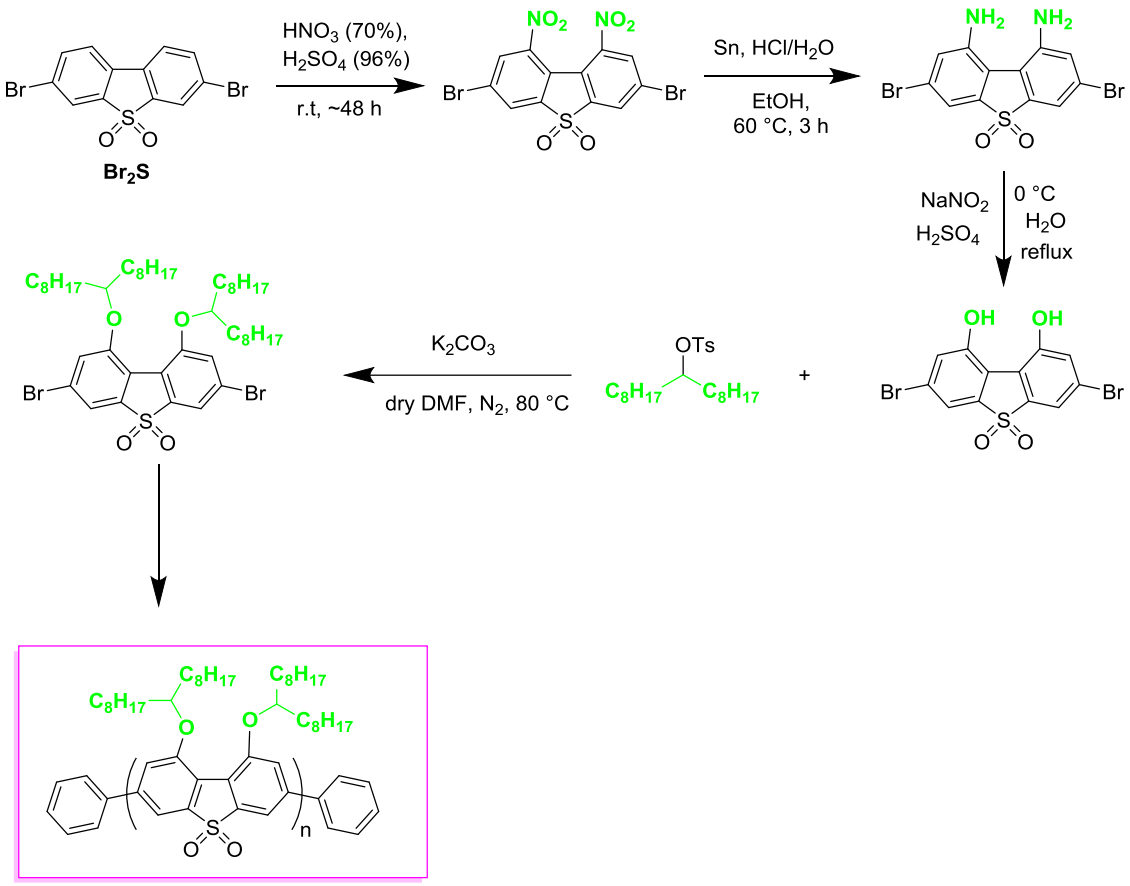


**Scheme: 5.1** Suggested synthetic route to 1,9-dialkoxy-3,7-dibromodibenzothiophene-*S*,*S*-dioxide homo polymer to enhance the solubility.

### 5.2.2 Novel dibenzothiophene-*S*,*S*-dioxide co-polymers with different donor units

After successfully preparing 1-functionalised dibenzothiophene-*S*,*S*-dioxide monomers, they could also be co-polymerised with a number of other different electron rich units not only the fluorene unit, such as the carbazole unit (see **Figure 5.5**).

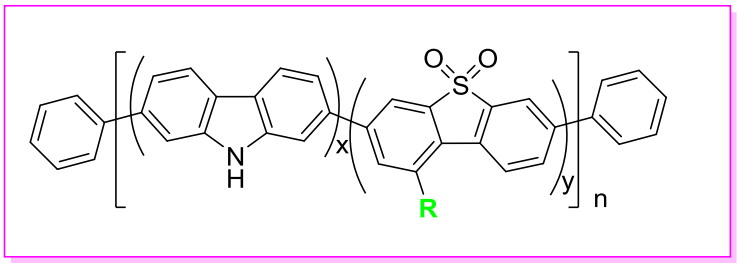


**Figure 5.5:** Structures of carbazole/1-functionalised dibenzothiophene-*S*,*S*-dioxide co-polymers, that could also be prepared.

### 5.2.3 Synthesis of new thermally activated delayed fluorescence (TADF) materials

Organic electroluminescence is a process of electro-excitation, where an electron and hole are recombined in an OLED device. The formation of excitons in the excited state statistically results in 25% of excitons going to the singlet state and 75% going to the triplet state. Thermally activated delayed fluorescence is a mechanism to improve the efficiency of OLED devices by harvesting the triplet excitons back to the singlet state. The discovery of new TADF emitters, which are more efficient and have higher stability, requires suitable electron donor (D) and electron acceptor (A) units. Dibenzothiophene-*S*,*S*-dioxide can be used as an acceptor unit with a suitable donor unit such as acridine. As future work, novel trimers could be synthesised by di-substitution of **Br$_2$S-R** at positions 3 and 7 using the Buchwald-Hartwig procedure with acridine or other donor units (see **Scheme 5.2**)

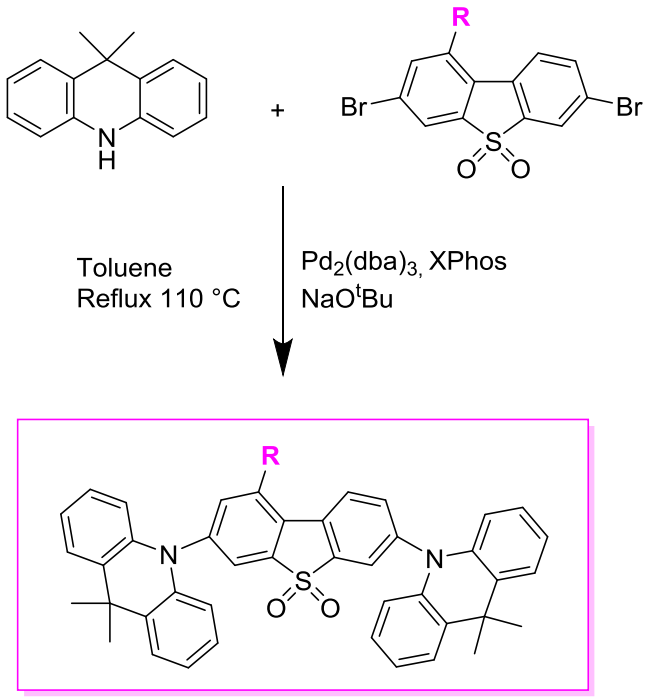


**Scheme 5.2:** Suggested synthetic route for the coupling of acridine to positions 3 and 7 of **Br$_2$S-R**.

Another idea includes a special design based upon the rigid accepting moiety **S** in the core and three symmetrical donor moieties attached to positions 1, 3, and 7. This would allow the effect of substitution of one more donor moiety at position 1 of the **S** unit on the TADF properties to be investigated (see **Scheme 5.3**).

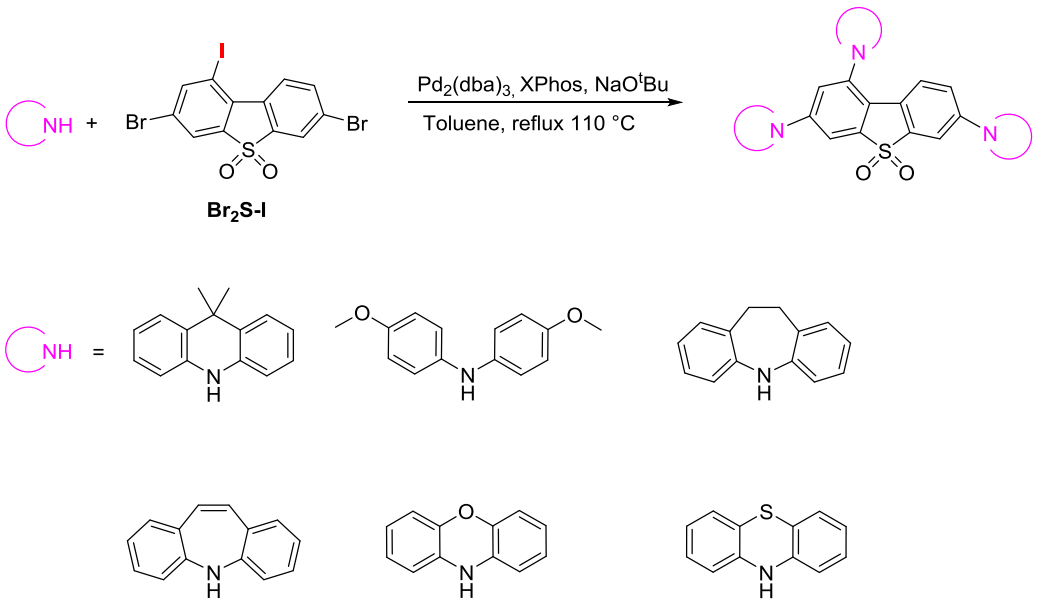


**Scheme 5.3:** Suggested synthetic route for the coupling of **Br2S-I** to cyclic arylamines.

# CHAPTER 6

# Appendices

---

**6.1**

**Table 6.1** Optimisation of nitration of 3,7-dibromodibenzothiophene-*S*,*S*-dioxide **$Br_2S$** to 1-nitro-3,7-dibromodibenzothiophene-*S*,*S*-dioxide (**$Br_2S$-$NO_2$**) at different reaction conditions at room temperature and scaling up the nitration reaction.

| | | | | **$Br_2S$-$NO_2$** | | | |
|---|---|---|---|---|---|---|---|
| **$Br_2S$**, amount | $HNO_3$, concen-tration, amount | $H_2SO_4$ (96%), amount | Time, h | Yield, % | *Purity, %* | Yield, % after recryst. (solvent) | *Purity, % (after recryst.)* |
| 0.20 g | 90 % 0.5 mL | 6 mL | 5.5 | 88.4 | *96* | | |
| 2.00 g | 90 % 5 mL | 60 mL | 8 | 99.0 | *90* | 39.1 ($CHCl_3$) | *95* |
| 2.00 g | 90 % 5 mL | 40 mL | 6 | 100 | *90* | 64.7 (dioxane) | *96* |
| 2.00 g | 90 % 5 mL | 20 mL | 5 | 100 | *95* | | |
| 2.00 g | 70 % 5 mL | 40 mL | 6 | 99.1 | *90* | 82.4 (dioxane) | *94* |
| 2.00 g | 70 % 10 mL | 20 mL | 6 | 94.9 | *92* | 33.0 % (dioxane)[a] | *99* |
| 20.0 g | 90% 50 mL | 200 mL | 7 | 100 | *87* | | |
| 7.50 g | 90 % 30 mL | 75 mL | 27 | 100 | *83* | 95.1 (dioxane) | *90* |
| 10.0 g | 70 % 50 mL | 100 mL | 24 | 96.8 | *90* | 72.2 (dioxane) | *96* |
| 20.0 g | 70 % 50 mL | 400 mL | 12 | 100 | *73* | 85.4 (dioxane) | *85* |
| 32.6 g | 70 % 160 mL | 330 mL | 23 | 97.7 | *93* | 95.1 (dioxane) | *90* |
| 159 g | 70 % 0.8 L | 1.6 L | 21 | 98.4 | *97* | 83 (dioxane) | *99* |

| | | | | | | | |
|---|---|---|---|---|---|---|---|
| 161 g | 70 %<br>0.82 L | 1.63 L | 21 | 96.6 | *98* | 83<br>(dioxane) | *99* |

[a] After several recrystalllisations from dioxane to obtain analytically pure sample.

### 6.2 Testing the stability of $Br_2S$ towards Pd/C reduction.

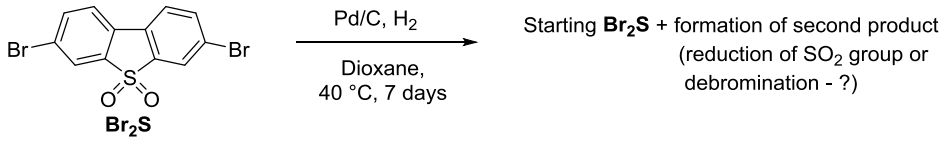


A round bottom flask (25 mL) was charged with 3,7-dibromo dibenzothiophene-*S*,*S*-dioxide **($Br_2S$)** (0.208 g, 0.556 mmol), dioxane (10 mL) and 10% Pd/C (0.210 g), and the flask was closed using a septum flushed with nitrogen. Then the flask was flushed with hydrogen, leaving a hydrogen balloon connected to the flask during the test. The mixture was stirred with heating at 40 °C for 7 days. The mixture was filtered through a bed of celite, washed with ethyl acetate (4 × 10 mL), and the solvent evaporated to yield a brown powder (0.286 g). TLC showed two spots. $^1$H NMR spectroscopy shows many overlapped peaks relating to two or more different compounds and some smaller unidentified peaks. Needs further investigation.

### 6.3 Attempted reduction of 1-nitro-3,7-dibromodibenzothiophene-*S*,*S*-dioxide ($Br_2S$-$NO_2$) with Pd/C under a hydrogen atmosphere.

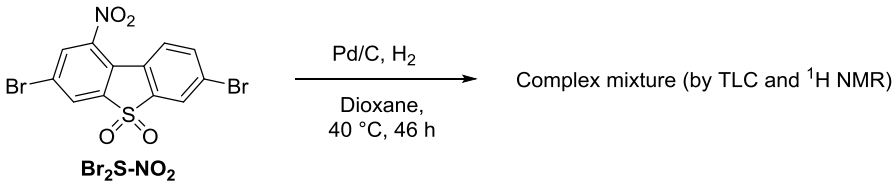


A round bottom flask (25 mL) was charged with 1-nitro-3,7-dibromo dibenzothiophene-*S*,*S*-dioxide **($Br_2S$-$NO_2$)** (0.201 g, 0.482 mmol) and 10% Pd/C 0.208 g). The flask was flushed with $H_2$ through the septum, dioxane (10 mL) was added, and the mixture was sonicated for few minutes for the more efficient removal of an air, before being flushed again with $H_2$. A new portion of dioxane was then added (10 mL) due to bad solubility of the **$Br_2S$-$NO_2$** (still not full dissolution), and the temperature was raised to 40 °C (full dissolution) and the mixture was stirred at this temperature for 46 hours. The mixture was then cooled to room

temperature, filtered through a bed of celite and washed with ethyl acetate (4 × 10mL). The combined organic layers were evaporated to yield the crude product (0.170 g, 94%) as a brown powder. $^1$H NMR spectroscopy showed a complex mixture of several products. Needs further investigation.

### 6.4 Testing the stability of $Br_2S$ towards Sn/HCl reduction.

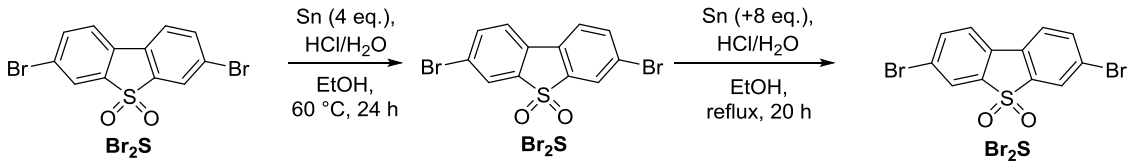


A small flask (5 mL) with a stirring bar was charged with 3,7-dibromodibenzothiophene-*S*,*S*-dioxide (**$Br_2S$**) (100 mg, 0.267 mmol) and ethanol (2.0 mL). Concentrated (37%) HCl (0.2 mL) and water (0.5 mL) were added and the mixture was stirred for 10 minutes (white coloured suspension was observed). Tin powder (127 mg, 1.06 mmol) was added in portions over 5 minutes with stirring. The mixture was stirred with heating at 60 °C for 24 h. Monitoring the reaction by TLC in different solvent systems did not show the appearance of new spots even after 19 h; only the spot for the starting material **$Br_2S$** was identified. $^1$H NMR spectroscopy was done after 24 hours from a probe sample, which also showed only starting material, **$Br_2S$**.

An additional portion of tin powder (250 mg, 2.09 mmol), concentrated (37%) HCl (0.25 mL), and ethanol (2 mL) were added and the mixture was stirred under reflux for a further 20 hours. The colour changed to pale yellow with the mixture changing to an emulsion. Monitoring the reaction by TLC after 44 hours showed only the spot corresponding to starting material **$Br_2S$**. $^1$H NMR probe also confirmed that only starting material **$Br_2S$** was present in the reaction mixture. The test was therefore stopped, the mixture was diluted with water (15 mL), and the solid was filtered off, washed with water until pH ~ 7 and dried to yield a slightly yellowish powder (235 mg, 235%). This solid was extracted with ethyl acetate, the solvent was evaporated and the residue was dried to yield starting material **$Br_2S$** (25 mg, 25%) as a white powder, which showed $\delta_H$ (400 MHz, $CDCl_3$): 7.94 (d, $J$ = 1.6 Hz, 2H), 7.78 (dd, $J$ = 8.2, 1.8 Hz, 2H), 7.64 (d, $J$ = 7.6, 2H).

### 6.5 Attempt to synthesise 1-cyano-3,7-dibromodibenzothiophene-*S*,*S*-dioxide (**Br$_2$S-CN**).

To a 2-neck round bottom flask, sodium nitrite (0.314 g, 4.55 mmol) and conc. $H_2SO_4$ (40 ml) were added. The sodium nitrite was added slowly over a period of 40 minutes and the solution was stirred vigorously at 0 °C. The solution was then heated to dissolve all of the sodium nitrite. The solution was then cooled back to 0 °C and a solution of **Br$_2$S-NH$_2$** (1.00 g, 2.57 mmol) in $H_2SO_4$ was added. This was left stirring at 0 °C for 18 h. Crushed ice was added to the solution which afforded a precipitate. This was filtered off, washed with water (10 mL) and immediately taken up in 40 ml of water. This was then slowly added to a solution of copper sulfate (1.85 g, 7.41 mmol) and sodium cyanide (2.08 g, 42.4 mmol) dissolved in water. The mixture was then heated to reflux for 3 h. The solution was hot filtered and dried to afford starting compound **Br$_2$S-NH$_2$** (0.296 g, 30%). The mother liquor was collected and evaporated, yielding 3,7-dibromo-1-hydroxydibenzothiophene-*S*,*S*-dioxide (**Br$_2$S-OH**) (0.455 g, 45%).

### 6.6 Attempt to synthesise 1-cyano-3,7-dibromodibenzothiophene-*S*,*S*-dioxide (**Br$_2$S-CN**).

**Br$_2$S-NH$_2$** (0.700 g, 1.95 mmol) and $H_2SO_4$ (25 ml) were charged into a 2-neck round bottom flask. To this, water (20 mL) was added dropwise, keeping the temperature below 30 °C during the addition. The solution was then cooled to 0 °C. A solution of sodium nitrite (169 mg, 2.44 mmol) was prepared by dissolving in water (4 mL). This was added dropwise to the **Br$_2$S-NH$_2$** solution over 30 minutes. The solution was left to stir at 0 °C for 2 h. During this time, a solution of sodium cyanide (1.62 g, 49.0 mmol) dissolved in water (10 mL) was prepared. This solution was added dropwise over 30 minutes to the reaction mixture, which was then allowed to reach room temperature and was left to stir for 67 h. The temperature was raised to 50 °C and allowed to stir for 1 h. The mixture was then cooled to room temperature, filtered and the solid was dried by vacuum filtration, to yield the crude product (0.612 g, 86%) which was shown by $^1$H NMR spectroscopy to be a mixture of **Br$_2$S** (32%), **Br$_2$S-OH** (53%) and **Br$_2$S-NH$_2$** (15%).

## 6.7 Attempted trials and failed reactions on substitution of $NH_2$ group in $Br_2S$-$NH_2$ by SR group using Cu-catalysed reaction with $Na_2S_2O_3$ and alkylbromides.

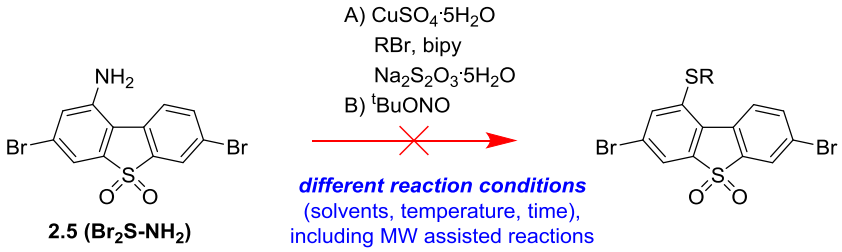


### Attempt to synthesise 1-(2-ethylhexylthio)-3,7-dibromodibenzothiophene-*S*,*S*-dioxide ($Br_2S$-SEtHex).

Sodium thiosulfate (0.910 g, 3.60 mmol), bipyridine (0.008 g, 0.051 mmol), $CuSO_4 \cdot 5H_2O$ (0.015 mg, 0.051 mmol), 2-ethylhexyl bromide (0.63 mL, 3.60 mmol) and methanol/water (2.5 mL/2.5 mL) were charged into a 3 neck round bottom flask. The solution was stirred at 80 °C for 2 h. To this, **$Br_2S$-$NH_2$** (0.201 g, 0.514 mmol) and isopentylnitrite (0.10 mL, 0.771 mmol) were added to the reaction mixture. Stirring at 80 °C was continued for 8 h, then stirring was continued for a further 12 h at r.t. Solution is extracted with diethyl ether (4 × 10 mL) and the solvent is evaporated to yield a yellow powder (0.130 g, 48.8%). The by-product was washed with THF and this solution was passed through a silica column to afford a pale yellow solution. This was deemed to be pure enough by TLC to combine with the initial product. The combined solids were then purified by flash chromatography on silica gel using Tol : DCM, 1:1 as eluent to a afford mixture of products **$Br_2S$-$NH_2$** (0.154 g, 58%) and **$Br_2S$** (0.005 g, 0.013 mmol, 1.9%).

### Attempt to synthesise 1-butylthio-3,7-dibromo-dibenzothiophene-*S*,*S*-dioxide ($Br_2S$-SBu).

Sodium thiosulfate (0.910 g, 3.60 mmol), bipyridine (0.008 g, 0.051 mmol), $CuSO_4 \cdot 5H_2O$ (0.015 g, 0.051 mmol), 1-bromobutane (0.63 mL, 3.60 mmol) and methanol/water (2.5 mL/2.5 mL) were charged into a microwave vial. The solution was stirred and subjected to microwave irradiation at 80 °C for 2 h. To this, **$Br_2S$-$NH_2$** (0.201 g, 0.514 mmol) and

isopentyl nitrate (0.10 mL, 0.77 mmol) were added. The mixture was then irradiated in a microwave reactor in a four stage process: 80 °C for 1 h, 80 °C for 2 h, 80 °C for 3 h and 80 °C for 4 h. The solution was then extracted with diethyl ether (4 × 10 mL) and the solvent was evaporated to yield a yellow powder (0.093 mg, 39%). The product was purified by flash chromatography on silica gel using Tol : DCM, 1:1 as eluent to yield a yellow solid powder (0.007 g, 2.9%).

**Attempt to synthesise 1-hexylthio-3,7-dibromodibenzothiophenes-*S,S*-dioxide ($Br_2$S-SHex).**

Sodium thiosulfate (0.440 g, 1.75 mmol), bipyridine (0.006 g, 0.025 mmol), $CuSO_4 \cdot 5H_2O$ (0.011 g, 0.025 mmol), 1-bromohexane (0.25 mL, 1.75 mmol) and ethanol/water (1.7 mL/0.9 mL) were charged into a test tube. The solution was stirred at 80 °C for 2 h. To this, **$Br_2$S-$NH_2$** (0.097 g, 0.25 mmol) and isopentyl nitrate (0.05 mL, 0.375 mmol) were added. Stirring at 80 °C was continued for 8 h. Reaction was brought to room temperature and stirring was continued for a further 32 h. TLC showed only the starting compound **$Br_2$S-$NH_2$**.

**Attempt to synthesise 1-hexylthio-3,7-dibromo-dibenzothiophenes-*S,S*-dioxide ($Br_2$S-SHex).**

Sodium thiosulfate (0.440 g, 1.75 mmol), bipyridine (0.006 g, 0.025 mmol), $CuSO_4 \cdot 5H_2O$ (0.011 g, 0.025 mmol), 1-bromohexane (0.25 mL, 1.75 mmol) and DMF/water (1.7 mL/0.9 mL) were charged into a test tube. The solution was stirred at 80 °C for 2 h. To this, **$Br_2$S-$NH_2$** (0.097 g, 0.25 mmol) and isopentyl nitrate (0.05 mL 0.375 mmol) were added. Stirring at 80 °C continues for 8 h. Reaction was brought to room temperature and stirring was continued for a further 32 h. Reaction was stopped and solvent was evaporated to give (0.735 g, 636%). Product was purified by flash chromatography on silica gel using PE : iPrOH, 20:1 as eluent, isolating no compound.

**Attempt to synthesise 1-hexylthio-3,7-dibromodibenzothiophenes-*S,S*-dioxide (Br$_2$S-SHex).**

Sodium thiosulfate (0.440 g, 1.75 mmol), bipyridine (0.006 g, 0.025 mmol), $CuSO_4 \cdot 5H_2O$ (0.011 g, 0.025 mmol), 1-bromohexane (0.25 mL, 1.75 mmol) and acetonitrile/water (1.7 mL/0.9 mL) were charged into a test tube. The solution was stirred at 80 °C for 2 h. To this, **Br$_2$S-NH$_2$** (0.097 g, 0.25 mmol) and isopentyl nitrate (0.05 mL 0.375 mmol) were added. Stirring at 80 °C was continued for 8 h. Reaction was brought to room temperature and stirring was continued for a further 32 h. TLC showed only the starting compound **Br$_2$S-NH$_2$.**

**Attempt to synthesise 1-hexylthio-3,7-dibromodibenzothiophenes-*S,S*-dioxide (Br$_2$S-SHex).**

Potassium thiosulfate (0.462 g, 1.75 mmol), bipyridine (0.006 g, 0.025 mmol), $CuSO_4 \cdot 5H_2O$ (0.011 g, 0.025 mmol), 1-bromohexane (0.25 mL, 1.75 mmol) and ethanol/water (1.7 mL/0.9 mL) were charged into a test tube. The solution was stirred at 80 °C for 2 h. To this, **Br$_2$S-NH$_2$** (0.097 g, 0.25 mmol) and isopentyl nitrate (0.05 mL, 0.375 mmol) were added. Stirring at 80 °C was continued for a further 8 h. Heating was stopped and stirring was continued for a further 32 h at r.t. TLC showed only the starting compound **Br$_2$S-NH$_2$.**

**Attempt to synthesise 1-hexylthio-3,7-dibromodibenzothiophenes-*S,S*-dioxide (Br$_2$S-SHex).**

Potassium thiosulfate (0.462 g, 1.75 mmol), bipyridine (0.006 g, 0.025 mmol), $CuSO_4 \cdot 5H_2O$ (0.011 g, 0.025 mmol), 1-bromohexane (0.25 mL, 1.75 mmol) and DMF (3 mL) were charged into a test tube. The solution was stirred at 80 °C for 2 h. To this, **Br$_2$S-NH$_2$** (97 mg, 0.25 mmol) and *t*-butyl nitrite (0.05 mL, 0.375 mmol) were added. Stirring at 80 °C was continued for a further 4.5 h. The reaction was then quenched with water, evaporated to give (242 mg, 209%). TLC showed only the starting compound **Br$_2$S-NH$_2$.**

**Attempt to synthesise 1-hexylthio-3,7-dibromodibenzothiophenes-*S,S*-dioxide (Br$_2$S-SHex).**

Potassium thiosulfate (0.462 g, 1.75 mmol), bipyridine (0.006 g, 0.025 mmol), $CuSO_4 \cdot 5H_2O$ (0.011 g, 0.025 mmol), 1-bromohexane (0.25 mL, 1.75 mmol) and DMSO (3 mL) were charged into a test tube. The solution was stirred at 80 °C for 2 h. To this, **Br$_2$S-NH$_2$** (0.097 g, 0.25 mmol) and *t*-butyl nitrite (0.05 ml, 0.375 mmol) were added. Stirring at 80 °C was continued for a further 4.5 h. The reaction was then quenched with water, evaporated to give (0.232 g, 200%). The crude product was then purified by flash chromatography on silica gel using THF as eluent, yielding by-product **Br$_2$S** (0.016 g, 0.042 mmol).

## 6.8 Supplementary information

Electronic Supplementary Information (ESI) available: $^1$H NMR, $^{13}$C NMR, MS, and GPC data for synthesised monomers and polymers.